Regional District of Fraser-Fort George

Collaborative Disaster Risk Reduction and Climate Adaptation Project

Prepared by BGC Engineering Inc. for:

Fraser Basin Council

July 8, 2025

Project 0511013

Pioneering responsible solutions to complex earth science challenges

July 8, 2025 Project 0511013

Fraser Basin Council
Suite 507, 1488 – 4th Avenue
Prince George, BC V2L4Y2

Attention: Kim Menounos, Senior Manager, Interior Regional Programs

Collaborative Disaster Risk Reduction and Climate Adaptation Project

Please find the above-noted report attached. We appreciate the opportunity to work with you on this challenging and interesting project.

Should you have any questions, please do not hesitate to contact the undersigned.

Yours sincerely,

BGC Engineering Inc.
per:

[redacted]

Kris Holm, M.Sc., P.Geo.
Principal Geoscientist

SUMMARY

The Regional District of Fraser-Fort George (RDFFG, the District), City of Prince George, District of Mackenzie, Village of McBride, Village of Valemount, Lheidli T'enneh First Nation, and McLeod Lake Indian Band are engaged in a District-wide "collaborative disaster risk reduction and climate adaptation (CDRRCA)" project. The CDRRCA project is being completed in the traditional territories of Lheidli T'enneh First Nation, McLeod Lake Indian Band, and the Simpcw First Nation.

The project partners aim to reduce risks and increase the resilience of communities within the RDFFG to natural hazards in a changing climate.

In support of this major goal, the CDRRCA advances three activities:

- *Hazard assessment*: Mapping steep creek alluvial fans, landslide and flood hazards
- *Exposure assessment*: Identifying valued assets and their exposure to mapped hazards at a regional scale
- *Recommendations*: Actions to advance CDRRCA goals as part of a multi-year plan extending beyond project completion.

Together, the project outcomes inform emergency management, mitigation planning, policy development, and regional understanding of how changes in climate could affect the identified hazards.

In summary, BGC characterized 271 alluvial fans and 1,232 landslide locations in the vicinity of settled areas across the District. BGC identified 24,000 km^2 within the District where the presence of a mapped steep (>30%) slope, greater than 1% estimated susceptibility to deep-seated earth slides, or the presence of an inventoried landslide, indicate areas of interest for potential landslide hazard.

BGC identified 2,770 km^2 of floodplains on all watercourses with catchments larger than 10 km^2 and completed Tier 2 floodplain mapping for 180 km of watercourses in the vicinity of Tabor Creek at Prince George, Fraser River at McBride, Fraser River at Tete Jaune Cache, Naver and Hixon Creeks at Hixon, and McLennan River and Swift Creek at Valemount (Drawing 03). The more detailed Tier 2 maps show estimated 200-year (0.5% AEP) flood hazard extents, velocities and depths under current conditions and with projected climate change.

The exposure assessment identified people and assets in hazard areas across the RDFFG and within each project partner's jurisdiction. In summary, the RDFFG is home to almost 100,000 people and contains about $17B in buildings[1], 58,000 km of roads, 1,400 km of railways, and 11,000 km of linear utilities. Of these, BGC identified about 10,000 people, $3B in development, 13,000 km of roads, and 2,000 km of linear utilities as being located in flood, alluvial fan, or landslide hazard areas of interest.

[1] Estimated total value of parcel improvements in the RDFFG (BC Assessment, 2023), plus total estimated value of buildings located on First Nations reserves (NRCAN, 2022b)

BGC delivered project results through documentation, data, and digital maps. Two-page fact sheets summarize findings for each project partner. Given the large study region, spatial deliverables are provided as Geographic Information Systems (GIS) data layers. The RDFFG has licensed Cambio Earth Systems (Cambio™) and provided access to project partner representatives (staff members). Cambio supplements existing local government platforms with access to spatial deliverables in a format for operational risk management. Data provided includes hazard and asset data layers, hazard exposure results for individual assets and hazard types, lidar topography and satellite-based InSAR analysis[2], a weather and snowpack module, and topographic measurement tools.

The recommendations included in this project inform collaboration between project partners towards a multi-year plan for disaster risk reduction and climate adaptation. The recommendations are intended to be read by different groups within each partner organization. For development and community services, recommended next steps include review of land use regulations, incorporating tools to support implementation, and a developing an approach to collaborate between the private and public sector. BGC also provides recommendations for further engagement, the incorporation of results into protective services (emergency management), and further assessments to resolve data gaps.

As a key message, BGC notes that the decentralized environment of natural hazard risk management in BC requires collaboration between parties with different responsibilities but shared needs to reduce risk. Regional coordination to share knowledge of hazard and exposure builds capacity by enabling many parties to advance their specific risk management objectives.

While the completed work focused on regional hazard and exposure, a second phase of the CDRRCA project will initiate in 2025. The second phase of work will broaden hazards to include heat and drought and will include further work to support development decision making in hazardous lands. The second project phase includes all project partners and will extend through 2027. The intended outcome is an informed approach to develop plans and regulations around land use, including Development Permit Areas, greater staff capacity to use hazard information to make development decisions, and increased community awareness of geohazards.

[2] Interferometric Satellite Aperture Radar (InSAR) analysis was completed as part of landslide hazard characterization, as described in Appendix G.

TABLE OF REVISIONS

Date	Revision	Remarks
May 30, 2025	DRAFT	Issued for comments
July 8, 2025	FINAL	

CREDITS AND ACKNOWLEDGEMENTS

BGC would like to acknowledge the following contributors to this project:

- Kris Holm, Richard Carter, Elisa Scordo, Matthieu Sturzenegger, Melissa Hairabedian, Gemma Ferland, Matthew Buchanan, Matthew Teelucksingh, Sebastian Martijena, Julia Kimball, Corey Scheip, Carie-Ann Hancock, Hamish Weatherly, Mike Porter, Patrick Grover, Lauren Hutchinson, Caio Stringari, Marc-Andre Brideau, Katherine Johnston, and Jane Wang.

BGC is also grateful for the coordination, leadership and support of Fraser Basin Council and the lead project partner, Regional District of Fraser-Fort George:

- *Fraser Basin Council*: Kim Menounos, Patience Rakochy, Scott Brown, and Terry Robert.
- Regio*nal District of Fraser-Fort George*: Kenna Jonkman and Blaine Harasimiuk.

BGC is grateful for the support and input provided by project partners, and guidance provided by advisors:

- *Project partners:* Regional District of Fraser-Fort George, Lheidli T'enneh First Nation, McLeod Lake Indian Band, Village of Valemount, Village of McBride, District of Mackenzie, and City of Prince George.
- *Advisors:* Gord Hunter, Ministry of Transportation and Transit (MOTT), Brendan Miller, Ministry of Forests (MoF), Ministry of Water, Land, and Resource Stewardship (WLRS), Ministry of Emergency Management and Climate Resilience (EMCR), and Joseph Shea, University of Northern British Columbia (UNBC).

LIMITATIONS

BGC Engineering Inc. ("BGC") prepared this document[3] for Fraser Basin Council (the "Client"). BGC is not liable for any loss, injury, or damages arising from any unapproved use or unauthorized modification of this document.

Any use or reliance which a third party makes of this document is the responsibility of the third party and is at such third party's own risk. BGC accepts no responsibility for damages, if any, suffered by any third parties as a result of their use of this document.

This document may include or rely upon estimates, forecasts, or modeling analyses (e.g., results or outputs of numerical modeling) that are based on available data. Such estimates, forecasts, or modeling analyses do not provide definitive or certain results. The Client is solely responsible for deciding what action (if any) to take based on any estimates, forecasts, or modeling analyses.

BGC prepared this document in accordance with generally accepted practices for similar services in the applicable jurisdiction. BGC makes no warranty (either express or implied) related to this document. BGC is not responsible for any independent conclusions, interpretations, extrapolations, or decisions made by the Client or any third party based on this document. The record copy of this document in BGC's files takes precedence over any other copy or reproduction of this document.

[3] References in these Limitations to the "document" include the document to which these Limitations are attached, any content contained in this document, and any content referenced in this document but located in one of BGC's proprietary software applications (e.g., Cambio).

TABLE OF CONTENTS

LIST OF TABLES

LIST OF FIGURES

LIST OF DRAWINGS

LIST OF APPENDICES

1.0 INTRODUCTION

1.1 General

The Regional District of Fraser-Fort George (RDFFG, the District), City of Prince George, District of Mackenzie, Village of McBride, Village of Valemount, Lheidli T'enneh First Nation, and McLeod Lake Indian Band are engaged in a District-wide "collaborative disaster risk reduction and climate adaptation (CDRRCA)" project. As lead partner, RDFFG retained Fraser Basin Council (FBC) to coordinate the project with BGC Engineering Inc. (BGC) completing the technical work[4]. The CDRRCA project is supported by the Union of BC Municipalities Disaster Risk Reduction-Climate Adaptation fund. It is guided by an advisory committee composed of project partner representatives, Ministry of Transportation and Transit (MOTT), Ministry of Forests (MoF), and University of Northern BC (UNBC).

The project partners aim to reduce risks and increase the resilience of communities within the RDFFG to natural hazards in a changing climate. In support of this, the CDRRCA advances three major activities:

1. Hazard assessment: Mapping flood, steep creek alluvial fans, and landslide hazards.
2. Exposure assessment: Identifying people and assets in mapped hazard areas.
3. Recommendations: Actions to advance CDRRCA goals as part of a multi-year plan extending beyond project completion.

The project outcomes are intended to inform emergency management, mitigation planning, policy development, and regional understanding of how changes in climate could affect the identified hazards.

The CDRRCA project is being completed in the traditional territories of several First Nations. The central part of RDFFG lies in the traditional territory of Lheidli T'enneh First Nation, with reserves in the vicinity of Prince George, British Columbia (BC). The northern part of the District is in the traditional territory of Tsek'ehne First Nation, including McLeod Lake Indian Band. Although their reserve lands are further south, traditional territories of Simpcw First Nation occupy large parts of southern RDFFG, including the Robson Valley. The RFFFG also extends close to the traditional territory of West Moberly First Nation in the North, Nak'azdli Whut'en territory in western RDFFG with one reserve on Great Beaver Lake, and Nazko First Nation with three reserves fringing the southern border of RDFFG along Blackwater River.

1.2 Report Organization

Table 1-1 outlines the structure of this report. The main report summarizes objectives, approach, key findings, and recommendations. The appendices provide additional background, technical methodologies, and results presented as tables, maps, and charts. Appendix I (Exposure Results spreadsheet), Appendix L (Geospatial Data), and Appendix M (Project Partner Fact Sheets) are provided as separate files.

4 Work is being completed under the terms of a September 1, 2023 contract between BGC and FBC.

Table 1-1 Report organization.

Section	Title	Description
Main Report	Main Report	Project overview, background, assessment framework, approach, results, and recommendations.
Appendix A	Terminology	Key terms used in the report.
Appendix B	Data Compilation	Key previous assessments (complete citation list provided in Main Document).
Appendix C	Geohazard Event Inventory	Inventory of recorded damaging hazard events within the RDFFG.
Appendix D	Study Area Background	Geologic, physiographic, and hydroclimatic project context.
Appendix E	Clear-water Flood Hazard Assessment Methods	Analysis approach for Tier 1 and 2 flood mapping.
Appendix F	Steep Creek Hazard Assessment Methods	Analysis approach for Tier 2 steep creek (alluvial fan) hazard characterization.
Appendix G	Landslide Hazard Assessment Methods	Analysis approach for Tier 1 and 2 landslide inventory and mapping.
Appendix H	Hazard Exposure Analysis Methods	Analysis approach for the characterization of valued assets in hazard areas.
Appendix KI	Hazard Exposure Analysis Results	Tabular summary of hazard exposure analysis results.
Appendix J	Gaps and Limitations	Summary of key gaps and limitations identified during assessment.
Appendix K	Metadata	Information about geospatial data compilation.
Appendix L	Geospatial Data	Geospatial data package (geodatabase).
Appendix M	Results Fact sheets	Two-page project summaries for each project partner.

1.3 Key Users

This project is intended to inform parties with diverse roles and responsibilities around disaster mitigation, preparedness, response, and recovery. Table 1-2 provides examples of roles and types of decision making that this project is intended to support. The list is not exhaustive.

Table 1-2 Intended users of project deliverables.

Community Roles	Typical Use-Case	Type of Decision-Making Support
Development Services: • Building Inspection and Bylaw Services	"I want to check whether a site of interest falls within a specific hazard area, and whether further actions may be needed"	Binary (Yes/No)
Development Services: • Planning Services **Community and Protective Services:** • Emergency Services **Financial Services:** • Asset management **Corporate Services:** • Information Technology	"I want to review regional hazard inventories to prioritize areas for further assessment and management". "I want to review hazards and exposed assets to develop emergency preparedness and response plans."	Prioritization and planning.
Contracted service providers: Qualified Professionals	"I want information to support my further assessment of areas as required by a client or authority, and in accordance with professional practice standards"	Decision support and implementation.

1.4 Cambio Earth Systems

Given the large study region, all spatial deliverables are provided in digital (GIS) format to facilitate use by project partners in their own platforms where available. Static drawings show areas mapped but are not intended for day-to-day decision support. The RDFFG has licensed Cambio Earth Systems (Cambio^{TM}) and provided access to project partner representatives (staff members[5]). Cambio is a secure earth science web application with a digital map knowledge base and tools for hazard monitoring and operational management. For this project, Cambio provides access to spatial deliverables, including hazard and asset data layers and hazard exposure results. It also provides additional access to applications including a remote-sensed model with lidar and satellite-based InSAR analysis[6], a weather and snowpack module, and topographic measurement tools. The current project does not include Cambio add-in modules for program implementation (e.g., inspections, monitoring, instrumentation) or the Cambio mobile application for field inspections. However, the data layers provide a foundation to add such tools as may be needed in the future to support planning, policy, regulation or protective services.

[5] Provided under subscription terms between RDFFG and Cambio Earth Systems Inc. dated December 18, 2024.

[6] Interferometric Satellite Aperture Radar (InSAR) analysis was completed as part of landslide hazard characterization, as described in Appendix G.

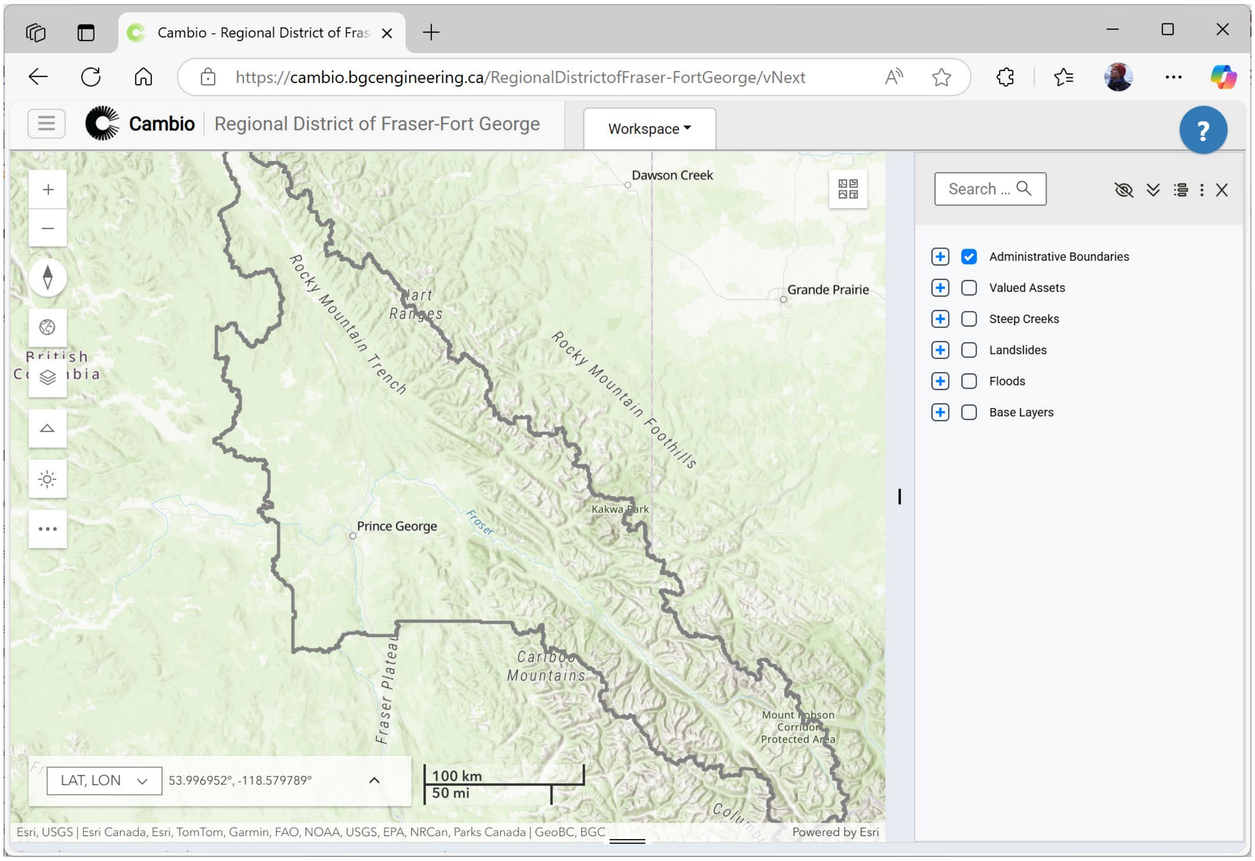

Figure 1-1 Cambio Earth Systems, with a layer list (right) showing groups of spatial data layers accessed through the tool.

1.5 Assessment Framework

The CDRRCA project applies a well-established framework for understanding and managing risk (e.g., Strouth & McDougall, 2021). This section describes that framework, starting with a conception of how risk is created from the overlap of hazard, exposure, and vulnerability (Figure 1-2).

Figure 1-2 Risk is a function of the interaction between hazard, exposure, and vulnerability.

- Risk is the potential for loss caused by future hazard events at a specific location, infrastructure, person, or group. Quantitatively, risk is the product of some adverse consequence (e.g., number of lives lost, economic loss, days of service disruption) and the probability of that loss occurring. It is a function of the interaction between the hazard, the exposed element at risk, and the vulnerability of that element to the hazard (Figure 1-2).
- Hazard refers to the process type, likelihood of impact, and intensity (e.g., flow depth, velocity) of impact at an exposed element.
- Exposure describes the quantity, value, and characteristics of the elements that are at risk, like people, buildings, infrastructure, economic activities, and things of social and cultural value.
- Vulnerability describes the probability of loss given an exposed element is impacted by a hazard with a given intensity. Vulnerable infrastructure is more likely to be damaged when impacted, while resilient infrastructure – and communities more broadly – are more likely to function and recover.

Disaster management in BC is highly decentralized, involving parties with diverse roles and responsibilities spread across both the public and private sector. Figure 1-3 illustrates a step-wise, pro-active approach to understand, make decisions, and take actions to reduce natural hazard risks. As a collaborative study, this project addresses earlier steps in the process, focusing on a question shared by all parties with disaster risk reduction goals: where are the hazards in relation to what we value? The project outcomes inform a broader range of future activities at a site-scale than can be accommodated by a single project or responsible party. These include further work to quantify vulnerability and risk for specific assets, develop policy and regulation for hazardous lands, and implement risk-reduction measures. Steps to reduce risk and increase resilience may unfold over multiple years and include multiple phases and projects.

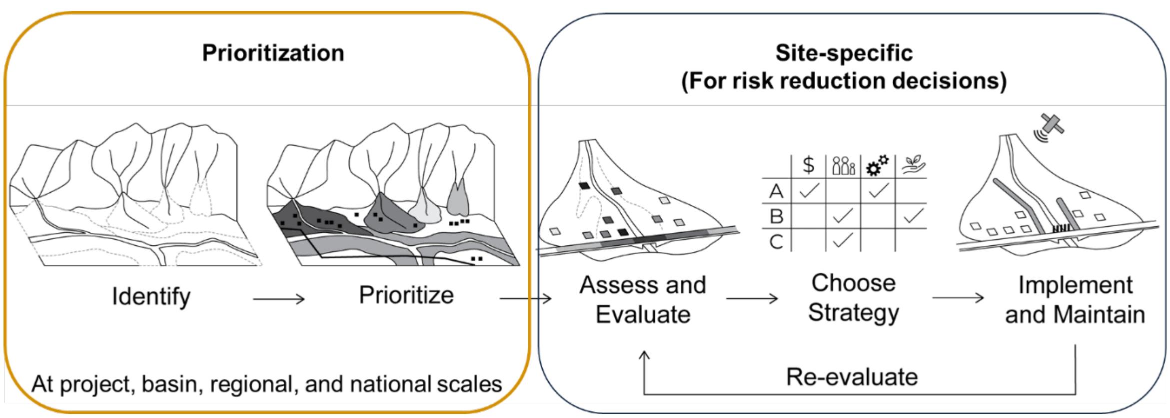

Figure 1-3 Conceptual illustration of steps in a pathway to risk reduction. This study focuses on steps outlined in the left (orange) box.

1.6 Level of Detail

Table 1-3 defines a three-tiered approach to describe levels of detail in hazard assessments. These tiers are commonly applied to flood hazard mapping and have been generalized to define assessment levels of detail for floods, steep creeks (alluvial fans) and landslides in this project.

Table 1-3 Description of hazard mapping "Tiers" representing different levels of detail.

Level	Description	Application to this study
Tier 1	Hazard Identification (screening-level) - Hazard identification maps help identify hazard areas across large spatial extents using desktop approaches.	Landslide susceptibility, floodplain identification (Section 4.2) Landslide inventory, susceptibility, and areas of interest (Section 4.4);
Tier 2	Base-level Mapping - further refine the Tier 1 results to better characterize hazards over larger areas and are a pre-cursor to more costly detailed flood mapping using hydraulic models. These are more cost-effective to prepare for larger areas using lidar data (e.g. no bathymetric data is required for Tier 2 flood mapping).	Floodplain mapping (Section 4.2); Alluvial fan characterization (Section 4.3).
Tier 3	Detailed Mapping - Further refines estimates of hazard extents and characteristics across a range of scenarios at greater detail than base level maps by including survey data and includes considerations for climate change. Detailed hazard maps include multiple hazard scenarios, delineation of flood construction-levels (FCLs), and can be used to inform policy, risk assessment, and risk management decisions.	Not applicable.

2.0 PROJECT OVERVIEW

2.1 Scope of Work

Table 2-1 describes elements of the CDRRCA assessment, which was based on a combination of desktop study, fieldwork, and engagement with project partners and the advisory committee.

Table 2-1 Overview of the project scope of work.

Work Phase	Activities	Tasks	Deliverables
1	**Project Management**		
1.1	Project management	Project administration	Project updates
2	**Knowledge Gathering & Engagement**		
2.1	Knowledge gathering and engagement	Data compilation and project partners and advisory engagement.	Confirmation of project objectives and supporting data for the assessment.
3	**Analysis**		
3.1	Hydroclimate	Characterisation of historical hydroclimate and hydrology, and quantification of climate change impacts. High-level qualification of indirect climate change effects to steep creeks and landslides.	Historical flood frequency estimates adjusted for projected climate change.
3.1	Flood (Tier 1)	Floodplain identification.	200-year (0.5% annual exceedance probability, AEP) flood extents.
3.1	Flood (Tier 2)	Flood mapping (select areas)	0.5% AEP flood scenarios for select areas, under current conditions and adjusted for projected climate change
3.3	Steep Creek (Tier 2)	Fan characterization	Alluvial fan hazard map
3.4	Landslide (Tier 1)	Landslide inventory; Landslide hazard mapping: InSAR analyses	Landslide inventory, landslide susceptibility map, InSAR analysis results
3.4	Population and Assets	Organization of population and asset data.	Asset data model.
3.5	Exposure	Spatial analyses of valued assets in hazard areas.	Hazard exposure maps and statistics.
4	**Field**		
4.1	Fieldwork (July 22-26, 2024)	Verification of desktop work.	Field notes and photos.
5	**Deliverables**		
5.1	Report and data	Reporting	Report, spatial data, Cambio.
5.2	Presentation	Presentation preparation	Presentation slide deck

BGC's followed the Engineers and Geoscientists BC (EGBC) Professional Practice guidelines for Legislated Flood Assessments in a Changing Climate in BC (EGBC, 2018), Flood Mapping in BC Professional Practice Guidelines (EGBC, 2017), BC Floodplain Mapping Guidelines (unpublished, in-progress[7]) and EGBC Professional Practice Guidelines for Landslide Assessments in BC (EGBC, 2023). The study framework also incorporated ideas from the United Nations International Strategy for Disaster Reduction (UNISDR) Sendai Framework (UNISDR, 2015). Specifically, the study framework focused on the first UNISDR priority for action, understanding disaster risk, and is a starting point for the remaining priorities, which focus on strengthening disaster risk governance, improving resilience, and enhancing disaster preparedness.

The project workflows are also consistent with analysis completed by BGC for the province-wide Disaster and Climate Risk and Resilience Assessment (DCRRA) (BGC, March 24, 2025)[8]. At a regional scale, the work is also consistent with previous assessments by BGC across large parts of British Columbia, including the Regional Districts surrounding the RDFFG and western Alberta (e.g., Holm et al., 2016; Holm et al., 2018).

2.2 Hazards Assessed

BGC assessed the following hazard types in the RDFFG:

- Clear-water floods: inundation due to an excess of clearwater discharge in a watercourse or body of water, submerging land outside the natural or artificial banks that is not normally under water. This term corresponds to "hydrotechnical hazards" (see Section 4.2 and Appendix E).
- Steep creek hazards on alluvial fans: processes on steep creeks that typically contain elevated concentrations of debris, often associated with avulsions, scour, and substantial bank erosion (i.e., debris floods and debris flows). Most stream channels within the study region are tributary creeks subject to steep creek processes (see Section 4.3 and Appendix F).
- Landslides: movement of rock, earth, or debris down a slope. Landslide velocities can range from nearly imperceptible to hundreds of km/hr (see Section 4.4 and Appendix G).

The assessment excluded the following hazard types:

- Failure of engineered structures (e.g., dams, dikes, culverts, bridges, engineered slopes)
- Flooding of stormwater and sewer infrastructure (pluvial flooding)
- Secondary hazard mechanisms (e.g., bank erosion, landslide-generated waves, ice jam floods)
- Hazards other than landslides, steep creeks, and floods (e.g., extreme heat and drought, snow avalanches), and landslide runout.

[7] Ministry of Forests is currently preparing draft floodplain mapping guidelines. These were considered as part of the project team's familiarity with interim content of these guidelines, which are unpublished at the time of publication of this document.

[8] Geospatial data delivered July 04, 2024.

BGC's work was based on desktop interpretation of remote-sensed imagery with fieldwork at representative sites. Appendix J lists gaps and limitations. The scope of work reflects current conditions, and changes to landscape, climate, and development may trigger a need for updates.

2.3 Engagement

Facilitated by FBC, BGC engaged with the project advisory committee and each project partner to gather local and traditional knowledge about hazard areas, obtain feedback about study priorities, and provide progress updates. Engagement presentations were distributed to participants following meetings held on the following dates:

Project advisory:

- December 19, 2023 (virtual)
- May 22, 2024 (virtual)
- July 23, 2024 (fieldwork connections)
- November 4, 2024 (virtual)
- January 15, 2025 (Prince George)
- February 6, 7, 2025 (Cambio Training)
- April 3, 2025 (MoF, MOTT Advisory)
- May 21, 2025 (virtual).

Project partners:

- February 22, 2024 (Village of McBride)
- February 28, 2024 (Village of Valemount)
- March 04, 2024 (Lheidli T'Enneh First Nation)
- March 07, 2024 (City of Prince George)
- March 08, 2024 (Mcleod Lake Indian Band)
- March 21, 2024 (District of Mackenzie)
- April 08, 2024 (RDFFG)
- June 07, 2024 (RDFFG)
- February 27, 2025 (RDFFG).

3.0 BACKGROUND

3.1 Project Setting

The RDFFG encompasses 51,000 km^2 in eastern British Columbia (BC) in the traditional territories of the Simpcw, West Moberly, and Lheidli T'enneh First Nations and McLeod Lake Indian Band (Drawing 01). The District includes four municipalities (City of Prince George, District of Mackenzie, Village of McBride, and Village of Valemount) and seven Electoral districts (A, C, D, E, F, G, H). The total census population is approximately 100,000 residents as of 2021 (Statistics Canada, 2021).

Appendix D summarizes the District's physiography, ecoregions, geology, hydroclimate, and projected climate change. This background provides context for the landslide, steep creek, and flood hazard mapping described in Section 4.0, with reference to Appendices E-G.

3.2 Previous Work

The RDFFG provided 61 reports to BGC as background materials for the project, including geotechnical and hydrotechnical site assessments, landslide, steep creek, flood, and snow avalanche hazard assessments, and terrain surveys. Appendix B lists the key studies BGC reviewed to inform the current project, with a focus on the following previous work:

- A geotechnical hazard assessment for Goslin and L'Heureux Creeks by Piteau Associates (November 1993).
- Robson Valley hazard land study by BGC (January 28, 1999).
- Detailed hazard assessment for Leona Creek (AMEC, August 14, 2012).
- Hydrotechnical report on Swiftcurrent Creek by DWB Consulting Services (February 17, 2017).
- Willox Creek emergency hazard assessment by BGC (October 30, 2020).
- Hydrologic and geomorphic assessment of Dore River by McElhanney (March 11, 2021).

3.3 Historical Hazard Events

Appendix D provides an inventory of about 100 historical hazard events in the RDFFG over the past century, which informed BGC's hazard characterization. Key data sources include the following:

- A text compilation of media reports of flooding, landslide, and avalanche events from 1808 to 2006 (Septer, 2007)
- DriveBC data for mud slides (debris flows) and washouts across the major highways of the study area, compiled by BGC from 2006 to 2022
- Canadian Disaster Database (Public Safety Canada, 2022)
- Preliminary Canadian Landslide Database (Brideau et al., 2025)
- BC MOTT event database for the area (G. Hunter, personnel communication July 2024).
- Geotechnical and hydrotechnical reports, where available
- Available academic sources.

Events were cataloged at a single location or landmark within a larger affected area. For example, a debris flow event in a single creek is referenced to the creek at the fan, and a geohazard event that affected a large geographical extent, such as riverine flooding, is related to a landmark in the affected area.

Data bias is inherent in historical accounts of past events due to gaps in recorded storms or geohazard events, because media reports tend to generalize effects of region-wide events (e.g., region-wide floods) rather than smaller and more localized impacts. The historical event inventory is not exhaustive, but the information contained within it can be used to identify the location of past geohazards events and associated consequences. These locations were referenced during geohazard identification (Section 4.0). Recorded events at steep creek fans are listed under the “Comments” field under “geohazard information” for a given site on *Cambio*.

3.4 Climate and Climate Change

Over the next decades, air temperatures in the RDFFG are projected to warm, resulting in more precipitation falling as rainfall instead of snow during the fall and spring, and less total rainfall during the summer months – suggesting that climatic conditions in the RDFFG will be wetter in the winter and drier in the summer by the end of century.

Appendix D summarizes RDFFG’s current climate setting and describes projected changes. Appendix E to Appendix G describe climate change effects on floods, steep creeks, and landslides. In summary, projected changes to climate have implications for the frequency, intensity, and seasonality of floods, steep creek hazards, and landslides. Methods for assessing climate change effects differ between hazard types and decision-making requirements. Given that site-specific effects require detailed information beyond the scale of this assessment, BGC qualitatively described the regional-scale factors that influence the sensitivity of steep creeks and landslides to climate change.

Compared to steep creeks and landslides, more information is available to estimate the effects of climate change on streamflow. As part of Tier 2 flood hazard mapping at five selected areas (Section 4.2.3), BGC analysed historic trends and projected future changes to develop 200-year (0.5% annual exceedance probability [AEP]) flood hazard scenarios adjusted to account for projected climate change[9]. Appendices E to G summarize climate change implications specific to each of the assessed hazard types.

[9] BGC applied a scaling factor to the estimated 200-year (0.5% AEP) flood based on climate projections from six Global Circulation Models (GCMs) and two emissions scenarios, RCP 4.5 and 8.5). See Appendix E for details.

4.0 HAZARD ASSESSMENT

4.1 Introduction

This section summarizes flood, steep creek and landslide hazard mapping completed within the RDFFG and used to characterize hazard exposure (Section 5.0). Appendices E-G provide a more detailed description of methods BGC used to assess each hazard type.

4.2 Floods

4.2.1 Background

Floods are defined as riverine flooding resulting from inundation due to an excess of clearwater discharge in a watercourse or body of water, submerging land outside the natural or artificial banks that is not normally under water. Historical flood events that have occurred within the RDFFG include riverine flooding from rainfall, snowmelt, ice-jams, and glacial runoff processes.

Appendix E describes the approaches used to characterize flood hazards at both a screening-level (Tier 1) and base (Tier 2) level of detail for select hazard areas (Section 4.2.3).

4.2.2 Floodplain Identification (Tier 1)

BGC adapted a province-wide Tier 1 floodplain layer as the basis for flood hazard exposure analysis. The Tier 1 layer provides approximate 200-year flood extents (0.5% annual exceedance probability, AEP) for all watercourses with catchments (watersheds) larger than 10 km^2 (Drawing 02). In areas where BGC completed more detailed (Tier 2) flood mapping, BGC adjusted the Tier 1 floodplain extents to correspond to the more detailed mapping. The floodplain layer represents the approximate 200-year flood extent. Locations within these extents may be subject to more frequent flooding, and the potential for larger floods to exceed mapped extents cannot be ruled out.

4.2.3 Flood Hazard Mapping (Tier 2)

Base-level or Tier 2 flood hazard mapping involves conducting hydraulic modelling and mapping using available lidar data as an improvement of screening-level mapping (Tier 1) and as a precursor to detailed mapping (Tier 3). Table 4-1 lists the five areas selected for Tier 2 flood hazard mapping based on review of available data and feedback from project partners. Drawing 03 shows the specific locations.

At the five selected locations, Tier 2 floodplain mapping provides 200-year (0.5% AEP) flood characteristics (extents, depth, velocity) under current conditions and with projected climate change. The mapping is intended to support planning decisions (e.g. for more detailed mapping), and to support emergency response plans for flood scenarios, but is not intended for regulatory use (e.g., Flood Construction Levels, FCL). While simplified, Tier 2 flood hazard maps are developed using similar methods to regulatory floodplain mapping (Tier 3) and can be refined in future.

Table 4-1 **Tier 2 floodplain mapping areas by Electoral Area.**

Watercourse (Electoral Area)	Watercourse Length of Mapping (km)
Tabor Creek at Prince George (D)	22
Fraser River at McBride (H)	58
Fraser River at Tete Jaune Cache (H)	36
Naver and Hixon Creeks at Hixon (E)	28
McLennan River and Swift Creek at Valemount (H)	36
Total	**180**

4.3 Steep Creeks

4.3.1 Background

A steep creek watershed consists of hillslopes, small feeder channels, a principal channel, and an alluvial fan composed of deposited sediments at the lower end of the watershed.

Steep creeks (here-in defined as having channel gradients steeper than 3°, or 5%) are subject to natural hazards involving a mixture of water and debris or sediment. These hazards typically occur on creeks and steep rivers with small watersheds (usually less than 100 km^2) in mountainous terrain, usually after intense or long rainfall events, sometimes aided by snowmelt and often worsened by previous forest fires. It is easiest to think about steep creek hazards as occurring in a continuum, as shown in Figure 4-1.

While steep creeks can produce clear-water floods, their most damaging processes are typically debris floods or debris flows. Debris floods occur when large volumes of water in a creek or river entrain (i.e., pick up) the gravel, cobbles and boulders on the channel bed. Debris flows involve higher sediment concentrations than debris floods. A common analogy for debris flow behaviour is wet concrete flowing down a steep channel.

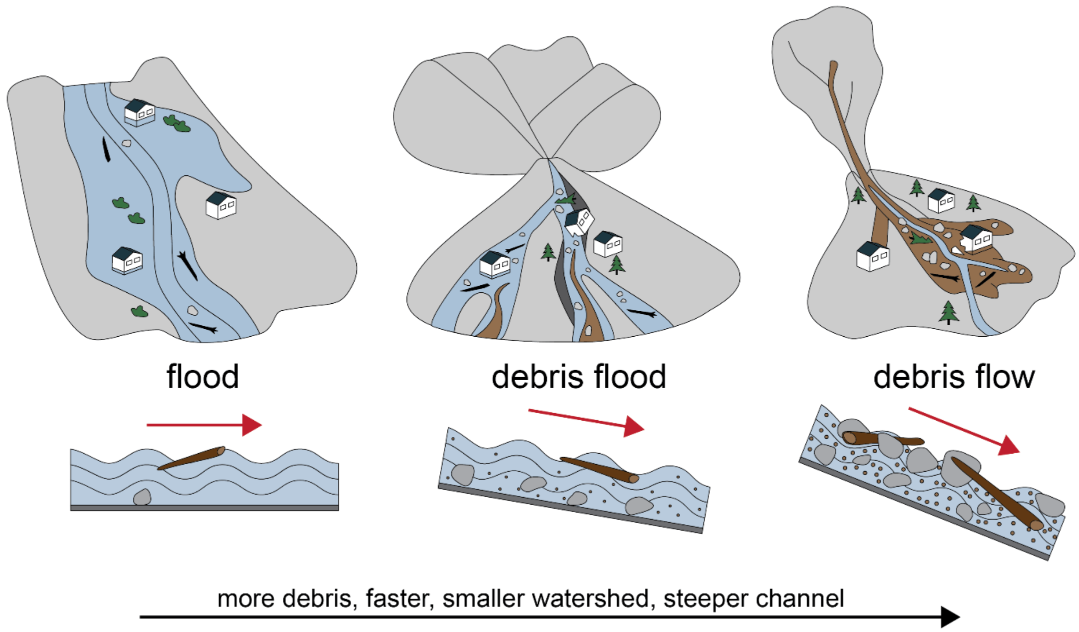

Figure 4-1 Main types of steep creek hazards.

4.3.2 Alluvial Fan Mapping

Alluvial fans form at the outlet of steep creeks when channels become less confined. Figure 4-2 shows an example of an alluvial fan landform visible with lidar topography.

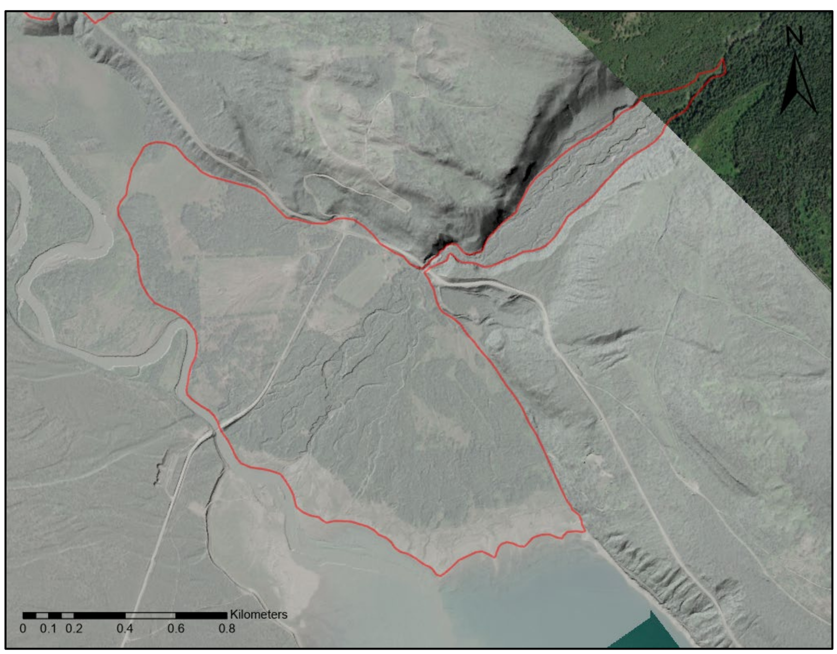

Figure 4-2 Example alluvial fan boundary, Packsaddle Creek, north end of Kinbasket Lake. Esri imagery overlain by lidar hillshade (Government of BC, 2016).

Appendix F describes steep creek hazard assessment methods. In summary, BGC used images, lidar, fieldwork, modelling tools and existing work to support the identification and characterization of alluvial fan landforms. BGC assessed watersheds upstream of each mapped fan to identify and characterize geohazard processes, but did not map the watersheds themselves. Figure 4-3 provides an example of hazard attributes assigned to Willox Creek fan, north of the Village of McBride.

Field	Example
Site Name	999215 - Willox Creek
Site Id	999215
Stream Name	Willox Creek
Steep Creek Dominant Process Type	Debris Flow
Mixed Process Types	-
Process Type Validation	Field
Fan Delineation Data	Lidar
Basin Sediment Supply	Supply Limited
Basin Activity Rating	Moderate
Fan Activity Rating	Moderate
Recorded Historical Event	Yes
Recorded Avulsion Event	Sat, Jul 4, 2020 3:13 AM
Recorded Event Type	Debris Flow
Recorded Event Date	Sat, Jul 4, 2020 3:13 AM

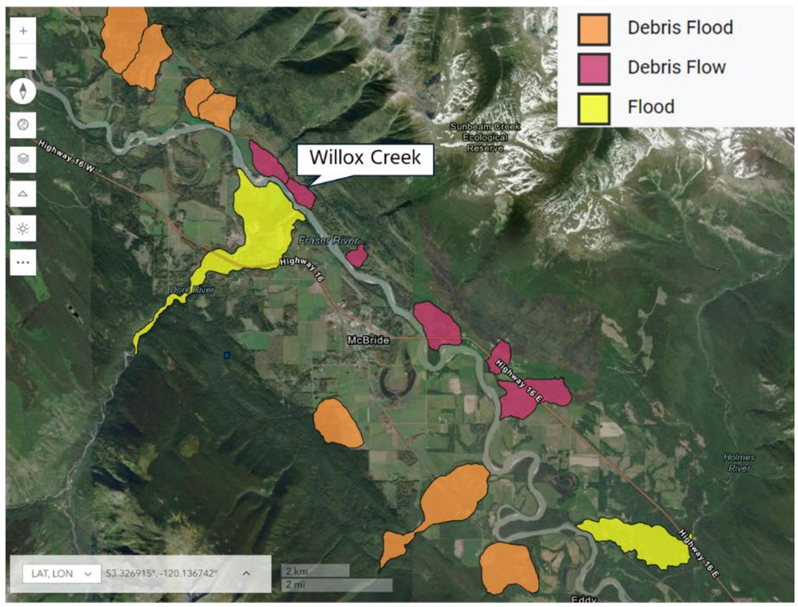

Figure 4-3 Example of steep creek hazard attributes defined for Willox Creek alluvial fan, north of the Village of McBride.

The results of steep creek hazard (alluvial fan) mapping formed the basis for hazard exposure assessment and are intended to support a range of use-cases. For land use regulation, alluvial fan boundaries can help define development permit areas (DPA) where further assessment may be required as a condition of development or building permits. Combined with hazard exposure, the inventory can support planning decisions (e.g., prioritizing areas for detailed mapping), hazard awareness building (e.g., community engagement), and emergency response planning (e.g., identifying access/egress routes during an emergency). At the level of detail of this study, the steep creek hazard mapping is not intended to indicate site-specific (e.g., asset-specific) hazard levels that will differ within a fan boundary.

4.4 Landslides

4.4.1 Background

A landslide is the movement of rock, earth, or debris down a slope (Hungr et al., 2014). Landslides range in size from rock fragments to hillslopes, in frequency from daily to millennia, and in speed from imperceptible to hundreds of kilometers per hour. Landslides can be further described based on the type of movement (e.g., Figure 4-4), the shape of the failure surface (i.e., rotational, planar), and how rapidly the material moves downslope (i.e., extremely slow to extremely rapid) (Table 4-2).

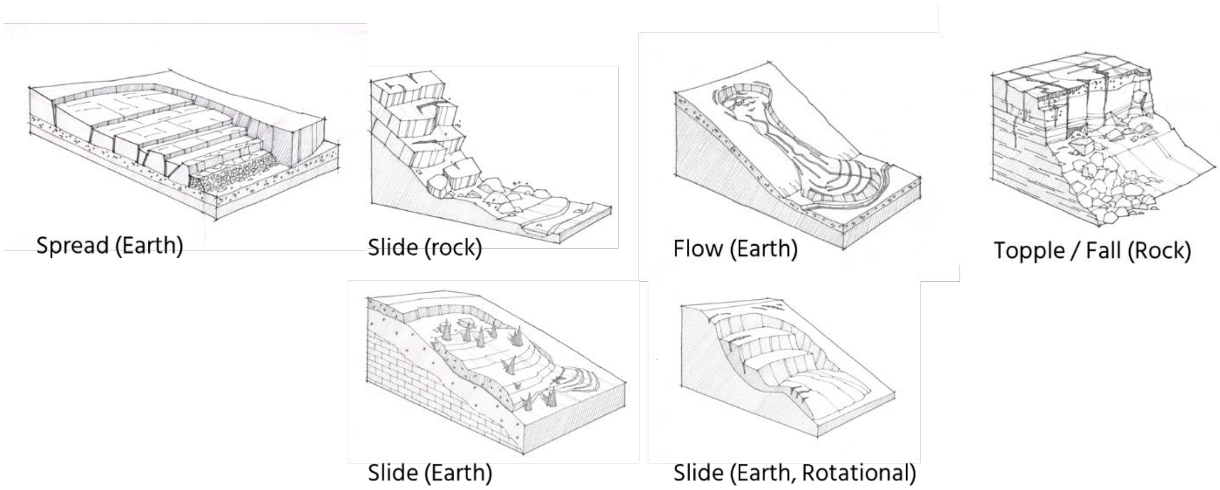

Figure 4-4 Schematic examples (not exhaustive) of landslide movement types, adapted from Hungr et al. (2014).

Table 4-2 Movement velocity categories (Hungr et al., 2014).

Description	Velocity (mm/s)	Typical Velocity
Extremely Rapid	$> 5 \times 10^{3}$	5 m/s
Very Rapid	$> 5 \times 10^{1}$	3 m/min
Rapid	$> 5 \times 10^{-1}$	1.8 m/hr
Moderate	$> 5 \times 10^{-3}$	13 m/month
Slow	$> 5 \times 10^{-5}$	1.6 m/year
Very Slow	$> 5 \times 10^{-7}$	16 mm/year
Extremely Slow	-	-

Sections 4.4.2 to 4.4.5 summarizes the step-wise approach BGC used to identify landslide hazard areas of interest at a District-wide scale based on a combination of landslide inventory, steep slope mapping, and landslide susceptibility mapping for deep-seated earth slides.

The results identify areas considered of interest for potential landslide hazard initiation. Assets located in these areas are considered “exposed” to landslide hazard (Section 5.0). The results inform decisions to undertake more detailed hazard assessment and monitoring of specific sites.

Appendix G provides more detailed description of landslide assessment methodology. Appendix J describes gaps and limitations of regional landslide hazard mapping that inform the use of project results. BGC emphasizes that the landslide exposure assessment completed at the regional scale of this project does not consider landslide runout from areas further upslope, or landslide retrogression behind the crest of escarpment slopes.

4.4.2 Landslide Inventory

BGC developed an inventory of landslide locations across the RDFFG based on available terrain data including lidar digital elevation models, imagery (satellite and airphotos), analysis of Interferometric Synthetic Aperture Radar (InSAR) data provided by TRE[10], and field checking of representative sites. Each landslide location is represented by a point location. BGC's point mapping convention followed the Preliminary Canadian Landslide Database (Brideau et al., 2025) with landslide locations placed at the approximate initiation location. BGC assigned landslide type, material (surficial, rock, anthropogenic) type, point location type (headscarp vs. deposit), and qualitative location confidence (low, moderate, high).

BGC notes that the landslide point inventory is not exhaustive. It does not imply a current level of activity or show extents of affected areas. However, the inventory identifies locations where known landslides exist and supports understanding of conditions at these locations (e.g., slope, geology). Appendix J tabulates limitations associated with landslide inventory mapping, implications, and opportunities to resolve.

4.4.3 Steep Slopes

BGC defined "steep" slopes within the RDFFG as those with a slope angle greater than 30% and a relief greater than 10 m vertical over 90 m horizontal. Jurisdictions across British Columbia commonly apply a slope gradient threshold (typically ranging from 20% to 30%[11]) to determine slope hazard development permit areas where a geotechnical assessment may be required as a condition of development approval.

BGC generated slope maps using a 'medium resolution digital elevation model" (MRDEM) (NRCAN, 2025), which is a raster with 30 m pixel size available District-wide. The map covers 19,000 km^2 (36%) of the RDFFG. Slopes exceeding 30% gradient and 10 m relief were assumed to have credible potential for landslide initiation and were included in the hazard exposure assessment.

BGC then compared the steep slope map with the landslide inventory to assess limitations of a steep slope map to capture the inventoried landslides. The results inform whether a steep slope map, on its own, is sufficient for the determination of hazard exposure to support decision

[10] Comparison of InSAR datasets dated April 4, 2015 to September 11, 2021.

[11] For example, City of Prince George uses a 20% threshold, and jurisdictions within the Thompson-Nicola Regional District and Columbia Shuswap Regional District commonly apply thresholds from 20-30%. Others do not specify a slope gradient and rely on case-by-case geotechnical review.

making, or if further work is needed to define landslide hazard areas of interest for slopes gentler than 30%. BGC determined the following:

- Of the 1,232 mapped landslide points, 825 (66%) occur on slopes gentler than 30%.
- The inventory includes 727 (roughly 60%) landslide points classified as soil slides, of which 632 (87%) occur on slopes gentler than 30%.

These results indicate that while steep slope maps can reasonably capture some landslide types (e.g. rockfall and rock slides), additional work is needed to define credible potential for landslides on slopes gentler than 30%. Such gentle terrain is also the area typically favoured for development. Appendix J tabulates additional limitations, including limitations related to the available resolution of topographic data, to identify steep slopes across the RDFFG.

4.4.4 Deep-seated Earth Slide Susceptibility

While using a gentler slope gradient threshold (e.g., choosing a 20% threshold) could capture more landslide-prone terrain, it also captures larger areas of stable terrain. To overcome the limitations of using slope criteria alone, BGC developed a landslide susceptibility map specifically calibrated to identify deep-seated earth slides (DSEs)[12] in glacial soils. This susceptibility map spans a large portion of British Columbia and is designed to include regions where DSEs are possible, while excluding areas where such landslides are unlikely (e.g., the Rocky Mountains).

Appendix G describes a multi-step process to generate the landslide susceptibility map covering a large portion of BC, including the RDFFG. The work was developed under BGC's research and development (R&D) program and shared within the RDFFG for this current project. The statistically-based analysis integrates a range of factors related to topography, geology, stream networks, and land cover. The results show the spatial probability an earth landslide is present in a location (Table 4-3). The estimate does not imply a hazard level (e.g., does not indicate a probability or magnitude of failure).

Table 4-3 Landslide susceptibility classes.

Class	Approximate Spatial Probability	Proportion of AOI
Low	< 1 %	86.3%
Moderate	1 - 10 %	9.2%
High	10 - 75%	3.2%
Very High	>75 %	1.3%

[12] The landslide inventory outlined in Section G-3 does not include classification of soil slides into earth slides and other processes such as debris slides. In the evaluation of the steep slope map (Section G-4), susceptibility model (Section G-5), and landslide AOI map (Section G-6), the term deep-seated earth slide (DSE) refers to all landslide points classified as soil slides.

4.4.5 Landslide Areas of Interest

Regulatory decision making requires the definition of areas where site-specific assessments may be warranted (e.g., required under bylaw where existing) to check for slope instability. Because the potential for landslides at any susceptibility cannot be entirely ruled out, the choice requires a tolerance for uncertainty. The objective is to capture as much unstable terrain as possible without encompassing too much stable terrain.

Within the RDFFG, a 1% (Low) landslide susceptibility threshold (Table 4-3) captures 364 of 632 soil slides identified on slopes gentler than 30% (e.g., the slides missed by steep slope criteria), while adding 2,450 km^2 (10%) of area. A more conservative threshold substantially increases the coverage area, and a less conservative threshold captures less landslides without substantially reducing the coverage area. BGC selected 1% as a reasonable threshold to identify areas of interest for further landslide assessment, given uncertainties and the information available. However, this threshold warrants further discussion (and potentially further model refinement) to inform adoption in regulation (e.g., slope DPAs).

Based on the results of the landslide inventory, steep slope mapping, and earth slide susceptibility mapping, BGC defined “Landslide Hazard Areas of Interest” (AOI) that meet one or more of the following criteria:

- Slope angle greater than 30% with a relief greater than 10 m vertical over 90 m horizontal
- Spatial probability of earth landslide presence greater than 1%
- Presence of an inventoried landslide.

The resulting Landslide Hazard AOI map covers approximately 24,000 km^2 (46 %) of the RDFFG and includes:

- 1,232 mapped landslide points (Section G-3)
- 19,000 km^2 of mapped steep slopes (Section G-4)
- 4,000 km^2 where spatial probability of a DSE is greater than 1 % (Section G-5)
- 1,500 km^2 where steep slope map and susceptibility criteria overlap.

While the Landslide Hazard AOI encompasses a relatively large proportion of the District, BGC notes that about 75% of the AOI is public (provincial) land. Assets within the Landslide Hazard AOI map are assumed as potentially exposed to landslide hazard, and results may inform decisions to undertake site-specific assessments in these areas (e.g. to inform a development decision). Landslide AOIs do not indicate hazard level, and the potential for landslides to occur outside AOIs cannot be entirely ruled out.

5.0 EXPOSURE ASSESSMENT

BGC analysed the mapped locations of people and assets in relation to hazard areas (Section 4.0). Where intersecting, people or assets are considered "exposed" to hazard (Figure 5-1). Being exposed to hazard does not imply a level of risk, which differs within hazard areas and between assets with different vulnerabilities. However, hazard exposure forms a basis to determine priorities and complete future steps of risk management.

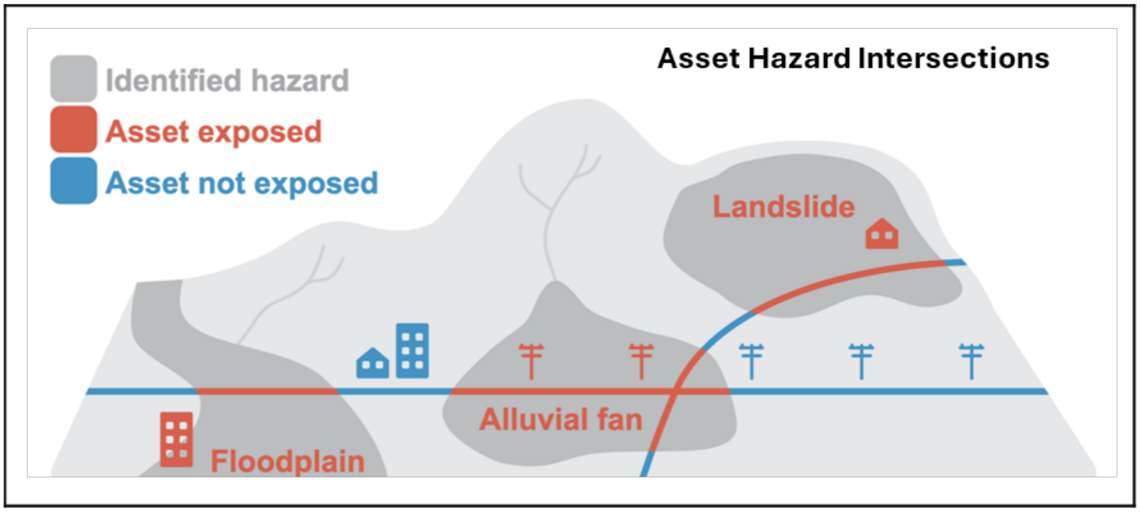

Figure 5-1 Simplified schematic of the hazard exposure analysis logic where exposure is defined as the spatial overlap between a mapped hazard area and a valued asset.

Table 5-1 shows the types of valued assets included in the assessment. Across the RDFFG, these include about 100,000 people, $17 Billion in buildings[13], 58,000 km of roads, 1,400 km of railways, and 11,000 km of linear utilities. Appendix I lists asset data sources and associated metadata. Appendix J provides a breakdown of identified data gaps for each asset group.

Appendix H describes the exposure analysis logic and workflow, and Figure 5-2 illustrates the analysis approach using parcel improvements exposed to flood hazard. The figure shows exposure in two ways that serve different use-cases:

1. Asset Hazard Intersections (Figure 5-2a) illustrates the intersection of assets with mapped hazard extents. This intersection addresses the question, "is the asset in the hazard area?", to inform a decision about individual locations.
2. Exposure Density (Figure 5-2b) shows hazard exposure within 100 m by 100 m (1 ha) grids. In this example, total exposure shows the assessed value of exposed parcel improvements per hectare. The grid addresses the question, "which areas have more concentrated hazard exposure?", to inform regional planning decisions.

[13] Estimated total value of parcel improvements in the RDFFG (BC Assessment, 2023), plus total estimated value of buildings located on First Nations reserves (NRCAN, 2022b)

Table 5-1 Asset data schema.

Asset Group			Name	Source
People			Population - Totals	Canadian Census (2021)
			Population – Demographic Breakdown (Census Statistics)	NRCAN (2022a)
Built Form	Parcel (With Improvements)		Parcel Improvement Values ($)	BC Assessment (Oct. 2023)
			Critical Facility	
	Buildings (First Nations Reserves)		Buildings (NRCAN replacement value)	NRCAN (2022b)
	Business		Businesses	Geografx
Cultural Values			Archeologic Site (density, count/ha)	Province of BC (2025)
Transportation	Roads	MOTT Roads	MOTT Roads - Exposure	BC Digital Road atlas; MOTT Road Network (2024)
		MOF Roads	MoF Roads - Exposure	
		Other Roads	Other Roads - Exposure	
	Railways		Railways - Exposure	ICI Society (2023)
Utilities	Petroleum Infrastructure		Petroleum (linear) - Exposure	
			Petroleum (points) - Exposure	
	Electrical Infrastructure		Electrical (linear) - Exposure	
			Electrical (points) - Exposure	
	Water Infrastructure		Water (linear) - Exposure	
			Water (points) - Exposure	
	Communication Infrastructure		Communication (linear) - Exposure	
			Communication (points) - Exposure	

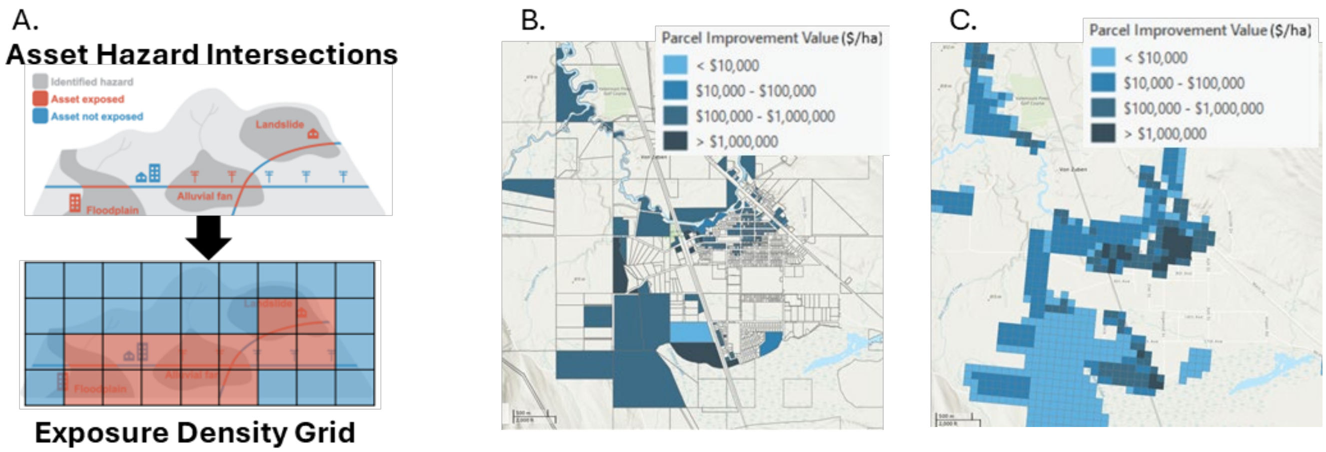

Figure 5-2 Schematic overview of the hazard exposure analysis workflow and results showing the analysis workflow (left), and outputs, which include hazard asset intersections (middle), and exposure density grid (right)

6.0 DELIVERABLES

Table 6-1 lists project deliverables, including drawings, tabular summaries of results, and access to digital maps and files.

Table 6-1 List of project deliverables.

Deliverable	Appendix or Dwg.	Description
Drawings	2-8	District-scale maps showing flood, landslide, and steep creek hazard mapping extents. Appended to the report. Intended to display the extent of areas mapped.
Exposure Results Tables	I	Total lengths, values, or counts of valued assets in hazard areas. Provided as separate file (Excel format) with tabs for each project partner. Intended as the primary tabular source of population and asset hazard exposure totals for each project partner.
Cambio™ Cloud Platform	-	Secure online access to hazard, asset, and exposure mapping for registered project partner users[14]. Intended for day-to-day operational access to hazard and exposure maps, baseline data, and geospatial tools. Provides understanding of hazards and hazard exposure to inform emergency planning, risk management resource allocation, and land use decisions. Platform to add additional instrumentation, inspection, and monitoring tools if required in future, complete updates, and add more detailed assessments when they become available.
Geospatial Data	L	ESRI geodatabase of spatial data layer deliverables. Intended to provide all spatial analysis outputs (hazard and exposure maps) in a format for GIS professionals. Provided as separate files. Appendix K provides metadata.
Project Fact Sheets	M	Two-page summaries of project objective and hazard exposure assessment results for each project partner. Intended to support engagement with staff, authorities, and the public.

[14] Cambio license is currently held by RDFFG with FBC project partners as authorized individual users, under terms outlined in a December 18, 2024 licensing agreement. The current license extends to December 31, 2025. The second project phase includes Cambio access through December 31, 2026.

Figure 6-1 shows hazard extents within each project partner jurisdiction; the same extents are shown at District-wide scale on Drawings 02 to 08. At the scale shown, hazards shown on static maps are intended to be illustrative (not for decision making).

Cambio (Figure 6-3) provides the secure way for project partners to interact with all hazard and exposure mapping results for day-to-day operations[15]. The fact sheets (Appendix M) provide the quickest way to access a snapshot of results for each project partner location (2-page summaries).

In summary, BGC characterized 271 alluvial fans and 1,232 landslide locations in the vicinity of settled areas across the District. BGC identified 2,770 km^2 of floodplains on all watercourses with catchments larger than 10 km^2 and completed Tier 2 floodplain mapping for 180 km of watercourses in the vicinity of Tabor Creek at Prince George, Fraser River at McBride, Fraser River at Tete Jaune Cache, Naver and Hixon Creeks at Hixon, and McLennan River and Swift Creek at Valemount (Drawing 03). The more detailed Tier 2 maps show estimated 200-year (0.5% AEP) flood hazard extents, velocities and depths under current conditions and with projected climate change (Section 3.4).

BGC identified 24,000 km^2 within the District where the presence of a mapped steep (>30%) slope, greater than 1% estimated susceptibility to deep-seated earth slides, or the presence of an inventoried landslide, indicate areas of interest for potential landslide hazard (Drawing 08).

Figure 6-2 summarizes the total population and number of asset types exposed to flood, steep creek, and landslide hazards across the entire RDFFG. Appendix M provides similar summaries for each project on fact sheets and is the easiest way to view simplified results at a glance. Appendix I provides detailed totals for all assets, for each partner jurisdiction, and Cambio provides all exposure results in map view, by hazard type.

Table 6-2 defines the precision of hazard exposure statistics reported in totals (Appendix I). Given uncertainties in the analysis of such a large dataset, totals should not be reported at a greater level of precision than shown in Table 6-2[16].

[15] A user guide to navigate tools available through the platform can be found **here**.

[16] Note that geospatial data deliverables are unrounded but are intended to be reported at a level of precision no higher than noted in Table 6-2.

Table 6-2 Rounding applied to asset exposure totals.

Value	Rounded to Nearest
100B+	10B
10B	1B
1B	100M
100M	10M
10M	1M
1M	100k
100k	10k
10k	1k
1k	100
100	10
10	1
1	1

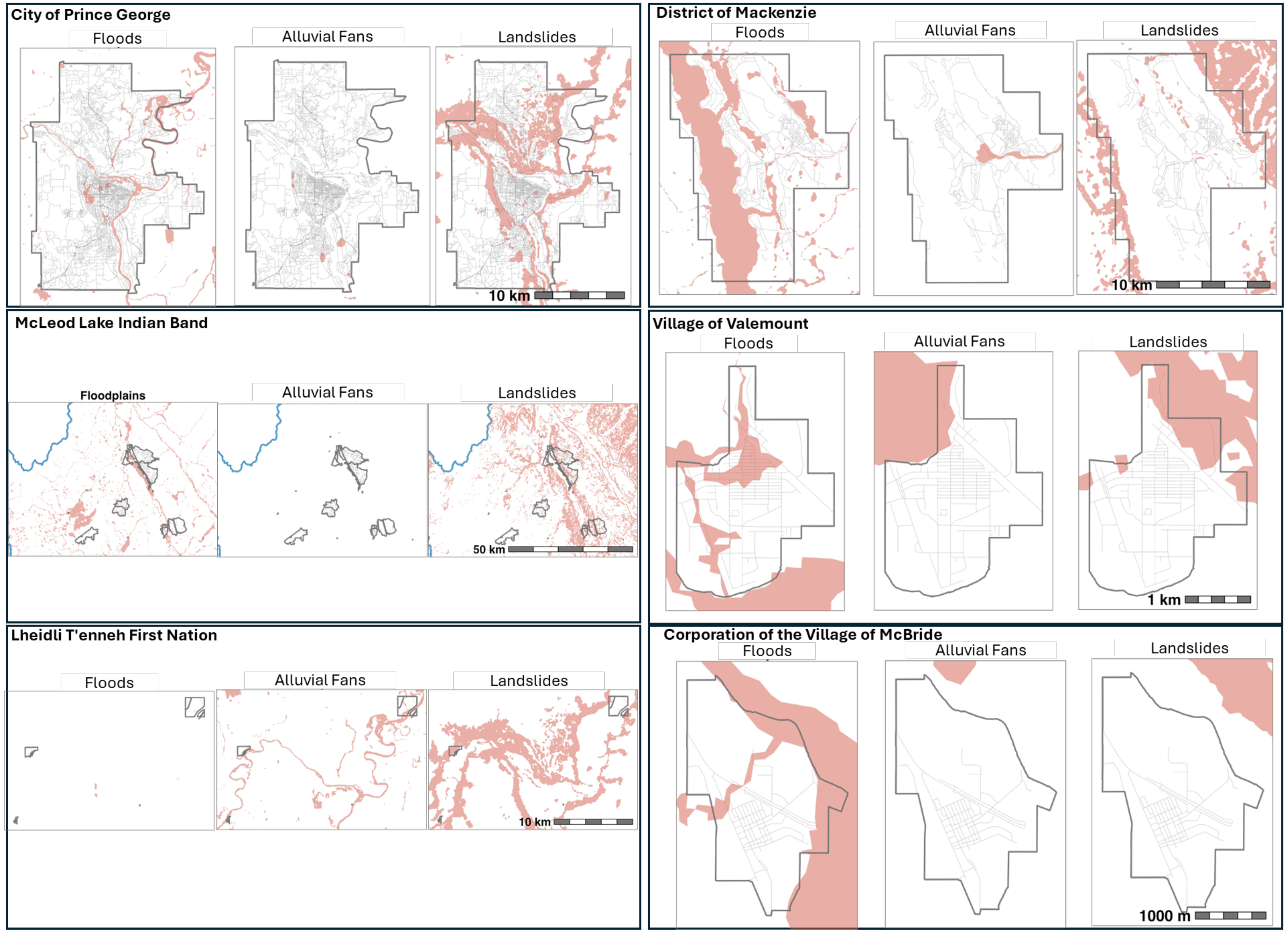
City of Prince George
Floods
Alluvial Fans
Landslides
10 km
District of Mackenzie
Floods
Alluvial Fans
Landslides
10 km
McLeod Lake Indian Band
Floodplains
Alluvial Fans
Landslides
50 km
Village of Valemount
Floods
Alluvial Fans
Landslides
1 km
Lheidli T'enneh First Nation
Floods
Alluvial Fans
Landslides
10 km
Corporation of the Village of McBride
Floods
Alluvial Fans
Landslides
1000 m

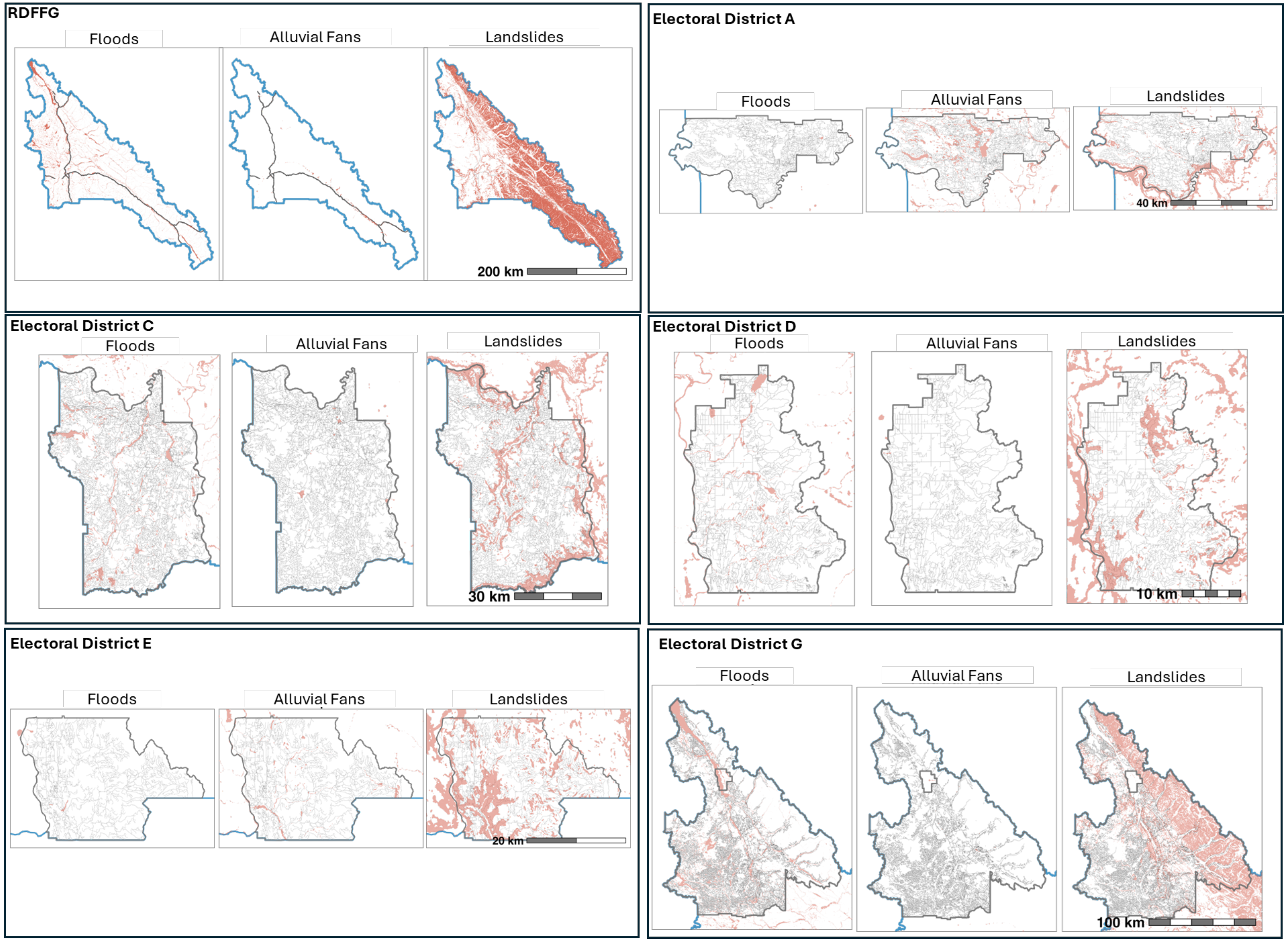
RDFFG
Floods
Alluvial Fans
Landslides
200 km
Electoral District A
Floods
Alluvial Fans
Landslides
40 km
Electoral District C
Floods
Alluvial Fans
Landslides
30 km
Electoral District D
Floods
Alluvial Fans
Landslides
10 km
Electoral District E
Floods
Alluvial Fans
Landslides
20 km
Electoral District G
Floods
Alluvial Fans
Landslides
100 km

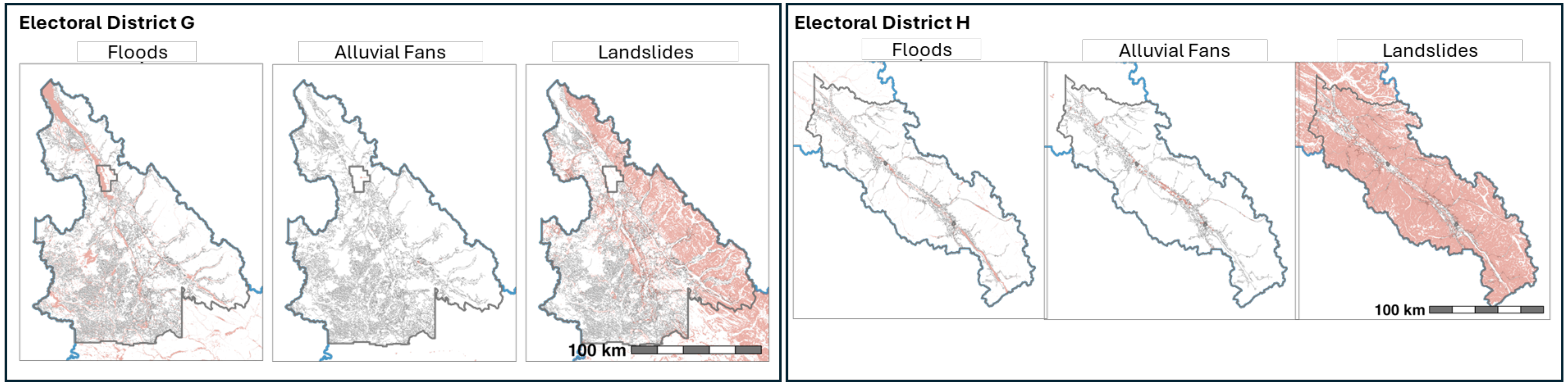

Figure 6-1 **Visual summary of hazard extents for each project partner. Hazard extents are shown in orange; blue outlines show jurisdictional boundaries. Similar extents are shown on project partner fact sheets.**

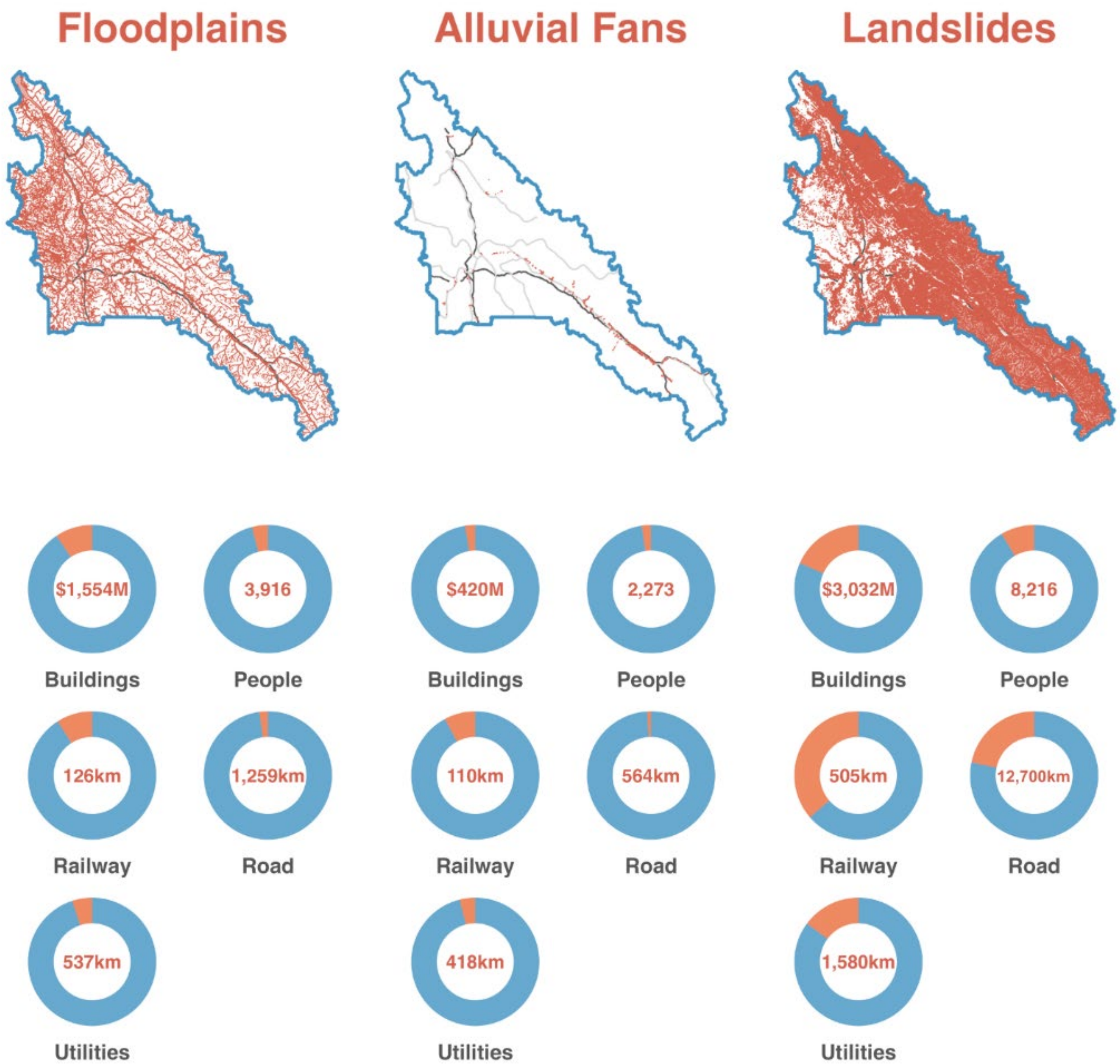

Figure 6-2 Summary of population and assets exposed to flood (floodplains), steep creek (alluvial fans), and landslide hazards for the entire RDFFG. The red areas within the maps represent mapped hazard areas. In the circular graphs, orange represents proportion exposed, blue represents the unexposed area.

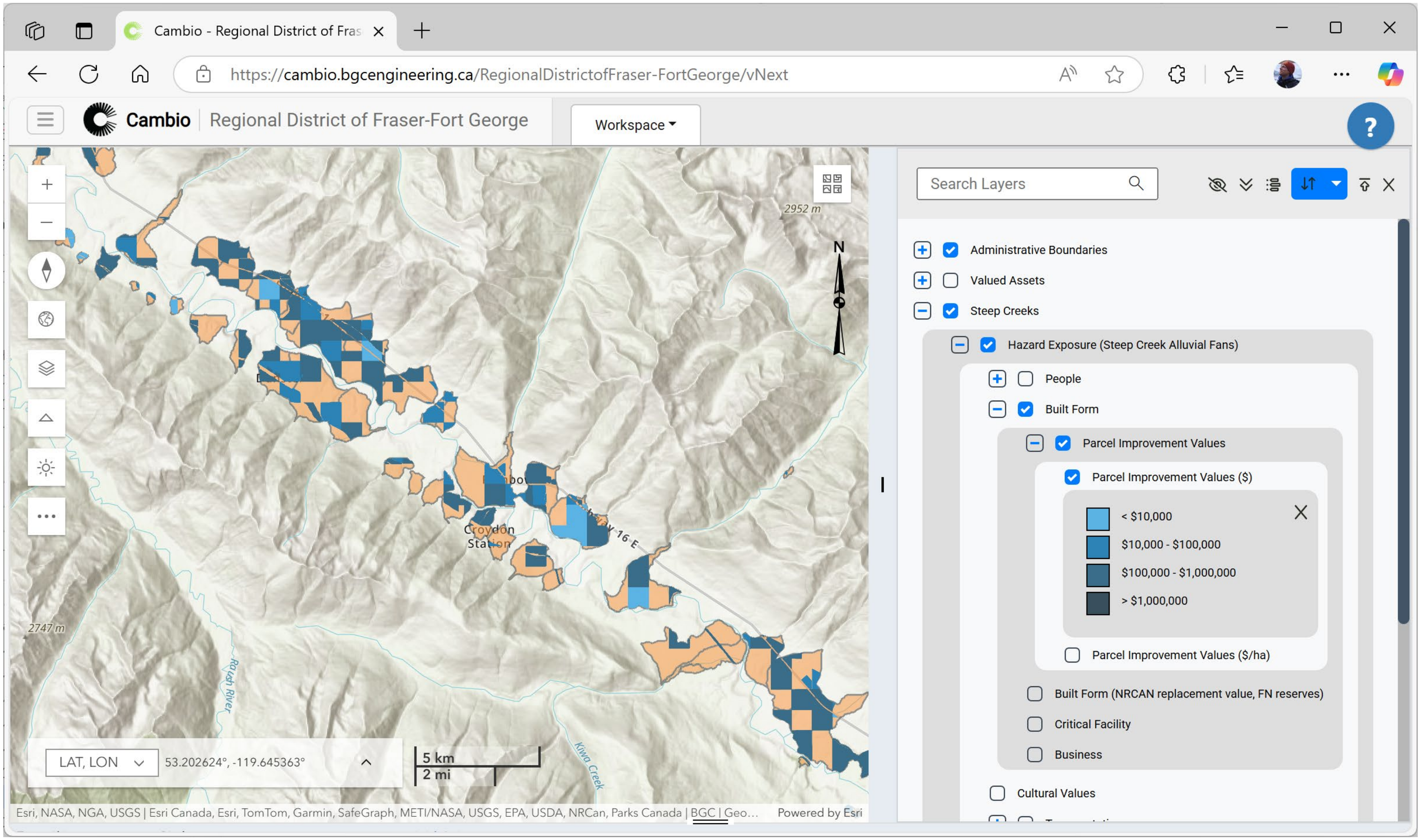

Figure 6-3 Screen capture example of Cambio showing parcel hazard exposure (blue shading) on alluvial fans (tan shading) in the Robson Valley.

7.0 GAPS AND LIMITATIONS

This assessment is based on information about natural systems, people, and the built environment that contain gaps and limitations. These gaps and limitations create uncertainties, and resolving these uncertainties over time will strengthen decision making.

Appendix J lists gaps and limitations of this assessment, identifies implications, and suggests opportunities to resolve. Appendix J does not include a complete list of assumptions, gaps and limitations that may be associated with externally sourced data, which may be accessed through the links or references listed in Appendix H.

BGC emphasizes that while this project identifies assets exposed to mapped hazards, no hazard mapping is ever 100% complete. Assets not identified as "exposed" fall outside the criteria used to indicate exposure but may be exposed in other ways – for example to scenarios larger than mapped or outside the scope of assessment. Because this project represents a snapshot in time, changed conditions for either valued assets or hazard conditions may result in hazard exposure not identified in this study.

BGC also emphasizes that the hazard types considered in this analysis do not have the same probability of occurrence or measure of probability (e.g., 1:200-year flood extent, compared to an alluvial fan formed from multiple events, compared to slope with at least a 1% chance of a landslide landform). As such, comparison of hazard exposure between hazard types should be done with caution.

8.0 RECOMMENDATIONS

8.1 Introduction

Table 8-1 lists recommendations for consideration by project partners, further expanded in Sections 8.2 to 8.4. The recommendations may require review by different groups within each project partner's organization and are intended to inform planning over a multi-year time horizon (e.g., 1 to 10-year planning).

Table 8-1 List of recommendations by type.

Section	Type	Description
8.2	Development and Community Services	• Supplement requirements (bylaws) with tools that support implementation of these requirements. • Collaborate with energy, transportation and utility operators within the RDFFG to leverage shared needs and goals around hazard and risk management. • Use results of the current project to support review and potential updates to policies and bylaws about development in hazardous lands. • Develop a plan for community education about flood, steep creek and landslide hazards, and to build staff capacity for decision making informed by the results of this project. • Engage with Cambio staff for training on the software platform used to provide deliverables.
8.3	Protective Services	• Review weather and hydrologic forecast and monitoring tools available through project deliverables for potential use in emergency preparedness and response. Review existing emergency preparedness plans with the results of this study. • In each of the Tier 2 mapping areas, consider the hydraulic models as a tool to quickly develop flood scenarios from flood forecasts for emergency response support.
8.4	Further Assessments	• Develop a longer-term roadmap to resolve identified gaps and complete more detailed assessments of areas selected by Project Partners as higher priority, based on this assessment and other factors communities may consider (outside the context of this project).

8.2 Development and Community Services

8.2.1 Program Implementation

Recommendation: Supplement requirements (bylaws) with tools that support implementation of these requirements. Develop a roadmap *and funding model for program implementation.*

Section 1.5 described a natural hazard and risk management framework for this project. However, it is important to distinguish project workflows from those of a jurisdiction managing programs, which reflect their own responsibilities and set requirements for work done by others.

While the Province of BC and Government of Canada provide supporting roles, development decisions in municipal or Electoral Areas are the responsibility of local governments[17]. First Nations hold decision making authority in reserve lands with Federal jurisdiction and through rights and title in traditional territories (Government of BC, 2018; Government of Canada, 2021) and the Canadian Constitution (Government of Canada, 1982).

The regulation of development in hazardous lands includes a professional reliance model, where QPs assess if a proposed development is 'safe for the use intended'. Jurisdictions making development decisions in hazardous lands may focus on the following:

- Setting requirements (regulation) that triggers work by third parties (e.g., proponents and QPs).
- Determining if requirements have been met (e.g., via professional reliance and any additional review process set by the authority).

The above roles are required elements of a regulatory process. Implementing the process also depends on QPs being able to deliver the required work at an acceptable standard of care with reasonable liability and budget.

BGC notes two additional needs of QPs that, if fulfilled, may lower both administrative overhead of the regulator and costs to a proponent:

- Providing operational tools that make it efficient for all parties (e.g., authority, proponents, and QPs) to navigate a process to obtain information, conduct assessments, and provide quality assurance.
- Providing the relevant parties with secure access to a geospatial knowledge base with inputs for the required work, and that enables delivery of results to the knowledge base (e.g., a virtuous cycle of improvement).

BGC suggests further discussion of these needs that considers both technical requirements and cost-benefit assessment of funding options. While it is relatively common to provide access to .pdf format reports, geospatial data management is typically the more critical factor affecting levels of effort. Section 8.2.2 provides further considerations for collaboration to build a digital knowledge base and tools.

8.2.2 Collaboration

Recommendation*: Use steps of risk management to clarify how energy, transportation and utility operators within the RDFFG can collaborate to advance shared hazard and risk management goals.*

[17] The Province of BC is responsible for subdivision approvals in Electoral Areas, but approvals are generally tied to local bylaws where existing.

Assets included in hazard exposure analysis are managed by a wide range of private and public parties. While communities require roads and utilities to function, the responsibility for their management largely depends on other parties (e.g., MOTT, Fortis BC, BC Hydro and CN Rail).

Figure 8-1 illustrates a ‘funnel’ of risk management steps, extending from baseline data about natural systems through increasingly site-specific steps of risk management. BGC has observed a higher capacity for resource and information sharing where common needs exist – often closer to the top of the funnel. In the decentralized environment of risk management in BC, collaboration about earlier steps is a high leverage way to support subsequent steps taken by individual parties at specific sites.

Considering collaboration through a risk management lens can also help clarify the limits of centrally managed (government) roles, beyond which a decentralized approach captures the fullest capacity of all parties managing their specific risks. For example, QPs completing site assessments for development approvals on the same alluvial fan require similar watershed inputs (a strong government role) to conduct site-specific work on individual properties (a strong proponent role).

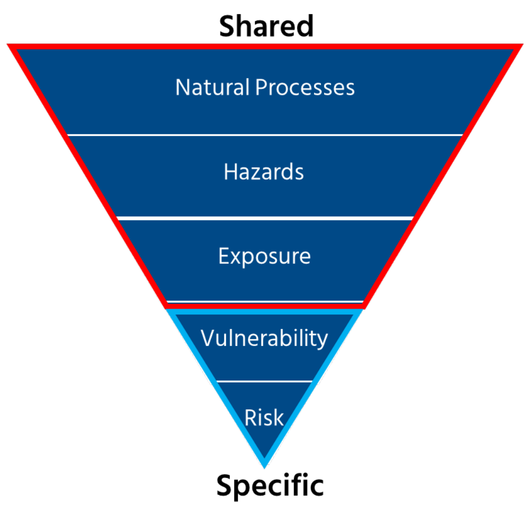

Figure 8-1 Conceptual illustration of risk management steps as a funnel, from a foundation shared by diverse parties (in red) to steps specific to the intended use of parties with different roles and responsibilities (in blue).

8.2.3 Policy and Regulation

Recommendation*: Use results of the current project to support review and potential updates or preparation of decision-making processes (policies and bylaws) about development in hazardous lands.*

Programs for hazard risk management are typically strongest where knowledge about risks is balanced by transparent decision-making tools (bylaws) about development (Figure 8-2). The current work has shifted knowledge further up the quadrants of Figure 8-2.

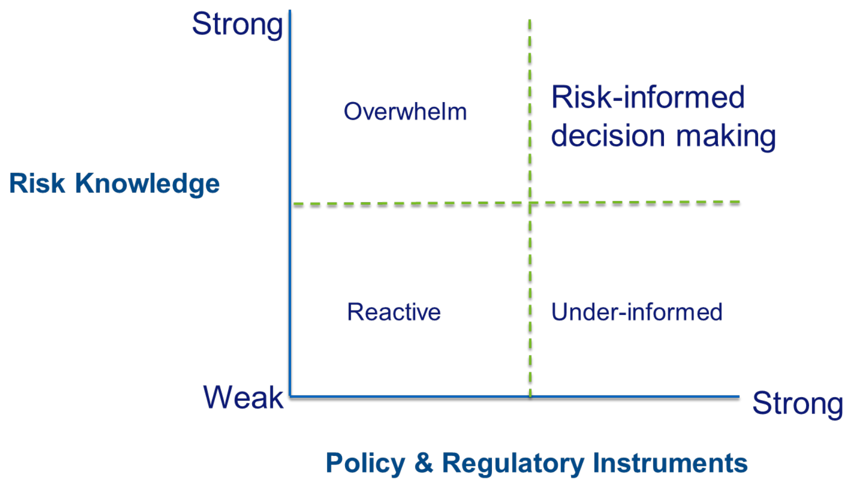

Figure 8-2 Conceptual illustration of a balance between risk knowledge and policy and regulation.

Building on the knowledge base advanced by the current work, Table 8-2 describes activities to support decision making process development (e.g., Official Community Plans and Development Permit Areas). In 2025-2026, the CDRRCA project will initiate a second phase to make progress in these three areas, with a focus on floods, steep creeks, and slopes (landslides). The intended outcome is an informed approach to develop plans and regulation around land use, help build staff capacity to use hazard information in development decisions, and increase community awareness of natural hazards.

Table 8-2 Activities to strengthen decision making processes and tools that will advance as part of a second CDRRCA project phase in 2025-2027.

Area	Activities	Outcomes
Regulatory Review (Geoscience, Planning, Legal)	Regional (project partners) scientific, planning, and legal review of language, policies, and procedures around the use of hazard maps and information in policy and bylaws.	Language basis of policy/bylaw review from perspective of geoscience, planning, and law.
Regulatory Review (Geospatial)	Review of existing mapping for the purpose of bylaw integration and online display (e.g. hazard mapping format and terminology alignment with policy/bylaw wording).	Geospatial (map) basis of policy/bylaw review.
Regulatory Process Recommendations	Policy recommendations related to the hazards in the project areas, with recommendations to resolve remaining gaps and uncertainties.	Recommendations for policy integration, gaps and remaining uncertainties.

8.2.4 Engagement

Recommendations:

- Develop a plan for community education about flood, steep creek and landslide hazards.

- Develop a plan to train staff in the application of results of this project.
- Engage with Cambio staff for training on the software platform used to provide deliverables for day-to-day operational access.
- The technical results of this study support more informed engagement at a community level, at a local scale that considers values distinct to a community.
- In support of these recommendations, the second phase of the CDRRCA project will include a half-day workshop with project partner staff. This workshop will inform subsequent review of regulation and policy review, as well as further public engagement.

For project partner staff accessing project results in Cambio, BGC notes that support is available as part of the licensing agreement. Cambio Earth Systems Inc. staff can arrange for a training session, on request.

8.3 Protective Services

8.3.1 Flood Monitoring

Recommendation*: Review weather and hydrologic forecast and monitoring tools available through project deliverables for potential use in emergency preparedness and response*.

Review existing emergency preparedness plans in light of the results of this study.

Real-time and forecasted precipitation and stream flows inform hazard management and emergency response. The Cambio software platform licensed by RDFFG to deliver the results of this study includes access to the following real-time information:

- Environment and Climate Change Canada (ECCC) maintains the Canadian Precipitation Analysis (CaPA) system, which provides estimates of hindcasted precipitation in 10 km by 10 km (at 60° N) grids across North America. ECCC also provides the Regional Deterministic Prediction System (RDPS) and High Resolution Deterministic Prediction System (HRDPS). These are 84-hour and 48-hour, respectively, forecast data (at hourly timesteps) that is produced four times a day at similar resolution to the CaPA data. The forecast dataset includes many climate variables, including forecasted precipitation.
- Real-time[18] Water Survey of Canada (WSC) streamflow and lake level monitoring data (e.g., Figure 8-3).
- Real-time Snow Data Assimilation System (SNODAS) data (e.g., Figure 8-4).

[18] i.e., information-refresh each time flow monitoring data is updated and provided by third parties.

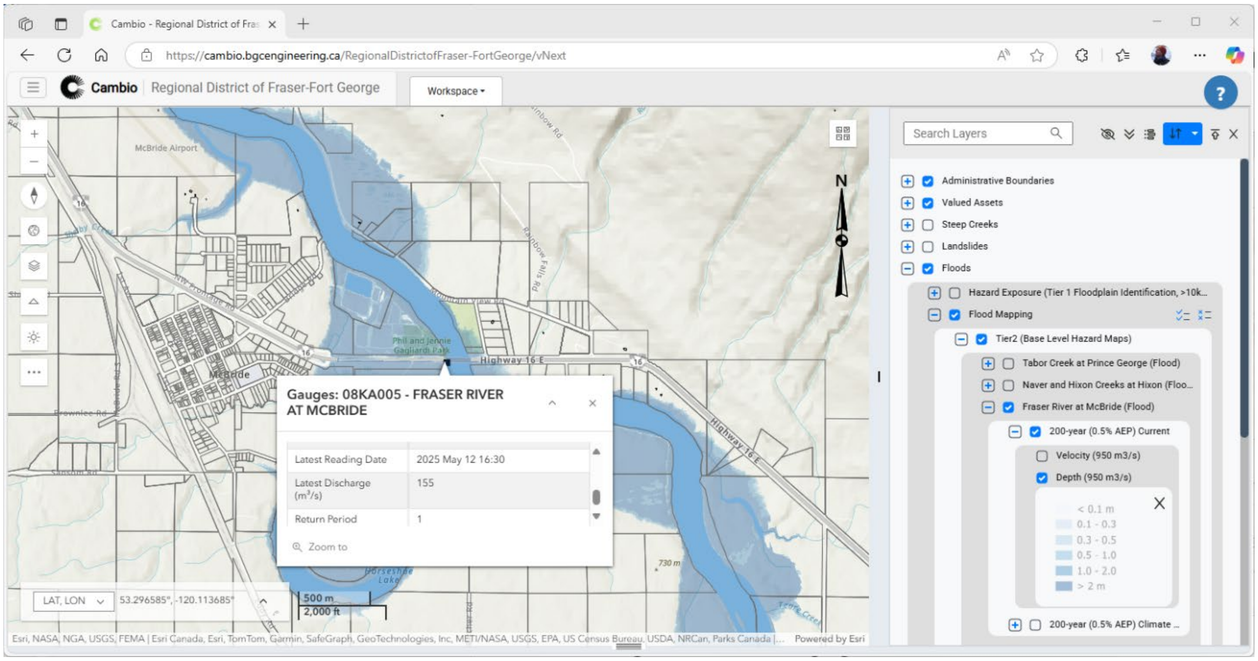

Figure 8-3 WSC near real-time gauging station on the Fraser River at McBride, within the extent of Tier 2 flood hazard mapping.

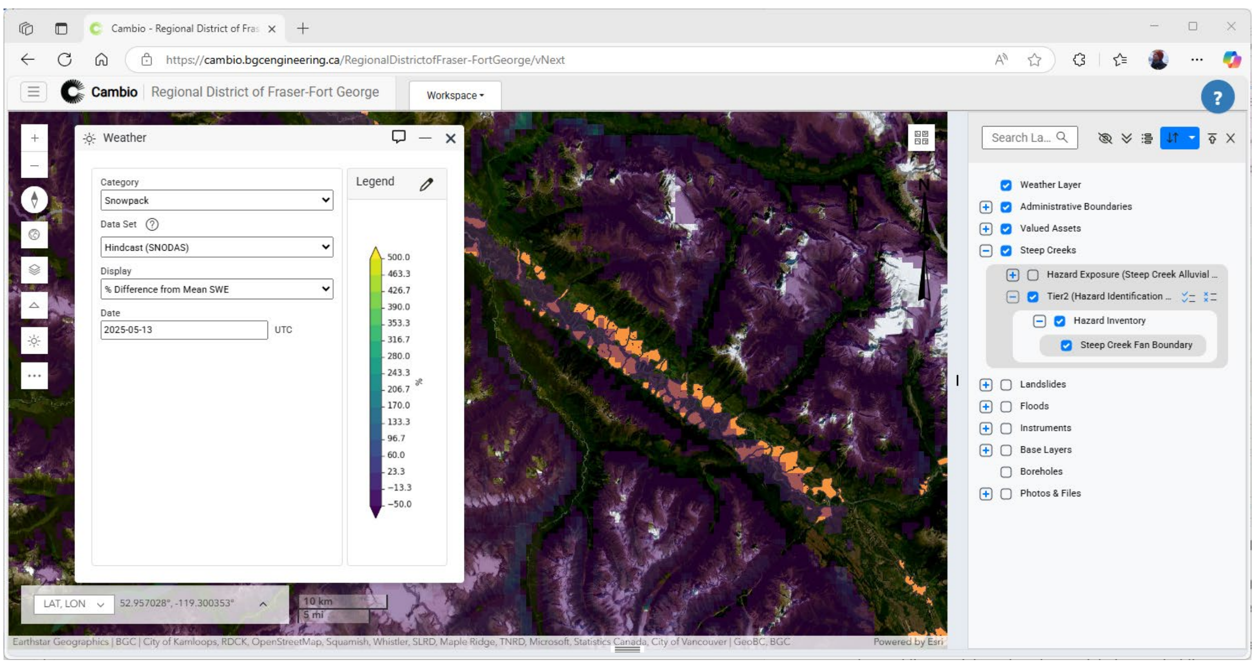

Figure 8-4 Real-time Snow Data Assimilation System (SNODAS) data indicating below-average snowpack in the Robson Valley area, as of May 13, 2025.

At the current level of study, these available monitoring tools are not yet tied to actions (e.g., do not support monitoring or warning for specific hazard thresholds). However, the monitoring tools do qualitatively inform emergency preparedness, such as to check existing flows in a mapped floodplain extent and determine what people and assets are in these areas.

8.3.2 Emergency Flood Modelling

Recommendation: *In each of the Tier 2 mapping areas, consider the hydraulic models as a tool to quickly develop flood scenarios from flood forecasts for emergency response support.*

The BC River Forecast Centre (RFC) provides daily 10-day forecasts of discharges at specific WSC gauges along rivers and creeks across BC, including the areas where BGC developed hydraulic models for flood hazard mapping. Flood forecasts indicate potential flooding but cannot provide any information on where the water is likely to go (extent), its characteristics (depth, velocity) and when (timing).

During a flood emergency, the hydraulic models used to prepare the Tier 2 flood hazard maps can potentially be re-run with forecast data. The results can help EOC directors issue evacuation alerts and orders with improved knowledge about the potential extent and characteristics of flooding.

8.4 Further Assessments

Recommendation: *Develop a longer-term roadmap to resolve identified gaps and complete more detailed assessments of areas selected by project partners as higher priority, based on this assessment and other factors communities may consider (outside the context of this project).*

Appendix J compiles gaps and limitations related to hazard, asset, and analysis workflows, their implications, and considerations to resolve. The following sections highlight select further work recommended in areas subject to flood, steep creek, and landslide hazards.

8.4.1 Floods

This assessment delivered base level (Tier 2) flood hazard maps for five high priority areas within the RDFFG. BGC recommends that these areas be advanced to detailed (Tier 3) mapping as required for use in regulation (bylaws).

Provincial funding for flood hazard mapping is currently available through the provincial Disaster Resilience and Innovation Funding Program (DRIF)[19]. The province is also undertaking detailed flood hazard mapping as part of the Flood Hazard Identification and Mapping Program (FHIMP), including one project on the Nechako and Fraser Rivers. BGC is not aware of any FHIMP projects planned for 2025 in the RDFFG. BGC suggests that FHIMP program administrators be made aware of the current work to avoid duplicating effort in the scoping of future mapping projects.

BGC notes that the detailed FHIMP flood mapping on the Nechako and Fraser Rivers will supersede the floodplain identification mapping completed in this project. The exposure analysis workflows developed by this project are designed for efficient updates once new hazard mapping becomes available. They can also be adapted to incorporate vulnerability criteria (e.g.,

[19] Disaster Resilience and Innovation Funding program - Province of British Columbia.

for flood consequence assessment). On their release, BGC recommends updating the exposure analysis to reflect findings of the FHIMP flood mapping; the results may inform subsequent flood management planning.

8.4.2 Steep Creeks

Most of the watercourses assessed this current study are steep creeks subject to debris floods and debris flows. The Willox Creek debris flow in July 2020, which destroyed one dwelling and impacted several others, is an example of the destructive power of steep creek hazards.

BGC recommends that Project Partners, in association with a Qualified Professional, develop a 10-year roadmap for detailed steep creek hazard mapping (Tier 3). The effort may require multiple cycles of external funding to advance (e.g., Provincial or Federal grants). However, it can greatly strengthen development regulation on alluvial fans and planning to avoid new development in the highest hazard areas.

The “Steep Creeks” tab in Appendix I (Hazard Exposure Results) lists inventoried steep creeks in each project partner jurisdiction with their attributes and hazard exposure totals. Combined with additional factors (e.g., community priorities outside the context of this project), fan hazard and asset attributes can be filtered to inform priorities for further assessment. For example, Table 8-3 lists the eleven steep creek geohazard areas with highest-rated basin activity[20], in descending order based on the assessed value of improvements. Filtering by other assets (e.g., roads or utilities) may yield a different list. BGC suggests that users view the inventory as a screening tool with consideration of their roles and responsibilities (e.g., a user responsible for roads may have different priorities than a user responsible for land development).

BGC notes that steep creeks subject to debris floods and debris flows exist within the RDFFG that were not mapped. For example, steep creeks crossing roads without a developed fan landform were not included in the inventory. BGC recommends project partners engage with the appropriate agency (e.g., MOTT) to further complete the hazard inventory for roads exposed to hazard at steep creek crossings.

[20] See Section 4.3 for a list of steep creek hazard attributes assigned to each fan, and Appendix F for further details.

Table 8-3 Alluvial fans containing at least High-rated basin activity, in descending order of exposed parcel improvement value. Parcel improvement 'rank' is in comparison to values on the 271 inventoried fans.

ID	Jurisdiction	Site Name	Dominant Process	Mixed Process	Relative Basin Activity	Population (Approx)[21]	Total Parcel Improvement Value	
							Value	Rank
999262	Village of Valemount	Swift Creek 2	Flood	Debris Flood/ Clearwater Flood	High	38	$6,400,000	9
999190	Village of Valemount	Swift Creek	Flood	Debris Flood/ Clearwater Flood	High	94	$5,800,000	10
999191	RDFFG Electoral Area H	Swiftcurrent Creek	Flood	Debris Flood/ Clearwater Flood	High	8	$4,200,000	13
999201	RDFFG Electoral Area H	Tete Creek	Flood	Debris Flood/ Clearwater Flood	High	6	$3,500,000	16
999060	RDFFG Electoral Area H	Crystal Creek	Debris Flow	Debris Flow/ Debris Flood	High	14	$2,700,000	20
999187	RDFFG Electoral Area H	Spittal Creek	Debris Flow	Debris Flow/ Debris Flood	High	24	$2,700,000	20
999070	RDFFG Electoral Area H	Wilson Creek	Debris Flow	-	High	8	$2,100,000	27
999134	RDFFG Electoral Area H	Leona Creek	Debris Flow	-	High	14	$1,800,000	33
999113	RDFFG Electoral Area H	Klapperhorn Creek	Debris Flow	-	High	8	$1,000,000	56
999184	RDFFG Electoral Area H	Small Creek	Flood	-	High	6	$420,000	85
999089	RDFFG Electoral Area H	Goslin Creek	Debris Flow	Debris Flow/Debris Flood	Very High	10	$400,000	88

.

[21] See uncertainties noted in Appendix J, for population data. Total shown is the maximum estimate of two sources: Fortin (2024), and NRCAN (2022).

8.4.3 Landslides

Landslide hazard AOIs define areas with landslide initiation potential based on slope and susceptibility criteria or the presence of previous landslides (Section 4.4).

Depending on site conditions, developed areas with steep escarpment[22] slopes may contain hazard exposure beyond the base (landslide runout) and behind the crest (landslide retrogression) that was not identified by this study. Some partners, such as the City of Prince George and Village of Valemount, have established Hazardous Condition Areas that include "significant slopes" (over 20% grade) and setback criteria[23]. However, the crest and toe of escarpment slopes have not been systematically delineated where existing.

BGC recommends further work to identify and prioritize escarpment slopes and develop a plan for their further assessment. The intended results may inform development permit areas for parcels wholly or partially within a setback from the top or bottom of a slope with a defined threshold angle and minimum height. BGC can provide further information on typical assessment approaches, on request.

[22] Escarpment slopes are steep, natural slopes that separate two relatively level land surfaces.

23 See Schedule B-2 of the City of Prince George Official Community Plan Bylaw 8383 (2011)

9.0 CLOSURE

This report contains sections under the supervision of different individuals. Kris Holm is the responsible author for the overall hazard exposure assessment (Main Report). Elisa Scordo is the overall responsible author for the flood hazard assessment (Appendix E). Matthieu Sturzenegger is the overall responsible author for steep creek and landslide assessments (Appendix F and Appendix G). Richard Carter is the responsible author for geospatial data analysis workflows (Appendix H).

We trust the above satisfies your requirements. Should you have any questions or comments, please do not hesitate to contact us.

Yours sincerely,

BGC Engineering Inc.
per:

[redacted]

Kris Holm, M.Sc., P.Geo.
Principal Geoscientist

Richard Carter, M.Sc.
Earth Scientist

[redacted]

Elisa Scordo, M.Sc., P.Ag., P.Geo.
Principal Hydrologist

[redacted]

Matthieu Sturzenegger, Ph.D., P.Geo.
Senior Engineering Geologist

Reviewed by:

Hamish Weatherly, M.Sc., P.Geo.
Principal Hydrologist

KH/HW/kj/mm

REFERENCES

AMEC Earth & Environmental. (2012, August 14). *Leona Creek Debris Flow Hazard 13292 Bunbury Road, Robson Valley Supplementary Informatio*n [Report]. Prepared for RDFFG.

BGC Engineering Inc. (2025, March 24). Disaster and Climate Risk and Resilience Assessment (DCRRA): Hazard Threat Analysis. Final Report prepared for Sage on Earth Consulting Inc. on behalf of Emergency Management and Climate Readiness (EMCR). Geospatial data delivered July 04, 2024.

Brideau, M.-A., Hancock, C.-A., Brayshaw, D., Lipovsky, P., Cronmiller, D., Friele, P., Geertsema, M., & Wells, G. (2025). Preliminary Canadian Landslide Database (10.0) [Data set]. Zenodo. https://doi.org/10.5281/zenodo.14585761

Engineers and Geoscientists of BC (EGBC). (2017). *Guidelines for Flood Mapping in BC*. Web link: APEGBC-Guidelines-for-Flood-Mapping-in-BC.pdf.aspx.

Engineers and Geoscientists of BC (EGBC). (2018). *Guidelines for Legislated Flood Assessments in a Changing Climate in BC*. Version 2.1. August 28. Web link: PP Guidelines - Legislated Flood Assessments in a Changing Climate in BC V.2.1

Engineers and Geoscientists of BC (EGBC). (2023). *Landslide Assessments in British Columbia*. Web link: Landslide Guidelines V4-1

Government of British Columbia (BC). (2016). British Columbia Emergency Management System (BCEMS) document. Available online at: https://www2.gov.bc.ca/assets/gov/public-safety-and-emergency-services/emergency-preparedness-response-recovery/embc/bcems/bcems_guide_2016_final_fillable.pdf [accessed; 09/14/2018].

Government of British Columbia. (2018). Declaration on the Rights of Indigenous Peoples Act. Victoria, BC: Queen's Printer.

Government of Canada. (1982). Constitution Act. Source: https://www.laws-lois.justice.gc.ca/PDF/Const_TRD.pdf.

Government of Canada. (2021). Bill C-15: United Nations Declaration on the Rights of Indigenous Peoples Act. Ottawa, ON: Queen's Printer.

Holm, K., Jakob, M. & Scordo, E. (2016). An inventory and risk-based prioritization of steep creek fans in Alberta. 3rd European Conference on Flood Risk Management: Innovation, Implementation, Integration. 18-20 October 2016, Lyon France.

Holm, K., Jakob, M., Kimball, S., Strouth, A., Esarte, A., & Camire, F. (2018). Steep creek geohazards risk and risk control assessment in the Town of Canmore, Alberta. Geohazards 7 Conference, Canmore, Canada.

Hungr, O., Leroueil, S., & Picarelli, L. (2014). The Varnes classification of landslide types, an update. *Landslides, 11*, 167-194. https://doi.org/10.1007/s10346-013-0436-y

Natural Resources Canada. (2022a). *Social Vulnerability to Natural Hazards in Canada*. Geological Survey of Canada Open File 8892

Natural Resources Canada. (2022b). *Physical Vulnerability to Natural Hazards in Canada*. Geological Survey of Canada Open File 8902

Public Safety Canada (2022). Canadian Disaster Database. https://www.publicsafety.gc.ca/cnt/rsrcs/cndn-dsstr-dtbs/index-en.aspx [Accessed 11/03/2023].

Septer, D. (2007). *Flooding and Landslide Events Southern British Columbia 1808-2006*. Ministry of Environment, Province of British Columbia.

Statistics Canada (2022). 2021 Census of Population. Source: Reference materials, 2021 Census

Strouth, A. & McDougall, S. (2021). Societal risk evaluation for landslides: historical synthesis and proposed tools. *Landslides, 18*, 1071–1085**. https://doi.org/10.1007/s10346-020-01547-8**

United Nations Office for Disaster Risk Reduction (UNISDR). (2015). *Sendai Framework for Disaster Risk Reduction – UNISRD*. Website accessed November 2018: https://www.unisdr.org/we/coordinate/sendai-framework

DRAWINGS

NOTES:
1. ALL DIMENSIONS ARE IN METRES UNLESS OTHERWISE NOTED.
2. THIS DRAWING MUST BE READ IN CONJUNCTION WITH BGC'S REPORT TITLED "COLLABORATIVE DISASTER RISK REDUCTION AND CLIMATE ADAPTATION PROJECTAND DATED JULY 2025.
3. BASE TOPOGRAPHIC DATA BASED ON ESRI WORLD TOPOGRAPHIC BASE MAP.
4. COORDINATE SYSTEM IS UTM ZONE 10 NAD1983.
5. BGC PREPARED THIS DRAWING FOR THE EXCLUSIVE USE OF BGC'S CLIENT IDENTIFIED ON THIS DRAWING. UNLESS BGC AGREES OTHERWISE IN WRITING, THIS DRAWING MUST NOT BE MODIFIED OR USED FOR ANY PURPOSE OTHER THAN THE SPECIFIC PURPOSE FOR WHICH BGC GENERATED IT. BGC SHALL HAVE NO LIABILITY FOR ANY DAMAGES, INJURY, OR LOSS ARISING FROM ANY UNAUTHORIZED USE OR MODIFICATION OF THIS DRAWING. THIRD PARTIES USE OR RELY UPON THIS DRAWING AT THEIR OWN RISK.

SCALE:	1:650,000
DATE:	JULY 2025
DRAWN:	MIB
REVIEW:	KH
APPROVED:	KH

CLIENT: REGIONAL DISTRICT of Fraser-Fort George

BGC

PROJECT: COLLABORATIVE DISASTER RISK REDUCTION AND CLIMATE ADAPTATION PROJECT

TITLE: PROJECT STUDY AREA

PROJECT No.:	DWG No.:
0511013	01

X:\Projects\0511013\GIS\Production\Reports\20250130_RDFFG_Maps\RDFFG_Report_Maps.aprx - Hazard_Maps

THIS DRAWING MAY HAVE BEEN REDUCED OR ENLARGED. ALL FRACTIONAL SCALE NOTATIONS INDICATED ARE BASED ON ORIGINAL FORMAT DRAWINGS.

NOTES:
1. ALL DIMENSIONS ARE IN METRES UNLESS OTHERWISE NOTED.
2. THIS DRAWING MUST BE READ IN CONJUNCTION WITH BGC'S REPORT TITLED "COLLABORATIVE DISASTER RISK REDUCTION AND CLIMATE ADAPTATION PROJECTAND DATED JULY 2025.
3. BASE TOPOGRAPHIC DATA BASED ON ESRI WORLD TOPOGRAPHIC BASE MAP.
4. COORDINATE SYSTEM IS UTM ZONE 10 NAD1983.
5. BGC PREPARED THIS DRAWING FOR THE EXCLUSIVE USE OF BGC'S CLIENT IDENTIFIED ON THIS DRAWING. UNLESS BGC AGREES OTHERWISE IN WRITING, THIS DRAWING MUST NOT BE MODIFIED OR USED FOR ANY PURPOSE OTHER THAN THE SPECIFIC PURPOSE FOR WHICH BGC GENERATED IT. BGC SHALL HAVE NO LIABILITY FOR ANY DAMAGES, INJURY, OR LOSS ARISING FROM ANY UNAUTHORIZED USE OR MODIFICATION OF THIS DRAWING. THIRD PARTIES USE OR RELY UPON THIS DRAWING AT THEIR OWN RISK.

SCALE:	1:650,000
DATE:	JULY 2025
DRAWN:	MIB
REVIEW:	KH
APPROVED:	KH

CLIENT: REGIONAL DISTRICT of Fraser-Fort George

BGC

PROJECT: COLLABORATIVE DISASTER RISK REDUCTION AND CLIMATE ADAPTATION PROJECT

TITLE: FLOODPLAIN IDENTIFICATION (TIER 1)

PROJECT No.: 0511013

DWG No.: 02

X:\Projects\0511013\GIS\Production\Reports\20250130_RDFFG_Report_Maps\RDFFG_Report_Maps.aprx - Hazard_Maps

THIS BAR MEASURES 100 mm AT FULL SIZE. ALL SCALES REFERENCED TO FULL SIZE

NOTES:

1. ALL DIMENSIONS ARE IN METRES UNLESS OTHERWISE NOTED.
2. THIS DRAWING MUST BE READ IN CONJUNCTION WITH BGC'S REPORT TITLED "COLLABORATIVE DISASTER RISK REDUCTION AND CLIMATE ADAPTATION PROJECTAND DATED JULY 2025.
3. BASE TOPOGRAPHIC DATA BASED ON ESRI WORLD TOPOGRAPHIC BASE MAP.
4. COORDINATE SYSTEM IS UTM ZONE 10 NAD1983.
5. BGC PREPARED THIS DRAWING FOR THE EXCLUSIVE USE OF BGC'S CLIENT IDENTIFIED ON THIS DRAWING. UNLESS BGC AGREES OTHERWISE IN WRITING, THIS DRAWING MUST NOT BE MODIFIED OR USED FOR ANY PURPOSE OTHER THAN THE SPECIFIC PURPOSE FOR WHICH BGC GENERATED IT. BGC SHALL HAVE NO LIABILITY FOR ANY DAMAGES, INJURY, OR LOSS ARISING FROM ANY UNAUTHORIZED USE OR MODIFICATION OF THIS DRAWING. THIRD PARTIES USE OR RELY UPON THIS DRAWING AT THEIR OWN RISK.

SCALE:	1:650,000
DATE:	JULY 2025
DRAWN:	MIB
REVIEW:	KH
APPROVED:	KH

CLIENT: REGIONAL DISTRICT of Fraser-Fort George

BGC

PROJECT: COLLABORATIVE DISASTER RISK REDUCTION AND CLIMATE ADAPTATION PROJECT

TITLE: FLOOD HAZARD STUDY AREA (TIER 2)

PROJECT No.: 0511013

DWG No.: 03

X:\Projects\0511013\GIS\Production\Reports\20250130_RDFFG_Maps\RDFFG_Report_Maps.aprx - Hazard_Maps

THIS BAR MEASURES 100 mm AT FULL SIZE. ALL SCALES REFERENCED TO FULL SIZE

NOTES:
1. ALL DIMENSIONS ARE IN METRES UNLESS OTHERWISE NOTED.
2. THIS DRAWING MUST BE READ IN CONJUNCTION WITH BGC'S REPORT TITLED "COLLABORATIVE DISASTER RISK REDUCTION AND CLIMATE ADAPTATION PROJECTAND DATED JULY 2025.
3. BASE TOPOGRAPHIC DATA BASED ON ESRI WORLD TOPOGRAPHIC BASE MAP.
4. COORDINATE SYSTEM IS UTM ZONE 10 NAD1983.
5. BGC PREPARED THIS DRAWING FOR THE EXCLUSIVE USE OF BGC'S CLIENT IDENTIFIED ON THIS DRAWING. UNLESS BGC AGREES OTHERWISE IN WRITING, THIS DRAWING MUST NOT BE MODIFIED OR USED FOR ANY PURPOSE OTHER THAN THE SPECIFIC PURPOSE FOR WHICH BGC GENERATED IT. BGC SHALL HAVE NO LIABILITY FOR ANY DAMAGES, INJURY, OR LOSS ARISING FROM ANY UNAUTHORIZED USE OR MODIFICATION OF THIS DRAWING. THIRD PARTIES USE OR RELY UPON THIS DRAWING AT THEIR OWN RISK.

SCALE:	1:650,000
DATE:	JULY 2025
DRAWN:	MIB
REVIEW:	KH
APPROVED:	KH

CLIENT: REGIONAL DISTRICT of Fraser-Fort George

BGC

PROJECT: COLLABORATIVE DISASTER RISK REDUCTION AND CLIMATE ADAPTATION PROJECT

TITLE: ALLUVIAL FAN INVENTORY

PROJECT No.: 0511013

DWG No.: 04

X:\Projects\0511013\GIS\Production\Reports\20250130_RDFFG_Report_Maps\RDFFG_Report_Maps.aprx - Hazard_Maps

THIS DRAWING MAY HAVE BEEN REDUCED OR ENLARGED. ALL FRACTIONAL SCALE NOTATIONS INDICATED ARE BASED ON ORIGINAL FORMAT DRAWINGS.

THIS BAR MEASURES 100 mm AT FULL SIZE. ALL SCALES REFERENCED TO FULL SIZE

X:\Projects\0511013\GIS\Production\Reports\20250130_RDFFG_Maps\RDFFG_Report_Maps.aprx - Hazard_Maps

NOTES:
1. ALL DIMENSIONS ARE IN METRES UNLESS OTHERWISE NOTED.
2. THIS DRAWING MUST BE READ IN CONJUNCTION WITH BGC'S REPORT TITLED "COLLABORATIVE DISASTER RISK REDUCTION AND CLIMATE ADAPTATION PROJECTAND DATED JULY 2025.
3. BASE TOPOGRAPHIC DATA BASED ON ESRI WORLD TOPOGRAPHIC BASE MAP.
4. COORDINATE SYSTEM IS UTM ZONE 10 NAD1983.
5. BGC PREPARED THIS DRAWING FOR THE EXCLUSIVE USE OF BGC'S CLIENT IDENTIFIED ON THIS DRAWING. UNLESS BGC AGREES OTHERWISE IN WRITING, THIS DRAWING MUST NOT BE MODIFIED OR USED FOR ANY PURPOSE OTHER THAN THE SPECIFIC PURPOSE FOR WHICH BGC GENERATED IT. BGC SHALL HAVE NO LIABILITY FOR ANY DAMAGES, INJURY, OR LOSS ARISING FROM ANY UNAUTHORIZED USE OR MODIFICATION OF THIS DRAWING. THIRD PARTIES USE OR RELY UPON THIS DRAWING AT THEIR OWN RISK.

SCALE:	1:650,000
DATE:	JULY 2025
DRAWN:	MIB
REVIEW:	KH
APPROVED:	KH

CLIENT: REGIONAL DISTRICT of Fraser-Fort George

BGC

PROJECT: COLLABORATIVE DISASTER RISK REDUCTION AND CLIMATE ADAPTATION PROJECT

TITLE: LANDSLIDE HAZARD INVENTORY

PROJECT No.: 0511013

DWG No.: 05

X:\Projects\0511013\GIS\Production\Reports\20250130_RDFFG_Maps\RDFFG_Report_Maps.aprx - Hazard_Maps

NOTES:
1. ALL DIMENSIONS ARE IN METRES UNLESS OTHERWISE NOTED.
2. THIS DRAWING MUST BE READ IN CONJUNCTION WITH BGC'S REPORT TITLED "COLLABORATIVE DISASTER RISK REDUCTION AND CLIMATE ADAPTATION PROJECTAND DATED JULY 2025.
3. BASE TOPOGRAPHIC DATA BASED ON ESRI WORLD TOPOGRAPHIC BASE MAP.
4. COORDINATE SYSTEM IS UTM ZONE 10 NAD1983.
5. BGC PREPARED THIS DRAWING FOR THE EXCLUSIVE USE OF BGC'S CLIENT IDENTIFIED ON THIS DRAWING. UNLESS BGC AGREES OTHERWISE IN WRITING, THIS DRAWING MUST NOT BE MODIFIED OR USED FOR ANY PURPOSE OTHER THAN THE SPECIFIC PURPOSE FOR WHICH BGC GENERATED IT. BGC SHALL HAVE NO LIABILITY FOR ANY DAMAGES, INJURY, OR LOSS ARISING FROM ANY UNAUTHORIZED USE OR MODIFICATION OF THIS DRAWING. THIRD PARTIES USE OR RELY UPON THIS DRAWING AT THEIR OWN RISK.

SCALE:	1:650,000
DATE:	JULY 2025
DRAWN:	MIB
REVIEW:	KH
APPROVED:	KH

CLIENT: REGIONAL DISTRICT of Fraser-Fort George

BGC

PROJECT: COLLABORATIVE DISASTER RISK REDUCTION AND CLIMATE ADAPTATION PROJECT

TITLE: DEEP-SEATED EARTH SLIDE SUSCEPTIBILITY

PROJECT No.: 0511013

DWG No.: 06

THIS DRAWING MAY HAVE BEEN REDUCED OR ENLARGED. ALL FRACTIONAL SCALE NOTATIONS INDICATED ARE BASED ON ORIGINAL FORMAT DRAWINGS.

THIS BAR MEASURES 100 mm AT FULL SIZE. ALL SCALES REFERENCED TO FULL SIZE

NOTES:
1. ALL DIMENSIONS ARE IN METRES UNLESS OTHERWISE NOTED.
2. THIS DRAWING MUST BE READ IN CONJUNCTION WITH BGC'S REPORT TITLED "COLLABORATIVE DISASTER RISK REDUCTION AND CLIMATE ADAPTATION PROJECTAND DATED JULY 2025.
3. BASE TOPOGRAPHIC DATA BASED ON ESRI WORLD TOPOGRAPHIC BASE MAP.
4. COORDINATE SYSTEM IS UTM ZONE 10 NAD1983.
5. BGC PREPARED THIS DRAWING FOR THE EXCLUSIVE USE OF BGC'S CLIENT IDENTIFIED ON THIS DRAWING. UNLESS BGC AGREES OTHERWISE IN WRITING, THIS DRAWING MUST NOT BE MODIFIED OR USED FOR ANY PURPOSE OTHER THAN THE SPECIFIC PURPOSE FOR WHICH BGC GENERATED IT. BGC SHALL HAVE NO LIABILITY FOR ANY DAMAGES, INJURY, OR LOSS ARISING FROM ANY UNAUTHORIZED USE OR MODIFICATION OF THIS DRAWING. THIRD PARTIES USE OR RELY UPON THIS DRAWING AT THEIR OWN RISK.

SCALE:	1:650,000
DATE:	JULY 2025
DRAWN:	MIB
REVIEW:	KH
APPROVED:	KH

CLIENT: REGIONAL DISTRICT of Fraser-Fort George

BGC

PROJECT: COLLABORATIVE DISASTER RISK REDUCTION AND CLIMATE ADAPTATION PROJECT

TITLE: STEEP SLOPES MAP

PROJECT No.: 0511013

DWG No.: 07

X:\Projects\0511013\GIS\Production\Reports\20250130_RDFFG_Maps\RDFFG_Report_Maps.aprx - Hazard_Maps

NOTES:
1. ALL DIMENSIONS ARE IN METRES UNLESS OTHERWISE NOTED.
2. THIS DRAWING MUST BE READ IN CONJUNCTION WITH BGC'S REPORT TITLED "COLLABORATIVE DISASTER RISK REDUCTION AND CLIMATE ADAPTATION PROJECTAND DATED JULY 2025.
3. BASE TOPOGRAPHIC DATA BASED ON ESRI WORLD TOPOGRAPHIC BASE MAP.
4. COORDINATE SYSTEM IS UTM ZONE 10 NAD1983.
5. BGC PREPARED THIS DRAWING FOR THE EXCLUSIVE USE OF BGC'S CLIENT IDENTIFIED ON THIS DRAWING. UNLESS BGC AGREES OTHERWISE IN WRITING, THIS DRAWING MUST NOT BE MODIFIED OR USED FOR ANY PURPOSE OTHER THAN THE SPECIFIC PURPOSE FOR WHICH BGC GENERATED IT. BGC SHALL HAVE NO LIABILITY FOR ANY DAMAGES, INJURY, OR LOSS ARISING FROM ANY UNAUTHORIZED USE OR MODIFICATION OF THIS DRAWING. THIRD PARTIES USE OR RELY UPON THIS DRAWING AT THEIR OWN RISK.

SCALE:	1:650,000
DATE:	JULY 2025
DRAWN:	MIB
REVIEW:	KH
APPROVED:	KH

CLIENT: REGIONAL DISTRICT of Fraser-Fort George

BGC

PROJECT: COLLABORATIVE DISASTER RISK REDUCTION AND CLIMATE ADAPTATION PROJECT

TITLE: LANDSLIDE HAZARD AREAS OF INTEREST

PROJECT No.: 0511013

DWG No.: 08

X:\Projects\0511013\GIS\Production\Reports\20250130_RDFFG_Report_Maps\RDFFG_Report_Maps.aprx - Hazard_Maps

APPENDIX A
TERMINOLOGY

A-1 TERMINOLOGY

This report refers to the following key definitions[1]:

- **Asset:** anything of value, including both anthropogenic and natural assets[2], and items of economic or intangible value.
- **Annual Exceedance Probability (AEP):** chance that a flood magnitude is exceeded in any year. For example, a flood with a 0.5% AEP has a one in two hundred chance (i.e., 200-year return period) of being exceeded in any year. While AEP is increasingly replacing the use of the term 'return period' to describe flood recurrence intervals, both terms are used in this document.
- **Clear-Water Floods:** riverine and lake flooding resulting from inundation due to an excess of clear-water discharge in a watercourse or body of water such that land outside the natural or artificial banks which is not normally under water is submerged. While called "clear-water floods", such floods still transport sediment. This term serves to differentiate from other flood forms such as landslide dam outburst floods, floods on alluvial fans or debris floods. Appendix E provides a comprehensive description of clear-water floods.
- **Steep-Creek Processes:** rapid flow of water and debris in a steep channel, often associated with avulsions and strong bank erosion. Steep creek processes carry larger volumetric concentrations of debris than clear-water floods. Steep creek processes are used in this report as a collective term for floods on alluvial fans, debris flows, and debris floods.
- **Consequence:** formally, the conditional probability that elements at risk will suffer some severity of damage or loss, given geohazard impact with a certain intensity (destructive potential). In this study, the term was simplified to reflect the level of detail of assessment. Consequence refers to the relative potential for loss between hazard areas. Consequence ratings consider both the value of elements at risk and the intensity (destructive potential) of a geohazard, but do not provide an absolute estimate of loss.
- **Elements at Risk:** assets exposed to potential consequences of geohazard events.
- **Exposure**: describes the quantity, value, and characteristics of the elements that are at risk, like people, buildings, infrastructure, economic activities, and things of social and cultural value.
- **Flood Mapping:** delineation of elevations on a base map, typically taking the form of flood lines on a map, that show the area that will be covered by water, or the elevation that water would reach during a flood event.
- **Hazard:** refers to the process type, likelihood of impact, and intensity (e.g., flow depth, velocity) of impact at an exposed element.
- **Resilience:** the ability of a system, community or society exposed to hazards to resist, absorb, accommodate to, and recover from the effects of a hazard in a timely and

[1] CSA (1997), EGBC (2017; 2018).

[2] Assets of the natural environment: these consist of biological assets (produced or wild), land and water areas with their ecosystems, subsoil assets and air (UNSD, 1997).

efficient manner, including through the preservation and restoration of its essential basic structures and functions.

- **Risk:** potential for loss caused by future hazard events at a specific location, infrastructure, person, or group. Quantitatively, risk is the product of some adverse consequence (e.g., number of lives lost, economic loss, days of service disruption) and the probability of that loss occurring. It is a function of the interaction between the hazard, the exposed element at risk, and the vulnerability of that element to the hazard.
- **Strahler Stream Order:** a classification of stream segments by their branching complexity within a drainage system. Strahler stream order is an indication of the significance in size and water conveying capacity at points along a river (Figure A-1).
- **Waterbody:** ponds, lakes and reservoirs.
- **Vulnerability:** describes the probability of loss given an exposed element is impacted by a hazard with a given intensity. Vulnerable infrastructure is more likely to be damaged when impacted, while resilient infrastructure – and communities more broadly – are more likely to function and recover.
- **Watercourse:** creeks, streams and rivers.

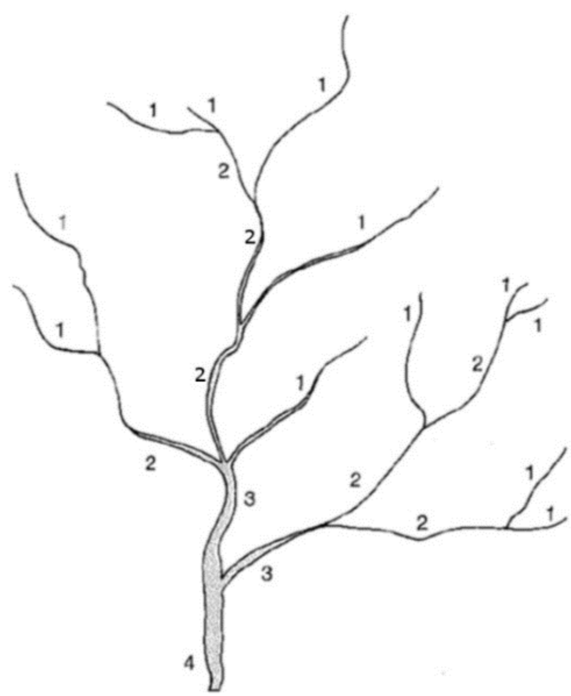

Figure A-1 Illustration showing Strahler stream order (Montgomery, 1990).

REFERENCES

Canadian Standards Association (CSA). (1997). *CAN/CSA – Q859-97 Risk Management: Guideline for Decision Makers*. CSA Group, Toronto, ON, pp. 55.

Engineers and Geoscientists of BC (EGBC). (2017). *Guidelines for Flood Mapping in BC*. Web link: https://www.egbc.ca/getmedia/8748e1cf-3a80-458d-8f73-94d6460f310f/APEGBC-Guidelines-for-Flood-Mapping-in-BC.pdf.aspx.

Engineers and Geoscientists of BC (EGBC). (2018). *Guidelines for Legislated Flood Assessments in a Changing Climate in BCC. Version 2.1*. https://www.egbc.ca/getmedia/f5c2d7e9-26ad-4cb3-b528-940b3aaa9069/Legislated-Flood-Assessments-in-BC.pdf.aspx.

Montgomery, C.W. (1990). *Physical Geology, 2nd edition*. WCB Publishers, Dubuque, IA, USA.

UNSD. (1997). Glossary of Environment Statistics. https://unstats.un.org/unsd/environmentgl/

APPENDIX B
DATA COMPILATION

Location			Project			Hazard Type			Reference
Name	River Basin	District	Project Title	Report/Paper (Y/N)	Spatial information?	Flooding?	Landslide?	Steep Creek?	Citation
Goslin and L'Heureaux Creeks		RDFFG	Geotechnical Hazard Assessments for Goslin and L'Heureux Creeks	Y	Y		Y	Y	Piteau Associates. (November 1993). Geotechnical Hazard Assessments for Goslin and L'Heureux Creeks [Report]. Prepared for Ministry of Transportation and Highways.
McBride		RDFFG	Debris Flow Assessment Proposed Subdivision W1/2 D.L. 3307 McBride, BC	Y	Y			Y	Agra Earth & Environmental. (May 8, 1996). Debris Flow Assessment Proposed Subdivision W1/2 D.L. 3307 McBride, BC [Report].
McBride, Sunbeam Creek		RDFFG	Geotechnical Hazard Assessment Lot 2, DL 11662, Plan 9602 McBride, BC	Y			Y	Y	Agra Earth & Environmental. (January 30, 1998). Geotechnical Hazard Assessment Lot 2, DL 11662, Plan 9602 McBride, BC [Report].
Robson Valley	Fraser	RDFFG	Robson Valley Hazard Land Study Lamming Mills to Albreda, BC	Y	Y		Y	Y	BGC Engineering Inc. (January 28, 1999). Robson Valley Hazard Land Study Lamming Mills to Albreda, BC [Report]. Prepared for RDFFG.
Robson Valley		RDFFG	Hazard Assessment Highway 16 Spittal and Leona Creeks Robson District	Y				Y	Ministry of Highways (MoH). (March 1999). Hazard Assessment Highway 16 Spittal and Leona Creeks Robson District [Report]. Prepared for Ministry of Highways.
Highway 16 near Cardinal Ranch	Fraser	RDFFG	Landscape and Stream Hazard Assessment of Torrented Stream Above Cardinal Ranch	Y	Y			Y	Firth Hollin Resource Science Corporation. (May 7, 1999). Landscape and Stream Hazard Assessment of Torrented Stream Above Cardinal Ranch [Report].
Swift Creek (Valemount)	Fraser	RDFFG	Swift Creek Fan Hazard Assessment	Y	Y	Y	Y	Y	BGC Engineering Inc. (August 12, 1999). Swift Creek Fan Hazard Assessment [Report]. Prepared for Regional District of Fraser-Fort George
Rainbow Creek		RDFFG	Geotechnical Hazard Assessment Rainbow Creek Fan	Y	Y		Y	Y	AGRA Earth & Environmental Ltd. (January 25, 2000). Geotechnical Hazard Assessment Rainbow Creek Fan McBride, BC [Report]. Prepared for RDFFG.
Willox Creek		RDFFG	Survey and Terrain Modeling for Landscape Hazard Assessment Willox Creek, McBride, BC	Y			Y	Y	Firth Hollin Resource Science Corporation. (January 31, 2000). Survey and Terrain Modeling for Landscape Hazard Assessment Willox Creek, McBride, BC [Report]. Prepared for RDFFG.
Willox Creek		RDFFG	Willox Creek Emergency Geohazard Risk and Mitigation Assessment	Y	Y		Y	Y	BGC Engineering Inc. (October 30, 2020). Willox Creek Emergency Geohazard Risk and Mitigation Assessment [Report]. Prepared for RDFFG.
Swiftcurrent Creek (Mount Robson)		RDFFG	Swift Current Creek Fan – Geotechnical Hazard Assessment	Y	Y	Y	Y	Y	AGRA Earth & Environmental Ltd. (February 3, 2000). Geotechnical Hazard Assessment Swift Current Creek Fan [Report]. Prepared for RDFFG.
Packsaddle Creek		RDFFG	Terrain Stability Assessment Packsaddle Creek	Y			Y	Y	Firth Hollin Resource Science Corporation. (February 18, 2000). Terrain Stability Assessment Report – Frac. W ½ DL 7369 Cariboo District, Packsaddle Creek [Report].
Selkirk, Tapli, McKirdy, Snowcourse, Home creeks (Valemount)		RDFFG	Geotechnical Hazard Assessment Selkirk, Tapli, McKirdy, Snowcourse, and Home Creek	Y	Y		Y	Y	AMEC Earth & Environmental. (February 23, 2001). Geotechnical Hazard Assessment Selkirk, Tapli, McKirdy, Snowcourse, and Home Creek [Report]. Prepared for RDFFG.
Robson Valley		RDFFG	Stream Survey, Terrain Analysis and Landscape Hazard Assessments for 13 Creeks in the Robson Valley Area	Y	Y	Y	Y	Y	Firth Hollin Resource Science Corporation. (March 2002). Stream Survey, Terrain Analysis and Landscape Hazard Assessments for 13 Creeks in the Robson Valley Area of British Columbia [Report]. Prepared for RDFFG.
Saranna, Dulles, Collett creeks (Dunster)		RDFFG	Geotechnical Hazard Assessment Saranna, Dulles, and Collett Creeks Dunster, BC	Y	Y	Y	Y	Y	AMEC Earth & Environmental. (March 11, 2002). Geotechnical Hazard Assessment Saranna, Dulles, and Collett Creeks Dunster, BC [Report]. Prepared for RDFFG.
Wilson, D, Booth, Alder creeks (Dunster)		RDFFG	Geotechnical Hazard Assessment Wilson, D, Booth, and Alder Creeks Dunster, BC	Y	Y	Y	Y	Y	AMEC Earth & Environmental. (April 10, 2002).Geotechnical Hazard Assessment Wilson, D, Booth, and Alder Creeks Dunster, BC [Report]. Prepared for RDFFG.
Hagan and Gort Creeks (Dunster)		RDFFG	Geotechnical Hazard Assessment Hagan and Gort Creeks Dunster, BC	Y	Y	Y	Y	Y	AMEC Earth & Environmental. (April 19, 2002).Geotechnical Hazard Assessment Hagan and Gort Creeks Dunster, BC [Report]. Prepared for RDFFG.
Leona Creek (Robson Valley)		RDFFG	Detailed Geological Hazard Assessment Leona Creek Watershed	Y	Y		Y	Y	AMEC Earth & Environmental. (December 9, 2004).Detailed Geological Hazard Assessment Leona Creek Watershed Robson Valley [Report]. Prepared for RDFFG.
Leona Creek (Robson Valley)		RDFFG	Leona Creek Debris Flow Hazard Reconnaissance	Y	Y		Y	Y	AMEC Earth & Environmental. (June 21, 2012). Leona Creek Debris Flow Hazard Reconnaissance 13292 Bunbury Road, Robson Valley [Report]. Prepared for RDFFG.
Leona Creek (Robson Valley)		RDFFG	Leona Creek Debris Flow Hazard Supplementary Information	Y	Y			Y	AMEC Earth & Environmental. (August 14, 2012). Leona Creek Debris Flow Hazard 13292 Bunbury Road, Robson Valley Supplementary Information [Report]. Prepared for RDFFG.
Swiftcurrent Creek (Mount Robson)		RDFFG	Hydrotechnical Summary Report Swiftcurrent Creek	Y	Y	Y	Y	Y	DWB Consulting Services Ltd. (February 17, 2017). Hydrotechnical Summary Report Swiftcurrent Creek [Report].
Miworth and Prince George	Nechako	RDFFG	Nechako River Bank Erosion Study	Y	Y	Y			GeoNorth Engineering Ltd. (June 30, 1998). Nechako River Bank Erosion Study [Report]. Prepared for Ministry of Environment, Lands, and Parks.
Dore River	Dore	RDFFG	Hydrologic and Geomorphic Assessment of the Dore River	Y	Y	Y			McElhanney Ltd. (March 11, 2021). Hydrologic and Geomorphic Assessment of the Dore River [Report]. Prepared for RDFFG.
Various	Various	Various	Flooding and Landslide Events Southern British Columbia 1808-2006	Y	Y	Y	Y	Y	Septer, D. (2007). Flooding and Landslide Events Southern British Columbia 1808-2006. Prepared for Ministry of Environment.
McBride		RDFFG	A landslide in glacial lae clays in central British Columbia	Y	Y		Y		Thomson, S., & Mekechuk, J. (1982). A landslide in glacial lake clays in central British Columbia. Canadian Geotechnical Journal. 19(3): 296-306. https://doi.org/10.1139/t82-036
Robson Valley	Multiple	Multiple	The Robson Valley Story	Y		Y			Wheeler, M. J. (2008). *The Robson Valley Story: A Century of Dreams* . Sternwheeler Pres.
Valemount		RDFFG	Landslide Inventory Map of the Valemount Area. A detailed methodological description	Y	Y		Y		Bornaetxea, T., Blais-Stevens, A., & Miller, B. (2023). Landslide Inventory Map of the Valemount Area, British Columbia, Canada. A Detailed Methodological Description. In: Alcántara-Ayala, I., et al. Progress in Landslide Research and Technology, Volume 1 Issue 2, 2022. Progress in Landslide Research and Technology. Springer, Cham. https://doi.org/10.1007/978-3-031-18471-0_27
Various	Various	RDFFG	Historical DriveBC Events	N	Y	Y	Y	Y	DriveBC. (2022). Historical DriveBC Events 2006-2022 [Data]. Retreived from https://catalogue.data.gov.bc.ca/dataset/historical-drivebc-events.
Various	Various	Various	An overview of recent large catastrophic landslides in Northern British Columbia	Y	Y		Y		Geertsema, M., Clague, J., Schwab, J. & Evans, S. (2006). An overview of recent large catastrophic landslides in Northern British Columbia, Canada. Engineering Geology. 83. 120-143. 10.1016/j.enggeo.2005.06.028.

APPENDIX C
GEOHAZARD EVENT INVENTORY

Year	Month	Type of Hazard	Location	Source	Description of Event
1911	June	Flood	Fraser River, Prince George	Septer (2007)	Spring runoff caused the Fraser River at Prince George to rise to a record level of 25 ft. causing the city to flood.
1913	June	Flood	Tete Jaune	Septer (2007)	On June 11, Tète Jaune flooded due to the sudden rise of the Fraser River. Heavy rains during the previous few days caused a sharp rise in the water levels. In Main Street, the water was 1.8 m deep and still rising.
1914		Landslide	McBride, Fraser River	Thomson and Mekechuk (1982)	The CNR line in central BC was built across an old landslide along the valley of the Fraser River near the city of McBride. The new failure occurred shortly after the completion of construction in 1914 and the railway was relocated just off the slide area by construction of the a timber pile tresle.
1915	June	Flood	Fraser River	Wheeler (2008)	In the middle of June, floods severely damaged new seeding and gardens. The water was reported to be four or five feet above water, and "has been higher than ever before in the memory of the oldest settlers." Joe Morgan nearly lost his 40 acre tract, a large part of which was hidden by water for several days. G.H. Riley, of Cariboo, had to take his boat and rescue his chickens. It has been reported that R. Veale's house at Cariboo was carried away by the water.
1917	December	Flood	Fraser River, Nechako River, Prince George	Septer (2007)	In 1917, an icejam at the junction of the Nechako and Fraser rivers caused flooding in low-lying portions of Prince George.
1920	June	Flood	Prince George	Septer (2007)	Heavy winter snows, late spring, little April-May runoff, warm days and nights in late May and June, accompanied by heavy thunderstorms built up water levels to danger points
1921	November	Flood	Fraser River, Nechako River, Prince George	Septer (2007)	A heavy icejam on the Nechako River near Prince George in the shallow water at the junction of the Fraser River flooded the main tracks and yard of the Canadian National Railway (CNR). Parts of Chinatown were flooded "halfway up the doors of the premises."At the Cache, (or Cottonwood Island) an island at the confluence of the Nechako and Fraser rivers, many houses flooded.
1928	May	Flood	Fraser River, Prince George	Septer (2007)	During the last few days of May, the Fraser River rose and caused flooding at Prince George. Floodwaters forced residents on the east side of George Street to resort to rafts and canoes.
1933	December	Flood	Nechako River, Prince George	Septer (2007)	Overnight December 18-19, an icejam near the mouth of the Nechako River caused the river to overflow in a number of places. Near Prince George, the CNR rail yard was flooded with 60 cm of water and sections of roadbed washed out.
1934	January	Debris flows (?) and Flood	Prince George	Septer (2007)	Heavy rains and mild weather caused serious washouts on railways near Prince George.
1936	May-June	Flood	Fraser River, Nechako River, Prince George	Septer (2007)	On June 1, the temperature was 34.4 degrees C in Prince George. The Fraser River at Prince George rose to within 1.5 m of the decking of the CNR rail bridge. According to CNR superintendent W.H. Cobey, it reached the highest recorded level since 1911. People in East Prince George were evaculated and trains were delayed.
1939	May	Flood	Fraser River, Nechako River, Prince George, Summit Lake, Crooked River	Septer (2007)	Warmer weather during May brought a rapid rise in the Fraser and Nechako Rivers resulting in the sloughs being filled to capacity and rivers running over the normal banks. Summit Lake was reported to be a full 15 cm higher than any previous record. Crooked River was running so fast that the freighters were making relays. Around May 19 near Prince George, the Fraser River backed up the Nechako River causing the lower floors of many homes on East-End flats to flood.
1945	May	Flood	Fraser River, Nechako River, Prince George	Septer (2007)	Following a five-day heat wave near Prince George the water levels of the Nechako and Fraser rivers neared the flood stage. Rising at nearly 2.5 cm an hour, it caused flooding of lowlands east of Prince George. Around May 31, the Fraser River was rising faster than during the week preceding the disastrous 1936 floods (weather conditions in 1945 were very similar to those in the 1936 flood year).
1948		Flood	Dunster, Fraser River, Holmes River	Wheeler (2008)	In the record flood of 1948, Leo Allgeier tethered his boat to the Fraser Bridge (in Dunster) and ferried people back and forth across the flooded fields to the hill below the highway. Talitha and Emile Rosin's house near the mouth of the Beaver River (formally called Holmes River) was flooded and they had to boat to it. They found that the sofa, which had been stored on the top of the cook top, was wet, indicating how high the river had rose.
1948	May	Flood	Fraser River, Giscome	Septer (2007)	Around May 17-18, the Fraser River inundated low-lying land at Giscome, 25 mi. (40 km) east of Prince George. This was the first reported flooding for the 1948 spring runoff. The Fraser River at Prince George rose 14 in. (35 cm) in 36 hours. At Willow River nearby, workmen built a log diversion to protect a bridge on the main highway.

Year	Month	Type of Hazard	Location	Source	Description of Event
1948	May-June	Flood	Fraser River, Prince George	Septer (2007)	Hot weather caused severe flood conditions in British Columbia and the Fraser River inundated parts of Prince George (although most of the damage from flooding in the mid-western parts of the province).
1948		Flood	Swift Creek	BGC (August 12, 1999)	Valemount resident recalls flood that occurred on Swift Creek in 1948.
1949	December	Flood	Nechako River, Prince George	Septer (2007)	Early on December 22, an icejam in the Nechako River caused flooding. The icejam was solid enough for a person to walk across the river. Overnight December 21-22, the river rose 1.2 m. At the confluence of the Nechako and Fraser rivers, 200 homes were threatened and 25 ac. (10 ha) of mill property was under water.
1954	May	Debris Flood (?) and Flood	Isle Pierre	Septer (2007)	On May 15 at 3:30 a.m., a washout 4.8 km east of Isle Pierre wrecked a westbound CNR passenger train. A sudden freshet caused a dam near a small lake 800 m upstream broke and undermined the east approach of the 90 cm culvert. A locomotive and two baggage cars of the 11-car passenger train dropped into a deep hole left by a washed-out culvert. Old-timers of the Isle Pierre district believed the accident was caused by the break up of a beaver dam broke in the small lake.
1955	January	Flood	Nechako River, Prince George	Septer (2007)	In January following unusual mild temperatures, the Nechako River flooded low-lying areas twice within two weeks. On January 19 and again in January 29, icejams backed up the Nechako River from where it flows into the frozen Fraser River. The Nechako River rose 2.4 m within a week (during a normal spring freshet, the Nechako River would usually not rise more than 1.5 m). Floodwaters and ice threatened the bridge linking Prince George with the John Hart Highway by straining the supports of this bridge across the Nechako River.
1955	June	Flood	Stone Creek, Bear Lake		A storm starting early on June 25 caused rivers and streams to flood their banks for many miles. Five bridges on the Trans-Provincial Highway, including the one at Stone Creek washed out while others were dangerously weakened. The village of Stone Creek was cut off in both north and south directions. According to old-timers, it was the “worst flood in 25 years.”
1955	October	Rockfall	Stone Creek	Septer (2007)	Rockfall debris caused a PGE speeder to jump the tracks killing two railway employees working on a Bridge and Buildings crew.
1958	October	Rockslide	Prince George		On October 1, rocks came down onto the Pacific Great Eastern Railway (PGE) line 30 mi. (48 km) north of Prince George. J.S. Broadbent, general manager of the PGE, said the slide was “a minor occurrence – it happens all the time.”
1960	September	Debris Flow	McBride	Septer (2007) and Canadian Disaster Database (2022)	On September 7 at 9:45 a.m., a landslide came down a steep ravine 28.8 km)west of McBride. The 3 m high mud and debris slide killed three of the highway construction workers. The swiftly moving rubble broke two-thirds of the way up of the 37.5 m ravine. Another man was injured while fifth man escaped. The slide was between 18-30 m wide as it plunged down the steep slopes of the about 45 m deep ravine. The debris was about 9 m deep. The slide occurred in loose clay and carried stumps and trees but little rock.
1964	June	Mud Slide	McBride, Snowshoe, Fraser River	Wheeler (2008)	A massive slide of mud and trees blocked the Fraser River 43 miles upstream of McBride. The river backed up about three miles, almost to Snowshoe, and diverted itself through a back channel. Bill Arnold saw the extent of the flood by boat and recalled that it took more than a year for the debris to clear.
1964	June	Flood	Fraser River, Nechako River, Prince George	Septer (2007)	The Fraser River reached a flood danger level. Near Prince George some 400 residents of “The Cache,” an island at the confluence of the Nechako and the Fraser Rivers, were evacuated
1965	October	Flood or Debris Flood (?)	Parsnip River	Septer (2007)	On October 26, heavy rain cut the railroad bridge across the Parsnip River, 144 km north of Prince George. Rail traffic on the PGE line between Prince George and the Peace River district was interrupted.
1967	June	Flood	Fraser River, Nechako River, Prince George	Septer (2007)	On June 6, the gauge under the old Fraser River bridge at Prince George reached 32.68 ft., the highest point since 1964. Water from the Fraser River backed up the Nechako River into the Island Cache, flooding a number of homes.
1968	December	Flood	Nechako River, Prince George	Septer (2007)	On December 27 and December 29, the Nechako River caused two flood waves near Prince George when icejams backed up the river. Bbout 150 people were forced from their homes on Cottonwood Island.
1969		Flood	Fraser River, Dome Creek	Wheeler (2008)	The Fraser River flooded a store to about a two foot depth. There was an inversion layer, the higher mountains around began to lose their snow covers, Dome Creek ran over its banks. The areas around its mouth where it ran into the Fraser River flooded, as the river remained firmly ice-covered.

Year	Month	Type of Hazard	Location	Source	Description of Event
1970	January	Flood	Nechako River, Fraser River, Prince George	Septer (2007)	On January 15, low temperatures of caused a sudden formation of ice on the Nechako River and the river levels to rise later that day at a steady 5 cm an hour, at one point rising 20 cm within 15 minutes. The rising waters caused backflow as the fast flowing Nechako River was running into an ice-jammed Fraser River. Residents were evacuated from Cottonwood Island and Island Cache. On January 17, the Nechako River finally spilled its banks, forcing more residents evacuated.
1972	June	Flood	Fraser River, Prince George, Cottonwood Island, McBride	Septer (2007) and Canadian Disaster Database (2022)	On June 2, the Fraser River at Prince George recorded an early peak of 31.75 ft, which was just under the 1948 peak. On June 13 north of Prince George, Highway 97 closed after the Pine River washed out the road near Pine Pass. There was "considerable" flooding on Cottonwood Island, a partially-dyked island at the junction of the Fraser and Nechako rivers and a total of 243 people were evacuated. Most of the low-lying land there was under 0.6-1.8 m of water, and 46 homes had been flooded. At South Fort George, just downstream from Prince George, an undetermined number of residents in a trailer court near the river were evacuated as about 1 ft. of water spilled over the banks. In McBride, five families were evacuated from the undyked Mountainview area near town. On June 14 at midnight, the Fraser River at Prince George reached a high of 34.22 ft., holding at that level.
1974	October	Earth Slide	McBride	BCG Landslide Database	Earth slide at CN Fraser Mile 4.25 triggered by increased pore pressure
1976	May	Flood	Nechako River, Fraser River, Prince George	Septer (2007)	Heavy rain, frost-free nights and a large snow pack in the Nechako drainage area caused a heavy runoff. On May 6, the Nechako River rose 1.5 m. Roads in the district washed out, cutting off some local residents. Overnight May 12-13, the Fraser River at Prince George rose 3 in. (7.5 cm) bringing it above the 30-ft. flood warning level.
1978	October	Debris Flow	Prince George	Septer (2007)	On October 30, a mudslide coming down in the Prince George BC Rail yard 3 km north of Prince George killed two PGE employees who were repairing a clogged drainpipe.
1979	November	Mudslide	Prince George	Septer (2007)	On the night of November 14, a mudslide in the Prince George BC Rail yard derailed a boxcar and seven butane-filled tanker cars. More than 0.5 m of mud covered about 45 m of track. The mud also pushed away a small bridge the company stored in the area. Mudslide was purported caused by heavy rain increasing the thawing of the ground.
1980	December	Flood	Fraser River, Penny, Aleza Lake, Upper Fraser	Septer (2007)	On December 17, a 5-km long icejam in the Fraser River near Penny backed up the water and caused flooding. The low-lying area around Penny was covered with ice "as far as the eye can see." More flooding was reported west of Penny near Aleza Lake. Icejams also cut a road near the community of Upper Fraser.
1986	May	Debris Flows, Debris Floods and Flood	Fraser River, McBride, Dore River, Tete Jeune, Prince George	Septer (2007)	Starting during the evening of May 26, and continuing for several days, high temperatures caused snow slides and rapid snowmelt runoff. It resulted in flow surges, debris flows and damage along many McBride area creeks, including a mudslide near McBride that cut off about 100 people. On May 26 around 9 p.m., a "wall of water" swept down the Dore River, flooding several basements, overturning vehicles and submerging Highway 16. The flood was caused by three snow slides in the headwaters of the south fork of the river which blocked the river with up to 15 m of ice. This ice dams eventually gave way causing material and water from all the slides to wash down the river. On May 31, flooding from the Fraser River occurred in Prince George with some basements flooded with water up to 30 cm deep.
1986	May	Debris Flows, Mud Flows	Goslin Creek	Piteau (1993), MoH (1999)	Major debris flow or mud flow in Goslin Creek on May 26 due to presence of major landslides that provide a continuing contribution of debris and warm weather. Caused flooding of residential property and highway 16.
1986	May	Mudslide	Bevier Creek, Dore River	Wheeler (2008)	On Monday, May 26, a mudslide roared down Bevier Creek on Mountain View Road. The slide washed out the road and flooded the residence of Kim and Lisanne Powell. The Powells were eating supper at the time and escaped with their young daughter just one step ahead of a ten-foot wall of mud. The Powell residence was hit again on Tuesday by the second slide, when the back walls collapsed and mud flowed through the home. Also on May 26th, the south fork of the Dore River was blocked by at least three avalanches. The the large ice dam gave way, a surge of water, mud and logs from all the slides washed down the river and flooded the residences and roads along the Dore River. A helicopter later flow emergency personnel through the gap in the avalance, estimated to be 50 ft high.
1986	May	Debris Flow	Spittal Creek	MoH (1999)	Debris flow on Spittal Creek, probably caused by warm weather, which caused flooding of Highway 16.

Year	Month	Type of Hazard	Location	Source	Description of Event
1986	May	Debris Flow	Eustis Creek	MoH (1999), Firth Hollins Resource Scienc Corp. (1999)	Debris flow on Eustis Creek (creek above Cardinal Ranch) which deposited mud and debris onto the property and Highway 16. Hay field downstream of Highway 16 covered by several inches of silt.
1988	July	Debris Flow	Valemont	BGC Landslide Database	Debris flow occurred at CN Albreda Mile 54.3 Klapperhorn, impacting CN bridge and Kinder Morgan TMPL pipeline.
1990	June	Debris Flow and Flood	Stone Creek, Bevier Creek, McBride	Septer (2007) and Canadian Disaster Database (2022)	On June 11, debris flow at Stone Creek washed out 100 m of Highway 97 and three houses in the Stoner area. The creek was five times and more its normal width of 8 m. On the evening of June 12, the sudden melt caused Bevier Creek to overflow its banks about 5 km north of McBride. The creek caused a slide described as a “wall of mud, boulders and snow.” At noon on June 14, a second and third slide came down.
1990	June	Flood	Fraser River, Prince George	Septer (2007)	On June 1 after rising 70 cm in 24 hours, the Fraser River at Prince George reached flood stage with the gauge at South Fort George reading 9.4 m. The rainy weather caused the rapid snowmelt in the Upper Fraser River basin. Spring snowpack conditions were similar to those in 1972, the year of the last major flood in Prince George. On June 2 at 4 p.m., the river peaked at 9.91 m, flooding parks and basements and forcing about a dozen families out of their homes.
1990	August	Landslide	McBride	Eggington (2005)	The Kendall Glacier rock avalanche occurred approximately 30 km northwest of McBride. The failure initiated on a rock slope above a glacier and produced about 0.2 Mm3 of debris that travelled 1.2 km. Thunderstorms likely produced isolated and perhaps heavy rain fall at the site.
1991	July	Debris Flow	Leona Creek	MoH (1999)	Debris flow on Leona Creek on July 25, caused flooding of residential property and Highway 16. Triggered by warm weather.
1993	May	Debris Flow, Mud flow	Goslin Creek	Piteau (1993), MoH (1999)	Debris flow or mud flow in Goslin Creek on May 13, 1993. Caused flooding of residential property and Highway 16.
1993	May	Debris Flow	Leona Creek	MoH (1999)	Debris flow on Leona Creek on May 13, caused flooding of residential property and Highway 16. Triggered by warm weather.
1994	Spring	Debris Flow	Cardinal Ranch	Firth Hollins Resource Science Corp. (1999)	Highway 16 approx. 5 km east of Cardinal Ranch (Spittal Creek?) was closed for several days in the spring of 1994 by a mud slide/debris torrent of 120 m width and 4 - 6 m depth.
1996	July	Debris Flow	Spittal Creek	MoH (1999)	Debris flow on Spittal Creek, probably caused by warm weather, which caused flooding of Highway 16.
1996	November	Flood	Nechako River, Prince George	Septer (2007) and Canadian Disaster Database (2022), GeoNorth Engineering Ltd. (June 30, 1998)	A combination of higher than average flow and a sudden cold snap led to a series of ice jamming events in the Lower Nechako River between November 19th and 25th. It resulted in severe flooding and localised bank erosion in Prince George. An ice jam five kilometres long raised water levels along the low-lying regions of Prince George, flooding industrial and residential areas.
1997	May - July	Flood	Nechako River, Fraser River, Mud River, Shelly, Miworth, Prince George, Goat River	Septer (2007)	During May and July, high flows on the Nechako River, the Fraser River and other tributaries caused severe bank erosion at many communities beyond any experienced in recent years, resulting in a series of evacuations. Early in July, high water on the Goat River washed out 1 km of Highway 16 between McBride-Prince George. Some private roads also washed out. By mid July, much of the Nechako River Park and Trail System in the City of Prince George was still under water.
1997	July	Debris Flow	Leona Creek	MoH (1999)	Debris flow on Leona Creek on July 6, caused flooding of residential property and Highway 16. Triggered by warm weather.
1997	August	Debris Flood	Spittal Creek	MoH (1999), Firth Hollins Resource Scienc Corp. (1999)	Debris flood on Spittal Creek on August 6 caused by intense rain and caused flooding of Highway 16. First surge crossed Hwy 16, covering the road with several inches of mud and debris (velocity of first wave clocked on speedometer at 25 mph/11.7 m/sec, discharge of about 66 cm/s). Second surge was mostly contained in the ditchline. Flow followed down the Hwy 16 ditch for several hundred meters, overtopped culverted hay field access and stopped 800 m west along Hwy 16. 408 mm SWE
1997		Debris Flow	Wilson Creek	AMEC (March 11, 2002)	Debris flow at Wilson Creek, caused flooding of residential property and Read Road. 408 mm SWE

Year	Month	Type of Hazard	Location	Source	Description of Event
1999		Debris Flow	Wilson Creek	AMEC (March 11, 2002)	Debris flow at Wilson Creek, caused flooding of residential property and Read Road.
1999		Rock Avalanche	Kendall Glacier	Geertema et al. (2006), Geertsema & Cruden (2008)	Rock avalanche at Kendall Cglacier near McBride, likely triggered by a thunderstorm.
2000		Debris Flow	Wilson Creek	AMEC (March 11, 2002)	Debris flow at Wilson Creek, caused flooding of residential property and Read Road.
2001	July	Earth Slide	Lucerne	BGC Landslide Database	Earth slide at CN West of Jasper causing a train locomotive to derail
2002	April	Mudslides and Flood	Prince George	Septer (2007)	Around April 13-14, Prince George received 32 mm of precipitation, more than than the average for the entire month of April. At least two homes and the main road to the airport flooded and 15-m deep washout occurred near Prince George. A couple of minor mudslides were reported in the region. During the late night of April 14, a mud, rock and debris slide came down that covered a 35-m section of the Trans-Canada Highway up to a depth of 3-4 m.
2002	June	Flood	Nechako River, Fraser River, Prince George	Septer (2007)	A combination of hot weather and rain caused the Skeena, Bulkley, Nechako and Fraser rivers, already running high from the summer melt of a snowpack that had not as large in 55 years, to rise. On June 19 in Prince George, the upper Fraser River passed the 9.4-m mark. In south Fort George, the river breached its bank.
2005	Unknown	Flood	King/Nevin Creek, Highway 16	MOTI	Flooding.
2005	January	Flood and Mudslide	Naver Creek, Hixon, MacKenzie, Rollston Creek	Septer (2007)	Early on January 24, two ice jams on Naver Creek flooded four homes and caused a closure of Highway 97 near Hixon. The largest jam grew overnight to a length of 1.5 km. The flow in Naver Creek was reported as three times normal. One the same day, a mudflow in the Pine Pass area about 20 km north of the MacKenzie junction temporarily closed Highway 97. Soon after the highway reopened to single lane alternating traffic, it was closed again just before noon when Rollston Creek jumped its banks due to flooding associated with higher than normal temperatures and heavy rain and snowmelt.
2006	Unknown	Debris flood/Flood	Hargraves Creek	MOTI	Debris deposition under MOTI bridge
2007		Flood	McBride, Fraser River	Wheeler (2008)	High water in the Fraser River east of McBride
2007	April	Unknown	McBride	DriveBC	Wash out 38 km east of McBride. The road was reduced to single lane alternating traffic.
2007	November	Post-fire debris flow	Moose Lake	MOTI	Debris flow following prescribed burn at Moose Lake, Highway 16.
2007	December	Flood	Nechako River, Prince George	Canadian Disaster Database (2022)	On December 10, 2007 an ice jam in the Nechako River that, at one point, stretched as long as 33 kilometres, caused localized flooding. A state of emergency was declared.
2008	March	Unknown	Bear Lake	DriveBC	Debris on Road 5 km south of Bear Lake. The road was reduced to single lane alternating traffic
2008	May	Flood	Fraser River, Nechako River, Prince George	Globe and Mail (May 23, 2008)	Around a dozen homes in a low-lying residential area of Prince George were placed on evacuation order on May 22 in response to rising water levels on the Fraser River at the city's eastern edge. The Fraser was moving so powerfully that its tributary, the Nechako River, could not fully flow into it and was beginning to back up on itself.
2008	July	Debris flow/Debris flood	Cottonwood Creek	MOTI	Cottonwood Creek and adjacent two drainages experienced flows on July 2.
2008	July	Unknown	Tete Jaune	DriveBC	Wash out 25 km east of Junction with Highway 5, in Tete Jaune Cache, resulting in single lane traffic
2008	July	Mud Slide	Tete Jaune	DriveBC	Mud slide on Highway 16, with the highway closed in both directions.
2008	January	Flood	Fraser River, Nechako River, Prince George	CBC News (Jan 7, 2008)	Water levels on the Nechako River reached their highest level in 200 years in early January after a large chunk of ice shifted creating new flooding in Prince George. Many homes and businesses in the River Road and Pulp Mill Road areas were flooded for the second time that winter. The flooding is a result of ice on the Nechako River and the nearby Fraser River blocking the normal flow of the rivers, affecting areas along the Nechako above the confluence of the two rivers.
2009	April	Unknown	Prince George	DriveBC	Wash out 22.5 km on Highway 97, south of Junction with Highway 16, 22.5 km south of Prince George. The road was reduced to single lane alternating traffic

Year	Month	Type of Hazard	Location	Source	Description of Event
2011	May	Flood	Cottonwood River, Willow River, Salmon River	CBC News (May 18, 2011)	River Forecast Centre put out flood warnings for the Cottonwood River and the Willow River. On May 17, one of the evacuated homes on the Cottonwood River was destroyed by provincial officials after erosion from the floodwaters left it half in the river, and several others remain at risk
2011	July	Flood	Fraser River, Prince George	CBC News (July 11, 2011)	A flood warning in the central interior of B.C. was extended from Prince George to Quesnel. About a dozen Prince George homes along Farrell Street were evacuated when water levels reached 9.61 metres, more than two metres above the average for this time of year.
2011	May	Mud Slide	Prince George	DriveBC	Mud Slide 30 km east of Prince George. The road was reduced to single lane alternating traffic
2012	Unknown	Debris Flow	McPhee Creek	MOTI	Minor debris and erosion impacts on Raush Valley road.
2012	May	Unknown	Bear Lake	DriveBC	Highway 97 closed in both directions 10 km north of Bear Lake because of a washout.
2012	April	Unknown	Prince George	DriveBC	Wash outs on Highway 16, 73 km east and 85 km east of Prince George in late April
2012	June	Flood	Tete Jaune	DriveBC	Flooding on Highway 16, closed at the junction with Highway 5, in Tete Jaune.
2012	June	Debris Flow	Leona Creek	AMEC (2012, June 21)	Debris flow on Leona Creek during the night of June 16-17. High flows eroded the toe of a previous rock slide in the upper channel of Leona Creek. Estimated volume of event was 5,000 to 10,000 cubic meters. Upstream of Highway 16, debris largely remained within channel and natural levees andartifical channel berms. Flow depths were up to 2 to 3 m. Large avulsion into old side channel. Local bridge crossing was destroyed. Debris came within 5 m of residence on fan. Debris deposited onto Highway 16 at depths up to 1 to 1.5 m.
2012	June	Debris Flow	Leona Creek	AMEC (2012, August 14)	Subsequent debris flow event on Leona Creek on June 23 caused by heavy rain-on-snow. Reached and blokced Highway 16, but primarily contained within the channel on the residential property that is crossed.
2012	August	Debris Flow	Leona Creek	AMEC (2012, August 14)	Debris flow on Leona Creek during the night of August 8-9 caused by heavy precipitation. Debris was deposited outisde of the channel banks on the side opposite from the site property.
2013	April	Unknown	Prince George	DriveBC	Debris on Highway 97, 10 km south of Prince George. Road reduced to single lane.
2013	May	Flood	Fraser River, Prince George	Prince George Citizen (May 16, 2013)	A rapid snowmelt and unseasonably high temperatures prompted a flood warning on May 14. In response to the rising waters Paddlewheel and Cottonwood Island parks were closed. No residential evacuation orders or warnings were issued by the city to those living in the flood plain.
2013	June	Mud Slide	Tete Jaune	DriveBC	Mud slide on Highway 16, 8 km west of junction with Highway 5, in Tete Jaune.
2014	Unknown	Landslide	Tete Jaune	MOTI	Landslide at Tete Jaune weigh scale. Approximately 500 m3 deposited on Highway 16.
2014	October	Unknown	Bear Lake	DriveBC	Debris on Road 3 km south of Bear Lake. The road was reduced to single lane alternating traffic
2014	May	Mud Slide	McBride	DriveBC	Mud slide 40 km west of McBride on Highway 16
2014	June	Mud Slide	Tete Jaune	DriveBC	Mud slide on Highway 16, 1 km east of junction with Highway 5, in Tete Jaune. Highway closed in both directions.
2014	September	Mud Slide	Tete Jaune, Leona Creek	DriveBC, MOTI	Mud slide on Highway 16, 8.8 km west of junction with Highway 5, in Tete Jaune Cache. Road reduced to a single lane. Debris flow on Leona Creek on September 24.
2015	March	Unknown	Bear Lake	DriveBC	Wash out on Highway 97, 2 km north of Bear lake. Road reduceds to single lane.
2016	July	Mud Slide	Hixon	DriveBC	Mud slide on Highway 97, 8 km north of Hixon. Road reduced to single lane.
2016	October	Rock Slide	Tete Jaune	DriveBC	Rock slide on Highway 16, 12.6 km east of junction with Highway 5, in Tete Jaune.
2016	October	Rock Slide	Jasper	DriveBC	Rock slide on Highway 16, west of Jasper. Highway closed in both directions.
2016	November	Unknown	Bear Lake	DriveBC	Wash outs at several locations along Highway 97, south of Bear Lake. Road reduced to single lane
2016	December	Flood	Fraser River, Nechako River, Prince George	CBC News (Dec 15, 2016)	A recent cold snap caused an ice jam near the confluence of the Fraser and Nechako Rivers. Prince George officials shut down a portion of the Heritage River Trail because of rising river levels.
2017	February	Unknown	Prince George	DriveBC	Wash out on Highway 97, 8.7 km north of junction with Highway 16, in Prince George. Single lane closed
2017	March	Mud Slide	Prince George	DriveBC	Mud slide on Highway 97, about 5 km north of Prince George. Single lane closed
2017	March	Earth Slide	Prince George	BGC Landslide Database	Mud Slide 4.7 km north of Prince George near 704-714 John Hart Hwy. Southbound lane closed for about 26 hrs.
2018	May	Unknown	McBride	DriveBC	Debris on road on Highway 16, 26 km west of McBride. Highway closed in both directions
2018	January	Flood	Nechako River, Prince George	CBC News (Jan 8, 2018)	A rapid change in temperature in Prince George, with temperatures dropping to below -30 C on Dec. 28 and then rising above freezing by Jan. 5 caused the Nechako River to flood the North Nechako neighbourhood on the northwest edge of the city. B.C. River Forecast Centre measured a 1.3-metre rise along the Nechako River over the weekend due the warming temperatures.
2020	April	Flood	Prince George	DriveBC	Washouts and flooding causing closures on many highways and roads (e.g., Highway 16, Highway 97) between Prince George and Vanderhoof around April 25th.

Year	Month	Type of Hazard	Location	Source	Description of Event
2020	June	Flood	Dore River	McElhanney (March 11, 2021)	On June 23/24, 2020, a large rainstorm coupled with snowmelt runoff resulted in extreme flows (peak discharge of 169 cms, corresponding to a 70 to 100 year return period event) in the Dore River, causing significant bank erosion between the Highway 16 bridge and the CN railway bridge. Multiple properties lost land due to the erosion.
2020	July	Debris Flows	Willox Creek, McBride	BCG (September 25, 2021)	A series of debris flows occurred on Willox Creek. High fines content debris flows on Willox Creek achieved flow velocities of 6 m/s in the confined channel sections and carried boulders up to 1 m diameter.
2020	July	Unknown	Prince George	DriveBC	Washout on Beaverley Road Eastbetween Blackwater Road and Muralt Road which caused the road to be closed in both directions
2020	August	Unknown	Hixon	DriveBC	Washout at Hixon Creek Rd on Highway 97 caused the road to be closed in both diections
2020	September	Flood	Dore River	McElhanney (March 11, 2021)	Flood event on the Dore River between September 1-3 with peak flows of 148 cms, equivalent to a 25-year return period event. Minimal additional bank erosion occurred following the previous flood in June.
2021	April	Landslide	Bednesti	Prince George Citizen (April 11, 2021)	On April 21, a landslide was reported along Highway 16 between Bednesti and Vanderhoof. The slide, which undercut a section of the highway, was caused by water flowing from the adjacent bank and pooling under the highway.
2021	April	Unknown	Baldy Hughes	DriveBC	Washout on Blackwater Rd between Punchaw Rd and Baldy Hughes. Road closed in both directions
2021	May	Unknown	Prince George	DriveBC	Washout on Louis Drive near Prince George between Emile Cres and Hubert Rd. Road closed in both directions.
2021	July	Landslide	Valemont	The Rocky Mountain Goat (Sep 8, 2021)	The slide began sloughing large amounts in mid-to-late July and sent large amount of debris towards Swift Creek which supplies the Village's drinking water and flows near private properties. As a result, an evacuation alert was issued for 40 properties downstream, but the alert was lifted Aug. 13th after geotechnical assessments and a decrease in falling debris.
2021	June/July	Flood	McBride	CBC News (June 30, 2021), The Rocky Mountain Goat (n.d.)	Rapid snow melt due to a heat wave in late June and early July caused the Fraser River to rise rapidly in the Robson Vallley, causing flooding at McBride. Low-lying areas were flooded, but the waters did not reach the the bridge deck of the Fraser River crossing.
2021	October	Landslide	Tete Jaune	DriveBC	Rock slide at Hwy 5/16 JCT at Tete Jaune causing Highway 16 to be closed in both directions.
2022	July	Flood	Prince George	Prince George Citizen (Jul 6, 2022)	A thunderstorm on July 5 brought sheets of rain that dumped for nearly a full half-hour and turned city streets into lakes, causing localized flooding that damaged some buildings. Some of the worst flooding was in the light industrial area around Queensway.
n.d.		Landslide	Valemont	Bornaetxea et al (2023)	A landslide inventory that covers roughly 1200 km2 was completed. 1286 landslides were compiled and classified into 11 categories and three levels of uncertainty.
n.d.		Landslide	Morkill River, Hellroaring Creek, Forgetmenot Creek, Cushing Creek	Froese (1998)	Includes inventory of landslides in the Morkill River, Hellroaring, Forgetmenot, and Cushing creeks watersheds based on airphoto analysis.
Ongoing	1946-	Earth Slide	Prince George	BGC Landslide Database	Ongoing earth slide along CN Nechako at Mile 23. Has been moving since 1946
Ongoing	2000-	Landslide	Amies Slide, Highway 16	MOTI	Slow creeper towards Fraser R., 25 -50mm every few years. 150m Hwy. 16 affected to centerline.
Ongoing	2000-	Landslide	Sugarbowl Slide, Hwy16	MOTI	Slow creeper 25 to 50mm every few years. 70m wide, across Hwy. 16.
Ongoing		Landslide	Hixon Hill Slide Highway 97	MOTI	Slow creeper 25 to 50mm every few years. Hwy. 97.

APPENDIX D
STUDY AREA BACKGROUND

D-1 PHYSIOGRAPHY

The RDFFG lies within the general physiographic regions of the Interior Plateau, the Rocky Mountain Trench (RMT), and the Columbia and Rocky Mountains (Holland, 1976). The northwestern portion of the district that lies within the Interior Plateau is further divided into the Fraser Basin, the Nechako Plateau, and the McGregor Plateau. This area is generally characterized by flat or gently rolling surfaces at low-lying elevations, incised by major river systems (Fraser, Nechako, Salmon, Muskeg, Willow) and their tributaries. Much of the area is covered in features from the last glaciation, including glacial lakes, eskers, meltwater channels, and drumlins. The Nechako River drains the Nechako Plateau and flows north and east to its confluence with the Fraser River at Prince George. Major tributaries of the Nechako include the Chilako River, located 15 km west of Prince George.

To the east of the low-lying plateau sits the Rocky Mountain Trench. The trench parallels a fault system between the Rocky Mountains and Columbia Mountains and is occupied by the Fraser River in its southern section and the Parsnip River in its northern. Between these two sections, the trench is dissected by the McGregor Plateau at McGregor River. Here, the western wall of the trench merges with the Fraser Basin, and the eastern wall is offset approximately 24 km northeast.

The Hart, Misinchinka, and Park ranges of the Rocky Mountains make up the border between the RDFFG and Alberta. In the most northeastern Hart Ranges, mountain peaks are moderately rugged, with elevations generally below 2,300 m. The Parsnip River flows northwest from the Parsnip Glacier in the Southern Hart Ranges through the northern RMT to its outlet at Williston Lake near Mackenzie. The Misinchinka Ranges, between the RMT and Azouzetta Lake, also have relatively low-lying rounded peaks (2,000 m) compared to the Park Ranges, which include the highest peak in the Rocky Mountains, Mount Robson, at 3,954 m. The Park Ranges are characteristically rugged, with knife-like ridges and cirque glaciers, dissected and drained by tributaries flowing into the Fraser River.

The Fraser River originates in the Rocky Mountains just south of Yellowhead Lake near the BC-Alberta border. It flows north and west through the RMT before exiting and turning south just north of Prince George. In total, the Fraser drains a 220,000 km^2 area, including major tributaries in the district, such as McLennan River, Raush River, Bowron River, McGregor River, Salmon River, Willow River, and Nechako River.

The Cariboo and Monashee ranges of the Columbia Mountains make up the southwestern border of the district to the Cariboo Regional District (CRD) and Thompson-Nicola Regional District (TNRD). Mountain summit elevations range from 2,100 to 3,600 m and, due to intense glaciation, exhibit glacial features including sharp peaks and sawtooth ridges carved by cirque glaciers and U-shaped trunk valleys.

D-2 ECOREGIONS

The RDFFG spans 16 ecosections[1] that divide eight ecoregions[2] (Demarchi, 2011). Figure D-1 illustrates the boundaries of each ecoregion and Table D-1 provides a summary of the characteristics of the ecosections.

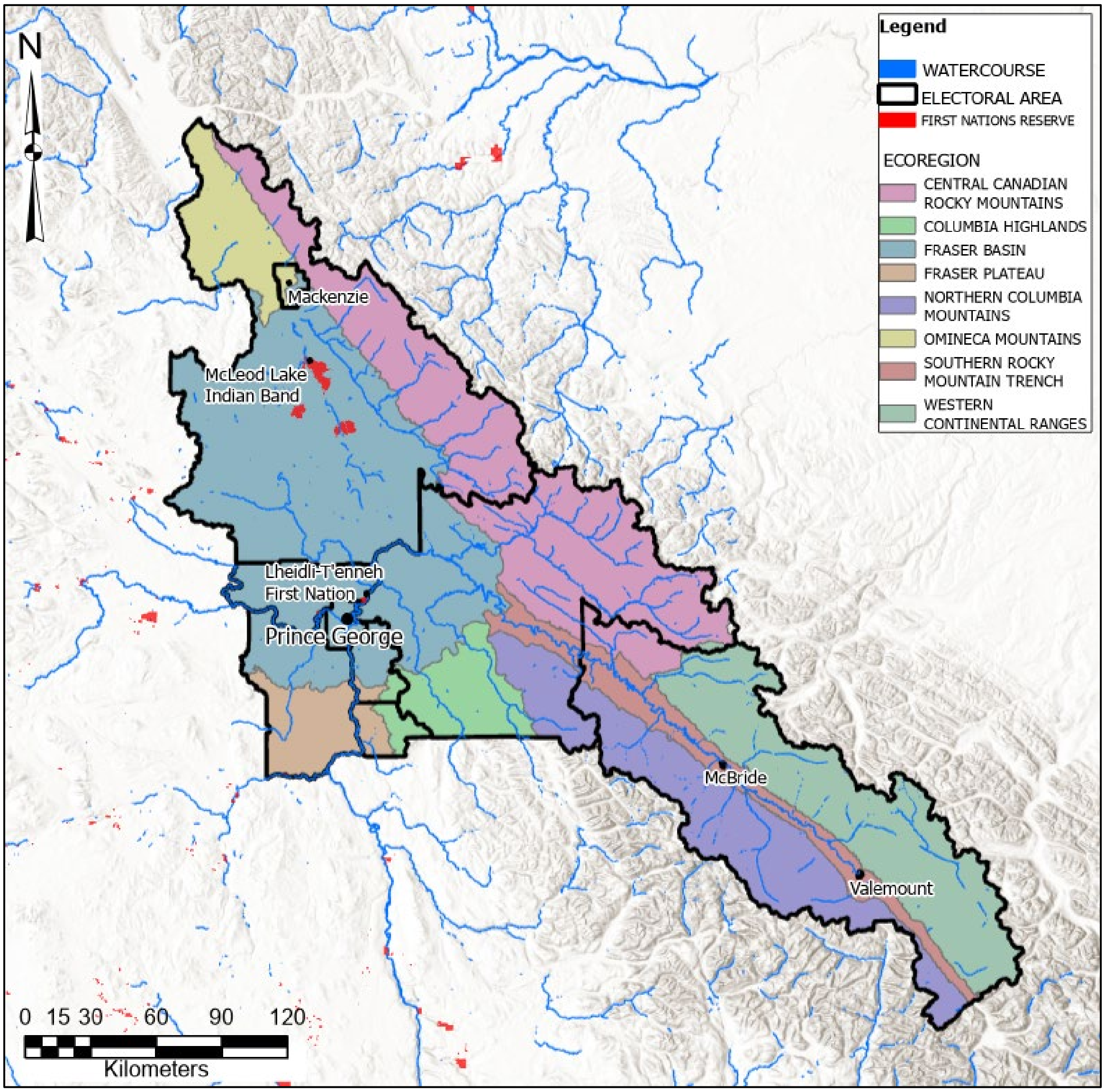

Figure D-1 Ecoregions within the RDFFG (Demarchi, 2011).

[1] Ecosections are areas with minor physiographic and macroclimatic or oceanographic variation. Ecosections are typically mapped at a 1:250,000 scale for resource emphasis and area planning (Demarchi, 2011).

[2] Ecoregions are areas with major physiographic and minor macroclimatic or oceanographic variation. Ecoregions are typically mapped at 1:500,000 scales for strategic planning (Demarchi, 2011).

Table D-1 Ecoregions and ecosections of the RDFFG (as defined by Demarchi, 2011 and shown on Figure D-1).

Ecoregion	Ecosection	Area Within RDFFG (km^2)	Physiography	Climate	Major Watersheds	Vegetation
Northern Columbia Mountains	Cariboo Mountains	5,931	High, rugged, ice-capped mountains and narrow valleys, with summits increasing in height to the south	Wet and humid conditions from easterly flowing Pacific air. Periods of intense cold and snow from cold Arctic air influxes.	Drained via the upper Fraser River by the Slim, Haggen, Dome, Wolverine, Goat, Milk, Dore, Castle, Raush streams	Sub-Boreal Spruce forests in the northwestern valley bottoms; Lower valleys have wet Interior Cedar-Hemlock forests; Mid-upper slopes Engelmann Spruce-Subalpine forests
	Northern Kootenay Mountains	284	High, rugged, ice-capped mountains	Highest precipitation in the ecoregion from moist Pacific air. In winter, Arctic air moves through the Rocky Mountain Trench, bringing cold spells to the valleys	North Thompson River, Adams River, Revelstoke reservoir, Duncan reservoir	
Columbia Highlands	Bowron Valley	2,401	Bordered by low highlands and ridges to the west, rugged mountains to the east, and rounded hills to the south. Glacial features such as eskers, drumlins, and meltwater channels are prevalent	Moist and cold; In the winter, cold, dense Arctic air brings heavy snowfall	Bowron River, Willow River; Naver, Abbay, and Sovereign streams	Sub-Boreal Spruce forests in the wide valleys and lower mountain slopes; Engelmann Spruce and Subalpine Fir forests on middle and upper mountain slopes
Fraser Plateau	Quesnel Lowland	886	Lowland trench	Arctic air from Fraser Basin enters readily; Precipitation from Pacific air over Columbia Mountains	Fraser River, Quesnel River, Cottonwood River, West Road/Blackwater	Sub-Boreal Spruce; Douglas-fir on south-facing slopes; Aspen, lodgepole pine, white spruce with higher elevations
	Nazko Upland	1,168	Rolling upland with areas of higher relief; Contains Fawnie and Nechako ranges shield volcanoes	Sub-continental; Cold winters, warm summers, maximum precipitation in late spring/early summer	Nechako River, West Road/Blackwater, Nazko	Sub-Boreal Pine-Spruce forests along West Road and Nazko river valleys; Engelmann Spruce-Subalpine Fir at highest elevations
Southern Rocky Mountain Trench	Upper Fraser Trench	2,609	Broad, flat, intermountain glacial plain	Moist and cool, with a distinct rainshadow from Valemount to McBride. Periods of extreme cold and snow from central interior Arctic air	Fraser River, McLennan River, Canoe River, Rausch River, Holmes River, Morkill River, Torpy River	Sub-Boreal Spruce forests above the Fraser and adjacent benchlands; Wetlands and muskegs in the northern portion; Cedar-Hemlock forests throughout
	Big Bend Trench	331	An intermountain plain predominantly filled by the Kinbasket Lake reservoir	High precipitation	Historically drained by the Columbia and Canoe rivers; Succour and Whitepine creeks	
Western Continental Ranges	Northern Park Ranges	7,101	High, rugged mountains (Park Ranges), mountain glaciers and moderately wide valleys	Cold and wet; Arctic air via Athabasca Valley or Rocky Mt Trench brings intense cold and snow	Fraser River, Forgetmenot River, Morkill River, Ptarmigan and Hugh Allen rivers	Sub-Boreal Spruce forests in upper Fraser; Interior Cedar-Hemlock forests in west-facing valleys; Engelmann Spruce-Subalpine forests in upper slopes
Fraser Basin	McGregor Plateau	6,021	Rolling upland that is a displaced portion of the Ricky Mountain Trench	Cool, moist climate; In winter, cold Arctic air can cause long periods of cold and snow	Upper Fraser River, lower Parsnip Riverlower McGregor River; lower Bowron and lower Willow rivers	Interior Cedar-Hemlock forests along eastern margin; Elsewhere dominated by Sub-Boreal Spruce forests
	Nechako Lowland	10,498	Flat or gently rolling lowland with dissection by the Fraser and Nechako rivers; Glacial features (eskers, drumlins, meltwater channels) throughout	Sub-boreal; Humid conditions in the summer due to surface heating; In the winter, long periods of intense cold and snowfall	Fraser River, Stuart, Nechako, Salmon, and Muskeg rivers	Lowland dominated by Sub-Boreal Spruce forests
	Babine Upland	546	Rolling upland with low ridges; Glacial features such as eskers, meltwater channels, and drumlins throughout	Humid and rainy conditions; Extreme cold and snow events in the winter	Sutherland and Fulton rivers into Babine Lake, Babine River, Nation River, Hautete, Middle, and Tacho	Sub-Boreal Spruce forests on lower slopes; Engelmann Spruce-Subalpine forests on mid and upper slopes
Central Canadian Rocky Mountains	Southern Hart Ranges	7,560	Transitional range of rounded mountains with some glaciers remaining in the south	Moist Pacific air stalls along western margin and brings heavy precipitation	Parsnip River, McGregor, Torpy, and Herrick rivers	Interior Cedar-Hemlock and Sub-Boreal Spruce forests on lower slopes; Engelmann Spruce-Subalpine forests on mid and upper slopes

Ecoregion	Ecosection	Area Within RDFFG (km^2)	Physiography	Climate	Major Watersheds	Vegetation
	Northern Hart Ranges	3,437	Rounded mountains	Heavy precipitation as rain and snow	Upper Clearwater River, Cucette Creek, Parsnip River, Pine, Burnt, and Sukunka rivers	Sub-Boreal Spruce forests in valley bottoms and low slopes; Wetlands in some flat-bottomed valleys; Engelmann Spruce-Subalpine forests on mid and upper slopes
	Misinchinka Ranges	301	Rugged, rounded mountains and deep, narrow valleys; area of transitional height	High precipitation; Moist Pacific air stalls over the mountains, and Arctic air lays in the Peace River Reach	Peace reach of the Williston Lake reservoir Clearwater River, Graham River	Boreal White and Black spruce forests in Ospika valley; Sub-Boreal Spruce in other valleys and low slopes; Engelmann-Spruce on higher slopes
Omineca Mountains	Parsnip Trench	1,888	Wide intermountain plain between the Omineca Mountains and the Rocky Mountains	Convective showers throughout the summer; Cold Arctic air brings heavy snowfall or rain during winter	Manson River, Nation River, Williston Lake reservoir	Sub-Boreal Spruce forests
	Manson Plateau	542	Rolling upland south of the Omineca Mountains	Pacific air and surface heating brings precipitation in the summer; Long periods of intense cold and snow in the winter	Nation River, Driftwood River, Takla Lake	Sub-Boreal Spruce in valley bottoms; Engelmann-Spruce on mid to upper slopes; Alpine Boreal Altai Fescue occur on high slopes and ridges

D-3 GEOLOGY

This section summarizes bedrock and surficial geology in the RDFFG to provide context on the fundamental earth processes that built the landscape assessed in this study.

D-3.1 Bedrock Geology

The RDFFG lies within the Western Cordillera and spans the Foreland, Omineca, and Intermontane morphogeologic belts. The Omineca Belt formed when the Intermontane superterrane, a mix of volcanic rocks from the Stikinia and Quesnellia volcanic arcs and marine sedimentary rocks, collided with the western margin of the ancient North American continent approximately 180 to 150 million years ago. This collision produced the metamorphosed rocks that make up the Columbia and Omineca mountains. This event caused the eastward and upward movement of the sedimentary rocks of the superterrane to form the Rocky Mountains, part of the Foreland fold and thrust belt. Thus, the rocks in this region are heavily folded and faulted. As illustrated in Figure D-2, bedrock is predominantly sedimentary in the eastern portion of the district and transitions to predominantly volcanic and metamorphosed rocks to the west.

The Columbia Mountains in the region are largely composed of sedimentary and meta-sedimentary rocks, mainly quartzite (Cariboo Mountains) and gneissic units (Monashee Mountains). The Park Ranges of the Rocky Mountains are made up of limestone and quartzite and are relatively less folded and faulted than the ranges to the east and west, the best example of these gently dipping beds being the peak of Mount Robson. To the northwest, the Hart Ranges differ from the Park Ranges in stratigraphy and structure due to late Tertiary uplift and dissection. The Misinchinka Ranges consist of sedimentary and metamorphic rocks, and coincide with the position of the Misinchinka schists, which lie along the east side of the RMT.

Approximately 55 million years ago, a faulting event occurred that essentially split the present day Rocky Mountains from the Columbia Mountains and formed the southern portion of the Rocky Mountain Trench. The geology of the trench consists of primarily younger and unconsolidated sedimentary rocks such as sandstones and conglomerates.

West of the trench, the Fraser Plateau and Basin are underlain by basaltic volcanic flows and sedimentary rocks of the Intermontaine Belt, with occurrences of Omineca schists and intrusives along the margin.

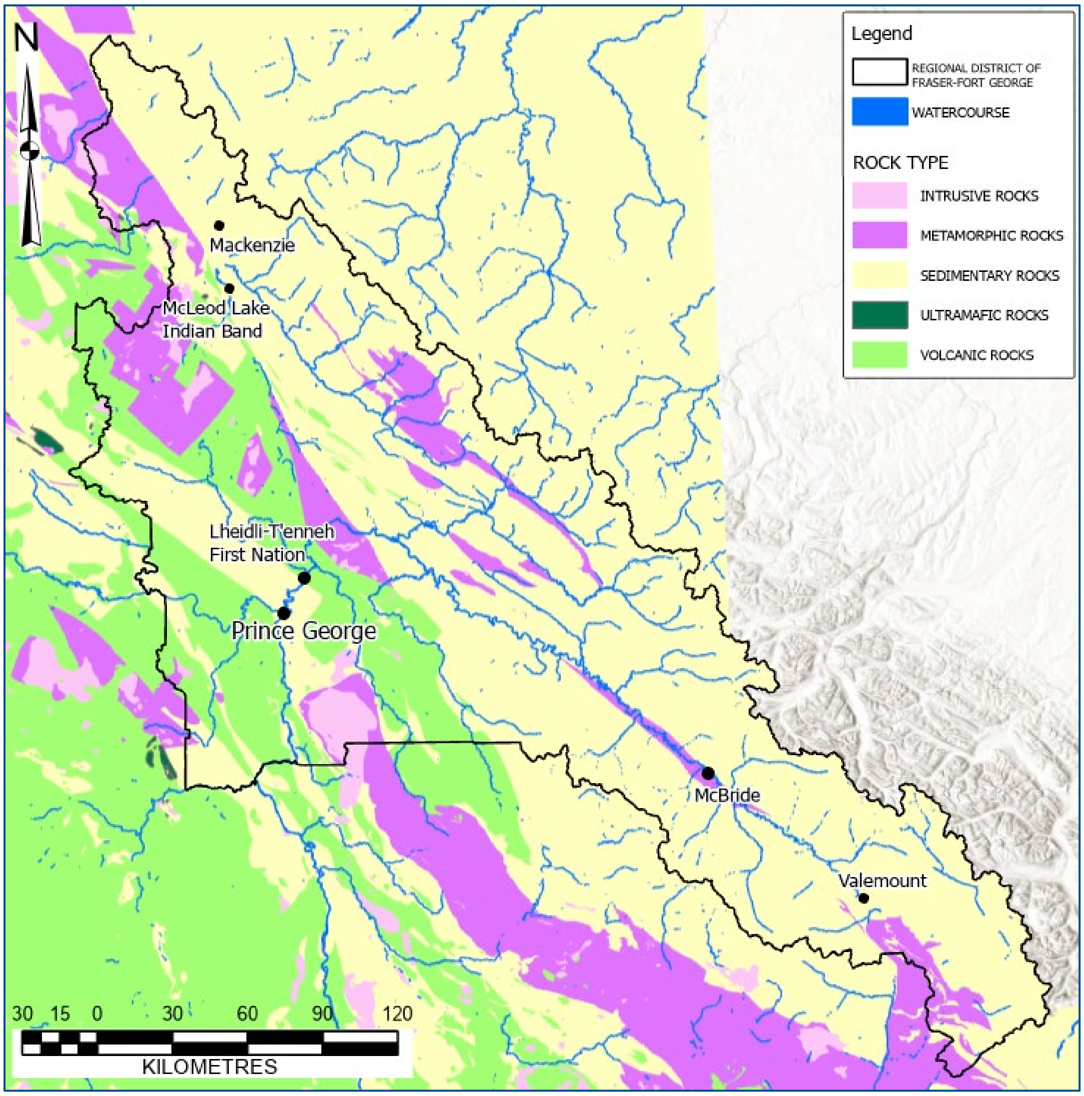

Figure D-2 Bedrock geology of the RDFFG. Digital mapping and bedrock classes from Cui et al. (2017).

D-3.2 Surficial Geology

Surficial geology features of the RDFFG are relics of glacial and post-glacial processes that took place between approximately 126,000 to 11,700 years before present while repeated advances and retreats of glaciers occurred across North America. Thick glaciers covered most of the RDFFG during the most recent glacial maximum, which occurred approximately 25,000 to 10,000 years ago (Holland, 1976; Church & Ryder, 2010; Clague & Ward, 2011). The region was influenced by montane glaciers advancing from local peaks, coalescing in valley bottoms, and subsequently retreating. As glaciers flowed across the landscape, they sculpted the bedrock into cirques, horns, comb ridges, and “U”-shaped valleys. Reduced mountainous glaciers and ice fields are still present within alpine areas of the Rocky and Columbia Mountains.

As the glaciers began to melt, they left extensive till and ice-contact deposits on mountain flanks and on plains elevated above contemporary river levels. Valley bottoms were typically covered with successions of advance-outwash gravel, diamictic sandy silt and gravel till, and recessional-outwash gravel. Retreating glacial ice also dammed river valleys throughout the RDFFG, forming extensive glacial lakes. Glacial Lake Fraser occupied the central interior, thought to cover 14,500 km^2 across Prince George, west to Vanderhoof, and south to its southern dam at Williams Lake (Miller et al., 2021). Intra-basin features developed as the westward retreating ice sheet allowed for subglacial channels to deliver large volumes of sediment and water into the lake. Large amphitheatre features are found where subaqueous fans have been incised by gently sloping, wide, flat-bottomed channels. The largest example of this is at Prince George, which is located on a large subaqueous fan that was developed by deposition from the Stuart River esker complex, incised by erosional channels and truncated by the Nechako River to the south. When the glacial dam at Williams Lake failed, glacial Lake Fraser drained rapidly, which caused liquefaction flowslides in the saturated silt and sand fan deposits.

Repeated glacial lake outburst floods filled the major river valleys and deposited sediment comprised primarily of silt, sand, and clay onto the valley floors (Fulton, 1965; Ryder et al., 1991). Terraces in glacial lake deposits that formed from these post-glacial streams and rivers are present within broad valleys (e.g., the Fraser) but have been heavily eroded in some smaller valley systems. Slopes that were over steepened by glacial processes release material and form colluvial deposits at the base of steep slopes. Slow earth slides and flows occur in weak, cohesive glacial and paraglacial soils – clay till, and glaciolacustrine silt and clay. A network of creeks and rivers drain steep mountain and valley slopes within the RDFFG and transport sediment to floodplains and alluvial fans, before ultimately being deposited into large lake basins or carried further downstream by large rivers. Available sediment supply in larger rivers is controlled by upstream sediment sources (e.g., bedrock-sourced landslides) and erosion of surficial deposits in valley bottoms (e.g., alluvial and glaciofluvial sediments).

D-4 HYDROCLIMATE

D-4.1 Hydroclimate

Averaged across the RDFFG over the period of 1961 to 1990, the mean annual temperature (MAT) is approximately 1.3ºC and the mean annual precipitation (MAP) is 1,100 mm, of which approximately 600 mm (55%) is snowfall (precipitation as snow [PAS]) (Table D-2). Seasonal precipitation is most abundant in the winter (350 mm) compared to the lowest abundance falling in the spring (200 mm) with a wide range across the RDFFG reflecting the physiographic diversity (Section D-1).

Table D-2 Historical (1961 to 1990) annual and seasonal climate statistics across the RDFFG (Wang et al., 2016).

Climate Variable	Historical Mean[1]	Range across the RDFFG
Annual		
Temperature (ºC)	1.3	-7.6 to +4.7
Precipitation[2] (mm)	1,100	400 to 3,200
Snowfall (mm)	600	150 to 2,500
Seasonal Precipitation		
Fall[3]	300	100 to 1,000
Winter[4]	350	100 to 1,000
Spring[5]	200	50 to 600
Summer[6]	250	100 to 850

Notes:

1. Historical climate is characterised based on the reference climate grid generated from the Parameter Regression of Independent Slopes Model (PRISM) interpolation method. Historical data are based on the CRU-TS 4.05 dataset (Harris et al., 2020).
2. Precipitation includes both rain and snow as a liquid equivalent.
3. September, October, and November.
4. December (previous year for an individual year), January, and February.
5. March, April, and May.
6. June, July, and August.

D-4.2 Climate Change

Air temperature is projected to warm due to climate change, resulting in an increase in the proportion of annual precipitation that is expected to fall as rainfall instead of snow, especially during the fall and spring. Precipitation is projected to increase as much as 30% in the fall and spring by the end of the century based on the “Fossil Fuel Development” emission scenario (Table D-3). In contrast, summer precipitation is projected to decrease by 5% by the end of the century under the same emission scenario. Precipitation projections suggest that climatic conditions in the RDFFG will be wetter in the winter and drier in the summer (Table D-3).

Table D-3 Projected annual and seasonal climate statistics across the RDFFG (Mahony et al., 2022).

Climate Variable	Historical Mean[1]	Mid-century[1,2,3]		End of Century[1,2,3]	
		Middle of the Road	Fossil Fuel Development	Middle of the Road	Fossil Fuel Development
Annual					
Temperature (ºC)	1.3	+2.8	+3.6	+3.7	+5.9
Precipitation[2] (mm)	1,100	+10	+10%	+15%	+20%
Snowfall (mm)	600	-15%	-20%	-20%	-40%
Seasonal Precipitation					
Fall[3]	300	+15%	+15%	+20%	+30%
Winter[4]	350	+10%	+10%	+10%	+15%
Spring[5]	200	+15%	+20%	+20%	+30%
Summer[6]	250	+5%	+0%	+5%	-5%

Notes:

1. The mean is based on an ensemble of projections across 13 Atmosphere-Ocean General Circulation Models (GCMs).
2. Projections assume an emission scenario of SSP2-45 for the “Middle of the Road” and SSP5-85 for “Fossil Fuel Development” scenario.
3. The mid-century projections cover 2041 to 2070 while the end of century projections cover 2071 to 2100.
4. Precipitation includes both rain and snow.
5. Snowfall was derived from temperature and/or precipitation values and is not a direct output of the climate models.
6. September, October, and November.
7. December (previous year for an individual year), January, and February.
8. March, April, and May.
9. June, July, and August.

The spatial distribution of changes to hydroclimate variables shows a larger increase in temperature and precipitation in the northern portion of the RDFFG (Figure D-3). An increase in snowfall is not expected anywhere in the RDFFG (Table D-3). The largest decrease in snowfall is expected in valley bottoms (Figure D-3).

Projected change to climate has implications for the frequency, intensity, and seasonality of floods, steep creek hazards, and landslides. Appendices E-G summarize climate change implications specific to each hazard type.

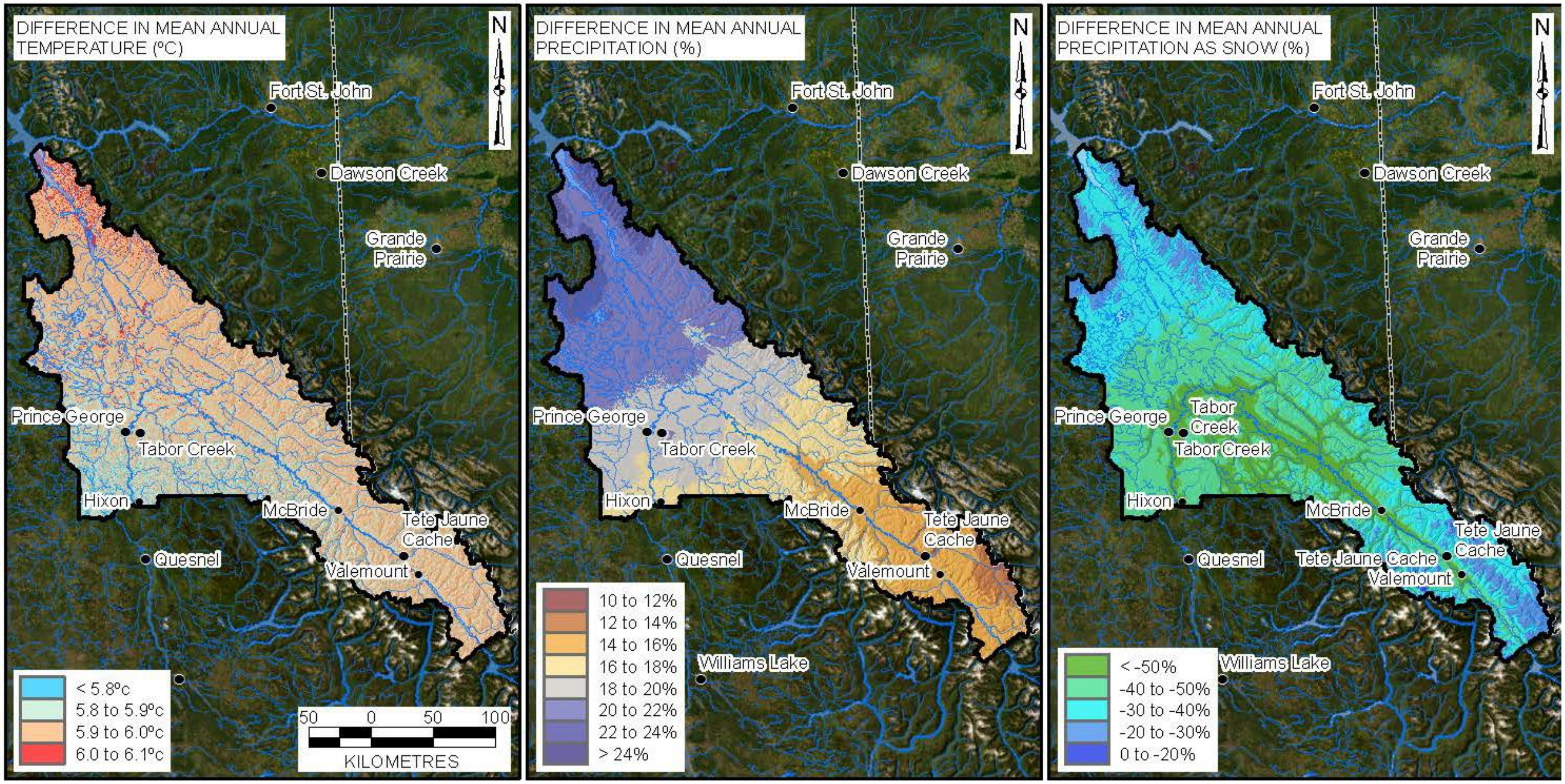

Figure D-3 **Future changes to temperature (a), precipitation (b), and snowfall (c) from historical (1961 to 1990) conditions assuming a Fossil Fuel Development scenario (SSP5-85) by the end of the century (2071 to 2100) across the RDFFG (Mahony et al., 2022).**

REFERENCES

Church, M. & Ryder, J. (2010). Physiography of British Columbia. In: R. Pike, T. Redding, R. Moore, R. Winkler & K. Bladon (Eds.) Compendium of forest hydrology and geomorphology in British Columbia. Victoria, B.C.: British Columbia Ministry of Forests, pp. 17–44.

Cui, Y., Miller, D., Schiarizza, P., & Diakow, L.J. (2017). *British Columbia digital geology*. British Columbia Ministry of Energy, Mines and Petroleum Resources, British Columbia Geological Survey Open File 2017-8, 9p. Data version 2019-12-19.

Demarchi, D.A. (2011). *Ecoregions of British Columbia*. Third Edition. Ministry of Environment. Victoria, British Columbia.

Fulton, R.J. (1965). Silt deposition in late-glacial lakes of Southern British Columbia. *American Journal of Science, 263*, 553-570.

Harris, I., Osborn, T.J., Jones, P., & Lister, D. (2020). Version 4 of the CRU TS monthly high-resolution gridded multivariate climate dataset. *Science Data, 7*, 109. https://doi.org/10.6084/m9.figshare.11980500

Holland, S. R. (1976). *Landforms of British Columbia: a physiographic outline*. British Columbia Department of Mines and Petroleum Resource. Bulletin no. 48.

Mahony, C.R., Wang, T., Hamann, A., & Cannon, A.J. (2022). A CMIP6 ensemble for downscaled monthly climate normals over North America. *International Journal of Climatology, 42*(11), 5871-5891. https://doi.org/10.1002/joc.7566

Miller, B.G.N., Iverson, R.M., Clague, J.J., Geertsema, M., & Roberts, N.J. (2021). Channel-amphitheatre landforms resulting from liquefaction flowslides during rapid drawdown of glacial Lake Fraser, British Columbia, Canada. *Geomorphology, 392*(1), 107898. https://doi.org/10.1016/j.geomorph.2021.107898

Ryder, J.M., Fulton, R.J., & Clague, J.J. (1991). The Cordilleran ice sheet and glacial geomorphology of southern and central British Columbia. *Géographie Physique et Quaternarie, 45*, 365-377. https://doi.org/10.7202/032882ar

Wang, T., Hamann, A. Spittlehouse, D.L., & Carroll, C. (2016). Locally downscaled and spatially customizable climate data for historical and future periods for North America. *PLoS One 11*, e0156720. https://doi.org/10.1371/journal.pone.0156720

APPENDIX E
CLEARWATER FLOOD HAZARD ASSESSMENT

E-1 INTRODUCTION

This appendix describes data sources and methods used by BGC Engineering Inc. (BGC) to identify and characterize clearwater flood geohazards within the Regional District of Fraser-Fort George (RDFFG). BGC used different approaches to characterize flood hazards at both a screening-level (Tier 1) and base-level (Tier 2) level of detail for select hazard areas. Each tier relies on an increasing amount of detail (Table E-1).

Table E-1 Description of Floodplain Mapping "Tiers" representing different levels of detail.

Level	Description
Tier 1	**Flood Hazard Identification (screening-level)** - Hazard identification maps help identify areas susceptible to flood inundation across large spatial extents using desktop approaches.
Tier 2	**Base-level Floodplain Mapping** - Flood Hazard Maps further refine the Tier 1 results to better characterize flood hazards over larger areas and are a pre-cursor to more costly detailed flood mapping using hydraulic models. The hydraulics in Tier 2 are modeled using a hydraulic model developed using lidar when available but do not include a bathymetric survey to define the channel geometry.
Tier 3	**Detailed-level Floodplain Mapping** - Further refines estimates of flood extents and characteristics across a range of scenarios at greater detail than base-level maps by including bathymetric survey data and includes considerations for climate change. Detailed Flood Hazard Maps includes multiple flood scenarios, delineation of flood construction-levels (FCLs), and can be used to inform policy, risk assessment, and risk management decisions.

E-2 APPROACH OVERVIEW

Riverine flooding resulting from inundation due to an excess of clearwater discharge in a watercourse or body of water, submerging land outside the natural or artificial banks that is not normally under water.

Historical flood events that have occurred within the RDFFG are generally due to flooding from rainfall, snowmelt, and glacial runoff processes (e.g., Figure E-1). The focus of the clearwater flood hazard assessment for the RDFFG is on riverine flooding from precipitation (rainfall or snowmelt driven) within natural watercourses and lakes. The assessment does not consider flooding due to other mechanisms such as failure of engineered structures (e.g., dams and dikes), and does not consider ice jam floods. Steep creeks subject to debris flows and debris floods are separately assessed, as described in Appendix F.

Figure E-1 Fraser River in flood near McBride, BC, due to snowmelt in the spring. Photo Credit: Sandra James (Rocky Mountain Goat, July 6, 2021)

Historical floodplain maps were previously developed by the Province of BC for select areas of the RDFFG based on the stationary 200-year return period, or 0.5% annual exceedance probability (AEP[1]), flood event (Table E-2). Maps within the Prince George area are in the process of being updated (Sites 1-3, Table E-2) as part of the federal Flood Hazard Identification and Mapping Program (FHIMP). The detailed floodplain mapping (Tier 3) are not yet publicly available and were not available for use in this study.

Table E-2 Summary of historical floodplain mapping within the RDFFG.

Site No.	Watercourse	Type	Electoral Area	Map Year
1	Chilako River	Floodplain	Prince George	1996
2	Fraser and Nechako Rivers at Prince George	Floodplain	Prince George	1997
3	Salmon River near Prince George	Floodplain	Prince George	1986
4	Naver and Hixon Creeks at Hixon	Floodplain	E	1993

[1] Annual Exceedance Probability (AEP) is the estimated probability that an event will exceed a specified magnitude in any year. For example, a flood with a 0.5% AEP has a one in two hundred chance of being reached or exceeded in any year. AEP is used alongside of 'return period' to describe flood recurrence intervals in this study

Flood areas across the RDFFG were identified from the following spatial sources:

1. Historical flood event inventory.
2. Prediction of floodplain extents for streams and rivers using terrain analysis.
3. Prediction of floodplain extents for selected rivers using hydraulic modelling.

Table E-3 summarizes the approaches used to identify and characterize clearwater flood hazard areas across the RDFFG.

Table E-3 Summary of clearwater flood identification approaches.

Approach	Hazard Assessed	Application
Historical flood event inventory	All mapped watercourses and waterbodies prone to clearwater flooding.	Identification of creeks and rivers with historical precedent for damaging floods. The historical flooding locations are approximate locations where known landmarks adjacent to a watercourse were flooded, or specific impact to structures (roads, houses) was reported in media. The historical flood event inventory is summarized in Appendix D.
Prediction of floodplain extents using terrain analysis (Tier 1)	All mapped watercourses without existing floodplain mapping.	Identification of low-lying areas adjacent to streams using a terrain-based flood hazard identification approach that was previously developed province-wide by BGC. This method provides screening level identification of flood inundation extents and depths for a 200-year flood event (0.5% AEP). Tier 1 mapping results area available in Cambio.
Prediction of floodplain extents using hydraulic modelling (Tier 2)	Selected flood hazard areas without existing floodplain mapping.	Method provides base level flood hazard mapping including flood inundation extents, flow depths, and velocities based on a lidar digital elevation model. Tier 2 mapping results are available in Cambio.

The following sections describe methods and data sources used to identify and characterize clearwater flood hazard areas as summarized in Table E-3. The results of the Tier 1 and 2 mapping were merged to provide one flood hazard layer for exposure analysis.

E-3 HISTORICAL FLOOD EVENT INVENTORY

BGC compiled a historical flood, steep creek, and landslide event inventory across the RDFFG and digitized the locations of historical events from Septer (2007), DriveBC (British Columbia Ministry of Transportation and Transit [BC MoTT], May 2024), hazard reports (e.g., McElhanney, March 11, 2021), and recent freshet-related floods and landslides sources (e.g., media reports), as compiled in Appendix C. Historical flood events were used to confirm flood-prone low-lying terrain outside of areas with historical floodplain maps.

E-4 DISTRICT-WIDE FLOOD HAZARD IDENTIFICATION (TIER 1)

District-wide Tier 1 floodplain identification was based on previous floodplain mapping developed by BGC (April 19, 2024), which was used to approximate the flood inundation extent for a 200-year (0.5% AEP) flood on mapped watercourses. Table E-4 summarizes the key data inputs used to develop the Tier 1 floodplain mapping layer including terrain, flow and water level data, and hydrographic features. Section E-4.1 summarizes methods used to develop the floodplain layer, and Section E-4.2 describes gaps and limitations.

Table E-4 Summary of key data inputs

Data Type	Description	Reference
Terrain	The COP-30 dataset has global coverage, at 30 m resolution in Canada, with an absolute vertical accuracy of <4 m and an absolute horizontal accuracy of < 6 m. This dataset comes from the TanDEM-X satellite mission (2011 to 2015).	Copernicus
Mean Daily Peak Flows	Annual maxima mean daily peaks flows were downloaded for analysis of the 200-year (0.5% AEP) flood at each hydrometric station. The watershed area reported by the WSC was used in the analysis.	WSC
Water Level	Mean daily water levels and discharge values were downloaded for rating curve development at each hydrometric station. The rating curve was used to estimate the corresponding water depth associated with the 200-year (0.5% AEP) flood at each hydrometric station.	WSC and USGS
Waterbodies	The hydrographic features in this dataset include waterbodies (e.g., lakes) that were used to merge with the Tier 1 floodplain map.	CanVec

E-4.1 Hazard Layer Development

BGC used the empirical approach “Global Floodplain” (GFPLAIN) by Nardi et al. (2019) as an efficient process to simulate floodplains over large areas, compared to methods optimized for detailed, smaller area assessment (e.g., hydraulic-based methods). The GFPLAIN method relies on an empirical model that relates flood depth to watershed area using the following equation, where *a* and *b* are constant coefficients [Eq. E-1].

$$Flood\ Depth = a(Watershed\ Area)^b \qquad \text{[Eq. E-1]}$$

BGC advanced this method beyond the approach described by Nardi et al. (2019) by developing regional coefficients to capture the diversity of BC across six ecozones (Figure E-2) (NRCan, 2010). Table E-5 summarizes the 561 WSC and USGS hydrometric stations used for analysis, which are distributed in each ecozone.

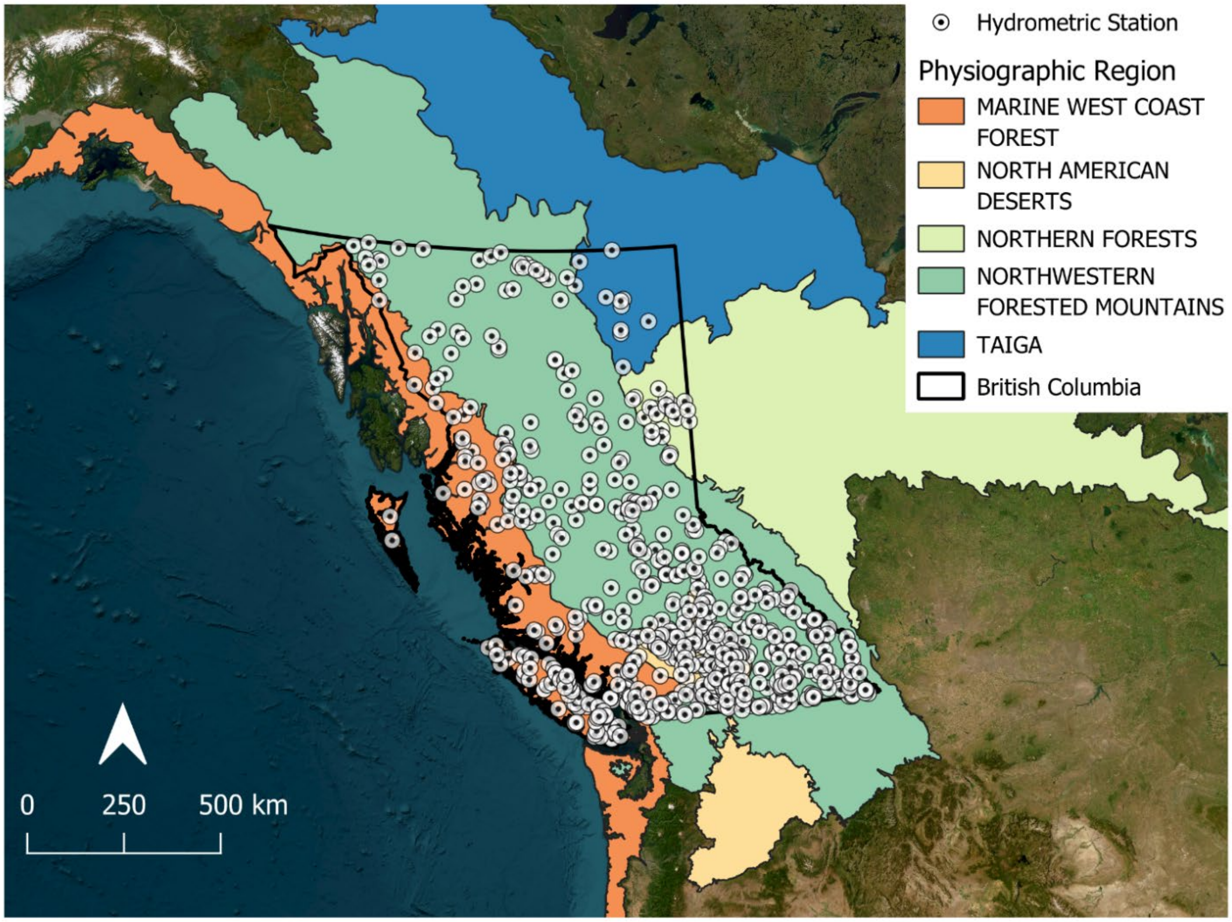

Figure E-2 Ecozones of BC and hydrometric stations used for the empirical modelling of floodplain depth.

Table E-5 Number of hydrometric stations analyzed in each ecozone.

ID	Ecozone	Number of Hydrometric Stations
1	Marine West Coast Forest	107
2	North American Desserts	69
3	Northern Forests	139
4	Northwestern Forested Mountains	208
5	Taiga	38

The 200-year (0.5% AEP) flood was estimated for each WSC station using a flood frequency analysis (FFA). The FFA was based on the Annual Maxima Series (AMS) using the mean daily flow (MDF) at every hydrometric station present in the six ecoregions. The minimum record length recorded at the gauge for use in the FFA was 10 years. The Generalised Extreme Value (GEV) distribution was fit to the AMS using the linear moments for parameter estimation (Zhang, Stadnyk, & Burn, 2019).

The water depth corresponding to the 200-year (0.5% AEP) flood was estimated using a rating curve to relate water depth[2] to streamflow. The rating curve is defined by a power law developed at each hydrometric station in the six ecozones. An example of a rating curve for the *Pack River at the Outlet of McLeod Lake* (07EE010) hydrometric station located in the Northwestern Forested Mountains ecoregion is shown in Figure E-3(a). In some cases, noise was present in the stage data for lower discharge values as shown in Figure E-3(b). The lower 10% of the discharge values and corresponding stage values were removed from the dataset to improve the power law fit for the higher discharge values. Note the rating curve is based on a subset of the entire discharge record, where stage data is available.

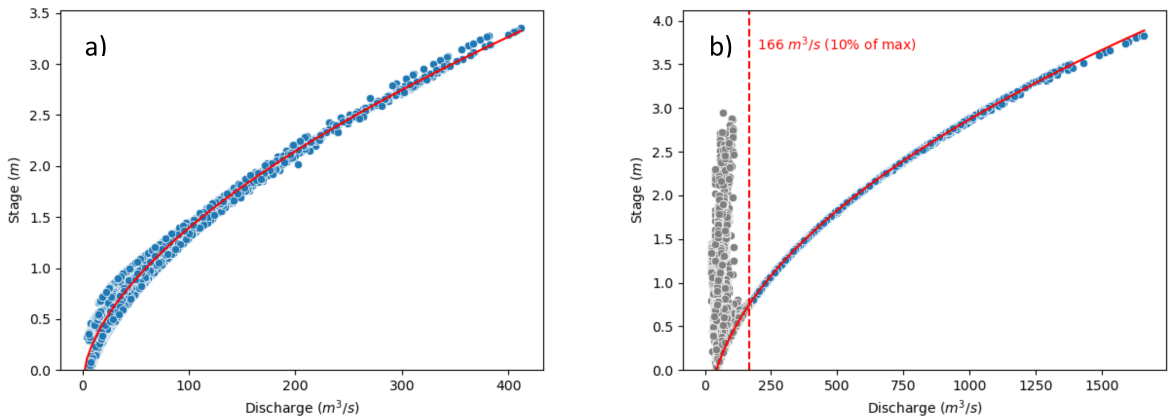

Figure E-3 Example rating curve for a) Pack River at the Outlet of McLeod Lake (07EE010) hydrometric station and b) Finlay River above Alie River (07EA005) hydrometric station. Both stations are in the Northwestern Forested Mountains ecoregion. Gray circles show data points removed from the analysis.

The water depth corresponding to the 200-year (0.5% AEP) flood and watershed area at each hydrometric station was subsequently used for the development of the regional coefficients within each ecoregion. The watershed area upstream of each hydrometric station is based on the published value provided by WSC.

Terrain analysis techniques were used to extract the stream network (in raster form) from the Copernicus 30 m DEM. Each stream network grid cell was assigned a flood depth using the watershed area based on the regional equation associated with an ecozone. This algorithm produces a gridded floodplain by identifying low-lying grid cells along a watercourse (Figure E-4). The floodplain extent is formed by the grid cells that are characterised by ground elevations that are lower than the corresponding flood elevation. The flood elevation is defined as the grid cell ground elevation plus the flood depth, expressed in meters.

The Python script and user manual of the GFPLAIN algorithm used for generating the Tier 1 floodplain map is accessible at https://github.com/fnardi/GFPLAIN with instructions for applications and reuse of the code.

[2] To build the rating curve, the flood depth was estimated by subtracting the minimum recorded stage elevation from the stage elevation corresponding to each discharge measurement. The flood depth is thus relative to the minimum stage elevation as opposed to the bottom of the channel at each station.

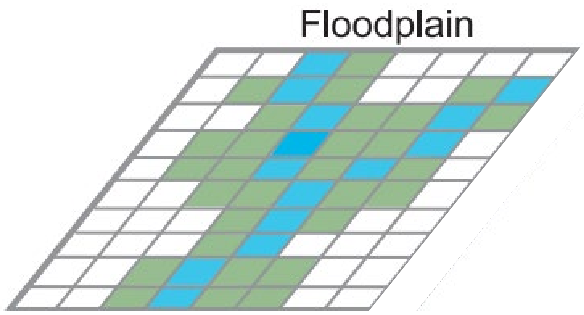

Figure E-4 Conceptual model of the gridded layer that is derived by defining grids as the 200-year (0.5% AEP) floodplain (green) whose elevations are lower than the corresponding stream network flow levels (blue) (Nardi et al., 2019).

The GFPLAIN methodology weakens in areas with low topographic relief especially where lakes and wetlands are present. As such, the CanVec database of waterbodies was merged with the Tier 1 floodplain to better define the lake extents. Each grid cell was assigned a unique identifier where 0=not flooded, 1=flooded, and 2 =waterbody (Table E-6 and Figure E-5).

Table E-6 Grid cell identifier and description.

Identifier	Description
0	Grid not considered flooded due to riverine, clearwater flooding.
1	Grid considered flooded due to riverine, clearwater flooding.
2	Grid considered to be a waterbody

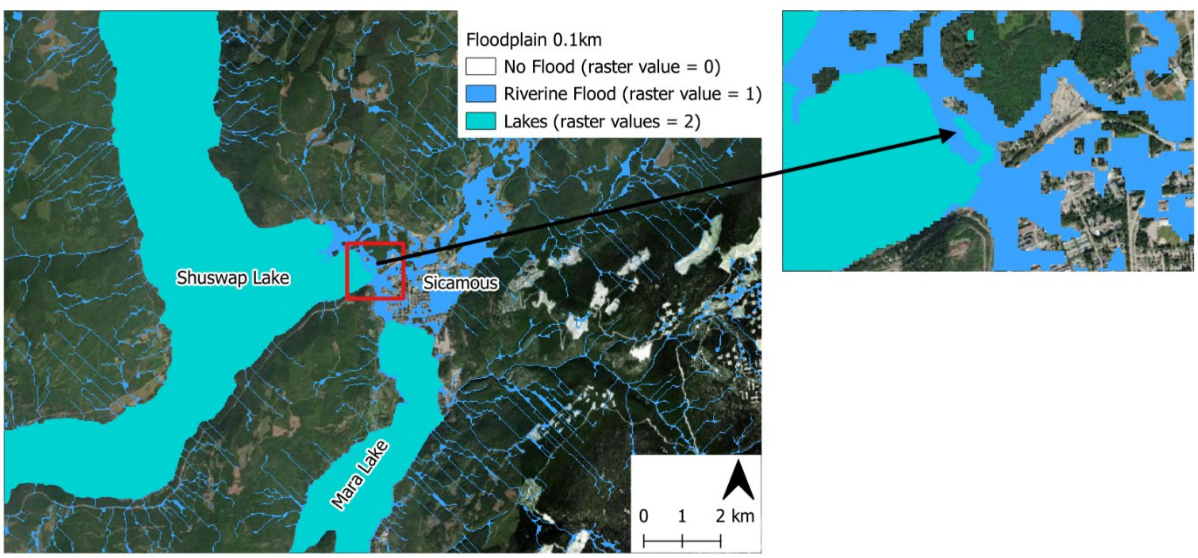

Figure E-5 Example of area where waterbodies were merged with the Tier 1 floodplain map.

Where existing, base level (Tier 2) floodplain mapping provides a more accurate simulation of 200-year flood extents. As such, BGC merged the Tier 1 floodplain layer with Tier 2 results for the 200-year flooded extent in each of the Tier 2 flood mapping areas described in Section E-5.

E-4.2 Gaps and Limitations

Appendix J compiles project gaps and limitations, including those related to flood hazard mapping.

In summary, BGC's mapping deliverable is intended as a screening tool for hazard identification and planning for more detailed floodplain mapping, in association with the hazard exposure analysis. While the mapping shows estimated 200-year flooded extents, it is not intended to show a specific flood scenario given all areas are unlikely to flood at the same magnitude at the same time.

Watercourses with less than 10 km^2 watershed areas are not shown. It is possible to prepare Tier 1 flood hazard maps for small catchments, but the utility of such mapping depends on objectives. Floodplain identification for small catchments can be unreliable in urban areas with stormwater management assets, and it does not fully represent hazard extents on small-catchment steep creeks subject to debris floods or debris flows. The chosen catchment cutoff (>10 km^2) reflects an objective to identify main-valley clear water floodplains for hazard exposure analysis.

Detailed (Tier 3) flood hazard mapping is required to consider effects of structural flood mitigation (e.g., dikes) or flow regulation (e.g., impacts of dams), which were not resolved at Tier 1 or 2 levels of detail.

E-5 SELECT BASE-LEVEL FLOOD HAZARD IDENTIFICATION (TIER 2)

Base-level or Tier 2 flood hazard mapping involves conducting hydraulic modelling and mapping using available lidar data without bathymetric survey data as an improvement to screening-level mapping (Tier 1) and as a precursor to detailed mapping (Tier 3).

BGC conducted base-level hydraulic modelling and mapping for five selected flood hazard areas for a total length of 180 km of mapping (Table E-7, Figure E-6). These areas were selected based on review of available data and feedback from participants about areas of concern for flooding and needs for improved flood policy. The selected areas include one area with historical floodplain maps (Naver and Hixon Creeks at Hixon: Ministry of Environment, Lands and Parks, October 1995) and four additional flood hazards area without previous floodplain mapping.

Tier 2 floodplain mapping provides 200-year (0.5% AEP) flood characteristics (flooding extents, depth, and velocity) under current conditions and with projected climate change. It is intended to support planning decisions (e.g. prioritizing areas for more detailed mapping), and to support emergency response plans for flood scenarios, but is not intended for regulatory use (e.g. Flood Construction Levels, FCL).

Table E-7 Selected Tier 2 floodplain mapping areas by Electoral Area.

Watercourse (Electoral Area)	Total Mapping (km)
Tabor Creek at Prince George (D)	22
Fraser River at McBride (H)	58
Fraser River at Tête Jaune Cache (H)	36
Naver and Hixon Creeks at Hixon (E)	28
McLennan River and Swift Creek at Valemount (H)	36
Total	180

This section describes the approach used to develop two-dimensional (2D) hydraulic models for base-level floodplain mapping of the selected watercourses. Included in this section are the methodologies used for developing the terrain of the channel and floodplain, a description of the modelling software used, hydrology inputs, the development of the hydraulic model, and the sensitivity analysis performed on the model.

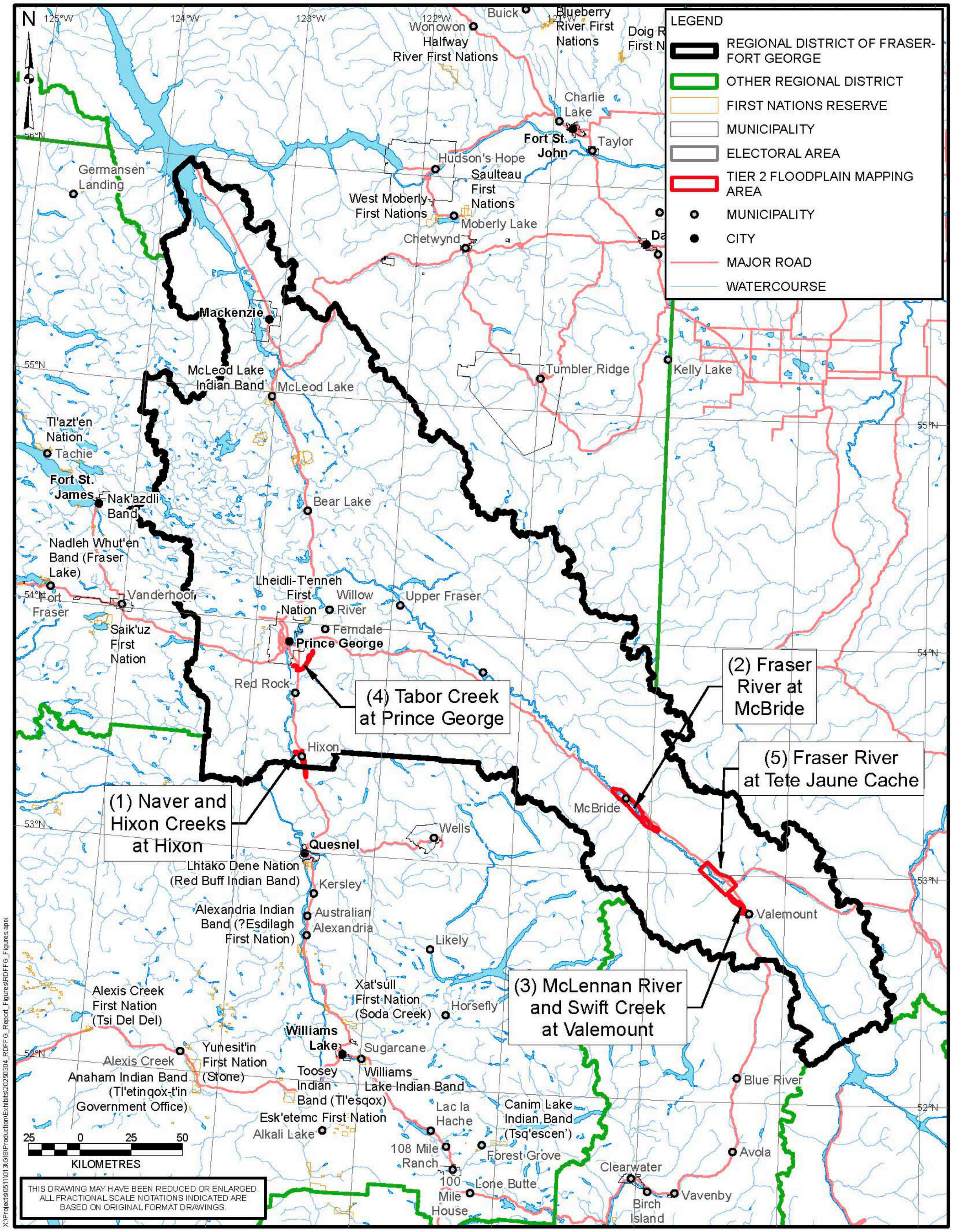

Figure E-6 Tier 2 floodplain mapping areas.

E-5.1 Hydrology Inputs

E-5.1.1 Hydrologic Regime

Winter precipitation typically falls as snow in the late fall and winter and remains stored on the ground until the spring melt period across the RDFFG. Nival (snowmelt dominant) hydrologic regimes have their annual maximum streamflow occur during the spring freshet. Streamflow typically declines after the peak, reaching low flows in late summer and fall because of low precipitation inputs and the depletion of the snowpack water supply. The monthly streamflow pattern is generally similar from year to year due to the energy available for snowmelt.

The present-day hydrologic regime of the upper Fraser River is dominated by snow accumulation in the fall/winter and a snowmelt freshet in the spring or early summer. Figure E-7 (top) displays the summary hydrograph for the *Fraser River at McBride* (08KA005) hydrometric station (watershed area: 6,890 km^2). The largest event occurred on June 12, 1972, with an instantaneous streamflow value of 1,422 m^3/s, approximately equal to a 110-year (0.9% AEP) flood. In the 71 years of recorded data, only one maximum annual discharge occurred during the fall (2010), with an instantaneous peak flow of 652 m^3/s.

The Dore River shares a similar hydrologic regime to the Fraser River. Figure E-7 (middle) displays the summary hydrograph for the *Dore River at McBride* (08KA001) hydrometric gauging station (watershed area: 409 km^2). Six of the 61 years of annual maximum flow occurred in the fall, although these peak flows occurred in years with low streamflow during the summer months due to a small snowpack. The largest event occurred on July 19, 2014, with an instantaneous streamflow value of 192 m^3/s, approximately equal to a 50-year (0.9% AEP) flood.

The Hixon Creek and Tabor Creek watersheds share similar nival-pluvial (snowmelt and rainfall) hydrologic regimes. These regimes are defined by an annual maximum streamflow during the spring freshet; however, large rain events in the fall also induce annual maximum streamflow in some years. Figure E-7 (bottom) displays the summary hydrograph for the *Naver Creek at Hixon* (08KE014) hydrometric station (watershed area: 658 km^2). This gauge has 17 years of mean daily streamflow data. The largest event occurred on May 20, 1956, with a daily mean streamflow value of 133 m^3/s.

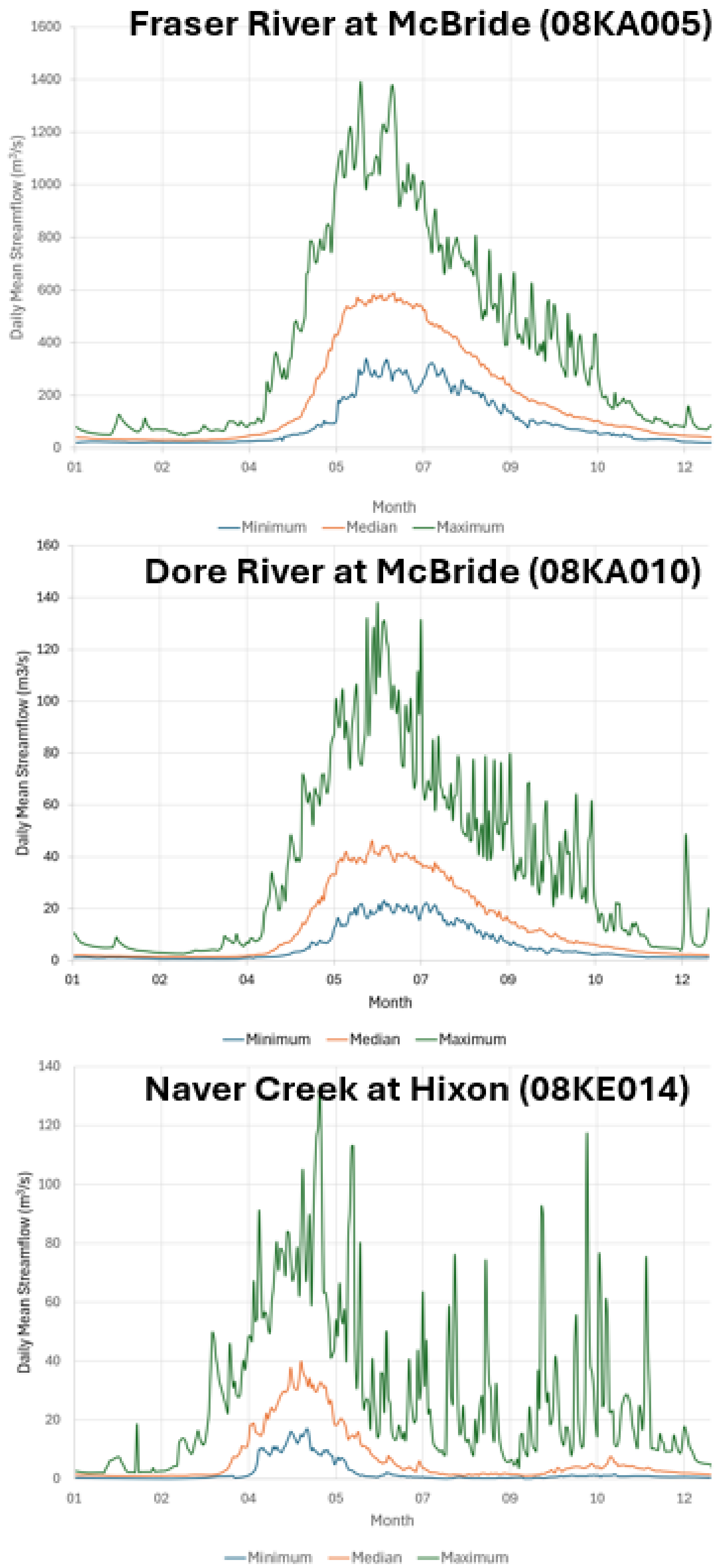

Figure E-7 Time series of daily mean streamflow data for *Fraser River at McBride* (08KA005) (top), *Dore River at McBride* (08KA010) (middle), and *Naver Creek at Hixon* (08KE014) (bottom) hydrometric stations.

E-5.1.2 Hydrology Methods

Instantaneous peak flows (IPFs) for the 200-year (0.5% AEP) flood were determined using a FFA based on historical records collected at WSC hydrometric stations. Table E-8 summarizes the FFA method used for each Tier 2 mapping area.

The two FFA methods were used based on whether the watercourse is gauged or ungauged:

1. Prorated FFA: A WSC hydrometric station is located on the same watercourse and the peak flow estimates from this station are prorated by the watershed area to the upstream model boundary location.
2. Regional FFA using the Index Flood Method for ungauged watercourses.

Table E-8 FFA methods used for each Tier 2 mapping area.

Watercourse	Method
Tabor Creek at Prince George	Index Flood (Region 1)
Fraser River at McBride	Pro-rated FFA
Fraser River at Tête Jaune Cache	Pro-rated FFA and Index Flood (Region 1)
Naver and Hixon Creeks at Hixon	Index Flood (Region 8)
McLennan River and Swift Creek at Valemount	Index Flood (Region 1)

E-5.1.2.1 Prorated Calculation

Prorated FFAs are conducted by prorating the flood quantiles estimated at the hydrometric station to the inflow location using Equation E-2.

$$\frac{Q_U}{Q_G} = \left(\frac{A_U}{A_G}\right)^n \qquad \text{[Eq. E-2]}$$

Where:

Q_U is the peak instantaneous flow rate at the ungauged site (m^3/s)

Q_G is the peak instantaneous flow rate at the gauged site (m^3/s)

A_U is the watershed area at the ungauged site (km^2)

A_G is the watershed area at the gauged site (km^2)

n is a site-specific exponent that is a function of watershed area (TAC, 2004).

An FFA was performed for the hydrometric stations with rivers within the model domain, summarized in Table E-9, to estimate the IPF for the 200-year flood. The FFA was performed on the annual maxima series using the largest IPF observed each year. For years where the IPF record was not available, the IPF was imputed using available annual maxima MDF based on a linear regression of paired IPF/MDF values. Flood quantiles were estimated using the GEV distribution (Zhang et al., 2019). The parameters of the distribution were calculated using either the *L*-moments[3] method of inference or the maximum likelihood estimate (MLE) depending on

[3] The l-moments method of inference was used to estimate the parameters of the GEV given the small sample size defined by the time periods

the period of record and fit of the data. Table E-9 summarizes the WSC stations that were used to estimate the 200-year return period event for the Fraser River at McBride and Fraser River at Tête Jaune Cache models.

Table E-9 Hydrometric stations used for pro-rated FFA.

Information	*Fraser River at McBride*	*Dore River near McBride*	*Fraser River at Red Pass*
Station ID	08KA005	08KA001	08KA007
Watershed Area (km^2)	6,890	409	1,710
Record Period	1953-2024	1915-1916, 1949-1952	1989-2022
Number of published instantaneous peak flows	71	61	33
Tier 2 modelling area	Fraser River at McBride	Fraser River at McBride	Fraser River at Tête Jaune Cache

The prorated FFA estimates the flood quantiles for the rivers in Table E-9. The model domain consists of other minor tributaries, in addition to the primary rivers. Under flooding conditions, it is unlikely for all tributaries to flood at the 200-year (0.5% AEP) event at the same time. As such, the inflow for the remaining tributaries were estimated by distributing the 200-year (0.5% AEP) IPF calculated at the 08KA005 gauge based on the watershed area.

E-5.1.2.2 Index Flood

The Index Flood is a method of regionalization that leverages short record lengths by “trading space for time”, where flood events at several hydrometric stations are pooled to estimate flood magnitude in a homogeneous region (Hoskin and Wallis, 1997). The RDFFG falls within two homogenous regions defined by BGC: Region 1 and 8 (Figure E-8). Region 1 is characterized by the influence of the Rocky Mountains whereas Region 8 has more influence from interior watersheds.

The index-flood method also requires the selection of an index-flood calculated at each hydrometric station in the region. The index-flood is intended to be a hydrological statistic that is reliable to calculate using short record (e.g., mean). The probability distribution of flood events at hydrometric stations in a homogeneous region are identical apart from a site-specific scaling factor, the index-flood. The parameters of the probabilitydistribution are estimated at each hydrometric station. These at-site estimates are combined using a weighted average to generate a regional estimate. The regional growth curve is thus a dimensionless quantile function common to every hydrometric station in the region and takes on the following form

$$\boldsymbol{X_T = \frac{Q_T}{Q_m}} \quad \text{[Eq. E-3]}$$

where X_T is the growth factor for return period T, Q_T is the flood magnitude at return period T, and Q_m is the index-flood magnitude. The flood magnitude at any return period is calculated using this relationship given the index-flood estimate. For additional information on the Index Flood approach, refer to Hoskin and Wallis (1997).

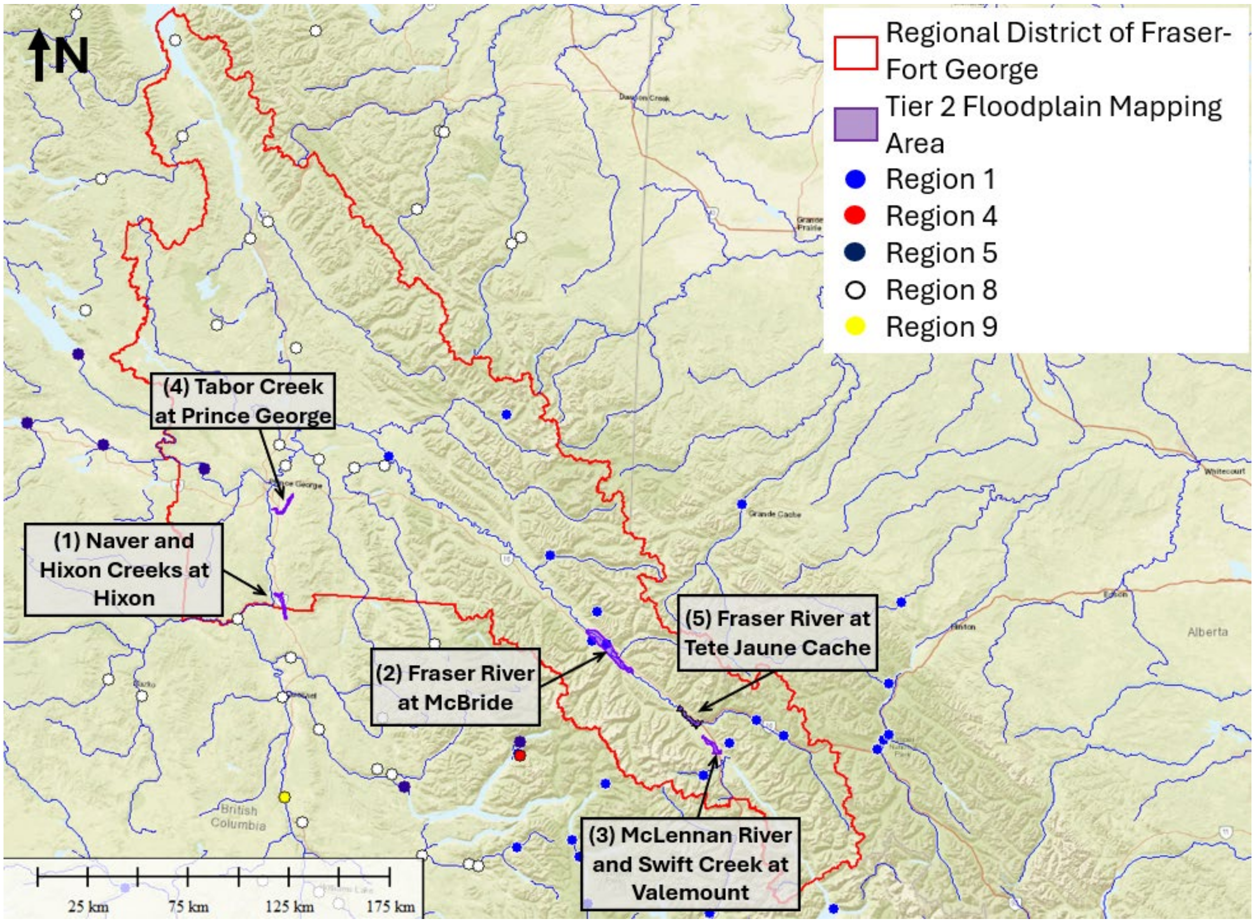

Figure E-8 Spatial distribution of the ten regions (only five shown in the figure).

The grown factor (X_T) for the 200-year (0.5% AEP) for both regions is listed in Table E-10.

Table E-10 Growth Factor (X_T) for the 200-year (0.5% AEP).

Region 1	Region 8
2.46	2.56

The index flood magnitude (IFM, Q_m) for Region 1 was calculated using the following equation for the mean annual maximum IPF.

$$\begin{aligned} log(Q_m) = & -9.9777 + 0.16182(MAT) + 0.0024786(PAS) \\ & + 0.75692(\log(Area)) + 0.18743(\log(CatchmentLength)) \\ & - 0.0040221(CN_{arcii}) - 0.055388(centroid_{longitude}) \end{aligned} \quad \text{[Eq. E-4]}$$

where:

Q_m = mean maximum annual discharge (m^3/s)

MAT = mean annual temperature (°C)

PAS = Precipitation as snow (mm)

Area = Watershed area (km^2)

CatchmentLength = Watershed length (km)

CN_{arcii} = Curve Number for antecedent moisture condition two

$Centroid_{longitude}$ = Watershed geometric centroid

The Q_m for Region 8 was determined from a machine learning model using a watershed's characteristics (e.g., watershed area, mean annual rainfall, mean annual snowfall, percentage of watershed area covered by lakes). The model was calibrated using data collected at hydrometric stations and the corresponding watershed characteristics and applied to ungauged watersheds to determine the Q_m at the crossings.

The 200-year (0.5% AEP) is calculated by multiplying the growth factor (X_T) with the index flood (Q_m) magnitude. In cases where there is some data at the gauge, it can be used to estimate the index flood. In this case, the index flood represents the mean annual maximum IPF.

E-5.1.3 Climate Change

Climate change is expected to affect the magnitude of flooding across the RDFFG. BGC reviewed streamflow projection datasets available from Pacific Climate Impacts Consortium (PCIC) and Intensity-Duration-Frequency (IDF) scaling factors from University of Western Ontario (Simonovic et al., 2015) to incorporate a climate change adjustment to the current 200-year flood event (0.5 % AEP) (Table E-11). The climate change adjustment factors ranged from 20% to 70% depending on location and the size of the watershed (Table E-12). Generally, a larger adjustment was applied for smaller watersheds (e.g., Naver and Hixon Creeks) because peak flows are projected to be increasingly rainfall generated, rather than snowmelt generated, under future climate change scenarios. The climate change adjustments are specific to both the location and flood magnitude (e.g. the same climate adjustment does not typically apply across all return period [AEPs]).

Table E-11 Climate change assessment data.

Data Source	Description	Application	How Data was Used
Continuous Streamflow Projections at Point Locations; Pacific Climate Impacts Consortium (PCIC, February 2020)	A hydrological model (VIC-GL) was driven by climate projections from six Global Circulation Models (GCMs) and two emissions scenarios, RCP 4.5 and 8.5).	For large watersheds where snowmelt drives flooding.	BGC calculated a scaling factor using a moving window FFA for the 200-year (0.5% AEP) flood and tabulated the results
Gridded Streamflow Scaling Factor (PCIC, January 2020)	Scaling factors calculated for the 200-year (0.5% AEP) across the Fraser and Peace River watersheds using one GCM (CanESM2) and one emission scenario (RCP 8.5)	For large watersheds where snowmelt drives flooding. Considered an upper estimate.	BGC tabulated the results for comparison.
Scaling Factor for historical Intensity-Duration-Frequency (IDF); University of Western Ontario (Simonovic, 2015)	Scaling factor calculated for the 200-year (0.5% AEP) 24-hour storm event using precipitation projections.	For small watersheds where convective storms drive flooding	BGC tabulated the results for comparison.

E-5.1.4 Hydrology and Climate Change Results

The hydrology and climate change results used for each Tier 2 mapping area are summarized in Table E-12.

Table E-12 Summary of flood scenarios for each Tier 2 mapping area.

Inflow Location	Watershed Area (km^2)	200-year (0.5% AEP) (m^3/s)	Climate-adjusted 200-year (0.5% AEP) (m^3/s)
Model 1: Tabor Creek at Prince George			
Tabor Creek (above Swede Creek)	65	29	40
Swede Creek	52	23	32
Unnamed Creek	23	10	14
Model 2: Fraser River at McBride			
Fraser River (upstream boundary)	4,400	970	1,170
Holmes River	800	175	215
Castle Creek	515	115	135
Raush River	1020	225	270
Dore River	408	250	300
Model 3: Fraser River at Tête Jaune Cache			
Fraser River (upstream boundary)	2,339	560	670
McLennan River	542	200	240
Tête Creek	150	140	165
Kiwa Creek	266	120	145
Model 4: Naver and Hixon Creeks at Hixon			
Naver Creek at the upstream boundary	481	102	174
Terry Creek	78	35	48
Pedley Creek	25	8	11
Hixon Creek	243	133	226
Model 5: McLennan River and Swift Creek at Valemount			
McLennan River (upstream boundary)	166	90	110
Hogan, Teepee, Crooked Creek	50	20	25
Swift Creek	132	60	75
Cranberry Creek	46	10	15

E-5.2 Hydraulic Model Development

E-5.2.1 Modelling Software

Results of the hydraulic analysis including flooding inundation extents, water depths, and flow velocities were estimated using the HEC-RAS (version 6.5) modelling software using the 2-dimentional flow option. HEC-RAS is a public domain hydraulic modelling program developed and supported by the United States Army Corps of Engineers (USACE) (Brunner & CEIWR-HEC, 2021).

E-5.2.2 Model Terrain

Detailed topographic data was used to represent the channel and floodplains for each model extent. BGC developed a 0.5 m x 0.5 m Digital Elevation Model (DEM) grid based on the lidar bare earth point cloud data retrieved from the LidarBC Portal[4]. Lidar data acquisition dates range from July 2019 to October 2019, except for the McBride area, where some sections were acquired between June 2020 and August 2021.

Since lidar captures only the water surface elevation in wetted areas, adjustments to either; 1) the channel geometry or 2) the discharge, can be applied if the discharge at the time of lidar acquisition is known:

1. Terrain Adjustment with a Projected Channel:
   The terrain model is modified by projecting a channel below the water surface. Water depths at specific locations are estimated using Manning's equation, based on the recorded discharge during lidar acquisition and an assumed cross-sectional channel shape (typically trapezoidal). Channel longitudinal slopes and top widths are derived from the lidar DEM. A 2D bathymetric channel surface is then interpolated from the estimated cross-sections.
2. Unadjusted Terrain with Recorded Discharge Correction:
   The lidar DEM is used without terrain modifications. The recorded discharge during the lidar acquisition is subtracted from the flood discharges used for modelling.

The second approach, unadjusted discharge with recorded discharge correction, was used for the Fraser River at McBride model, where a flood discharge using the lowest recorded value for the period of lidar collection was applied. In cases where the discharge at the time of the lidar acquisition is not known or when the channel conveyance is much smaller than the flood discharge being modeled, no adjustments were made. This was the case for the remaining four models, where the lidar DEM was used without adjustment due to the absence of discharge data during the lidar acquisition. The channel water surface elevation observed in the lidar DEM for these models was assumed to represent low-flow conditions.

E-5.2.3 Manning's n

In common with many hydraulic models, HEC-RAS 2D uses the Manning's roughness coefficient (Manning's n) to represent the hydraulic flow roughness. In floodplain areas, Manning's n varies with landcover. As a first step the model domain was split into land classes based on a 30-m resolution landcover dataset published by Natural Resources Canada (2019) (Table E-13). The land cover types within this dataset were associated to Manning's n values based on Chow (1959). Due to the lack of clear definition in the landcover dataset for the main channel area, channel polygons were generated to adjust the roughness values within the main channel. The spatial distribution of the Manning's values used in each model is presented within the corresponding model section.

[4] https://lidar.gov.bc.ca/

Table E-13 Associating land class with Manning's n.

Land Class	Manning's n
Temperate or sub-polar needleleaf forest	0.1
Sub-polar taiga needleleaf forest	0.1
Temperate or sub-polar broadleaf deciduous forest	0.1
Mixed forest	0.1
Temperate of sub-polar shrubland	0.07
Temperate of sub-polar grassland	0.035
Sub-polar or polar shrubland-lichen-moss	0.035
Sub-polar or polar grassland-lichen-moss	0.035
Wetland	0.044
Cropland	0.035
Barren lands	0.025
Urban or built-up	0.06
Water	0.034
Snow and ice	0.04

E-5.2.4 Hydraulic Structures

The flow constriction of the channel at bridges was accounted for by including the bridge embankments on either side of channel within the terrain model. However, the accuracy of the hydraulics at the crossing is uncertain without a survey to define the geometry of the bridge including the geometry and elevation of the bridge deck and soffit.

Several culverts are documented within the modelled areas (BC MoTI, 2017). At embankments with culverts having a diameter of 600 mm or larger or where multiple culverts are installed, notches were cut through the embankment in HEC-RAS via the terrain modification tool. These modifications allowed the water to pass from one side of an embankment to the other without explicitly modelling the culvert. An exception to this approach was made for three groups of culverts in the Tabor Creek at Prince George model. The modelled culverts correspond to the crossings at Willow Cale Forest Service Road and the railroad, located 1 km east (upstream) of the model outlet, as well as the Cariboo Highway crossing. Culverts smaller than 600 mm in diameter and undocumented culverts that might be within the modelled area were assumed to be blocked during the modelled flooding events.

E-5.2.5 Simulation Settings

The HEC-RAS 2D models were run using the shallow water equations with a Courant controlled time step[5]. The shallow water equations generally provide an accurate representation of flow

[5] The Courant number is the product of the velocity and the time step divided by the distance step. For a Courant controlled time step, the time step will be halved if the Courant number for any cell exceeds the maximum Courant number set by the user.

dynamics, especially in areas with sharp constrictions, expansions, or changes in flow direction (e.g., meander bends, bridges, etc.). The maximum Courant number was 2. The simulations were run until the inflows at the upstream end of the model were equal with the outflows at the downstream end of the model. The water surface tolerance[6] was set to 0.01 m, and the maximum number of iterations was set to 20 (default value).

E-5.2.6 Modelling Scenarios

Scenarios were modeled for both the stationary 200-year (0.5% AEP) and climate-adjusted 200-year (0.5% AEP) as summarized in Table E-12. Model results are presented in the following sections.

6 Used to compare the WSE difference between two consecutives iterations at each time step. If the difference is greater than the tolerance, the program continues to iterate for the current time step up to the maximum number of iterations.

E-5.3 Hydraulic Model Domains

E-5.3.1 Tabor Creek at Prince George

The model domain covers a 22 km section of Tabor Creek. The upstream limit of the model is located 7 km upstream (north) from the confluence with Swede Creek and the downstream limit is located approximately 300 m upstream from the confluence with the Fraser River (Figure E-9).

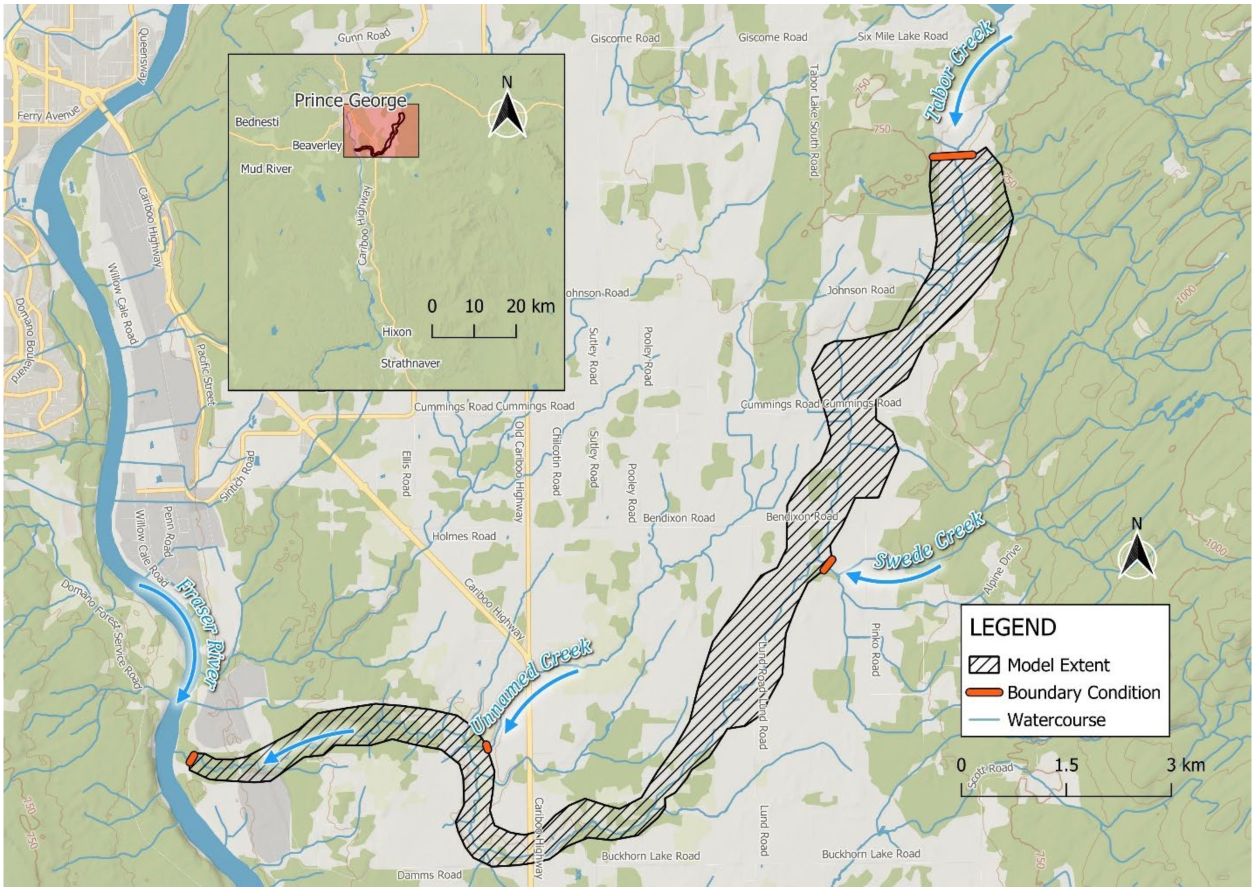

Figure E-9 Study area modelling domain for the Tabor Creek model. Watercourses from the National Hydrographic Network (NHN). Basemap from QGIS MapTiler Plugin[7].

Several tributaries contribute to the streamflow of Tabor Creek within the model domain, with the main tributaries being an unnamed creek and Swede Creek (Figure E-9). Each of these tributaries has a watershed area of approximately 16% the size of Tabor Creek's watershed area at the downstream limit of the model.

[7] MapTiler uses a variety of open source and commercial data sources to create its maps. The most common source is OpenStreetMap, with MapTiler also using data from the European Space Agency (ESA) and other open datasets for elements like satellite imagery, land cover, and elevation data.

The upstream boundary conditions for the unnamed creek, Swede Creek, and Tabor Creek were set as steady inflow hydrographs for both the 200-year (0.5% AEP) and climate-adjusted 200-year (0.5% AEP) flood events.

A normal depth assumption was applied to the downstream boundary of Tabor Creek. The friction slope was set to 1% (0.01 m/m), as measured from the bare earth lidar DEM.

E-5.3.1.1 Manning's n

Figure E-10 illustrates the Manning's n values used in the hydraulic model. Because the creek is only a few meters wide (approximately 5 m) through most of the domain, and its banks are well vegetated with trees and shrubs, the Manning's n estimate for the water land class value presented in Table E-13 was used as-is, without adjusting the roughness values within the main channel.

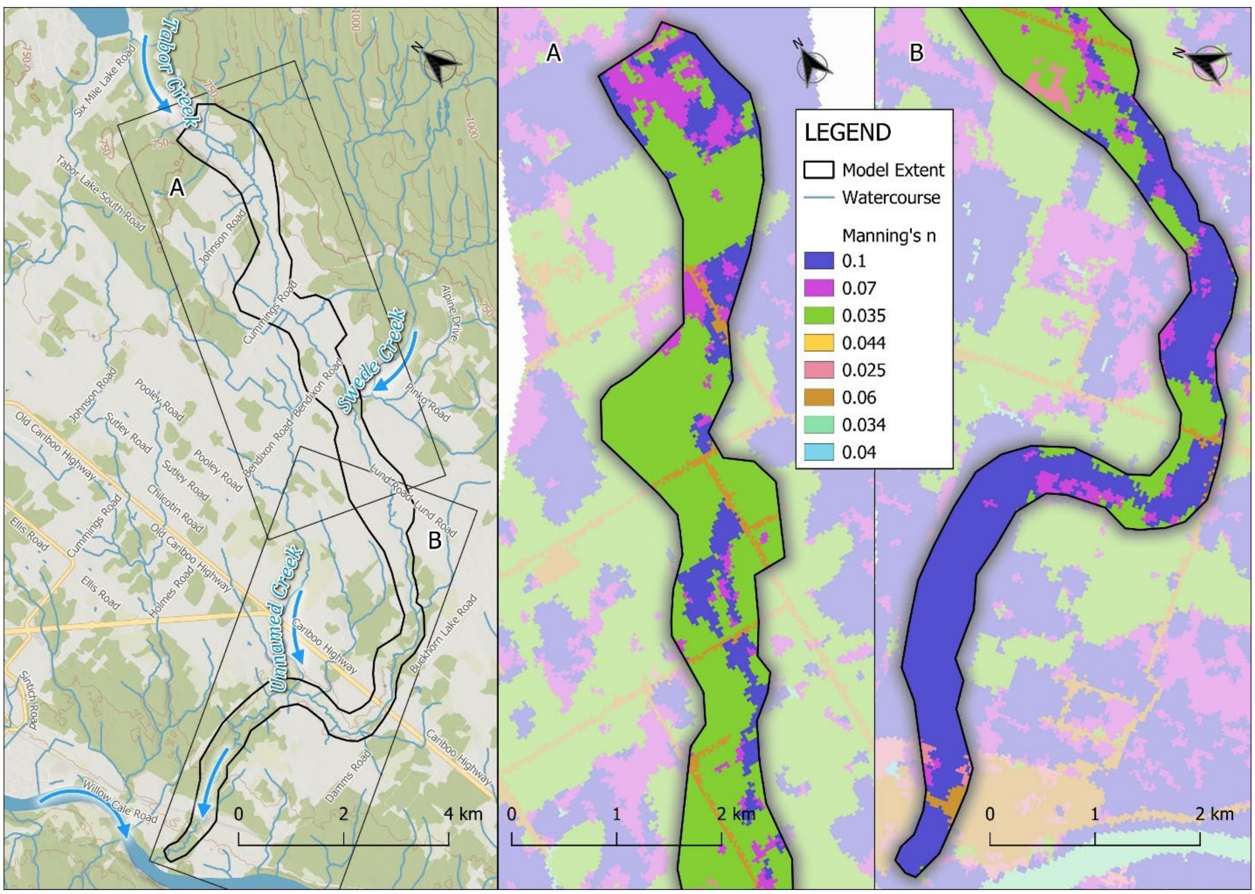

Figure E-10 Manning's n roughness layer defined for Tabor Creek at Prince George model.

E-5.3.1.2 Computational Mesh

For the Tabor Creek model, a base mesh resolution of 5 m was selected (Figure E-11). Breaklines were placed along terrain features such as road and railroad embankments. The final mesh consisted of over 480,00 computational cells.

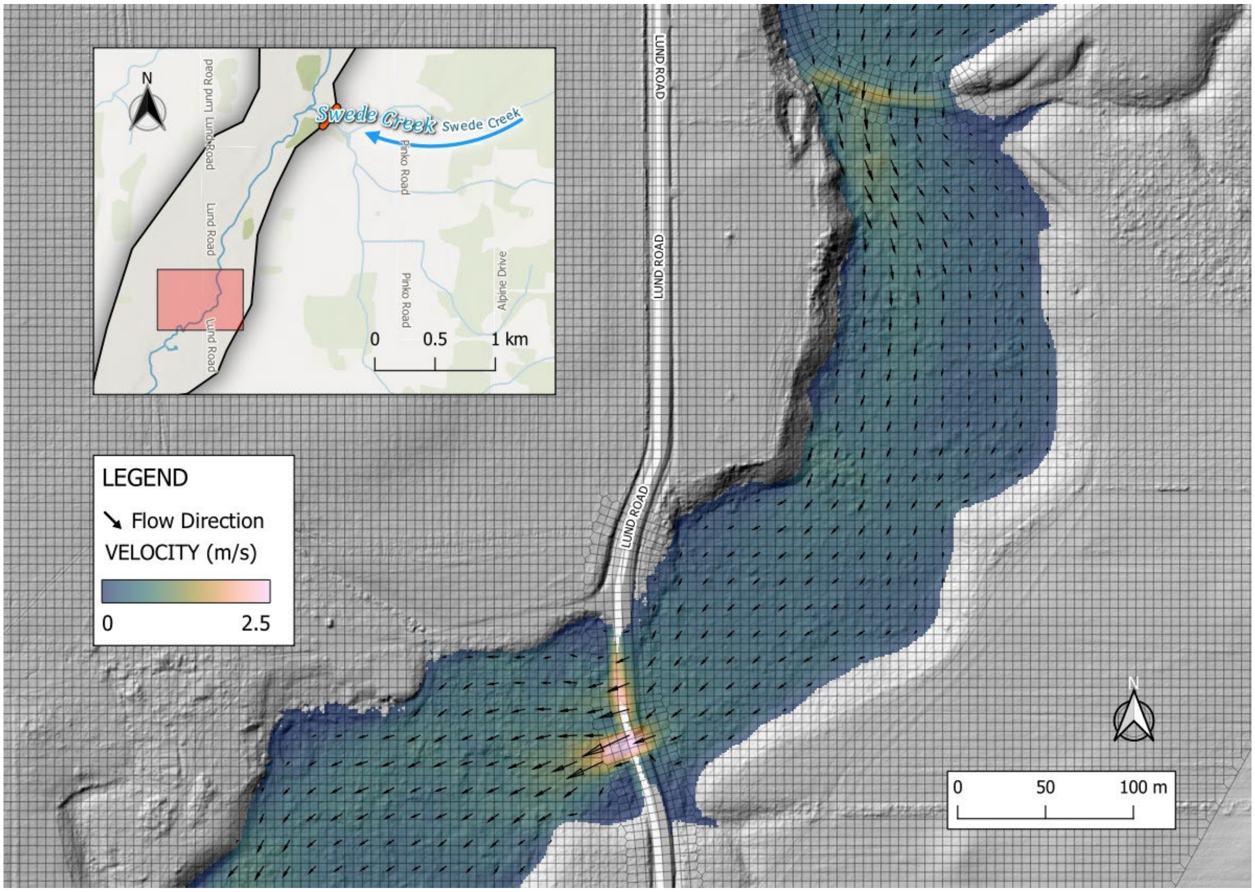

Figure E-11 Example of the mesh developed for the Tabor Creek at Prince George HEC-RAS model in the vicinity of Lund Road. Modelled flow velocities for the climate-adjusted 200-year flood event are overlaid on the DEM (hillshade). Arrow size is proportional to flow velocity.

E-5.3.1.3 Culverts

Three culvert groups were included in the Tabor Creek at Prince George model due to their proximity to the outlet and their influence on flow dynamics. These include the crossings at Willow Cale Forest Service Road (FSR), the CN railroad, and the Cariboo Highway. Further details on these culverts are provided in Table E-14.

Table E-14 Included culverts in Tabor Creek at Prince George model.

Location	Culvert Type	Number of Barrels	Dimensions	Invert Elevation (1)	Manning's n
Willow Cale FSR	Ellipse Concrete Culvert	1	3,000 mm x 5,000 mm (span x rise)	581.9 m	0.024
Railroad Crossing	Circular CSP	2	2,500 mm diameter	588.8 m	0.024
Cariboo Highway	Circular CSP	3	2,500 mm diameter	641.9 m	0.024

Note:

1. Inlet elevation as measured from the bare earth lidar, with outlet elevations assumed to be equal.

E-5.3.2 Fraser River at McBride

The model domain for the Fraser River at McBride covers a 54 km section of the Fraser River, starting 9 km upstream (southeast) from Raush River and ending 11 km downstream (northwest) from the confluence with Dore River. The model domain includes a section of Dore River, that extends approximately 4.5 km upstream from the confluence with the Fraser River (Figure E-12).

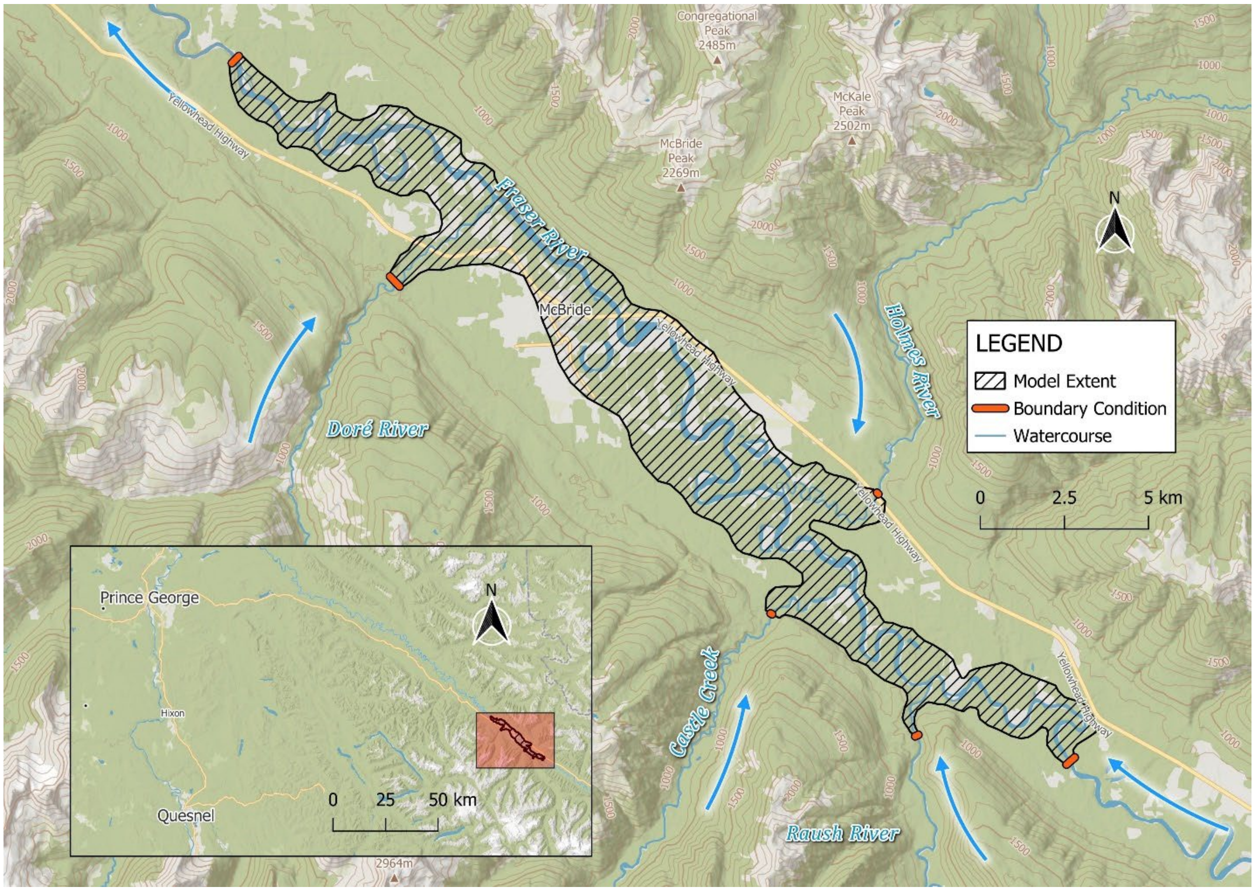

Figure E-12 Study area modelling domain for the Fraser River at McBride model. Selected watercourses from the National Hydrographic Network (NHN). Basemap from QGIS MapTiler Plugin[7].

Several tributaries contribute to the streamflow of the Fraser River within the McBride model domain, with the main tributaries being the Holmes River, Castle Creek, and Raush River. The watershed areas of these tributaries are 12%, 7%, and 15%, respectively, of the Fraser River watershed area at McBride. To distribute the inflows along the Fraser River, the peak flows estimated for the Fraser River at McBride were prorated based on the watershed areas of the Holmes River, Castle Creek, the Raush River, and the Fraser River at the upstream end of the model domain.

The upstream boundary conditions for Dore River, Holmes River, Castle Creek, Raush River, and Fraser River were set as steady inflow hydrographs for both the 200-year (0.5% AEP) and climate-adjusted 200-year (0.5% AEP) flood events. The lowest recorded discharge at Fraser

River at McBride WSC hydrometric station during the lidar acquisition (142 m^3/s) was prorated based on the tributaries' watershed areas and subtracted from the flood discharges presented in Table E-12.

A normal depth assumption was applied to the downstream boundary of the Fraser River. The friction slope was set to 0.02% (0.0002 m/m), as measured from the bare earth lidar DEM.

E-5.3.2.1 Manning's n

Figure E-13 illustrates the final Manning's n values used in the hydraulic model for the Fraser River at McBride. The Manning's n estimate for the water land class value presented in Table E-13 was reduced from 0.034 to 0.030, as the main channels have low gradient (0.02%–0.03%), except for Dore River, where it was increased to 0.040 to account for the presence of larger bed material (gravel to cobble sizes).

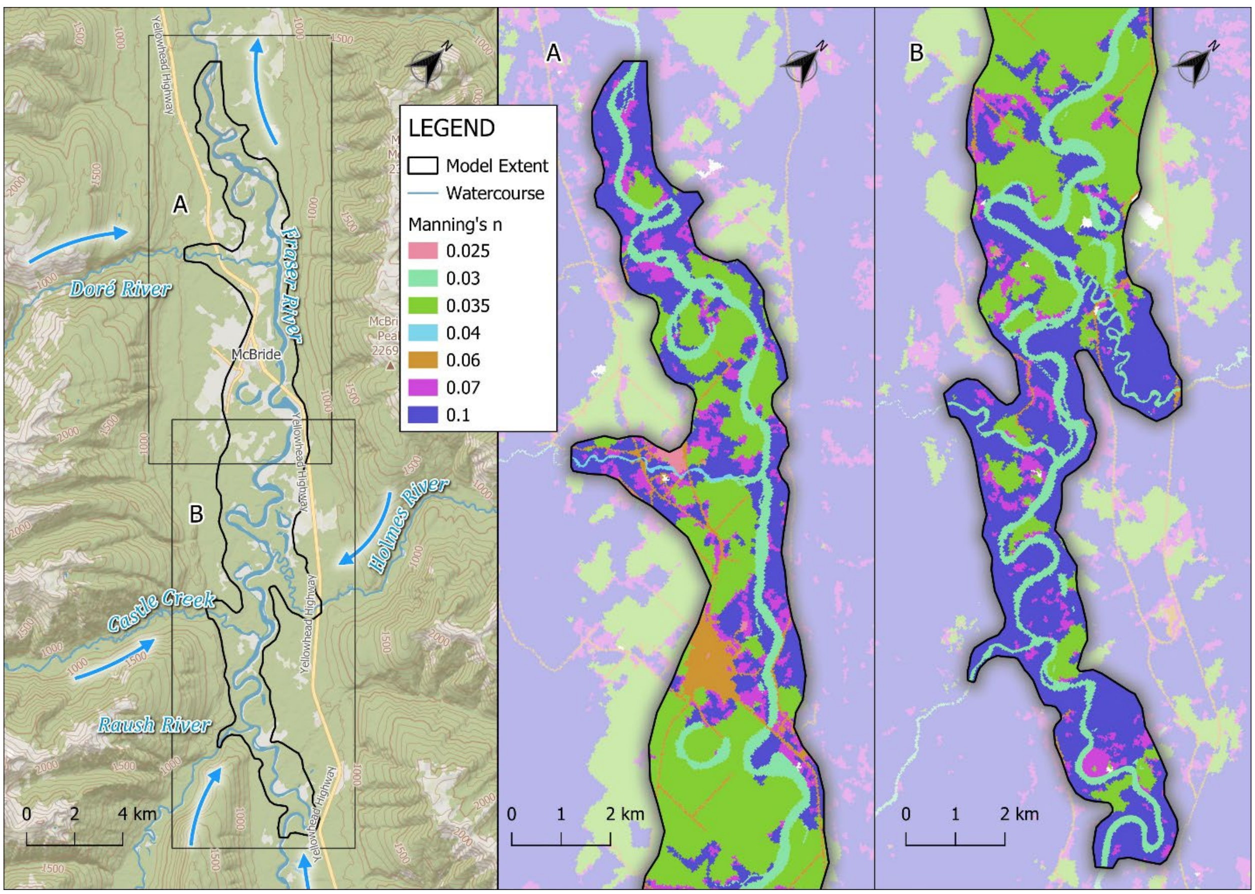

Figure E-13 Manning's n roughness layer defined for Fraser River at McBride model.

E-5.3.2.2 Computational Mesh

For the Fraser River at McBride model, a base mesh resolution of 20 m was selected (Figure E-14). Breaklines were placed iteratively along the channel centrelines (CL) to create a curvilinear mesh aligned with the main channel flows, with a resolution of 20 m. Breaklines were also placed along terrain features such as road and railroad embankments. The final mesh consisted of over 187,000 computational cells with an average cell face length of 20 m and an average cell area of 407 m^2.

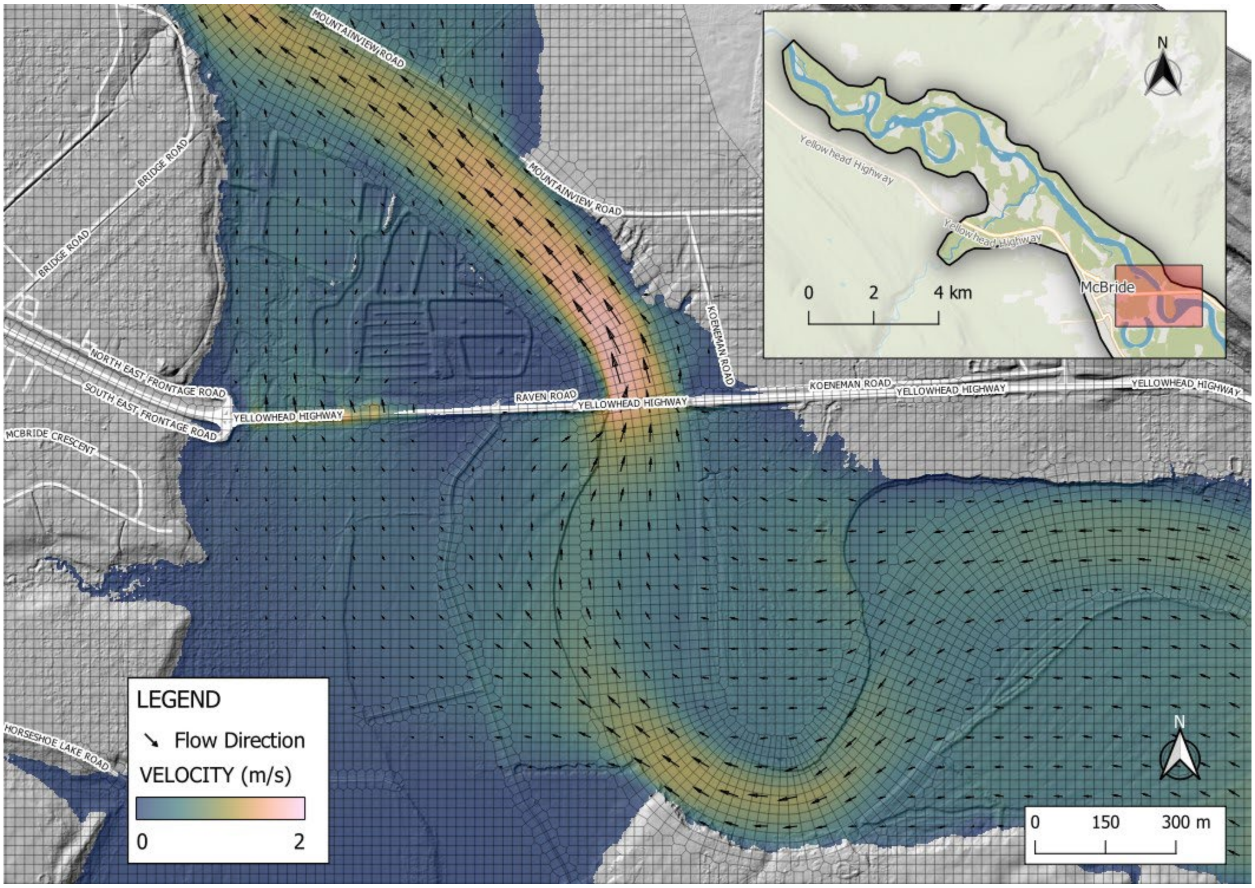

Figure E-14 Example of the mesh developed for the Fraser River at McBride HEC-RAS model in the vicinity of McBride Bridge. Modelled flow velocities for the stationary 200-year flood event are overlaid on the DEM (hillshade). Arrow size is proportional to flow velocity.

E-5.3.3 Fraser River at Tête Jaune Cache

The model domain spans approximately 28 km along the Fraser River, starting about 4 km upstream (east) from its confluence with McLennan River and extending to about 3.5 km downstream (northwest) of its confluence with Kiwa Creek. In addition to the Fraser River, the model domain includes a 4.6 km section of McLennan River and a 2.5 km section of Tête Creek (Figure E-15).

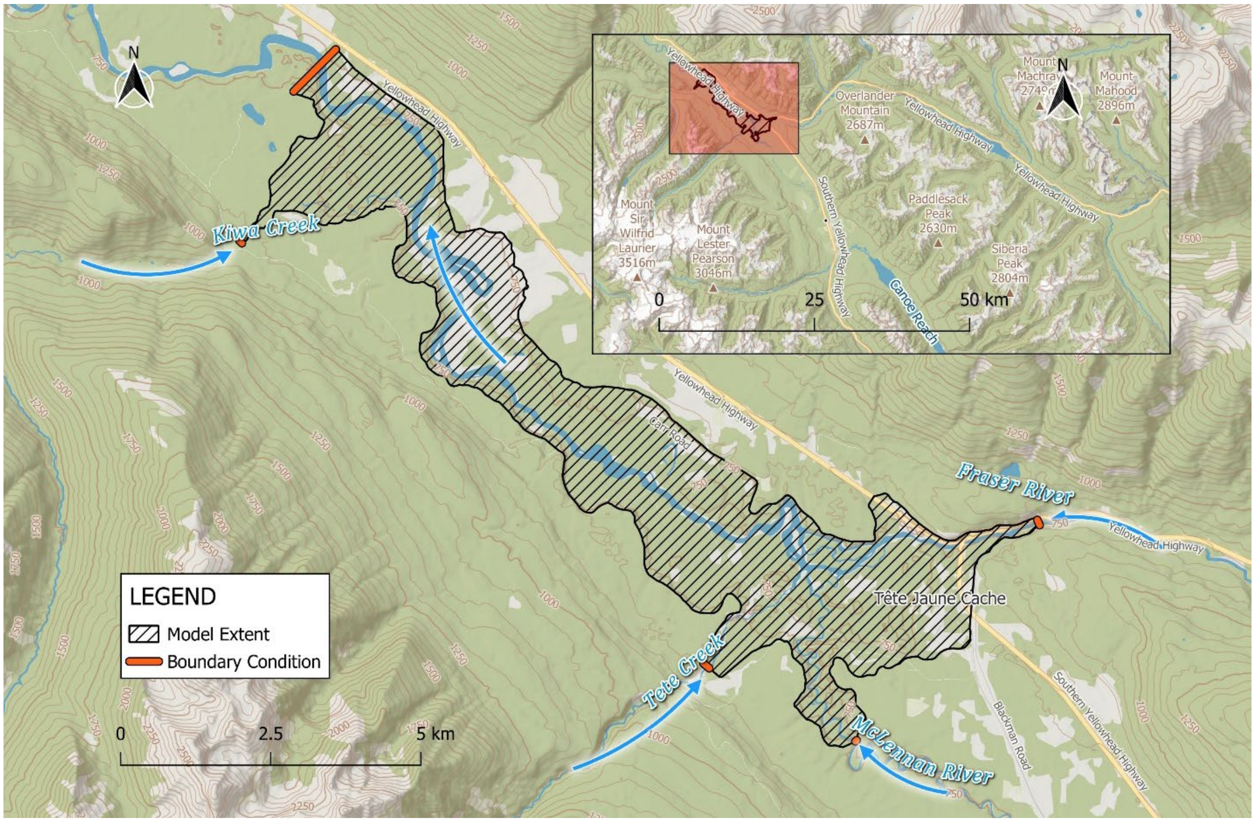

Figure E-15 Study area modelling domain for the Fraser River at Tête Jaune Cache model. Basemap from QGIS MapTiler Plugin[7].

Several tributaries contribute to the streamflow of the Fraser River within the model domain, with the main tributaries being McLennan River, Kiwa Creek, and Tête Jaune Creek. The combined peak flow estimates for the tributaries, along with the peak flow estimate for the Fraser River at the upstream boundary, were within 5% of the peak flow estimate at the downstream limit of the model. Therefore, no further adjustments were made.

The upstream boundary conditions for the Fraser River, McLennan River, Kiwa Creek, and Tête Jaune Creek were set as steady inflow hydrographs for both the 200-year (0.5% AEP) and climate-adjusted 200-year (0.5% AEP) flood events (Table E-12).

A normal depth assumption was applied as the downstream boundary of Fraser River. The friction slope was set to 0.03%, as measured from the bare earth lidar DEM.

E-5.3.3.1 Manning's n

The Manning's n estimates for the main channel areas of Tête Creek and Kiwa Creek were further refined from the baseline water land class values presented in Table E-13. These refinements account for increased channel gradient and ensure subcritical flow conditions, maintaining Froude numbers below 1. Final Manning's n values for both creeks were set to 0.07.

Along the Fraser River, several point bars are present, particularly at the confluence with the McLennan River and further downstream in the vicinity of Old Tête Jaune Road and railroad intersection, approximately 3 km northwest from the confluence. In these areas, Manning's n values were increased from 0.034 to 0.07 to reflect the rougher flow conditions caused by larger bed material (gravel to cobble size) and the presence of vegetated surfaces across the bars. Additionally, Manning's n values for three wetland areas located on the left side of the Fraser River floodplain near Tête Jaune Station were set to 0.044 to represent increased flow resistance due to wetland vegetation and terrain characteristics.

E-5.3.3.2 Computational Mesh

For the Fraser River at Tête Jaune Cache model, a base mesh resolution of 5 m was selected (Figure E-16). Breaklines were placed along the channel centrelines to create a curvilinear mesh aligned with the main channel flows, with a resolution of 5 m. Breaklines were also placed along terrain features such as road and railroad embankments. The final mesh consisted of over 1,147,100 computational cells with an average cell face length of 5 m and average cell area of 25 m^2.

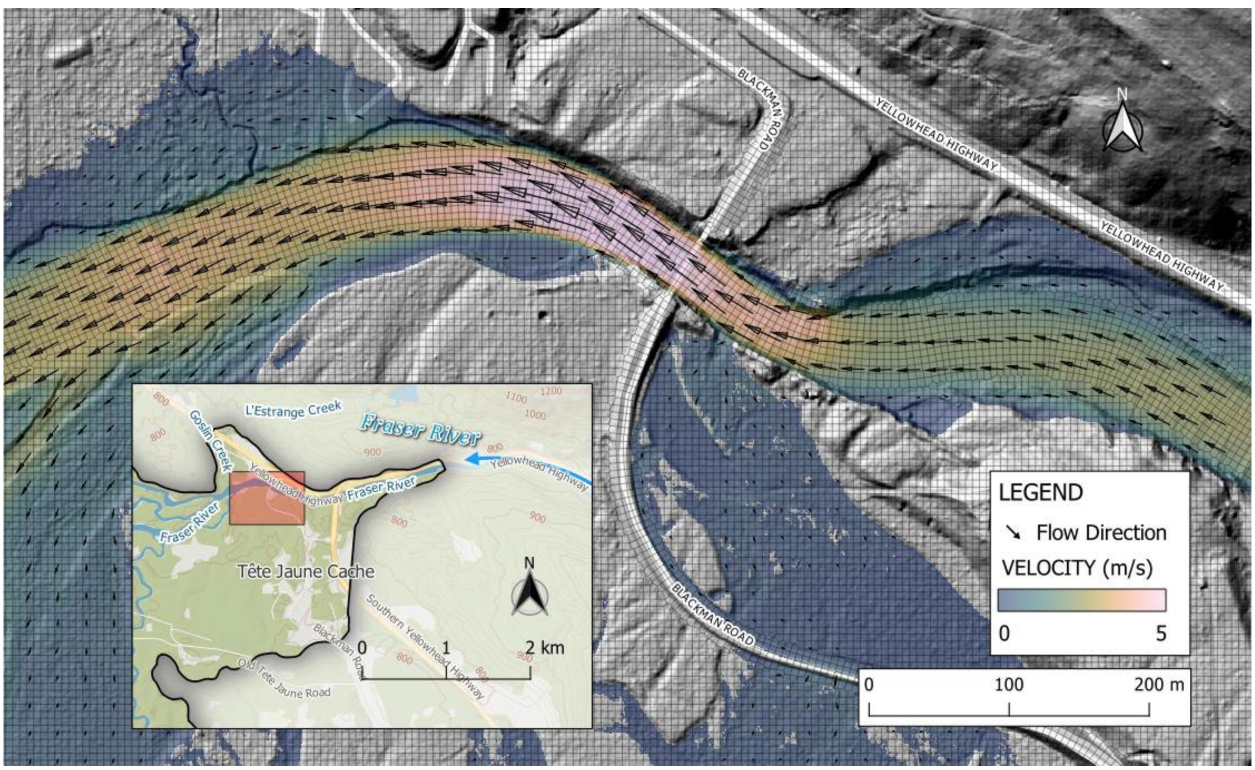

Figure E-16 Example of the mesh developed for the Fraser River at Tête Jaune Cache HEC-RAS model in the vicinity of the Blackman Road bridge. Modelled flow velocities for the stationary 200-year flood event are overlaid on the DEM (hillshade). Arrow size is proportional to flow velocity.

E-5.3.4 Naver and Hixon Creek at Hixon

The model domain for the Naver and Hixon Creek covers a 23.5 km section of Naver Creek, starting 2 km downstream (northwest) from Meadowbank Creek and ending 1.8 km upstream (east) from the confluence with the Fraser River (Figure E-17). The model domain includes a 3.5 km section of Hixon Creek.

Figure E-17 Study area modelling domain for the Naver and Hixon Creek at Hixon model. Selected watercourses displayed are from the National Hydrographic Network (NHN). Basemap from QGIS MapTiler Plugin[7].

Several tributaries contribute to the streamflow of Naver Creek within the model domain, with the main tributaries being Terry Creek and Pedley Creek. The watershed areas of these tributaries are 12% and 4%, respectively, of Naver Creek's watershed area at its confluence with Hixon Creek. To distribute the inflows along Naver Creek, the peak flows estimated for Naver Creek at Hixon Creek were prorated based on the watershed areas of Terry Creek, Pedley Creek, and Naver Creek at the upstream end of the model domain.

The upstream boundary conditions for Naver Creek, Terry Creek, Pedley Creek, and Hixon Creek were set as steady inflow hydrographs for both the 200-year (0.5% AEP) and climate-adjusted 200-year (0.5% AEP) flood events (Table E-12).

A normal depth assumption was applied to the downstream boundary of Naver Creek. The friction slope was set to 0.6% (0.006 m/m), as measured from the bare earth lidar DEM.

E-5.3.4.1 Manning's n

Figure E-18 illustrates the final Manning's n values used in the Naver and Hixon Creek at Hixon hydraulic model. The Manning's n estimate for the Hixon Creek main channel area was refined from the water land class value presented in Table E-13, increasing by 20% (from 0.034 to 0.041) to account for the presence of larger bed material compared to Naver Creek and the riffle-pool morphology observed during the field visit.

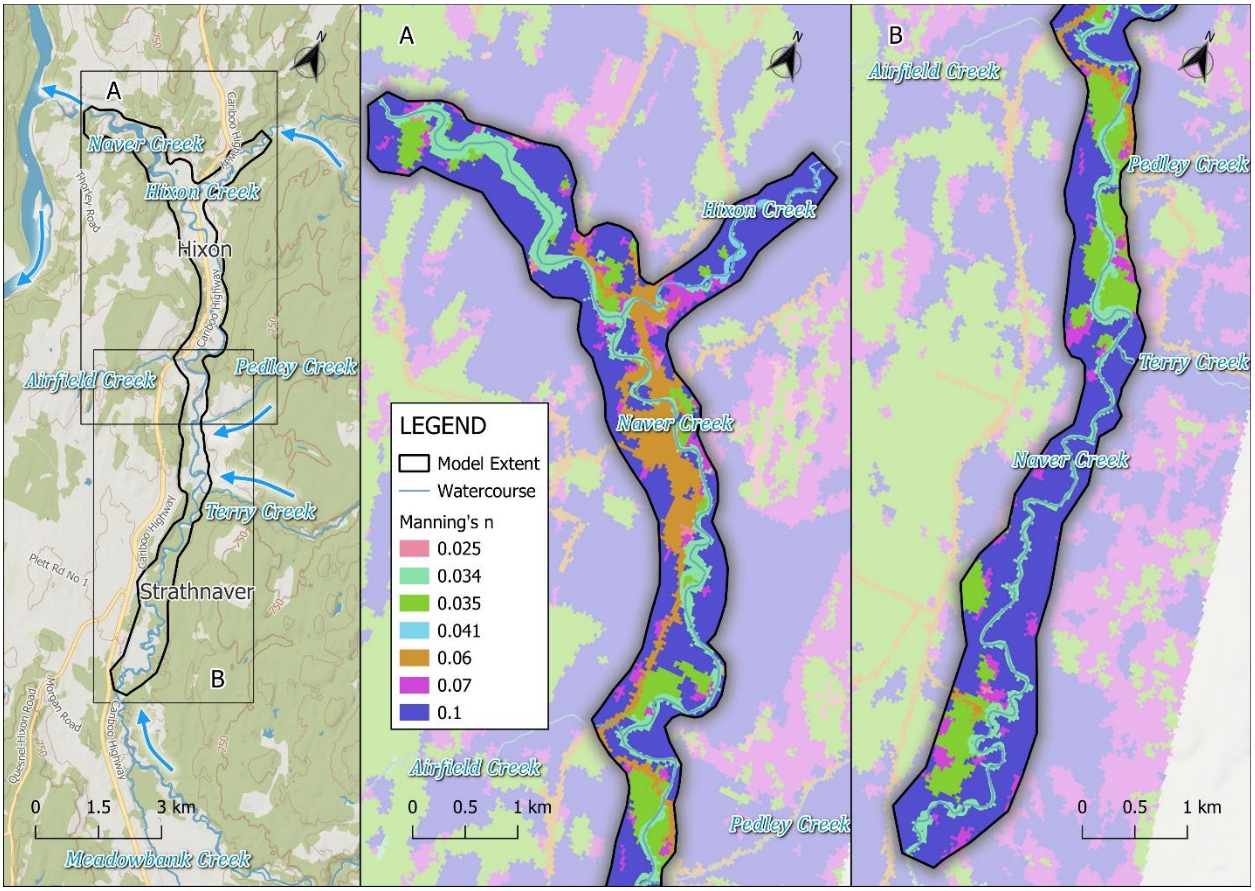

Figure E-18 Manning's n roughness layer defined for Naver and Hixon Creek at Hixon model.

E-5.3.4.2 Computational Mesh

For the Naver and Hixon Creek at Hixon model, a base mesh resolution of 5 m was selected (Figure E-19). Breaklines were placed along the channel centrelines (CL) to create a curvilinear mesh aligned with the main channel flows, with a resolution of 5 m for both Naver Creek and Hixon Creek. Breaklines were also placed along terrain features such as road and railroad embankments, and dikes or flood protection/mitigation structures. The final mesh consisted of over 448,000 computational cells with an average cell face length of 5 m and an average cell area of 25 m^2.

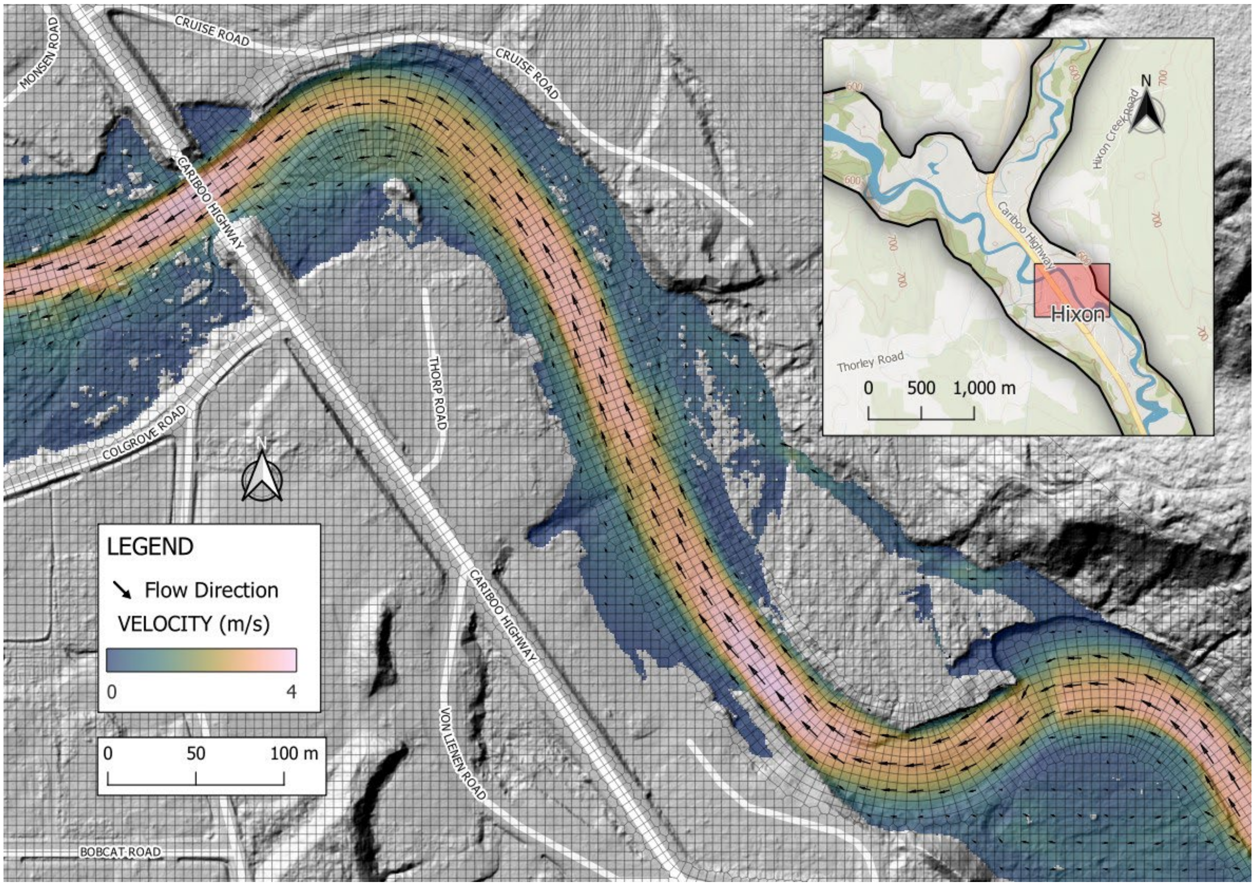

Figure E-19 Example of the mesh developed for the Naver and Hixon Creek at Hixon HEC-RAS model in the vicinity of the Canyon Creek bridge (Cariboo Highway). Modelled flow velocities for the climate-adjusted 200-year flood event are overlaid on the DEM (hillshade). Arrow size is proportional to flow velocity.

E-5.3.5 McLennan River and Swift Creek at Valemount

The model domain for the McLennan River and Swift Creek at Valemount study area covers a 30 km section of the McLennan River, starting 2.2 km southwest (upstream) from the confluence with Swift Creek and ending approximately 6 km southeast (upstream) from the confluence with the Fraser River. The model domain includes a 5.8 km section of Swift Creek (Figure E-20).

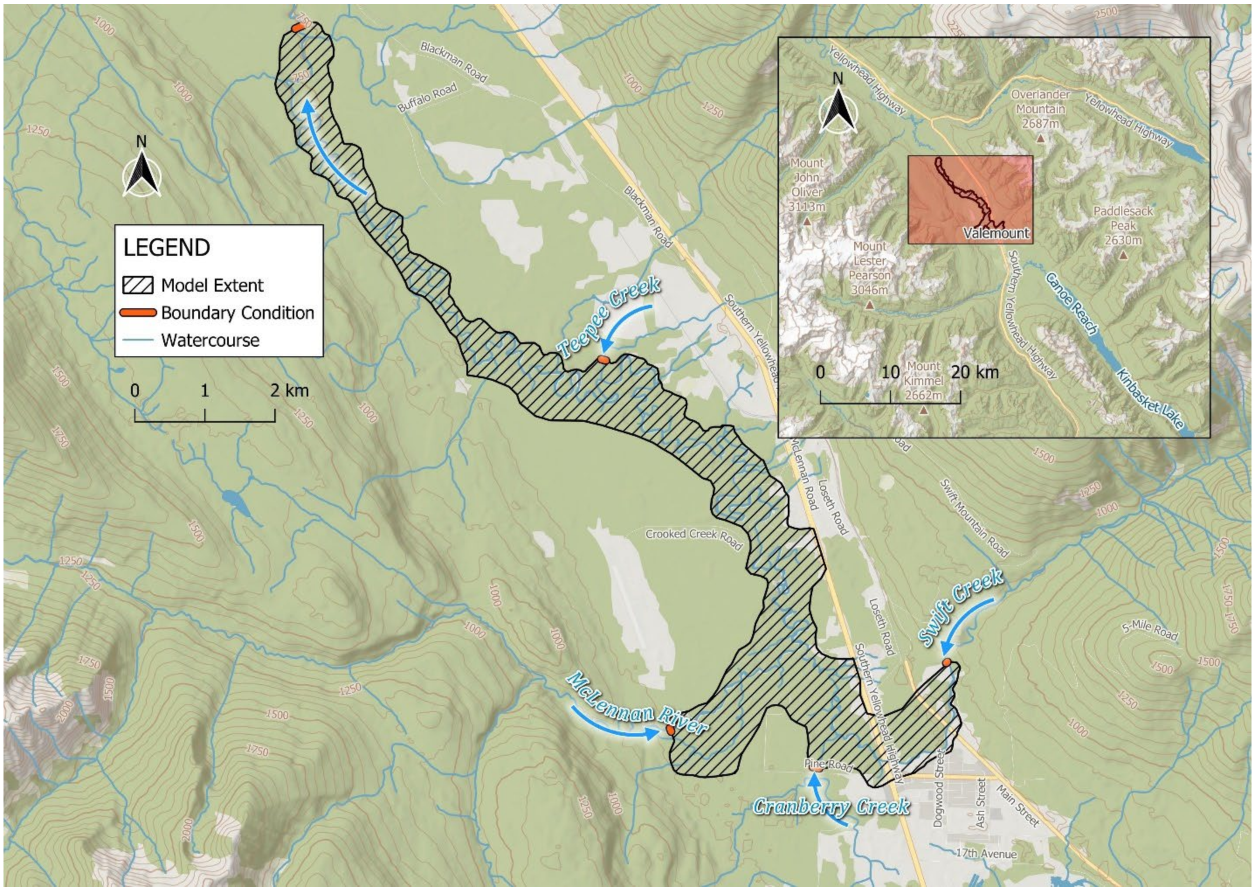

Figure E-20 Study area modelling domain for McLennan River and Swift Creek at Valemount model. Selected watercourses displayed are from the National Hydrographic Network (NHN). Basemap from QGIS MapTiler Plugin[7].

Several tributaries contribute to the streamflow of the McLennan River within the model domain, with the main tributaries being Swift Creek, Cranberry Creek, and Hogan-Teepee-Crooked Creek. The watershed areas of these tributaries are 28%, 10%, and 10%, respectively, of the McLennan River watershed area at the downstream limit of the model. The combined peak flow estimates for the tributaries, along with the peak flow estimate for the McLennan River at the upstream boundary, were within 2% of the peak flow estimate at the downstream limit of the model. Consequently, no further adjustments were necessary.

The upstream boundary conditions for McLennan River, Swift Creek, Cranberry Creek, and Teepee Creek were set as steady inflow hydrographs for both the 200-year (0.5% AEP) and climate-adjusted 200-year (0.5% AEP) flood events (Table E-12).

A normal depth assumption was applied to the downstream boundary of McLennan River. The friction slope was set to 0.05% (0.0005 m/m), as measured from the bare earth lidar DEM.

E-5.3.5.1 Manning's n

The Manning's n estimates for the McLennan River and Swift Creek main channel areas were further refined from the water land class values presented in Table E-13. This refinement accounts for the greater channel gradient and ensures the Froude number remains below 1. Manning's n values for the McLennan River were set to 0.04 between the confluence with Swift Creek and 1.5 km upstream, and 0.06 from this point upstream. For Swift Creek, Manning's n values were set to 0.04 from the confluence upstream to the railroad, and 0.06 upstream from this point.

E-5.3.5.2 Computational Mesh

For the McLennan River and Swift Creek at Valemount model, a base mesh resolution of 10 m was selected (Figure E-21). Breaklines were placed along the channel centrelines to create a curvilinear mesh aligned with the main channel flows, with a resolution of 10 m for both McLennan River and Swift Creek. Breaklines were also placed along terrain features such as road and railroad embankments, and dikes or flood protection/mitigation structures. The final mesh consisted of over 128,000 computational cells with an average cell face length of 10 m.

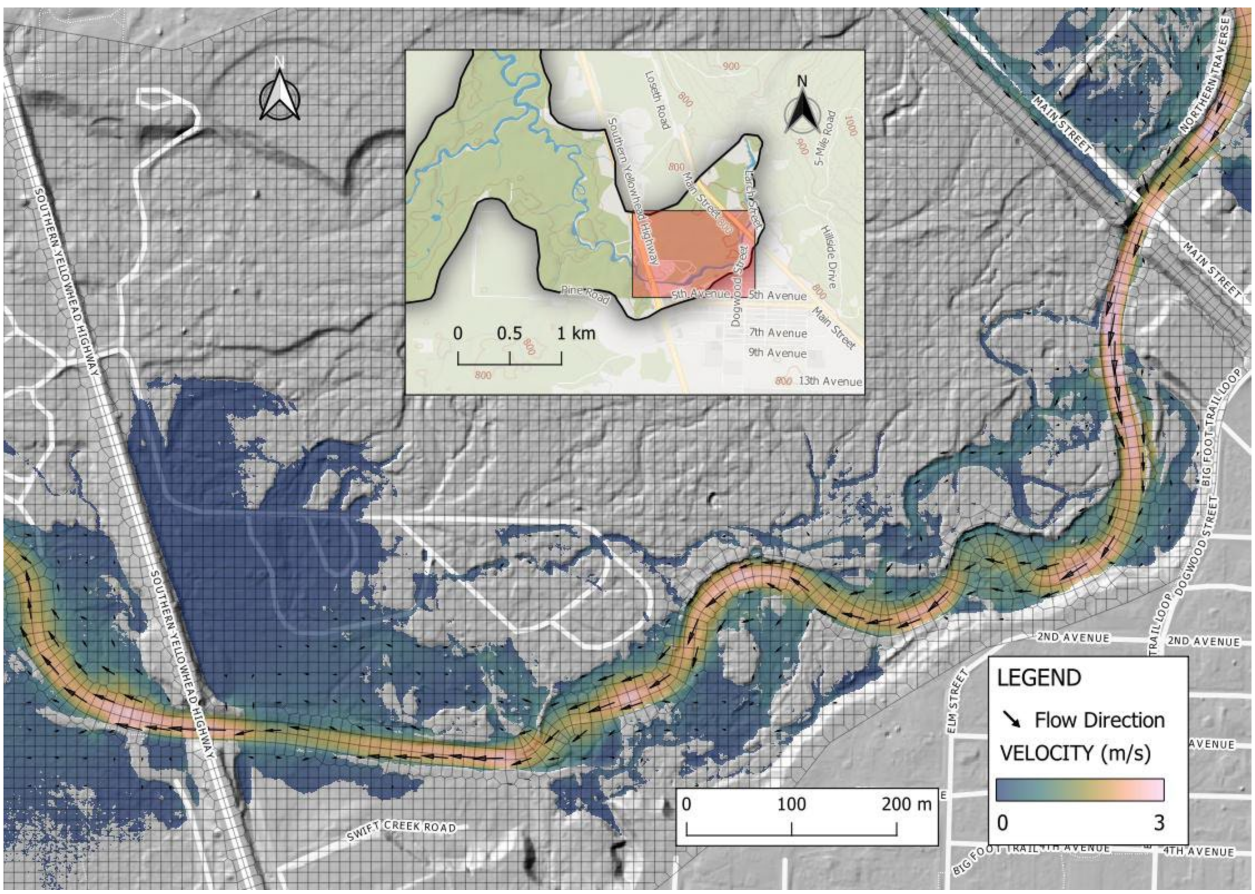

Figure E-21 Example of the mesh developed for the Swift Creek HEC-RAS model in the vicinity of Valemount. Modelled flow velocities for the climate-adjusted 200-year flood event overlaid on the DEM (hillshade). Arrow size is proportional to flow velocity.

E-5.4 Model Results

This section presents the results of the climate-adjusted 200-year (0.5% AEP) flood event at specific locations of interest. Results covering the entire study area extents, as well as the present day 200-year flood event, are available on Cambio™[8]. For context, the section also describes flood hazard extents in relation to the location of selected assets. Appendix H should be read for methods and limitations of the hazard exposure analysis.

E-5.4.1 Tabor Creek at Prince George

For both the 200-year flood event and the climate-adjusted 200-year flood event, the model predicts overtopping of the Willow Cale Forest Service Road (FSR), located approximately 1.2 km upstream (east) of the confluence with the Fraser River. This occurs because the capacity of the elliptical culvert beneath the FSR is exceeded. Approximately 400 m further upstream (east), water is predicted to pond behind the railroad embankment. However, the model indicates that the twin 2500 mm diameter culverts can convey the flood without causing overtopping of the embankment (Figure E-22).

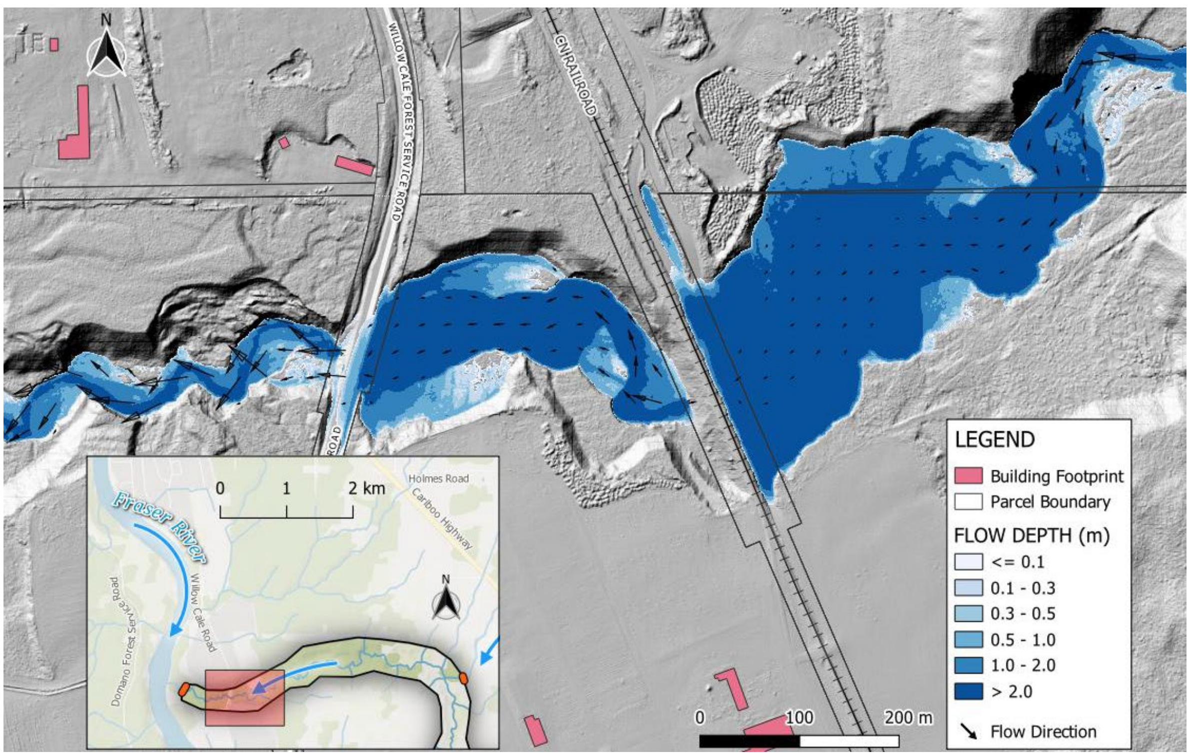

Figure E-22 Modelled climate-adjusted 200-year (0.5% AEP) Tabor Creek flood depth in the vicinity of Willow Cale FSR, overlaid on the DEM (hillshade). Arrow size is proportional to flow velocity. Building footprints from Microsoft (2023) database (additional buildings likely exist). Parcel boundaries from BC Assessment (2023).

---

[8] Cambio™ is a proprietary web-based application owned by Cambio Earth Systems Inc. Cambio™ helps manage certain types of geohazards along linear infrastructure. Cambio™ helps users organize hazard sites spatially, prioritize them for future action, build inspection and maintenance programs, and store certain information about the site history. The RDFFG has licensed Cambio Earth Systems (Cambio) and provided access to all partners. The current project does not include tools for program implementation (e.g. inspections, monitoring or hazard and asset management), but the data layers provide a starting point for such work as may be needed in future.

At the Cariboo Highway, flow is constricted by three 2500 mm diameter culverts beneath the roadway, resulting in elevated water levels upstream. Although the embankment is not overtopped, the model predicts flooding of nearby buildings (Figure E-23). The backwater effect is estimated to extend approximately 1 km upstream of the highway.

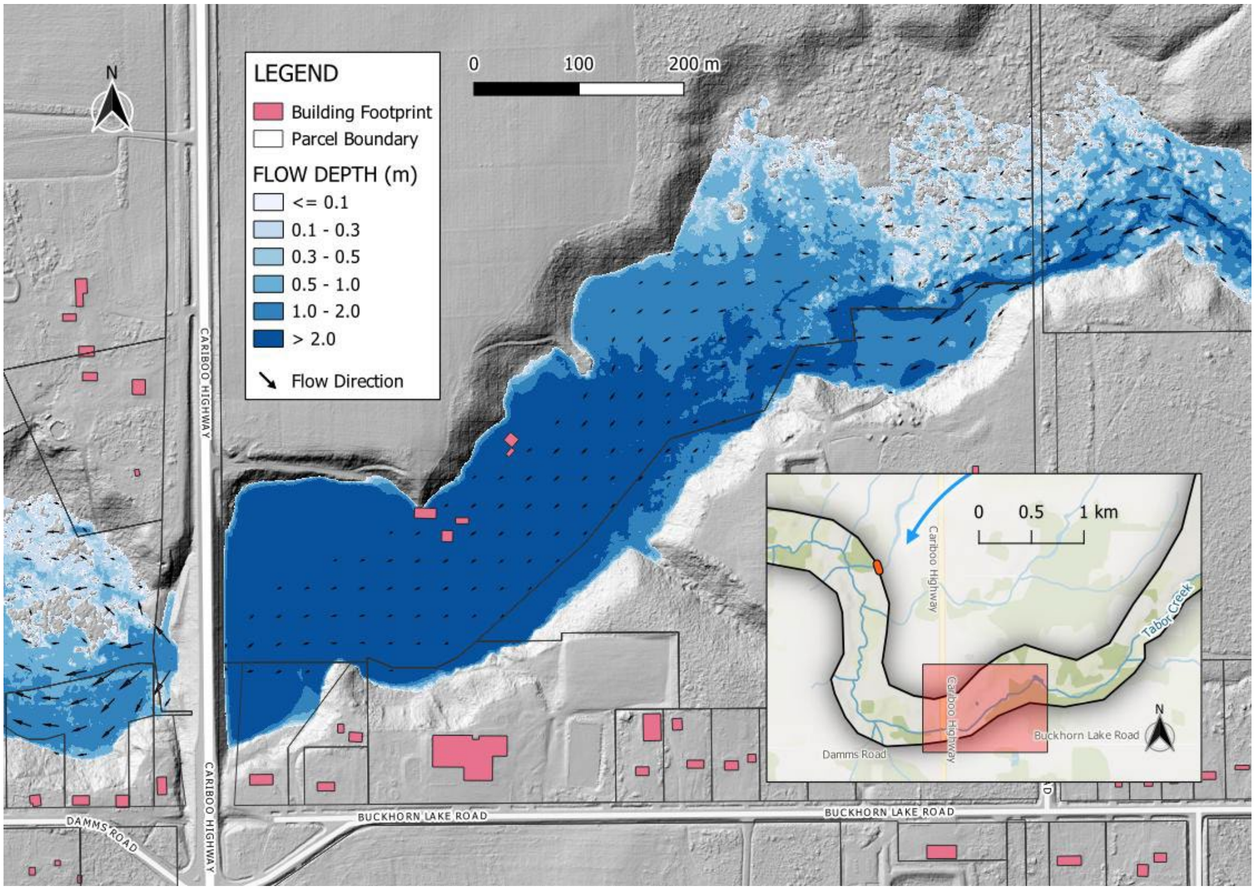

Figure E-23 Modelled climate-adjusted 200-year (0.5% AEP) Tabor Creek flood depth in the vicinity of Cariboo Highway, overlaid on the DEM (hillshade). Arrow size is proportional to flow velocity. Building footprints from Microsoft (2023) database (additional buildings likely exist). Parcel boundaries from BC Assessment (2023).

Upstream of Cummings Road, the model predicts flooding of buildings located along the right (west) floodplain of Tabor Creek (Figure E-24).

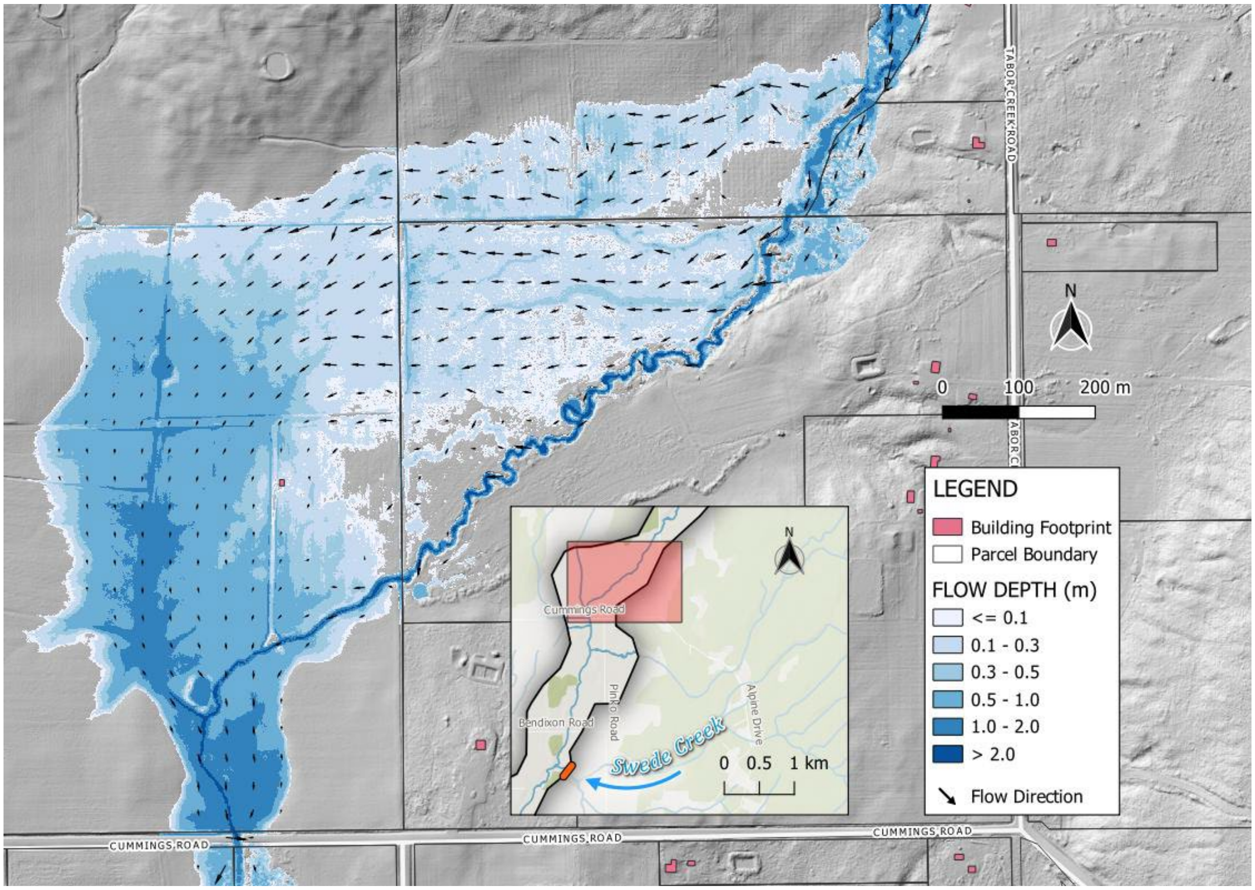

Figure E-24 Modelled climate-adjusted 200-year (0.5% AEP) Tabor Creek flood depth in the vicinity of Cummings Road, overlaid on the DEM (hillshade). Arrow size is proportional to flow velocity. Building footprints from Microsoft (2023) database (additional buildings likely exist). Parcel boundaries from BC Assessment (2023).

E-5.4.2 Naver and Hixon Creek at Hixon

For the climate-adjusted 200-year flood event, the model does not predict flooding of buildings along Hixon Creek or Naver Creek downstream of the Naver Creek and Hixon Creek confluence (Figure E-25). Approximately 250 m upstream and 800 m downstream from the confluence are two bridges: the Hixon Creek bridge (Cariboo Highway) and a CN railway bridge. Although the elevations of the soffits of both bridge decks are not known to BGC, the embankment elevations measured from the lidar DEM suggest that the soffits of the bridges are above the highest modelled water surface elevation (WSE), including sensitivity runs presented in Section E-5.5.

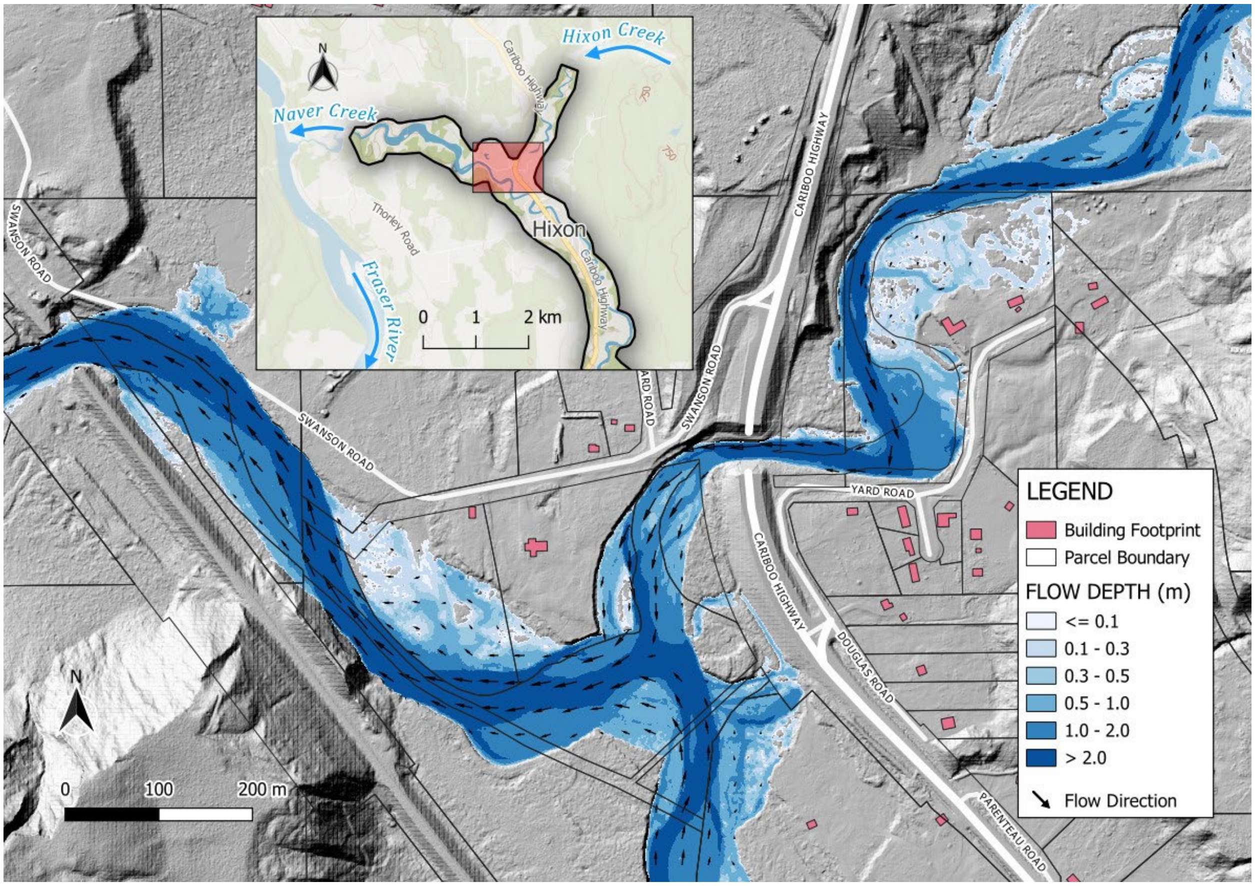

Figure E-25 Modelled climate-adjusted 200-year (0.5% AEP) flood depth in the vicinity of Naver Creek and Hixon Creek confluence, overlaid on the DEM (hillshade). Arrow size is proportional to flow velocity. Building footprints from Microsoft (2023) database. Parcel boundaries from BC Assessment (2023).

Along the left (west) floodplain of Naver Creek near Colgrove Road, the model predicts flooding of buildings (Figure E-26). While the elevation of the soffit of the Canyon Creek bridge (Cariboo Highway) deck is unknown to BGC, embankment elevations measured at 575.1 m from the lidar DEM suggest that the soffit is likely above the highest modelled WSE at 571.6 m, including the sensitivity runs presented in Section E-5.5.

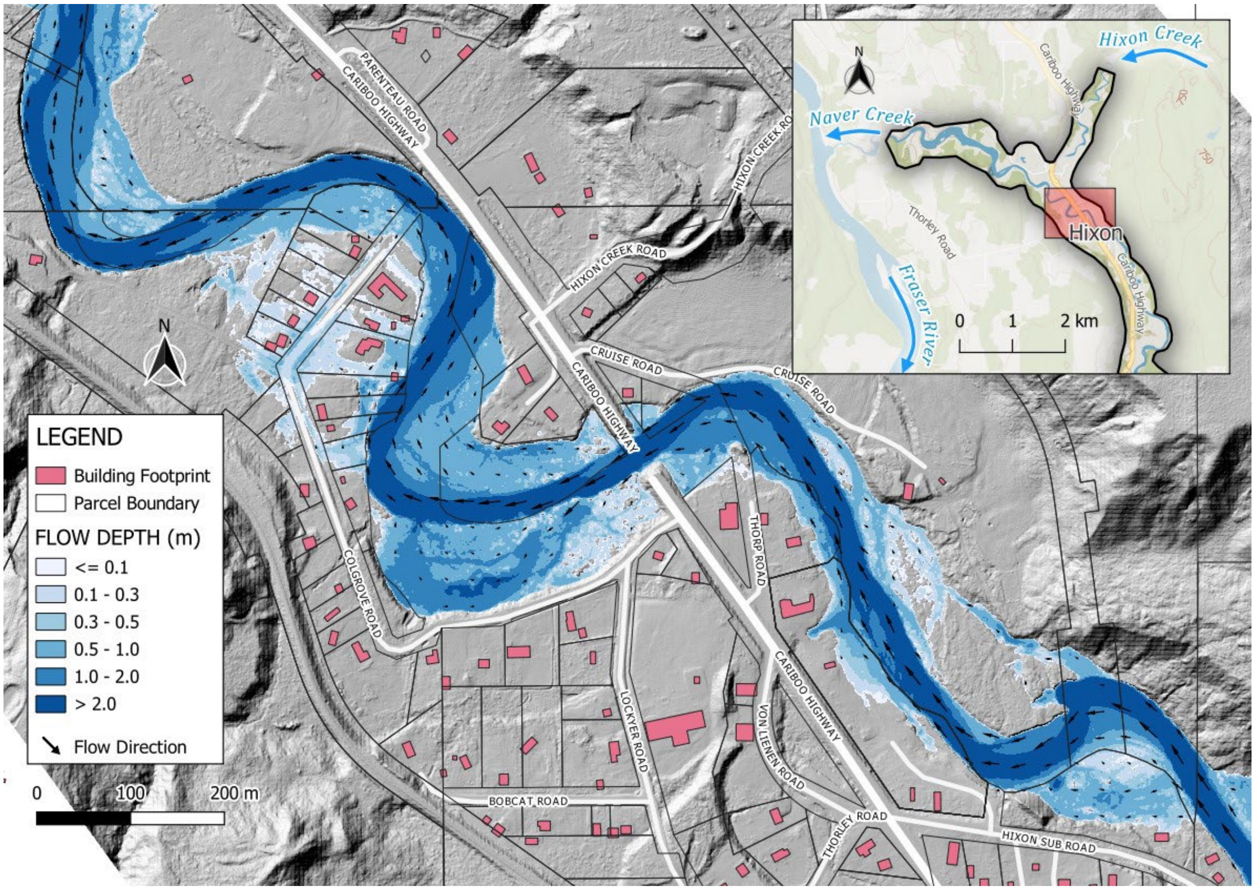

Figure E-26 **Modelled climate-adjusted 200-year (0.5% AEP) Naver Creek flood depth in the vicinity of the Canyon Creek bridge (Cariboo Highway), overlaid on the DEM (hillshade). Arrow size is proportional to flow velocity. Building footprints from Microsoft (2023) database (additional buildings may exist). Parcel boundaries from BC Assessment (2023).**

The model also predicts flooding of buildings along the left floodplain of Naver Creek near Sleepy Hollow Road (Figure E-27).

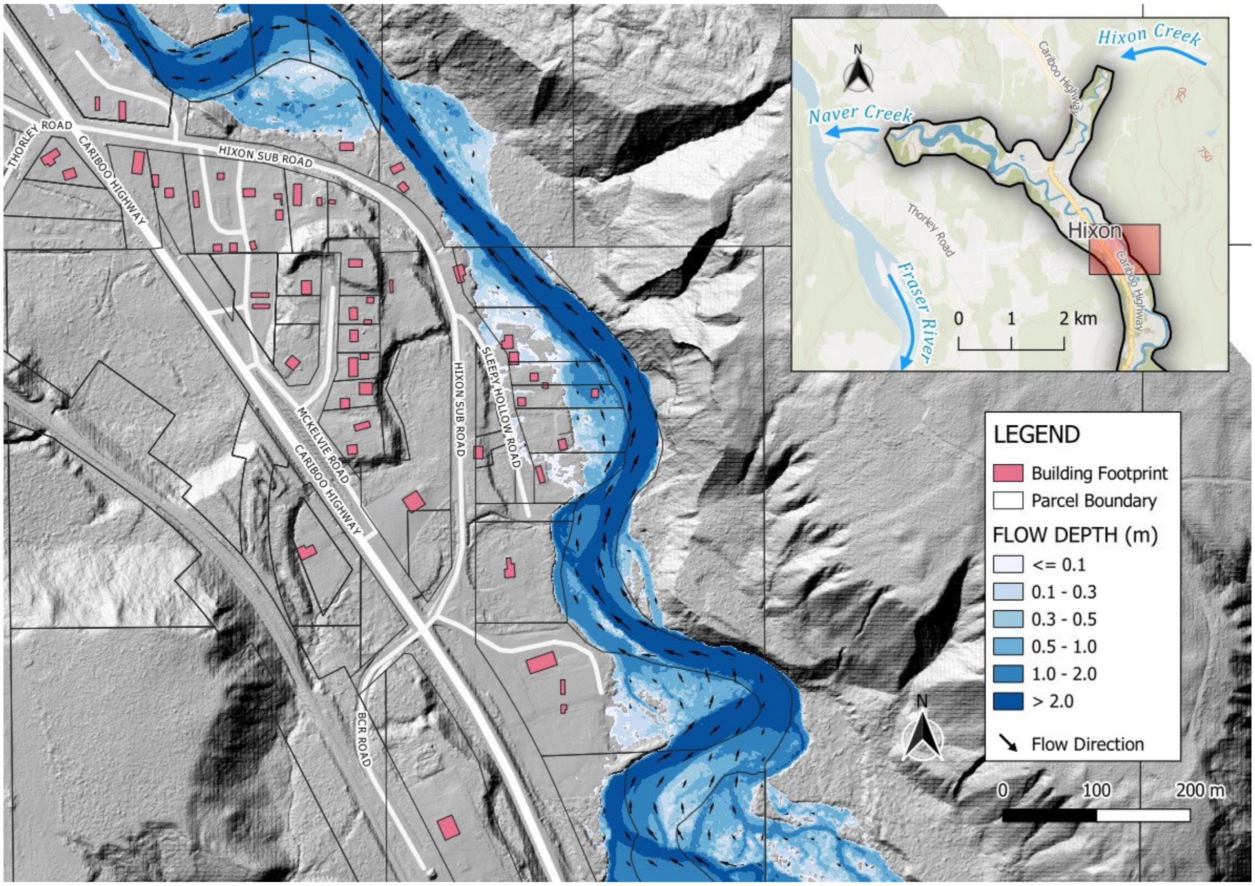

Figure E-27 Modelled climate-adjusted 200-year (0.5% AEP) Naver Creek flood depth in the vicinity of Hixon Sub Road, overlaid on the DEM (hillshade). Arrow size is proportional to flow velocity. Building footprints from Microsoft (2023) database (additional buildings likely exist). Parcel boundaries from BC Assessment (2023).

Upstream from the intersection of the Cariboo Highway and Hixon Sub Road, extending south along Naver Creek, the model does not predict flooding of buildings (Figure E-28 Although the elevation of the Lake Creek Road bridge deck soffit is unknown to BGC, embankment elevations derived from the lidar DEM are approximately 599.0 m. This suggests that the bridge may interact with channel flow, as the model predicts a WSE of 598.3 m.

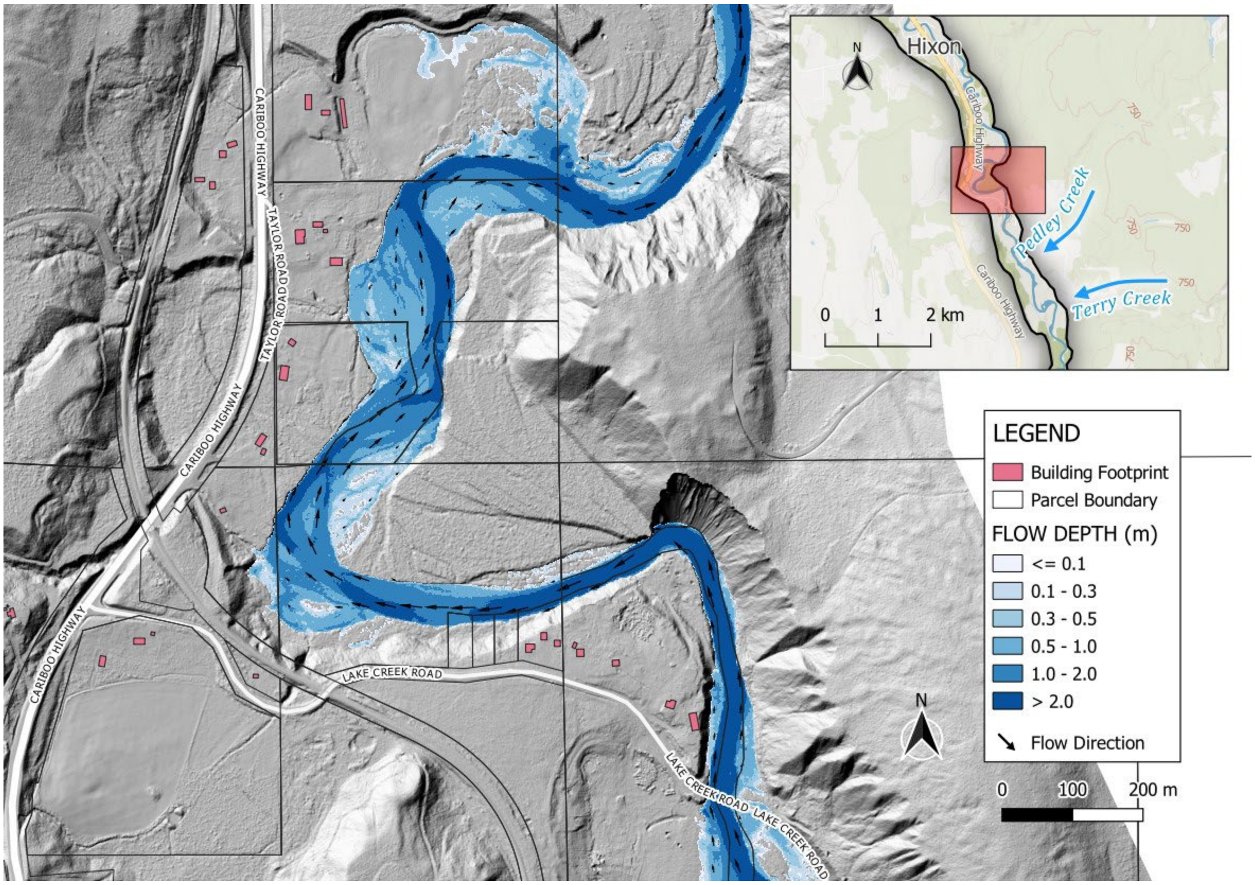

Figure E-28 Modelled climate-adjusted 200-year (0.5% AEP) Naver Creek flood depth in the vicinity of Lake Creek Road, overlaid on the DEM (hillshade). Arrow size is proportional to flow velocity. Building footprints from Microsoft (2023) database (additional buildings likely exist). Parcel boundaries from BC Assessment (2023).

E-5.4.3 Fraser River at McBride

For the climate-adjusted 200-year flood event, the model predicts flooding of buildings along the Dore River floodplain (Figure E-29). While BGC does not have data on the soffit elevations of the Museum Road and railroad bridges, embankment elevations measured from the lidar DEM are approximately 3 m above the highest modelled WSE, suggesting that flow is unlikely to interact with the bridge decks.

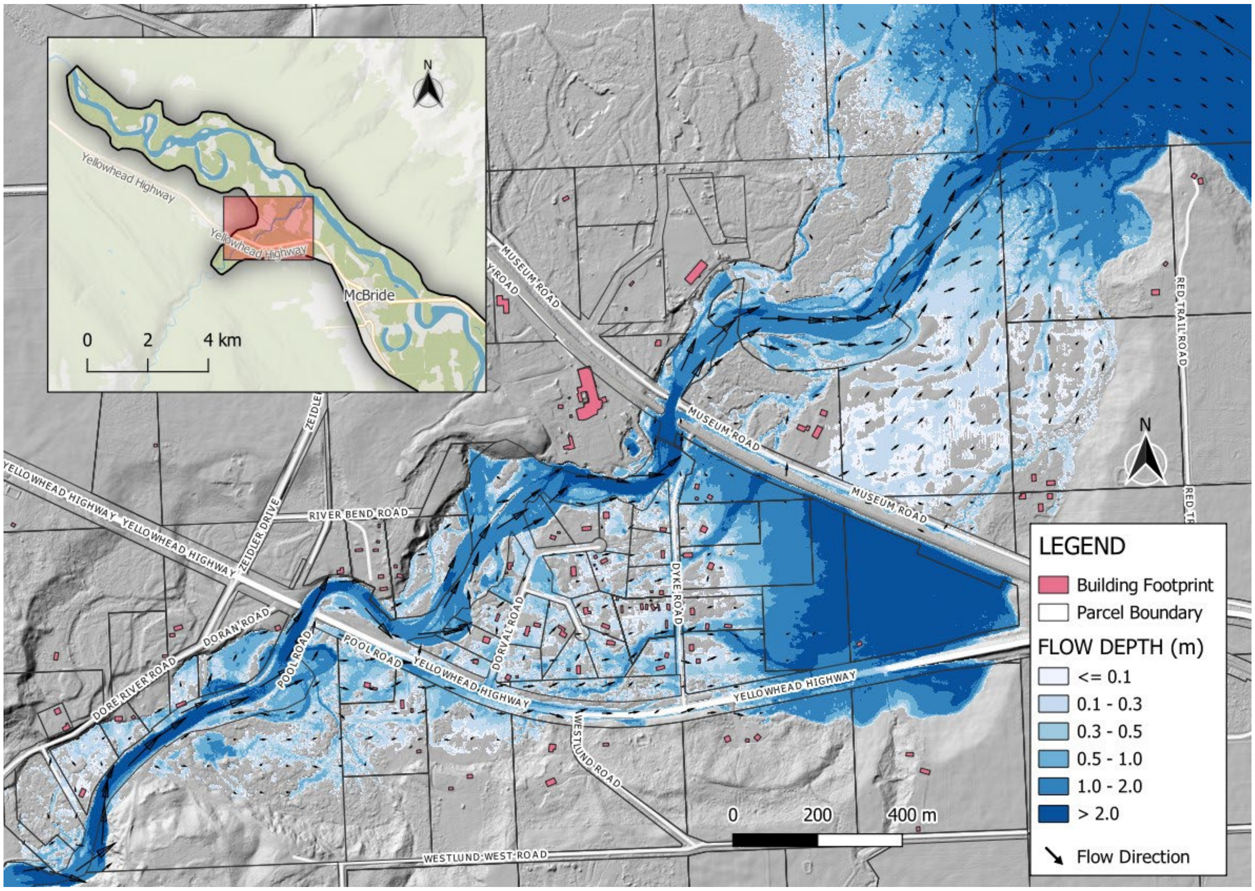

Figure E-29 Modelled climate-adjusted 200-year (0.5% AEP) flood depth along Dore River, overlaid on the DEM (hillshade). Arrow size is proportional to flow velocity. Building footprints from Microsoft (2023) database (additional buildings likely exist). Parcel boundaries from BC Assessment (2023).

Along the left (west) floodplain of the Fraser River near Mountainview Road, the model predicts flooding of buildings (Figure E-30). While BGC does not have data on the soffit elevation of the McBride Bridge (Yellowhead Highway), the embankment elevation at the bridge abutment measured from the lidar DEM, is approximately 1.3 m above the highest modelled WSE, suggesting that flow is unlikely to interact with the bridge deck. However, west of the bridge, the Yellowhead Highway slopes downward, and the model predicts overtopping the embankment for approximately 1 km along the highway centreline.

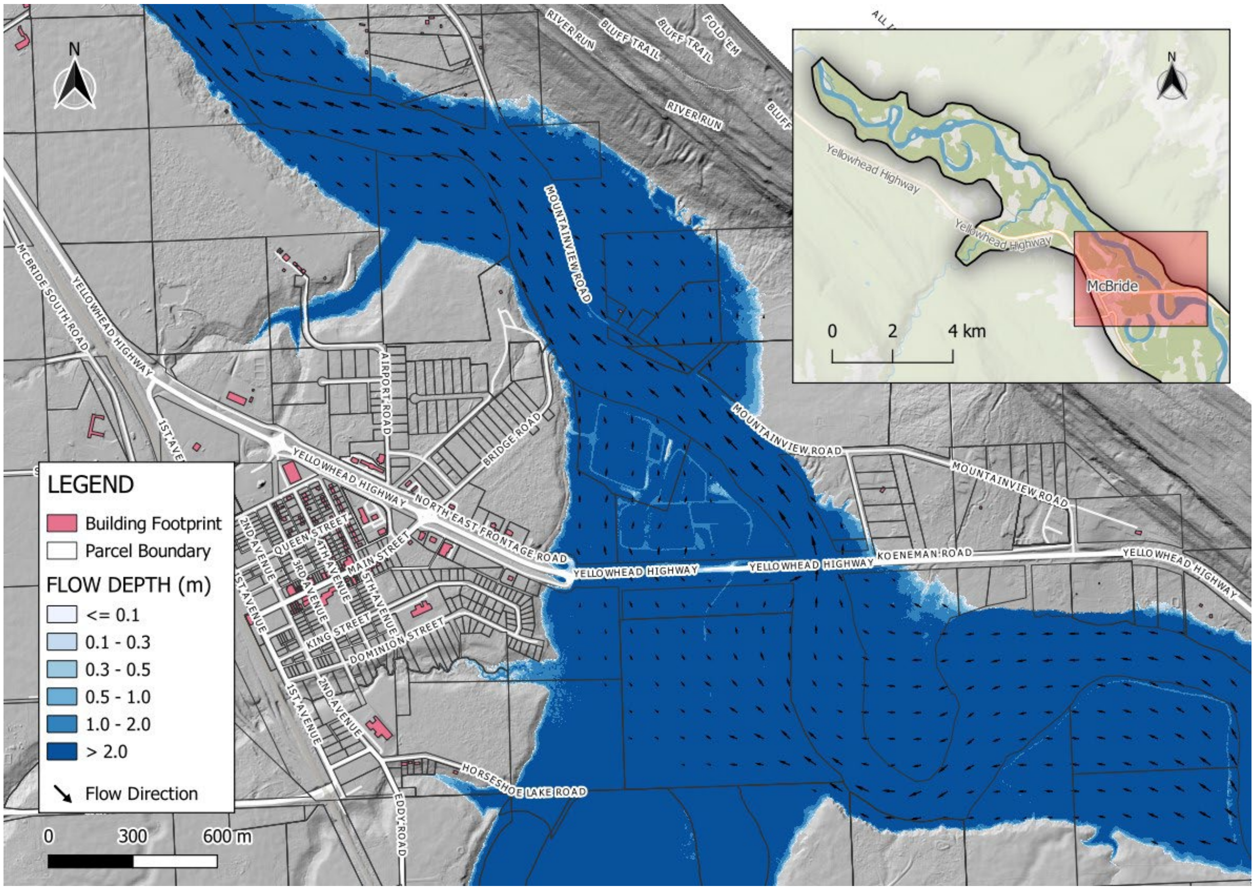

Figure E-30 Modelled climate-adjusted 200-year (0.5% AEP) flood depth along Fraser River in the vicinity of McBride, overlaid on the DEM (hillshade). Arrow size is proportional to flow velocity. Building footprints from Microsoft (2023) database and OpenStreetMap (additional buildings likely exist). Parcel boundaries from BC Assessment (2023).

The model also predicts flooding on Eddy Road for approximately 500 m in the vicinity of Castle Creek (Figure E-31).

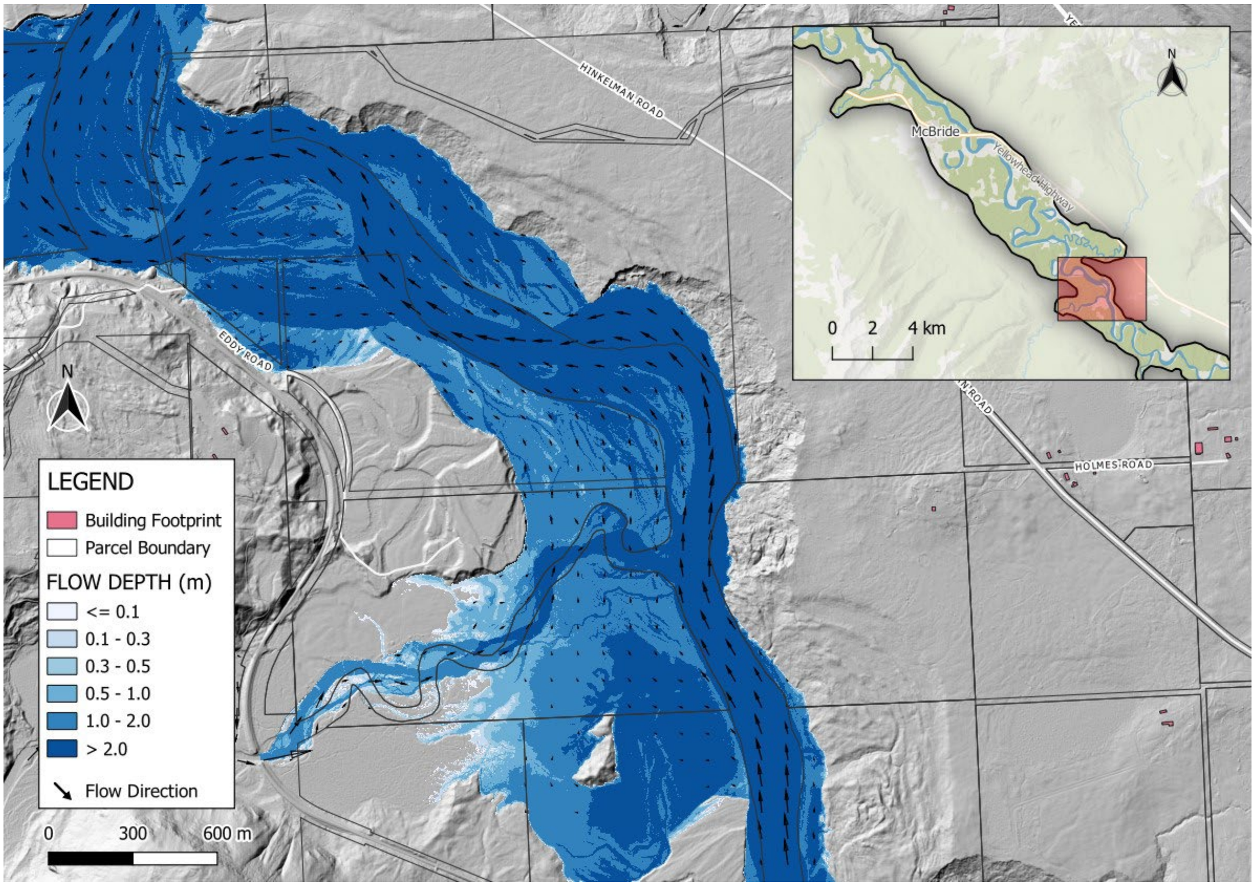

Figure E-31 Modelled climate-adjusted 200-year (0.5% AEP) Fraser River flood depth in the vicinity of Castle Creek, overlaid on the DEM (hillshade). Arrow size is proportional to flow velocity. Building footprints from Microsoft (2023) database and OpenStreetMap (additional buildings likely exist). Parcel boundaries from BC Assessment (2023).

E-5.4.4 Fraser River at Tête Jaune Cache

For the climate-adjusted 200-year flood event, the model does not predict inundation of buildings along the Fraser River adjacent to the Tête Jaune Cache community, including the confluences with the McLennan River and Tête Creek (Figure E-32).

Two bridges – the Yellowhead Highway Bridge (Highway 5) and the Blackman Road Bridge – are located approximately 650 m and 1500 m, respectively, downstream from the upstream boundary of the Fraser River model domain. Although soffit elevations for these bridges are unknown to BGC, lidar DEM data indicate that the embankment elevations are higher than the peak modelled WSE, including results from the sensitivity analyses presented in Section E-5.5. Specifically, for the Yellowhead Highway Bridge, the embankment elevation measured from the lidar DEM is 751.5 m, compared to the highest modeled WSE of 744.2 m. For the Blackman Road Bridge, the embankment elevation is 745.8 m, while the highest modeled WSE is 742.0 m.

Along the McLennan River, approximately 1.1 km downstream from its upstream boundary, two additional structures – the Old Tête Jaune Cache Road Bridge and a CN Railway Bridge – are present. Based on lidar DEM data, the CN Railway Bridge embankment (i.e., 746.8 m) appears to be above the highest modeled WSE (i.e., 738.9 m). In contrast, the Old Tête Jaune Cache Road Bridge shows signs of overtopping, as its embankment (i.e., 738.3 m) is below the highest modeled WSE (i.e., 738.5 m) by approximately 0.2 m (Figure E-32).

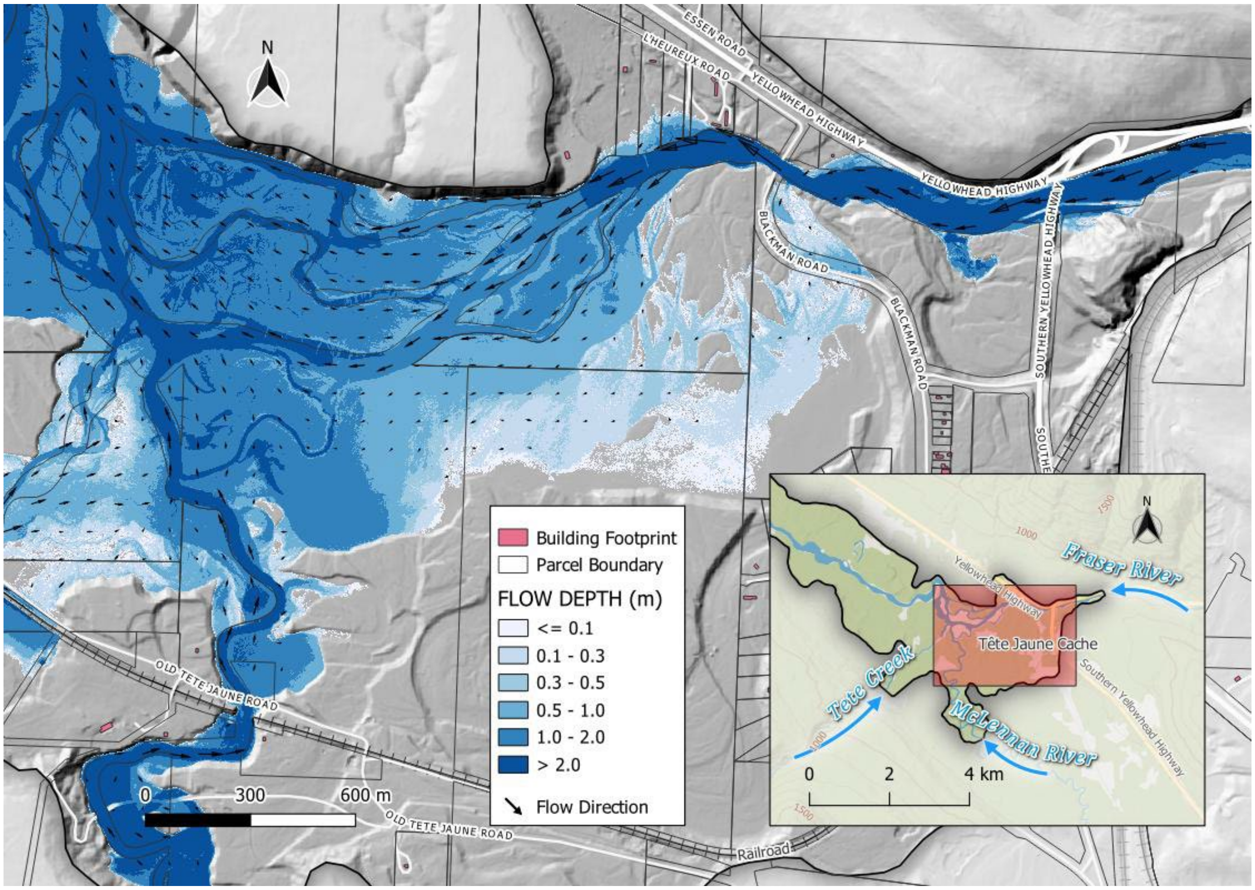

Figure E-32 Modelled climate-adjusted 200-year (0.5% AEP) flood depth at the confluence of Fraser River, McLennan River and Tête Creek, overlaid on the DEM (hillshade). Arrow size is proportional to flow velocity. Building footprints from Microsoft (2023) database (additional buildings likely exist). Parcel boundaries from BC Assessment (2023).

Flooding of buildings is predicted along the left (southwest) floodplain of the Fraser River downstream of its confluence with Tête Creek (Figure E-33). Within the Tête Creek sub-basin, two bridges – again, the Old Tête Jaune Cache Road Bridge and a CN Railway Bridge – are situated approximately 500 m downstream of the upstream model boundary. Lidar-based embankment elevations suggest both bridges have soffits above the modelled WSE, including in sensitivity scenarios evaluated in Section E-5.5. Specifically, for the Old Tête Jaune Cache Road Bridge, the embankment elevation measured from the lidar DEM is 743.5 m, compared to the highest modeled WSE of 742.7 m. For the CN Railway Bridge, the embankment elevation is 743.9 m, while the highest modeled WSE is 743.1 m.

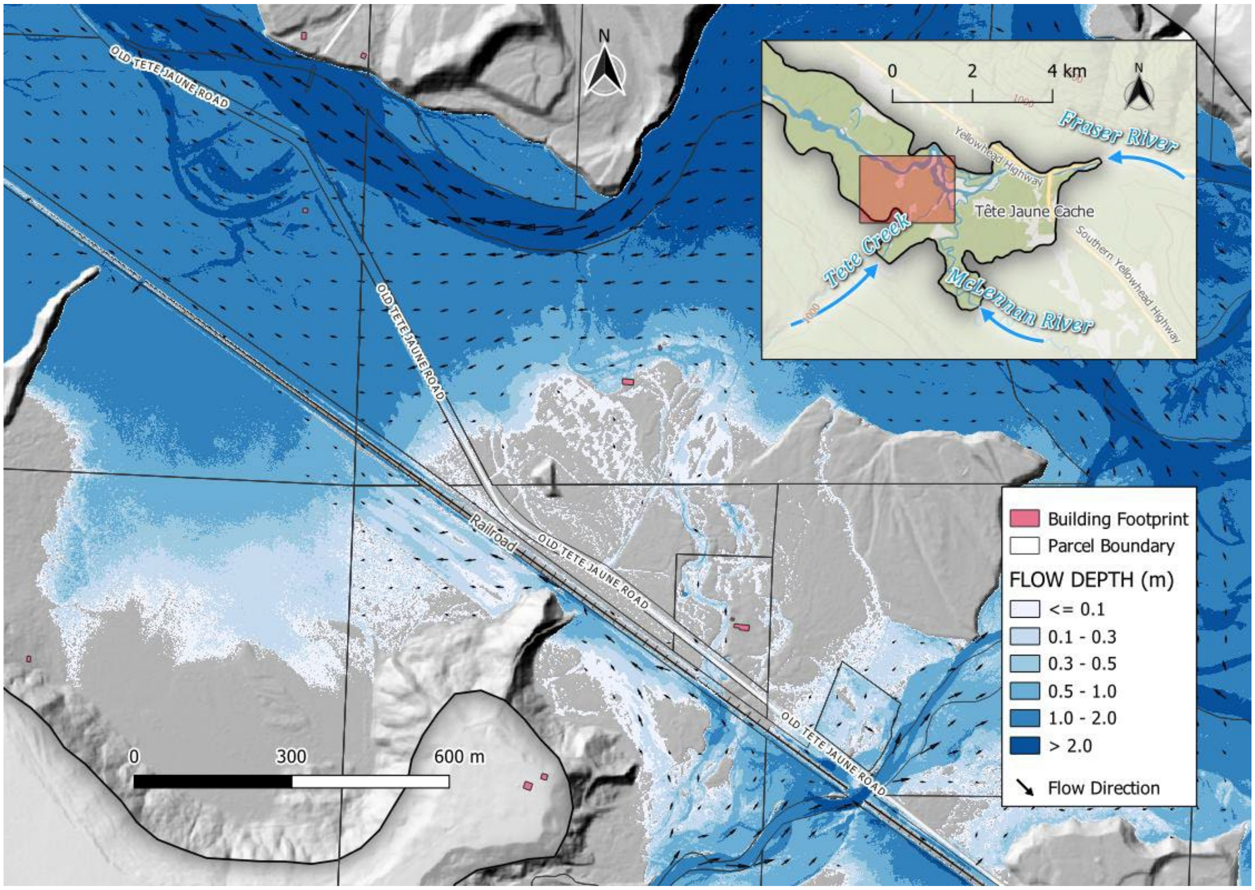

Figure E-33 Modelled climate-adjusted 200-year (0.5% AEP) flood depth downstream of the confluence of Fraser River and Tête Creek, overlaid on the DEM (hillshade). Arrow size is proportional to flow velocity. Building footprints from Microsoft (2023) database (additional buildings likely exist). Parcel boundaries from BC Assessment (2023).

Further downstream, in the vicinity of Old Tête Jaune Road and railroad intersection, flooding of both buildings and road infrastructure is predicted along the right and left floodplains of the Fraser River (Figure E-34).

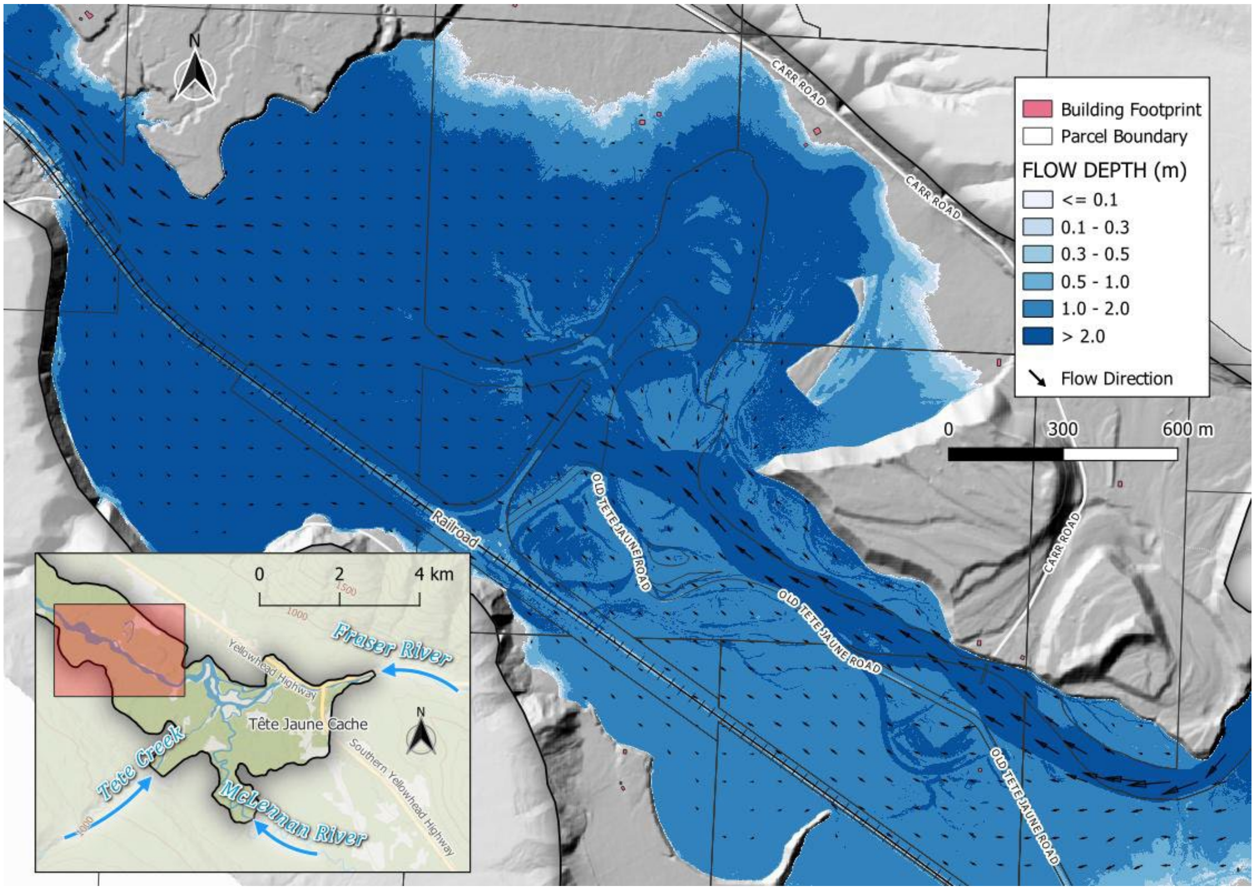

Figure E-34 Modelled climate-adjusted 200-year (0.5% AEP) Fraser River flood depth in the vicinity of Carr Road, overlaid on the DEM (hillshade). Arrow size is proportional to flow velocity. Building footprints from Microsoft (2023) database (additional buildings likely exist). Parcel boundaries from BC Assessment (2023).

In the vicinity of Kiwa Creek, the model does not predict flooding of buildings near its confluence with the Fraser River (Figure E-35). The building located on the left floodplain of Kiwa Creek, approximately 50 meters downstream from the railroad bridge, is situated on a terrain high point and is not expected to be flooded. Although the soffit elevation of the CN Railway Bridge is unknown to BGC and model outputs were clipped in the vicinity of the bridge, lidar-derived embankment elevations indicate that the bridge remains above the peak modeled WSE, consistent with the findings of the sensitivity analyses.

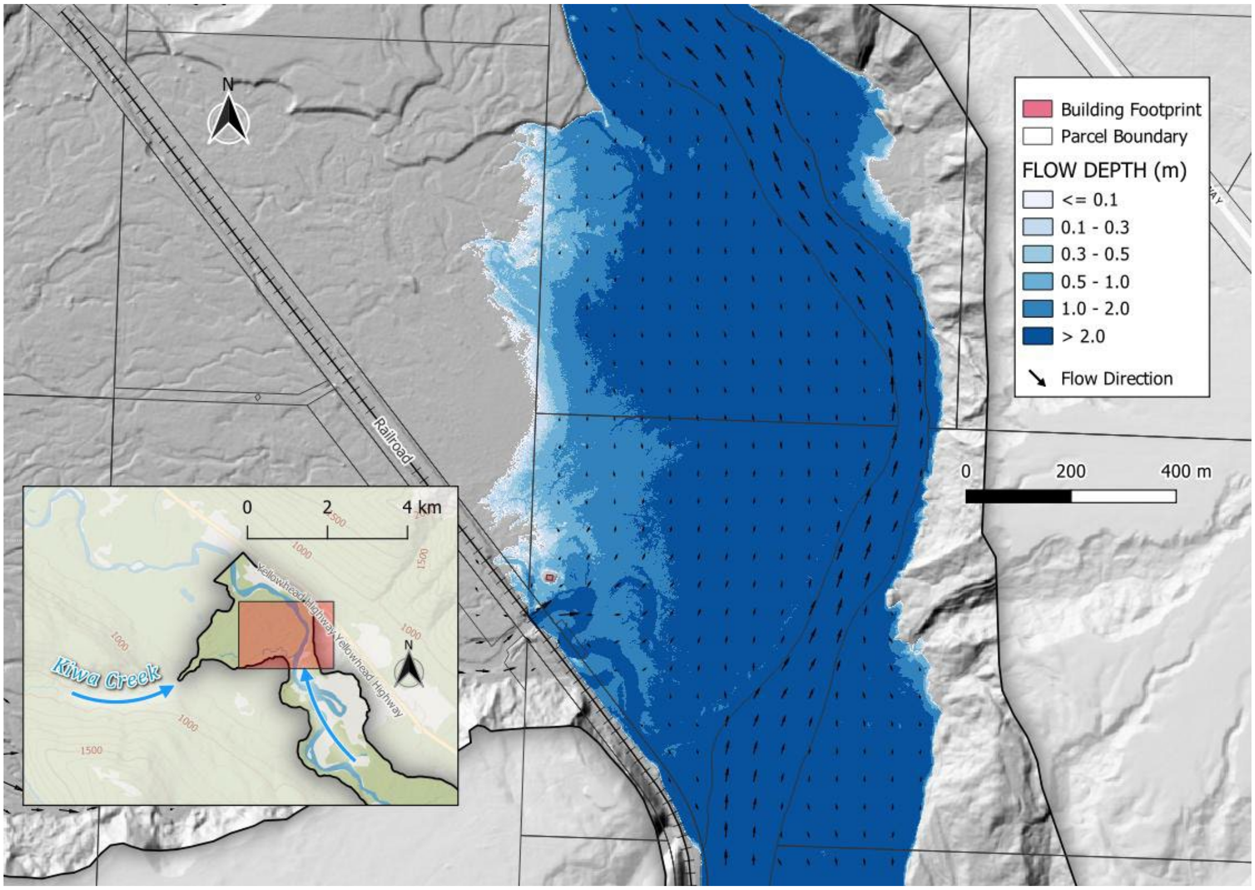

Figure E-35 Modelled climate-adjusted 200-year (0.5% AEP) flood depth at the confluence of Fraser River and Kiwa Creek, overlaid on the DEM (hillshade). Arrow size is proportional to flow velocity. Building footprints from Microsoft (2023) database (additional buildings likely exist). Parcel boundaries from BC Assessment (2023). The building footprint shown is located on a terrain high point and is not expected to be flooded.

E-5.4.5 McLennan River and Swift Creek at Valemount

Swift Creek is subject to both floods and debris floods, and is included in this study for both steep creek assessment and flood hazard mapping. This section addresses flood hazard mapping; see Appendix F for methods used to characterize the Swift Creek alluvial fan.

For the climate-adjusted 200-year flood event, the model predicts flooding of buildings along the Swift Creek floodplain (Figure E-36). While BGC does not have data on the soffit elevations of the Main Street and railroad bridges, embankment elevations measured from the lidar DEM are approximately 3.5 m above the highest modelled WSE, suggesting that flow is unlikely to interact with the bridge deck.

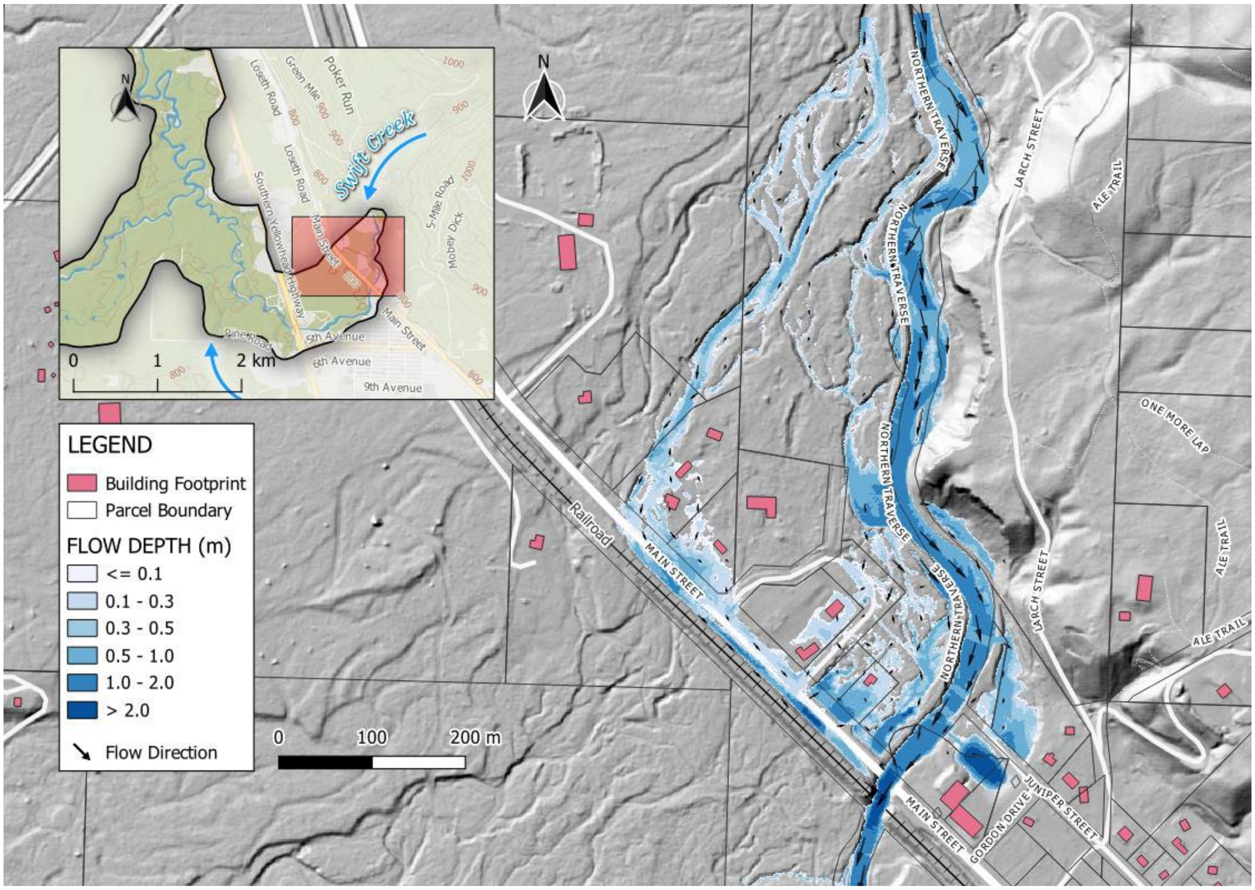

Figure E-36 Modelled climate-adjusted 200-year (0.5% AEP) Swift Creek flood depth in the vicinity of Main Street, overlaid on the DEM (hillshade). Arrow size is proportional to flow velocity. Building footprints from Microsoft (2023) database (additional buildings likely exist). Parcel boundaries from BC Assessment (2023).

Along the right (north) floodplain of Swift Creek near the Yellowhead Highway, the model predicts flooding of buildings (Figure E-37). While BGC does not have data on the soffit elevation of the Yellowhead Highway bridge, the embankment elevation at the bridge abutment, measured from the lidar DEM, is approximately 5 m above the highest modelled WSE, suggesting that flow is unlikely to interact with the bridge deck.

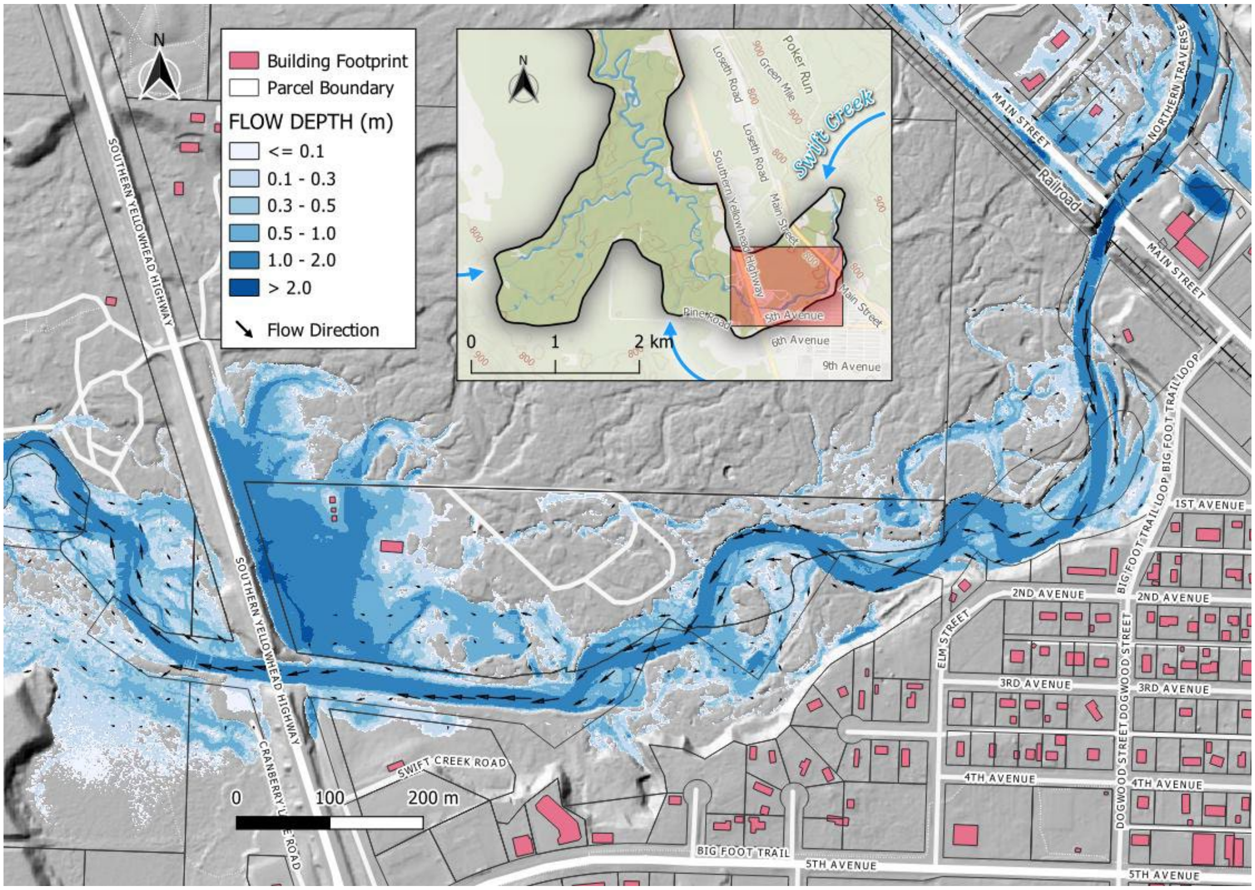

Figure E-37 **Modelled climate-adjusted 200-year (0.5% AEP) Swift Creek flood depth in the vicinity of the Yellowhead Highway, overlaid on the DEM (hillshade). Arrow size is proportional to flow velocity. Building footprints from Microsoft (2023) database (additional buildings likely exist). Parcel boundaries from BC Assessment (2023).**

Downstream of the McLennan River and Swift Creek confluence, the model does not predict flooding of buildings along the McLennan River during the climate-adjusted 200-year flood event (Figure E-38). The Crooked Creek Road bridge is located approximately 3.5 km downstream from the confluence. Although the elevation of the soffit of this bridge deck is not known to BGC, the embankment elevations measured from the lidar DEM are approximately 1 m above the highest modelled WSE, suggesting that flow is unlikely to interact with the bridge deck.

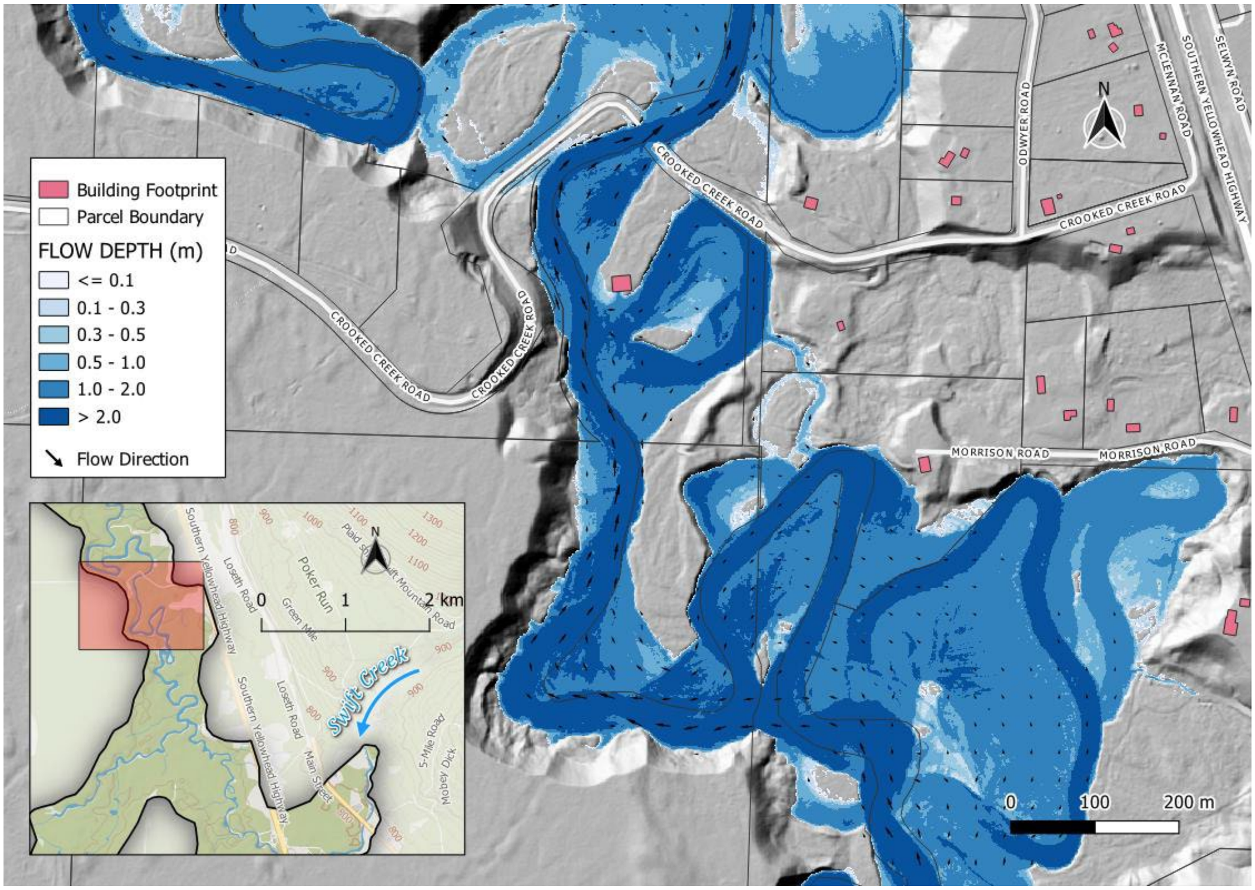

Figure E-38 Modelled climate-adjusted 200-year (0.5% AEP) McLennan River flood depth in the vicinity of Crooked Creek Road, overlaid on the DEM (hillshade). Arrow size is proportional to flow velocity. Building footprints from Microsoft (2023) database (additional buildings likely exist). Parcel boundaries from BC Assessment (2023).

E-5.4.6 Processed Data

The HEC-RAS models for each of the sites were run until they reached a steady state (i.e., the outflow of the model was equal to the total inflows). The results of the models were reviewed and the flow depths and velocities at the final time step was exported as a GIS raster layer. The flow depth and velocity rasters were reviewed in a GIS and additional cleaning of the results was performed to remove artifacts from the model run. The processed rasters for each site were then classified into discrete peak flood depths and velocities (Figure E-39) and imported into Cambio.

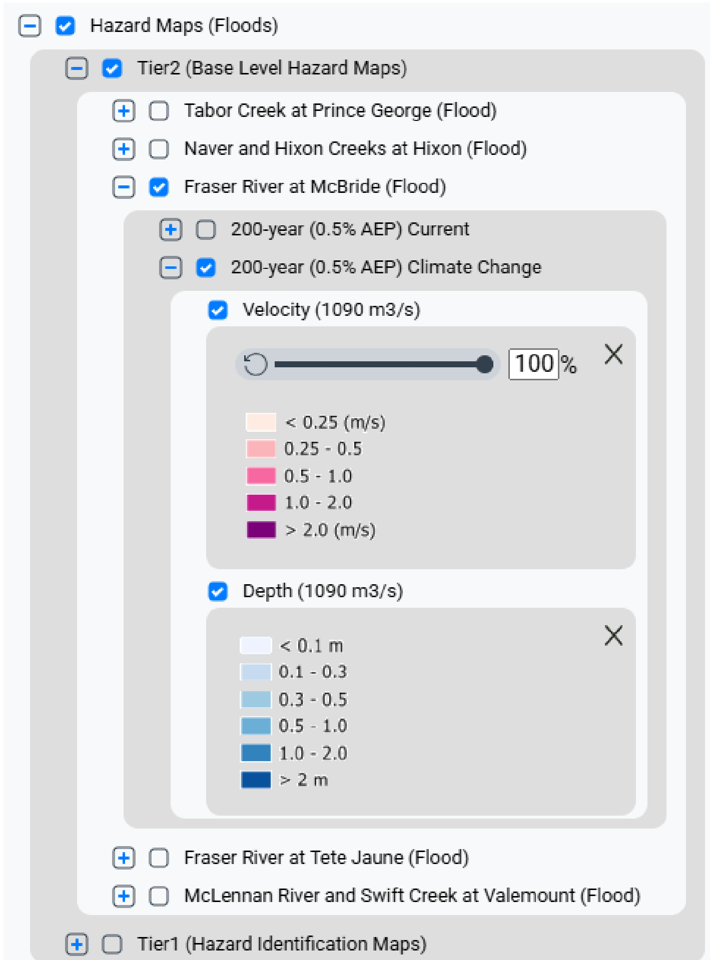

Figure E-39 Discrete flood velocities and flood depths used for display in Cambio, using Fraser River at McBride as an example.

E-5.5 Sensitivity Analysis

Ideally a model is calibrated and validated using paired high-water discharge and water level measurements (observational data) from past known events. However, no observational data was available from past flood events on all the five models presented herein. In lieu of observational data, a sensitivity analysis can be used to evaluate the model's sensitivity to different input parameters and to assess the impact of an input parameter on the modelled results. Additionally, there is uncertainty in the modeled discharges used in the models.

To address the uncertainty in the models, a sensitivity analysis was performed for each study area for the following parameters

- The roughness coefficient, Manning's n.
- The peak discharge.
- The friction slope at the downstream boundary condition
- The mesh resolution.

All sensitivity scenarios were performed on the stationary 200-year (0.5% AEP) flood event to evaluate the impact these input parameters could have on inundation extent within the study areas.

E-5.5.1 Tabor Creek at Prince George

The sensitivity analysis results indicated that a ±20% change in the Manning's n coefficient led to a ±4% change in the inundation extent and an ±7 cm change in the average WSE, suggesting that uncertainty in roughness coefficients has a limited impact on the inundation extents (Table E-15). Reducing the friction slope at the downstream boundary increased the WSE; however, the resulting backwater effect was confined to within 100 m of the model outlet and had a negligible influence on inundation extent. Similarly, halving the mesh size had little to no effect on the inundation extent indicating that the selected mesh resolution was sufficient.

Table E-15 Sensitivity analysis of Tabor Creek at Prince George HEC-RAS 2D model.

Parameter	Sensitivity Applied	Change in Inundation Extent	Change in WSE (cm)	
			Average	Std. Dev.
Manning's n	20% decrease	-4%	-7	3
	20% increase	+3%	+7	3
Discharge	10% increase	+4%	+8	4
	20% increase	+4%	+14	3
Friction Slope	Halving friction slope	0%	Not assessed	Not assessed
Mesh Resolution	Halving mesh cell size	2%	+2	2

E-5.5.2 Naver and Hixon Creek at Hixon

The sensitivity analysis results indicated that a ±20% change in the Manning's n coefficient led to a ±7% change in the inundation extent and an ±11 cm change in the average WSE, suggesting that uncertainty in roughness coefficients has a limited impact on the inundation extent (Table E-16, Figure E-40). Reducing the friction slope at the downstream boundary increased the WSE; however, the resulting backwater effect was confined to within 150 m of the model outlet and had a negligible influence on inundation extent. Similarly, halving the mesh size had little to no effect on the inundation extent indicating that the selected mesh resolution was sufficient.

Table E-16 Sensitivity analysis of Naver and Hixon Creek at Hixon HEC-RAS 2D model.

Parameter	Sensitivity Applied	Change in Inundation Extent	Change in WSE (cm)	
			Average	Std. Dev.
Manning's n	20% decrease	-7%	-11	5
	20% increase	+6%	+10	4
Discharge	10% increase	+5%	+8	3
	20% increase	+9%	+14	6
Friction Slope	Halving friction slope	0%	0	1
Mesh Resolution	Halving mesh cell size	0%	0	5

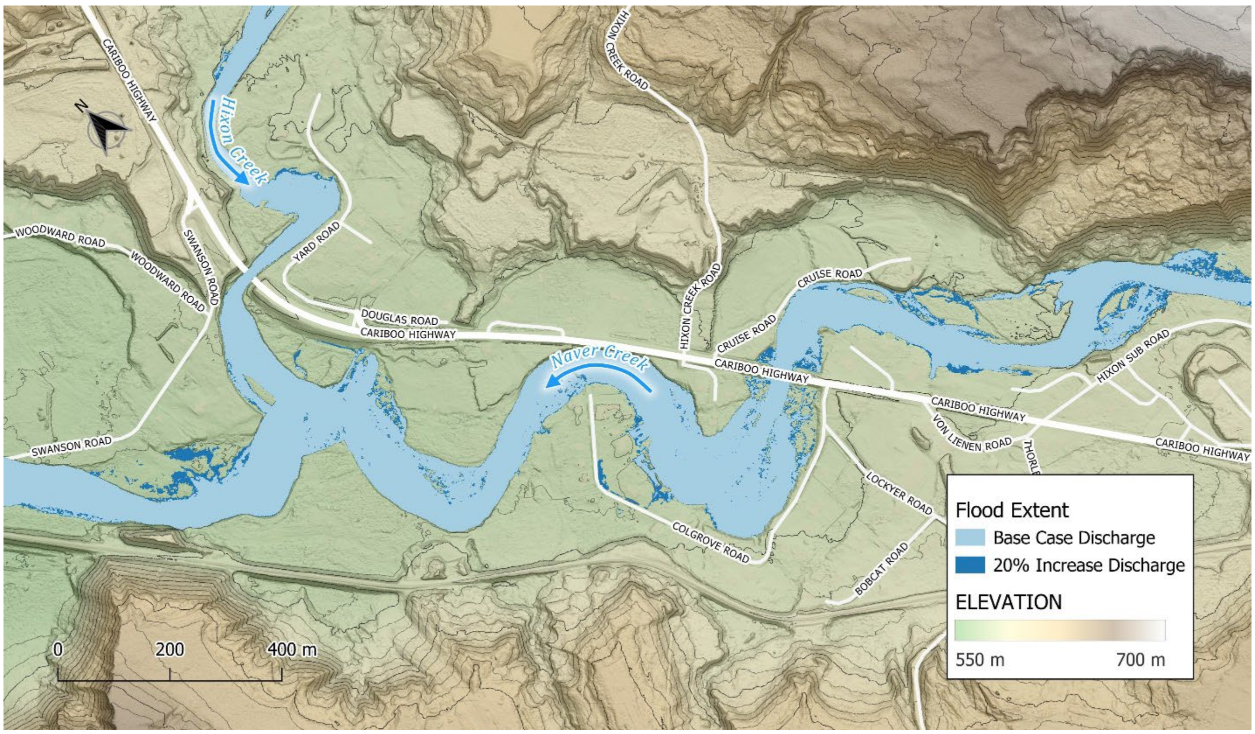

Figure E-40 Comparison of flood extent between the base case (0.5% AEP) and a scenario with a 20% increase in peak discharge in the vicinity of Naver Creek and Hixon Creek confluence, overlaid on the DEM (coloured multidirectional hillshade). Contour interval is 5 m.

E-5.5.3 Fraser River at McBride

The sensitivity analysis results indicated that a ±20% change in the Manning's n coefficient led to a ±3% change in the inundation extent and a ±38 cm change in the average WSE, suggesting that uncertainty in roughness coefficients has a limited impact on the inundation extent (Table E-17). Reducing the friction slope at the downstream boundary increased the WSE. Given the shallow gradient in the river, the resulting backwater effect extended 12 km upstream from the model outlet; however, it had a negligible influence on inundation extent. Halving the mesh size had little to no effect on the inundation extent.

Table E-17 Sensitivity analysis of Fraser River at McBride HEC-RAS 2D model.

Parameter	Sensitivity Applied	Change in Inundation Extent	Change in WSE (cm)	
			Average	Std. Dev.
Manning's n	20% decrease	-3%	-38	18
	20% increase	+3%	+37	17
Discharge	20% increase	+4%	+53	19
Friction Slope	Base slope from 0.020% to 0.015%	0%	+11	17
Mesh Resolution	Halving mesh cell size	0%	-4	8

E-5.5.4 Fraser River at Tête Jaune Cache

The sensitivity analysis results indicated that a ±20% change in the Manning's n coefficient led to a ±4% change in the inundation extent and a ±11 cm change in the average WSE, suggesting that uncertainty in roughness coefficients has a limited impact on inundation extent (Table E-18). Reducing the friction slope at the downstream boundary increased the WSE. Given the shallow gradient, the resulting backwater effect extended 15 km upstream from the model outlet; however, it had a negligible influence on inundation extent. Halving the mesh size had little to no effect on the inundation extent indicating that the selected mesh resolution was sufficient.

Table E-18 Sensitivity analysis of Fraser River at Tête Jaune Cache HEC-RAS 2D model.

Parameter	Sensitivity Applied	Change in Inundation Extent	Change in WSE (cm)	
			Average	Std. Dev.
Manning's n	20% decrease	-4%	-12	7
	20% increase	+4%	+10	9
Discharge	20% increase	+5%	+15	10
Friction Slope	Halving friction slope	1%	+1	4
Mesh Resolution	Halving mesh cell size	0%	-1	3

E-5.5.5 McLennan River and Swift Creek at Valemount

The sensitivity analysis results indicated that a ±20% change in the Manning's n coefficient led to a ±4% change in the inundation extent and a ±12 cm change in the average WSE, suggesting that uncertainty in roughness coefficients has a limited impact on the inundation extent (Table E-19). Reducing the friction slope at the downstream boundary increased the WSE. The resulting backwater effect extended 2 km upstream from the model outlet; however, it had a negligible influence on inundation extent.

Table E-19 Sensitivity analysis of McLennan River and Swift Creek at Valemount HEC-RAS 2D model.

Parameter	Sensitivity Applied	Change in Inundation Extent	Change in WSE (cm)	
			Average	Std. Dev.
Manning's n	20% decrease	-4%	-12	5
	20% increase	+3%	12	5
Discharge	25% increase	+6%	+26	12
Friction Slope	Halving friction slope	0%	+1	6

E-5.6 Hazard Mapping Uncertainties and Limitations

Appendix J lists hazard mapping uncertainties and limitations and provides options to resolve as part of future work. In summary, uncertainties relate to the calibration of models, a need to collect further data on river bathymetry, considering geomorphic factors in hazard mapping, and conducting updates as conditions change over time. BGC notes that effort to resolve gaps and uncertainties is more cost-effective if the hazard mapping is treated as an asset to be maintained on a periodic basis, rather than material to be replaced once obsolete. This way, further refinements can build on previous work, avoiding duplication of effort.

REFERENCES

BC Assessment (2023, October 20). Parcel boundaries and BC Assessment data [Dataset]. Retrieved from https://www2.gov.bc.ca/gov/content/data/finding-and-sharing/bc-data-catalogue

BGC Engineering Inc. (2024, April 19). Mapping for Floodplain Identification (Stage 1). [Report]. Prepared for BC Hydro.

British Columbia Ministry of Transportation and Infrastructure (BC MoTI). (2017). *Culverts* [Dataset]. Retrieved from https://catalogue.data.gov.bc.ca/dataset/ministry-of-transportation-mot-culverts

British Columbia Ministry of Transportation and Transit (BC MoTT). (2024, May). *Historical DriveBC events* [Dataset]. Retrieved from https://catalogue.data.gov.bc.ca/dataset/historical-drivebc-events

Brunner, G. W., & CEIWR-HEC. (2021). *HEC-RAS River Analysis System 2D Modeling User's Manua*l. Retrieved from www.hec.usace.army.mil.

Chow, V.T. (1959). Open-channel hydraulics. New York, McGraw-Hill, 680 p.

Hoskin, J.R.M. & Wallis, J.R. (1997). *Regional Frequency Analysis: An Approach Based on L-moments*. Cambridge University Press, UK. http://dx.doi.org/10.1017/cbo9780511529443

McElhanney Ltd. (2021, March 11). *Hydrologic and Geomorphic Assessment of the Dore River* [Report]. Prepared for RDFFG.

Microsoft (2023). *Microsoft Building Footprints for Canada* [Dataset]. Extracted November 14, 2023, from https://github.com/Microsoft/CanadianBuildingFootprints

Ministry of Environment, Lands and Parks (1995, October). *A Design Brief on the Floodplain Mapping Project for Naver and Hixon Creeks near Hixon, BC*. File: 35100-30/100-5229, Victoria, BC.

Nardi, F., Annis, A., Di Baldassarre, G., Vivoni, E.R., & Grimaldi, S. (2019). GFPLAIN250 m, a global high-resolution dataset of Earth's floodplains. *Scientific Data, 180309* (2019). https://doi.org/10.1038/sdata.2018.309

Natural Resources Canada. (2010). Terrestrial Ecozones. Retrieved from: https://sis.agr.gc.ca/cansis/nsdb/ecostrat/gis_data.html

Natural Resources Canada (NRC), Canada Centre for Remote Sensing. (2019). 2015 Land cover of Canada [GIS Data]. Retrieved from https://open.canada.ca/data/en/dataset/4e615eae-b90c-420b-adee-2ca35896caf6

Pacific Climate Impacts Consortium, University of Victoria, (2020, January). VIC-GL BCCAQ CMIP5: Gridded Hydrologic Model Output. Downloaded from https://www.pacificclimate.org/data/gridded-hydrologic-model-output in 2024.

Pacific Climate Impacts Consortium (PCIC), University of Victoria, (2020, February). VIC-GL BCCAQ CMIP5 RVIC: Station Hydrologic Model Output. Downloaded from https://pacificclimate.org/data/station-hydrologic-model-output on February 1, 2021

Rocky Mountain Goat. (2021, July). Rapid Melt: Fraser River flooding in photos. Accessed from www.therockymountaingoat.com/2021/07/rapid-melt/

Septer, D. (2007). *Flooding and landslide events southern British Columbia 1808-2006*. Retrieved from http://www.env.gov.bc.ca/wsd/public_safety/flood/pdfs_word/floods_landslides_south1.pdf

Simonovic, S.P., Schardong, A., Srivastav, R., & Sandink, D. (2015). *IDF_CC Web-based Tool for Updating Intensity-Duration-Frequency Curves to Changing Climate – ver 6.5*. Western University Facility for Intelligent Decision Support and Institute for Catastrophic Loss Reduction, open access https://www.idf-cc-uwo.ca

Transportation Association of Canada (TAC). (2004). *Guide to bridge hydraulics, 2nd ed*. Thomas Telford, London.

Zhang, Z., Stadnyk, T.A., & Burn, D.H. (2019). Identification of a preferred statistical distribution for at-site flood frequency analysis in Canada. *Canadian Water Resources Journal, 45*(1), 43-58. https://doi.org/10.1080/07011784.2019.1691942

APPENDIX F
STEEP CREEK HAZARD ASSESSMENT METHODS

F-1 INTRODUCTION

This appendix describes methods used by BGC Engineering Inc. (BGC) to identify and characterize steep creek geohazards within the Regional District of Fraser Fort George (RDFFG). This appendix is organized as follows:

- Section F-2 provides background information and key terminology on steep creek geohazards, and a high-level introduction to climate change effects on steep creek geohazards.
- Section F-3 describes methods and criteria used to identify and classify steep creek geohazard areas.
- Sections F-4 describes the fan and watershed attributes rated for each geohazard area.

F-2 BACKGROUND

Steep creeks (here-in defined as having channel gradients steeper than 3°, or 5%) are typically subject to a spectrum of sediment transport processes ranging from clear-water floods to debris floods to hyper-concentrated flows to debris flows, in order of increasing sediment concentration. They can be referred to collectively as hydrogeomorphic processes because water and sediment (in suspension and bedload) are being transported. Depending on process and severity, hydrogeomorphic processes can cause local landscape changes.

These processes are continuous in space and time, with floods transitioning into debris floods upon exceedance of critical bed shear stress thresholds to mobilize most grains of the surface bedload layer. At high fines concentrations, hyperconcentrated flows develop. Debris flows are typically triggered by side slope landslides or progressive bulking with erodible sediment, a process observed specifically after wildfires at moderate to high burn severity. Dilution of a debris flow through partial sediment deposition on lower gradients (less than approximately <15°) channels and tributary injection of water can lead to a transition towards hyper-concentrated flows and debris floods and eventually floods. Some steep creeks can be classified as hybrids, implying variable hydrogeomorphic processes at different return periods.

Figure F-1 summarizes the different hydrogeomorphic processes.

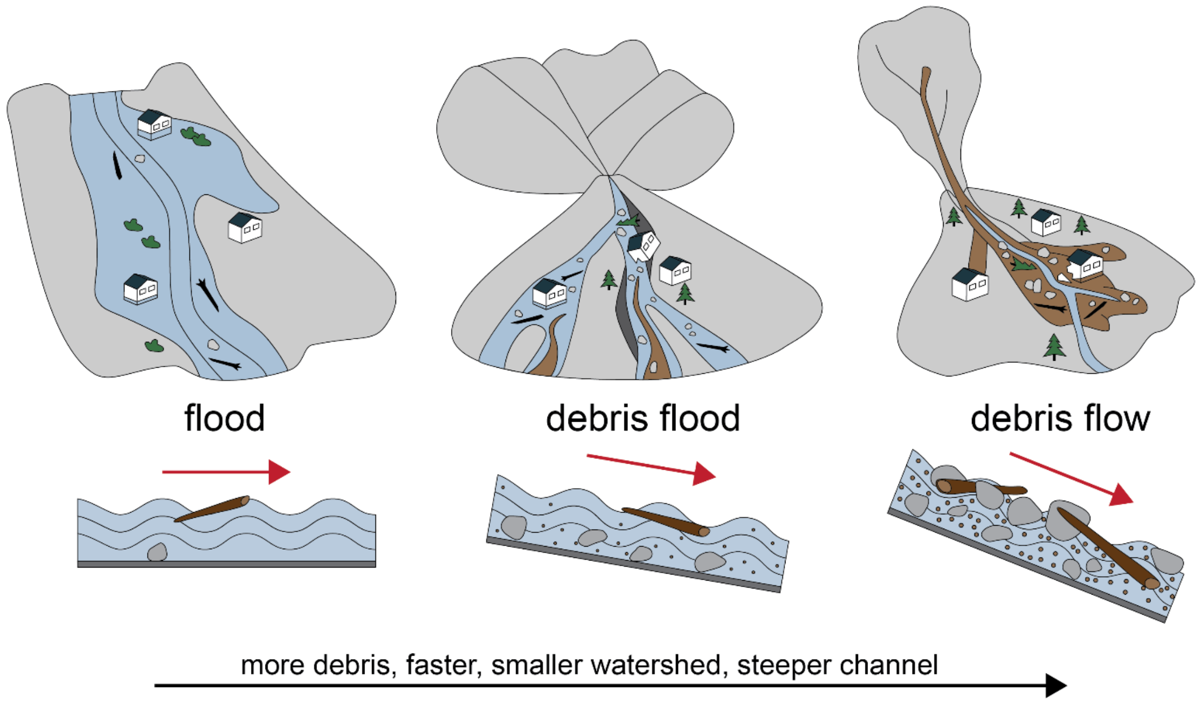

Figure F-1 Hydrogeomorphic processes.

F-2.1 Steep Creek Watersheds and Fans

A steep creek watershed consists of hillslopes, small feeder channels, a principal channel, and an alluvial fan composed of deposited sediments at the lower end of the watershed. Figure F-2 provides a typical example of a steep creek in the RDFFG. Alluvial fans in mountainous environments can be subject to the range of steep creek processes shown in Figure F-1.

While generalizations can be made about geohazard processes affecting alluvial fans, each watershed and fan is unique in the type and intensity of mass movement and fluvial processes, and the hazard and risk profile associated with such processes. Figure F-3 schematically illustrates two fans side by side. The steeper one on the left is dominated by debris flows and perhaps rock fall near the fan apex, whereas the one on the right with the lower gradient is likely dominated by debris floods.

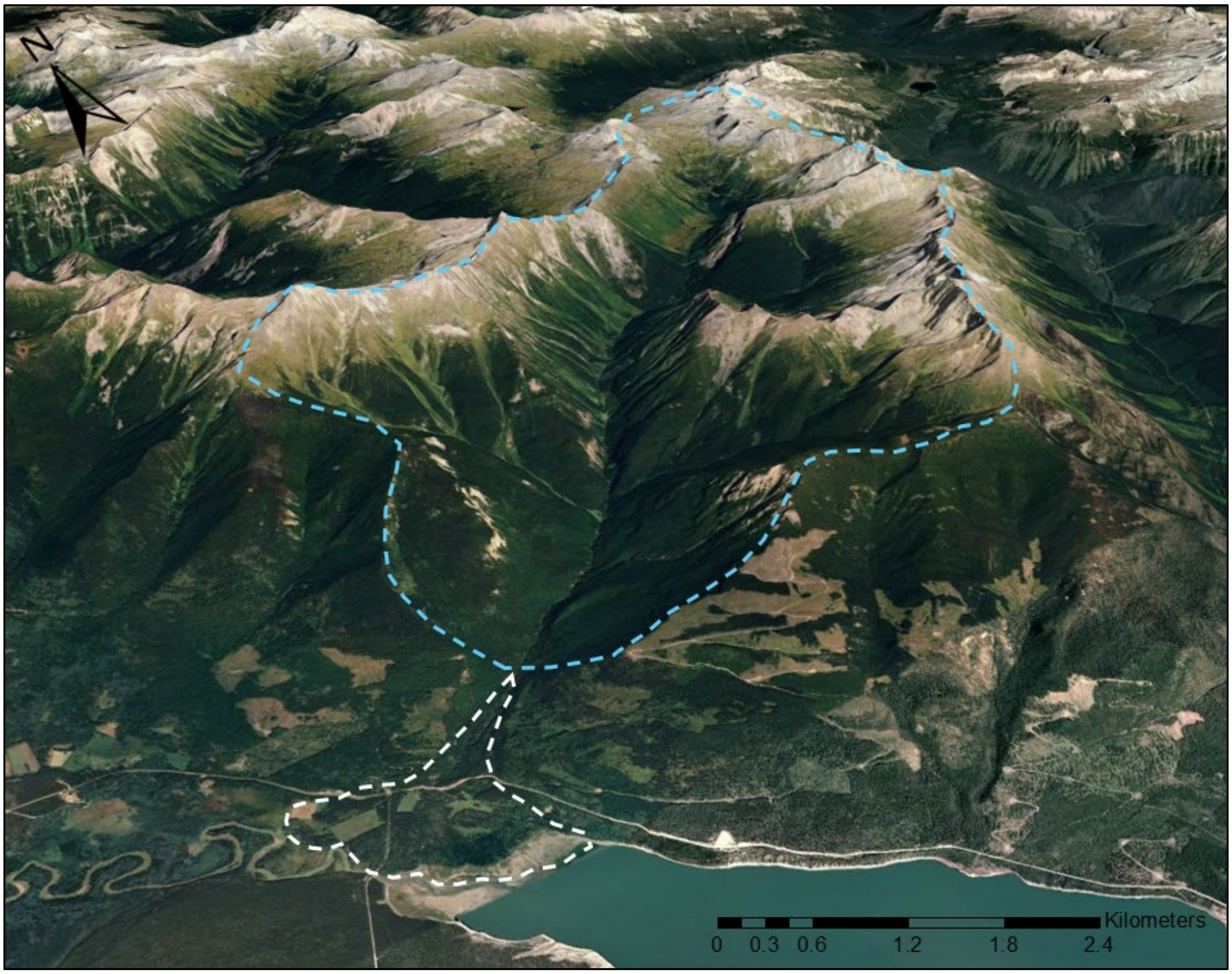

Figure F-2 A typical steep creek watershed and fan (Packsaddle Creek) located near Valemount in the RDFFG, with Kinbasket Lake in the foreground. The approximate watershed and fan boundary are outlined in blue and white, respectively. Imagery: Google Earth, 2019.

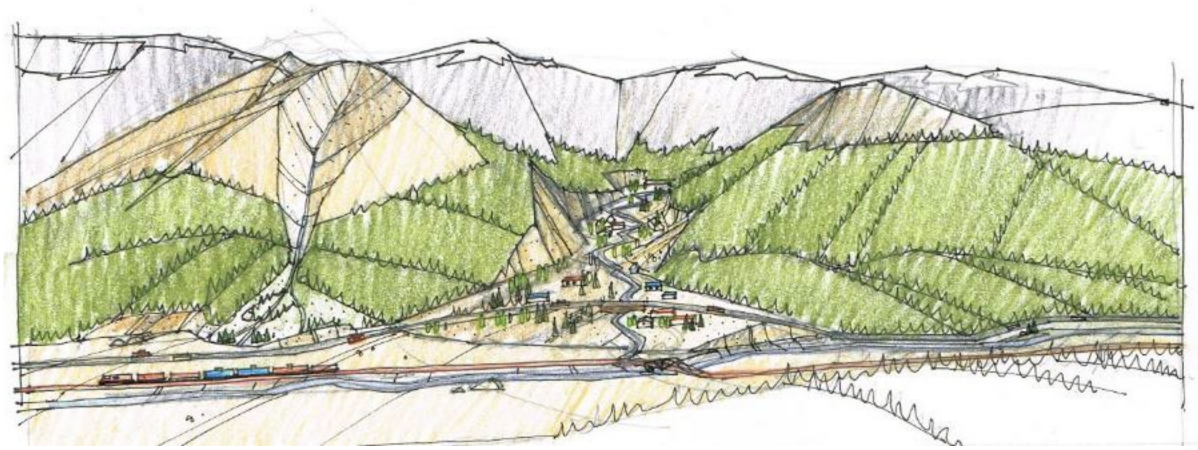

Figure F-3 Typical steep and low-gradient fans feeding into a broader floodplain. On the left a small watershed prone to debris flows has created a steep fan that may also be subject to rock fall processes. On the right a larger watershed prone to debris floods has created a lower gradient fan. Development and infrastructure are shown to illustrate their interaction with steep creek geohazard events. Artwork: Derrill Shuttleworth.

In steep creek basins (or watersheds), most mass movements on hillslopes directly or indirectly feed into steep mountain channels from which they begin their journey downstream. Viewed at the scale of the catchment and over geologic time, distinct zones of sediment production, transfer, erosion, deposition, and avulsions may be identified within a drainage basin (Figure F-4).

Steep mountain slopes deliver sediment and debris to the upper channels by a variety of landslide processes (e.g., rock fall, rock slides, debris avalanches, debris flows, slumps and raveling). Debris flows and debris floods characteristically gain momentum and sediments as they move downstream and spread across an alluvial fan where the channel enters the main valley floor. Landslides may also create temporary dams that pond water, which can fail catastrophically. In these scenarios, a debris flood or debris flow may be initiated in the channel that travels further than the original landslide.

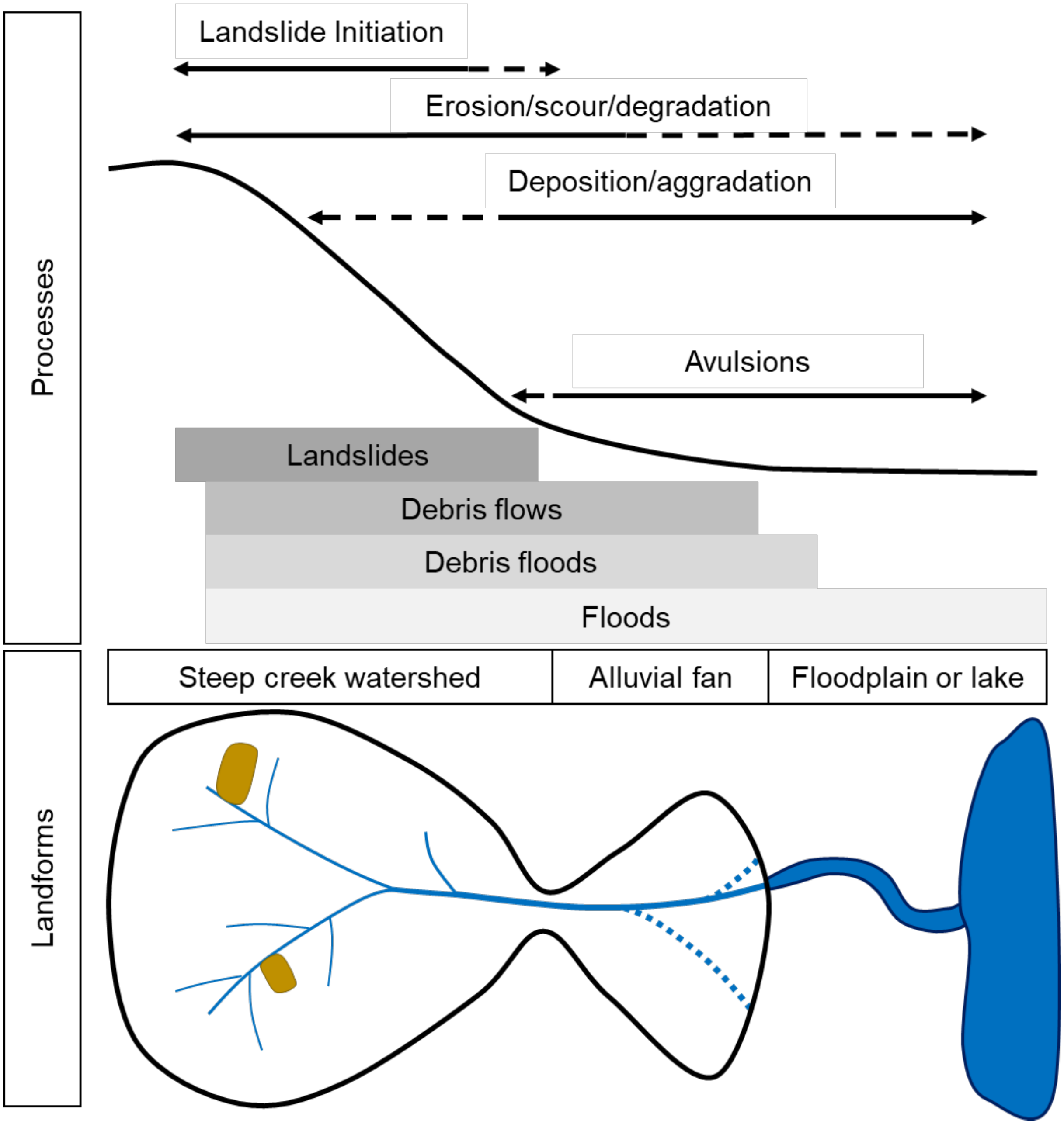

Figure F-4 Schematic diagram of a steep creek watershed system that shows the principal zones of distinctive processes and sediment behaviour. The alluvial fan is thought of as the long-term storage landform with a time scale of thousands to tens of thousands of years. Sketch developed by BGC from concepts produced by Schumm (1977), Montgomery & Buffington (1997), and Church (2013).

The alluvial fan represents a mostly depositional landform at the outlet of a steep creek watershed. Alluvial fans are dynamic and potentially dangerous (hazardous) landforms that represent the approximate extent of past and future hydrogeomorphic processes. This landform is more correctly called a colluvial fan when formed by debris flows because debris flows are classified as a landslide process, and an alluvial fan when formed by clear-water floods (those which do not carry substantial bedload or suspended load) or debris floods. For simplicity the term alluvial fan is used herein irrespective of geohazard type. “Classic” alluvial fans are roughly triangular in planform, but most fans have irregular shapes influenced by the surrounding topography. Redistribution of sediments from the upper steeper fan to the lower flatter fan, primarily through bank erosion and channel scour, is common (Lau, 2017; de Haas et al., 2024).

Stream channels on the fan are prone to avulsions, which are rapid changes in channel location, due to natural cycles in alluvial fan development and from the loss of channel confinement during hydrogeomorphic events (e.g., Kellerhals & Church, 1990; van Dijk et al., 2009; 2012; de Haas et al., 2017; Zubrycky et al., 2021; de Haas et al., 2024). If the alluvial fan is formed on the margin of a still water body (lake, reservoir, ocean), the alluvial fan is termed a fan-delta. These landforms differ from alluvial fans in that sediment deposition at the margin of the landform occurs in still water, which invites in-channel sediment aggradation due to a pronounced morphodynamic backwater effect. This can increase the frequency and possibly severity of avulsions (van Dijk et al., 2009; 2012).

The term “paleofan” is used to describe portions of fans interpreted as no longer active (under present climate and geomorphic/geological setting) and entirely removed from the channel processes described previously (i.e., with negligible potential for channel avulsion and flow propagation) due to deep channel incision (Kellerhals & Church, 1990). BGC mapped only one paleofan in the RDFFG; the fan located at Redmountain Creek is divided into the active and inactive (paleofan) portions of the fan.

Some paraglacial fans are located throughout the RDFFG. These are defined as fans primarily deposited shortly after the landscape was deglaciated (Ryder, 1971a; 1971b; Church & Ryder, 1972). Paraglacial fans are found overlying broad terraces bordering large river systems in the RDFFG (e.g., along the Fraser River between Valemount and Sinclair Mills). Unlike paleofans, paraglacial fans are not necessarily inactive. Thus, the term paleofan is only applied to paraglacial fans if the stream had incised into the fan and removed the connection between the stream and the landform.

F-2.2 Debris Flows

‘Debris flow’, as defined by Hungr, Leroueil, and Picarelli (2014), is a very rapid, channelized flow of saturated debris containing fine grained sediment (i.e., sand and finer fractions) with a plasticity index of less than 5%. Debris flows originate from a single or distributed source area(s) from sediment mobilized by the influx of ground or surface water. In areas with limited vegetation, or where wildfires have removed vegetation, abundant rilling and gullying may deliver sediment to the main channel and form debris flows. In those cases, no single source is required to initiate or maintain debris-flow mechanics.

Debris flows travel in confined channels bordered by steep slopes. In confined channels, the flow volume, peak discharge, and flow depth increase, and the debris becomes sorted along the flow path. Flow velocities typically range from 1 to 10 m/s, although very large debris flows from volcanic edifices, often containing substantial fines, can travel at more than 20 m/s along much of their path (Major, Pierson, & Scott, 2005). The front of the rapidly advancing flow is steep and commonly followed by several secondary surges that form due to particle segregation and upwards or outwards migration of boulders. Hence, one of the distinguishing characteristics of coarse granular debris flows is vertical inverse grading, in which larger particles are concentrated at the top of the deposit. This characteristic behaviour leads to the formation of lateral levees along the channel that become part of the debris-flow depositional record (de Haas et al., 2024). Similarly, depositional lobes are formed where frictional resistance from unsaturated coarse-grained or large organic debris-rich fronts is high enough to slow and eventually stop the motion of the trailing liquefied debris.

Due to their high flow velocities, peak discharges during debris flows are at least an order of magnitude larger than those of comparable return period floods but can be 50 times larger or more (Jakob & Jordan, 2001; Jakob et al., 2016). Channel banks can be severely eroded during debris flows, although lateral erosion is often associated with the trailing flow characterized by lower volumetric sediment concentrations. The most severe damage caused by debris flows results from direct impact of large clasts or coarse woody debris against structures that are not designed for the impact forces (Jakob, Stein, & Ulmi, 2012). Linear infrastructure such as roads, and railways are subject to damage from debris flows either from direct impact or erosion. Buried infrastructure can be damaged by debris flows if it is first exposed by erosion and then impacted by boulders or woody debris.

Debris flow avulsions are likely in poorly confined channel sections and on the outside of channel bends where debris flows tend to superelevate. A sudden loss of confinement and decrease in channel slope cause debris flows to decelerate and slow the advancing bouldery front, which blocks the channel. Further flows are often deflected by the slowing front, leading to secondary avulsions and the creation of distributary channels on the fan. Because debris flows often display surging behaviour, in which bouldery fronts alternate with hyperconcentrated afterflows, the cycle of coarse bouldery lobe and levee formation and afterflow deflection can be repeated several times during a single event (Iverson, 2014).

F-2.3 Debris Floods

Church and Jakob (2020) define debris floods as “floods during which the entire bed, barring the very largest clasts, becomes mobile for at least a few minutes and over a length of at least 10 times the channel width”. Accordingly, debris floods represent flood flows with high transport of gravel to boulder size material. Debris floods typically occur on creeks with channel gradients between 5 and 30% (3 and 17º) but can also occur on lower gradient gravel bed rivers.

Due to their initially relatively low sediment concentration, debris floods can be more erosive along low-gradient alluvial channel banks than debris flows. Channel and bank erosion introduce large amounts of sediment to the fan where they accumulate (aggrade) in channel sections with decreased slope. Debris floods can also be initiated on the fan itself through rapid bed erosion and entrainment of bank materials, as long as the stream power is high enough to transport some of the largest clasts in the channel bed (the grain size diameter for which 84% of the grain sizes are finer (D_{84}) – MacKenzie, Eaton, & Church., 2018). Because typical long-duration storm hydrographs fluctuate several times over the course of the storm, several cycles of aggradation and remobilization of deposited sediments on channel and fan reaches can be expected during the same event (Jakob et al., 2016). Similarly, debris floods triggered by outbreak floods may lead to single or multiple surges irrespective of hydrograph fluctuations that can lead to cycles of bank erosion, scour and infill. This is important for interpretations of field observations as only the final deposition or scour can be measured.

Church and Jakob (2020) developed a three-fold typology for debris floods (Figure F-5). Identifying the correct debris-flood type is key in preparing for numerical modeling and hazard assessments. Type 1 debris floods are a result of flows with a sufficient magnitude and shear stress to mobilize the channel bed. Type 2 debris floods are initiated by the transition of a debris flow to a debris flood in the channel or from a debris flow in a tributary channel entering a larger channel. Type 3 debris floods are associated with landslide dam outbreak floods (LDOF).

Hyperconcentrated flows are a special case of debris floods that are typical for volcanic sources areas or fine-grained sedimentary rocks. They can occur as Type 1, 2 or 3 debris floods. The term "hyperconcentrated flow" was defined by Pierson (2005) based on sediment concentration as "a type of two-phase, non-Newtonian flow of sediment and water that operates between normal streamflow (water flow) and debris flow (or mudflow)". The use of the term "hyperconcentrated flow" should be reserved for volcanic or weak sedimentary fine-grained slurries.

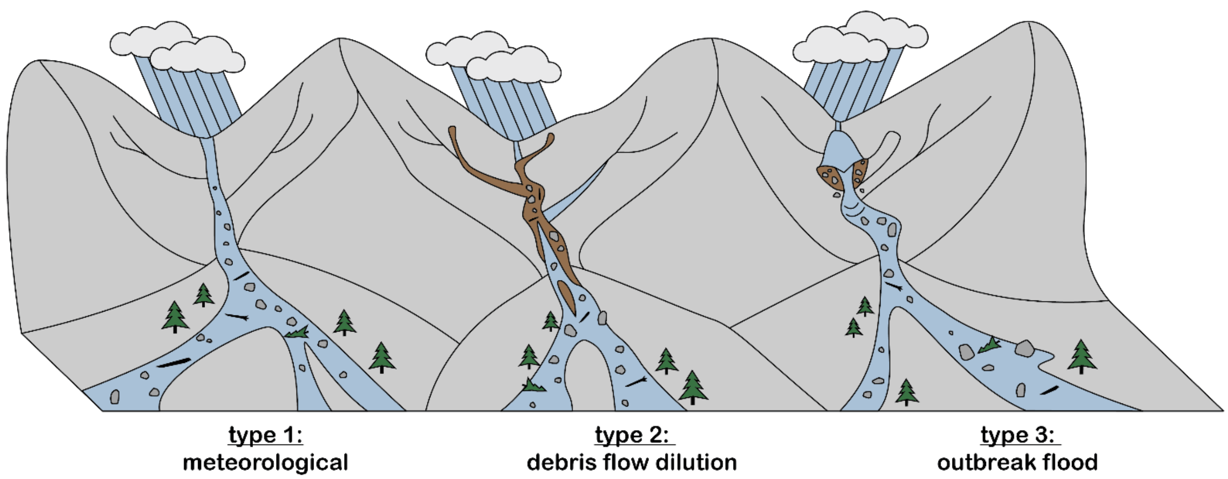

Figure F-5 Debris-flood types.

F-2.4 Clear-water Floods on Alluvial Fans

Clear-water floods are defined in Appendix E as "riverine and lake flooding resulting from inundation due to an excess of clear-water discharge in a watercourse or body of water such that land outside the natural or artificial banks which is not normally under water is submerged." In Appendix E, clear-water flood hazard is estimated based on historical and 3rd-party floodplain maps, historical events, existing hydraulic studies, hazard extent, and 200-year flood inundation modelling (Tier 1) (Nardi et al., 2019).

The potential for clear-water floods on alluvial fans depends on parameters such as evidence for previous avulsion, avulsion mechanism, and LDOF potential, which are discussed in Section F-4.

F-2.5 Climate Change

Climate change is expected to impact steep creek geohazards both directly and indirectly through complex feedback mechanisms (Stoffel et al., 2024). Given that hydrological and mass movement processes are higher order effects of air temperature increases, their prediction is highly complex and often site-specific. Changes to short duration (one hour and less) rainfall intensities are particularly relevant for post-fire situations in debris-flow generating watersheds. Within the year to a few years after a wildfire affecting large portions of a given watershed, short duration and high intensity rainfall events are much more likely to trigger debris flows or debris floods, than prior to a wildfire event.

Regional climate change projections indicate that the climate in BC is projected to warm, resulting in higher precipitation (especially in spring) expected to fall increasingly as rainfall. Appendix D provides additional details on BGC's climate change for this project.

While quantitative effects of climate change on steep creek hazard frequency and magnitude were not addressed at the scale of study, supply of sediment to steep creek channels helps indicate a range of potential effects. Steep creek basins can be generally categorized as being either:

- Supply-limited: Debris available for transport is a limiting factor on the magnitude and frequency of steep creek events. In other words, once debris in the source zone and transport zone has been depleted by a debris flow or debris flood, another event even with the same hydro-climatic trigger will be of lesser magnitude; or,
- Supply-unlimited: Debris available for transport is not a limiting factor on the magnitude and frequency of steep creek events, and another factor (such as precipitation frequency/magnitude) is the limiting factor. In other words, there is always an abundance of debris along a channel and in source areas so that whenever a critical hydro-climatic threshold is exceeded, an event will occur. The more severe the hydro-climatic event, the higher the resulting magnitude of the debris flow or debris flood.

Further subdivisions into channel supply-limited and unlimited, and basin supply-limited and unlimited are possible but were not considered further for this study.

The sensitivity of the two basic types of basins to increases in rainfall (intensity and frequency increases) differ (Figure F-6):

- Supply-limited basins would likely see a decrease in individual geohazard event magnitude, but an increase in their frequency as smaller amounts of debris that remains in the channel are easily mobilized (i.e., more, but smaller events).
- Supply-unlimited basins would likely see an increase in hazard magnitude and a greater increase in frequency (i.e., significantly more, and larger events).

Supply-limited basins can transition into supply-unlimited due to landscape changes. For example, sediment supply could be increased by wildfires, landslide occurrence, or human activity (e.g., related to road building or resource extraction). In the case of wildfires, the impact on debris supply is greatest immediately after the wildfire, with its impact diminishing over time as vegetation regrows. Wildfires are known to both increase the sediment supply and lower the precipitation threshold for steep creek events to occur. More details on wildfire are provided in Section F-2.6.

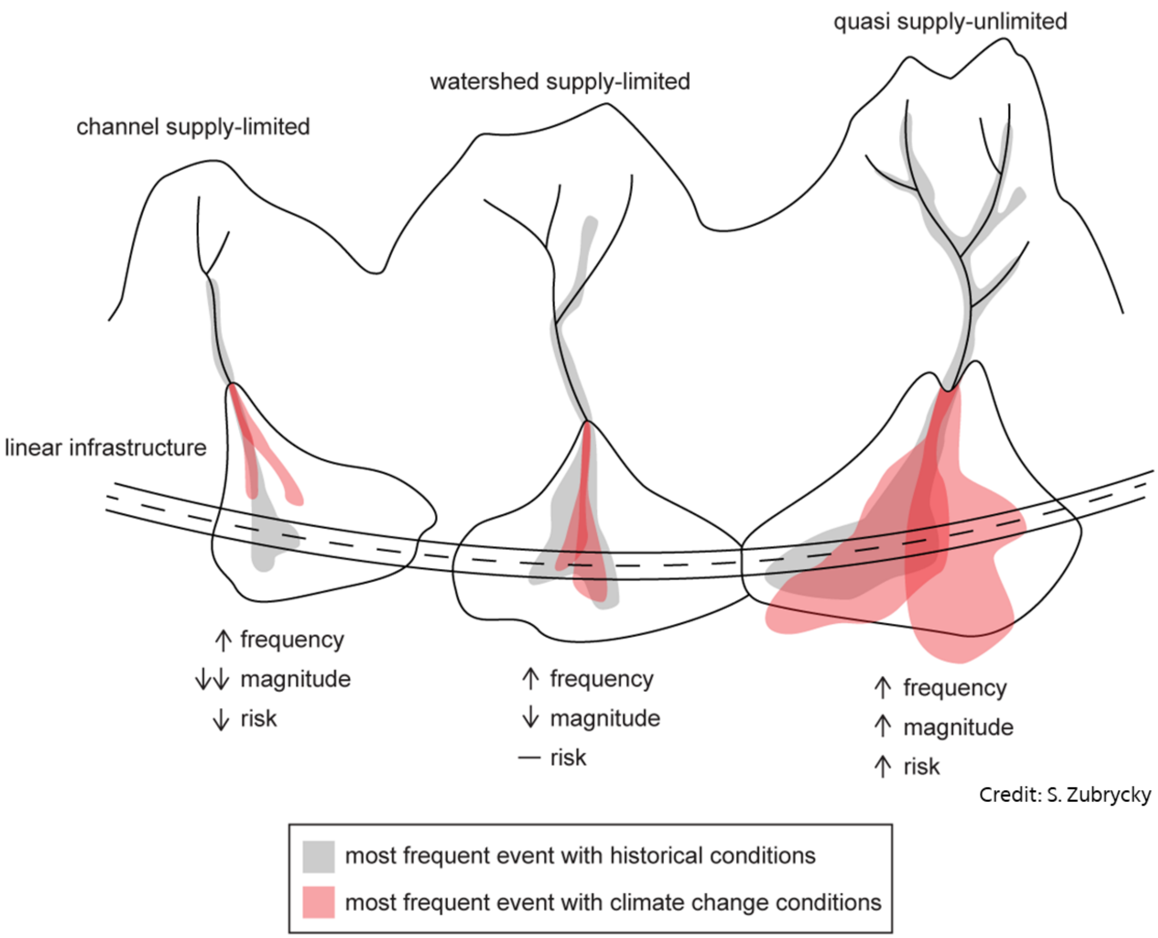

Figure F-6 Steep creek hazard sensitivity to climate change – supply-limited and supply unlimited basins.

F-2.6 Wildfires

Wildfires are well-documented to increase the likelihood and magnitude of geohazards (e.g., Gartner et al., 2024) and changes in water quality (Jordan, 2012; Elliot et al., 2024; HealthLink BC, January 2024). Potential wildfire effects on steep creek geohazards include:

- Increase in frequency and potential magnitude of debris flood and debris flows due to the increased availability and mobility of sediment and increase in rainfall runoff.

- Lower rainfall threshold for erosion and flooding, resulting in more frequent debris flow and debris flood initiation.
- Increase in landslide dam and LDOF potential.
- Increased overland flooding and potential related erosion may occur on open slopes, outside of channelized areas.

The increase in debris flood and debris flow likelihood and magnitude is temporary, and both the likelihood and magnitude subside with time, as vegetation re-establishes on hillslopes and soil stability is regained (Figure F-7).

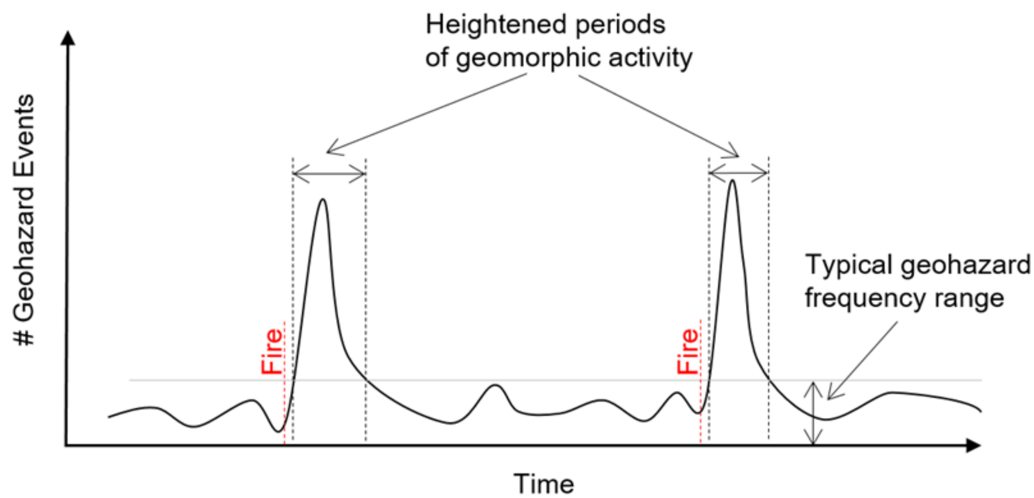

Figure F-7 Schematic diagram showing the temporary increase in geohazard activity following fire. Depending on the rate of watershed recovery, the peaks can last for one to twenty years following the fire. Schematic prepared by BGC.

Most runoff-generated post-wildfire debris floods and debris flows typically occur within the first two to three years following a fire (Cannon & Gartner, 2005; DeGraff et al., 2015; Graber, Thomas, & Kean, 2023). Widespread landslide-generated debris-flow activity is less likely, but possible in the decades following the fire due to the decay of burned or partially burned tree roots, which reduce soil cohesion (DeGraff et al., 2015; Hancock & Wlodarczyk, 2025).

Most post-wildfire impacts on water quality are observed within the first year or two after the wildfire (Jordan, 2012; Raoelison et al., 2023), although channel erosion and sediment transport may be elevated for several years after the wildfire (Eaton, Moore, & Giles, 2010).

As of 2023, BGC does not know of any reports of post-wildfire geohazards in the Robson Valley. There have been post-wildfire debris flows in the area of the 2024 Jasper wildfire complex (Brideau et al., 2025). While these geohazards are currently relatively uncommon in the RDFFG, BGC interprets that under our warming climate, they will likely occur more frequently in the future. In the current report, BGC did not specifically evaluate changes in geohazards due to wildfires.

F-3 STEEP CREEK GEOHAZARD IDENTIFICATION

Steep creek geohazard identification for the RDFFG focused on the delineation of alluvial fans, as these are the landforms commonly occupied by elements at risk. The boundaries of alluvial fans (e.g., Figure F-8) define the steep creek geohazard areas. Watersheds upstream of each mapped fan were assessed to identify geohazard processes and to rate attributes (Section F-4) but were not mapped.

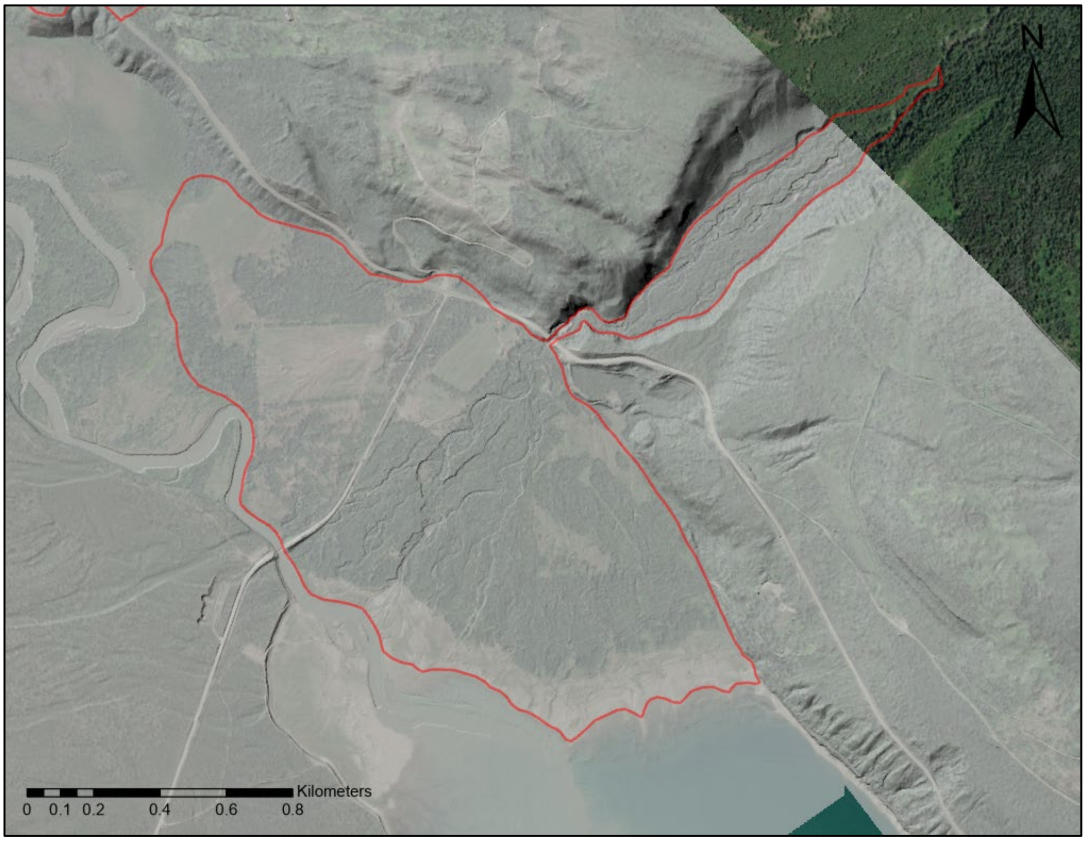

Figure F-8 Example alluvial fan boundary at Packsaddle Creek at the north end of Kinbasket Lake. Esri imagery overlain by lidar hillshade (Government of BC, 2016).

F-3.1 Fan Inventory

Fan extents were manually delineated in an ESRI ArcGIS Online web map based on a review of previous mapping (e.g., Bruce Geotechnical Consultants, January 28, 1999), and from hillshade images built from the coverage of lidar Digital Elevation Models (DEM). At sites where lidar DEMs were not available, low resolution (approximately 25 m)[1] Canadian Digital Elevation Model (CDEM) terrain models, aerial photographs, and satellite imagery available within ArcGIS were used for terrain interpretation. A total of 271 developed fans were mapped within the RDFFG.

1 CDEM resolution varies according to geographic location. The base resolution is 0.75 arc second along a profile in the south-north direction and varies from 0.75 to 3 arc seconds in the east-west direction, depending on location. In the SLRD, this corresponds to approximately 25 m grid cell resolution (Government of Canada, 2016).

The accuracy of each fan's boundary and hazard rating depends, in part, on the resolution of the available terrain data. Lidar DEMs, where available, provide 1 m or better resolution (e.g., Figure F-9). Mapped fan boundaries, even where lidar coverage is available, are approximate, but are less certain where lidar coverage was not available. For areas without lidar coverage, the minimum fan size and characteristics that can be mapped at regional scale with the available information is about 2 ha. Local variations in terrain conditions over areas of 1 to 3 ha, or over distances of less than about 200 m, may not be visible. Specific site investigations could allow refinement of the locations of the fan boundaries mapped by BGC.

Figure F-9 Example of oblique lidar hillshade and 20 m contours showing alluvial fans near Dunster. Lidar data from Government of BC.

While the presence of a fan indicates past geohazard occurrence, the lack of a fan on a steep creek does not necessarily rule out the potential for future geohazard occurrence. As such, the fan inventory completed in this study should not be considered exhaustive. In addition, in some cases, BGC does not rule out the potential for steep creek geohazards to extend beyond the limit of the mapped fan boundary. The fan boundary approximates the extent of sediment deposition since the beginning of fan formation[2]. Geohazards can potentially extend beyond the fan boundary due to localized flooding, where the fan is truncated by a lake or river, in young landscapes where fans are actively forming (e.g., recently deglaciated areas), or where large landslides (e.g., rock avalanches) trigger steep creek events larger than any previously occurring.

[2] Most of the alluvial fans mapped in this study represent the accumulation of sediment over the Holocene period (since about 11,000 years BP).

F-3.2 Geohazard Process Type Identification

BGC used terrain interpretations to assign each creek as “dominantly” subject to debris flows, debris floods, or clear-water floods. The term “dominant” refers to the process type that primarily controlled hazard assessment methodology and ratings. Recognizing that there is a continuum between clear-water floods and debris flows, BGC notes the following assumptions:

- Fans classified as subject to debris flows may also be subject to floods and debris floods at lower return periods (debris flows may transition to watery after flows in the lower runout zone and after the main debris surge).
- Fans classified as subject to debris floods may be subject to clear-water floods, but generally not to debris flows.
- Fans classified as subject to clear-water flood are dominated by clear-water floods.

BGC verified or modified the interpreted geohazard process types following published guidance (Wilford et al., 2004; de Haas et al., 2024) and the following information sources:

- The geomorphology of fans and their associated watersheds observed in the available airphotos and imagery
- Field observations of past geohazard deposits and their interpreted geohazard process type (BGC completed fieldwork from July 22, 2024 to July 26, 2024)
- Records of previous events.

In some cases, remotely sensed (lidar and air photo) or field observations indicated that the stream may be subject to mixed processes (i.e., the alluvial fan may be subject to debris flow and debris flood processes). In this case, the watershed was assigned the more conservative classification (i.e., debris flow is a more conservative rating than debris flood and flood, and debris flood is the more conservative rating than flood.).

Steep creek process type classification is subject to the following limitations:

- Creeks at the transition between debris flows and debris floods may generate either type of process and do not fall clearly into one category or another. The classification describes the potential dominant process type but does not consider the geomorphic or hydroclimatic conditions needed to trigger events. In rare occasions, channels may be classified as “debris flow” or “debris flood” without evidence for previous such events.
- Watershed conditions that affect hydrogeomorphic process types may not be considered. For example, a fan could be located at the outlet of a gentle valley, but where a debris-flow tributary enters near the fan apex. In this situation, debris flows could run out onto a fan that is otherwise subject to floods or debris floods from the main tributary.

F-4 FAN & WATERSHED ATTRIBUTES

The fan and watershed attributes characterized in this study are watershed activity (Section F-4.1), fan activity (Section F-4.2), avulsion evidence (Section F-4.3), channel confinement (Section F-4.4), and LDOF potential (Section F-4.5).

F-4.1 Watershed Activity

BGC assigned a rating (Table F-1) to describe the relative frequency of sediment mobilization and connectivity of sediment sources to the main channel of a watershed. For example, Figure F-10 shows a debris-flow watershed with numerous fresh landslide scarps connected to the main channel by evident feeder channels, which BGC evaluated as a High watershed activity. In comparison, a treed basin with no visible sediment sources proximal to the main channel would receive a Low or Very Low rating. The rating criteria differ by process type, as the level of debris-flow activity in a watershed is dependent on the availability of debris from landslides within the watershed, while debris-flood activity encompasses the presence of sediment sources and evidence of material entrainment in and along the main channel.

Table F-1 Relative basin activity for steep creeks organized by dominant process type.

Basin Activity	Description	Characteristic Observations	
		Debris-flood dominated steep creeks	Debris-flow dominated steep creeks
Very Low	• Minimal sediment sources. • Supply limited watershed.	• Negligible sediment sources in or along channel or in tributaries.	• Absence of landslide scars or erodible terrain. • Basin is treed. • Several rounded slopes.
Low	• Identifiable sediment sources, but most show limited evidence of activity or connectivity. • Supply limited watershed	• Minimal sediment sources in or along channel and any existing channel material is not easily mobilized (e.g., dense till, partially bedrock controlled).	• Some exposed soil or rock occurs. • Absence of fresh landslide scars or debris below exposed terrain. • Absence of channel deposits. • Basin and channel are mostly treed
Moderate	• Active sediment sources, but the material is not easily mobilized AND is not connected to the main channel or fan. • Supply limited or unlimited watershed.	• Sediment sources are present in or along channel. • Channel material is not easily mobilized (e.g., dense till, partially bedrock controlled) • Tributaries with identifiable sediment sources (e.g., debris-flow tributaries) typically stall before reaching main channel. • Main channel often has variable width.	• Sediment sources are present on slopes (e.g., presence of landslide scars in soil or rock). • Source material or in channel deposits are not easily mobilized (e.g., coarse, angular colluvium, dense till, or partially bedrock controlled). • Landslide deposits typically stall before the main channel.
High	• Active sediment sources, but the material is either not easily mobilized, or not clearly connected to the main channel or fan. • Supply unlimited watershed	• Numerous, actively producing source areas along main channel and tributaries (i.e., debris slides, debris avalanches, raveling in lacustrine, glaciofluvial, or morainal sediments); • Evidence of temporary sediment storage along main channel.	• Numerous, actively producing source areas on slopes or in channel. • Channel is choked with debris, but the material is not easily entrained (e.g., coarse angular colluvium) • Source material could be easily entrained (e.g., talus, loose glacial deposits, volcanic), but there is no clear connection between the sources and main channel (e.g., hanging valley).
Very High	• Active sediment sources that could be easily mobilized and are well connected to the main channel or fan. • Supply unlimited watershed	• Numerous, actively producing source areas along main channel and tributaries (i.e., debris slides, debris avalanches, raveling in lacustrine, glaciofluvial, or morainal sediments); • Source material could be easily entrained. • Tributaries with identifiable sediment sources (e.g., debris-flow tributaries) deposit straight into main channel.	• Numerous, actively producing source areas on slopes or in channel. • Channel choked with debris. • Easily entrained source materials along channels (e.g., talus, glacial deposits, volcanics)

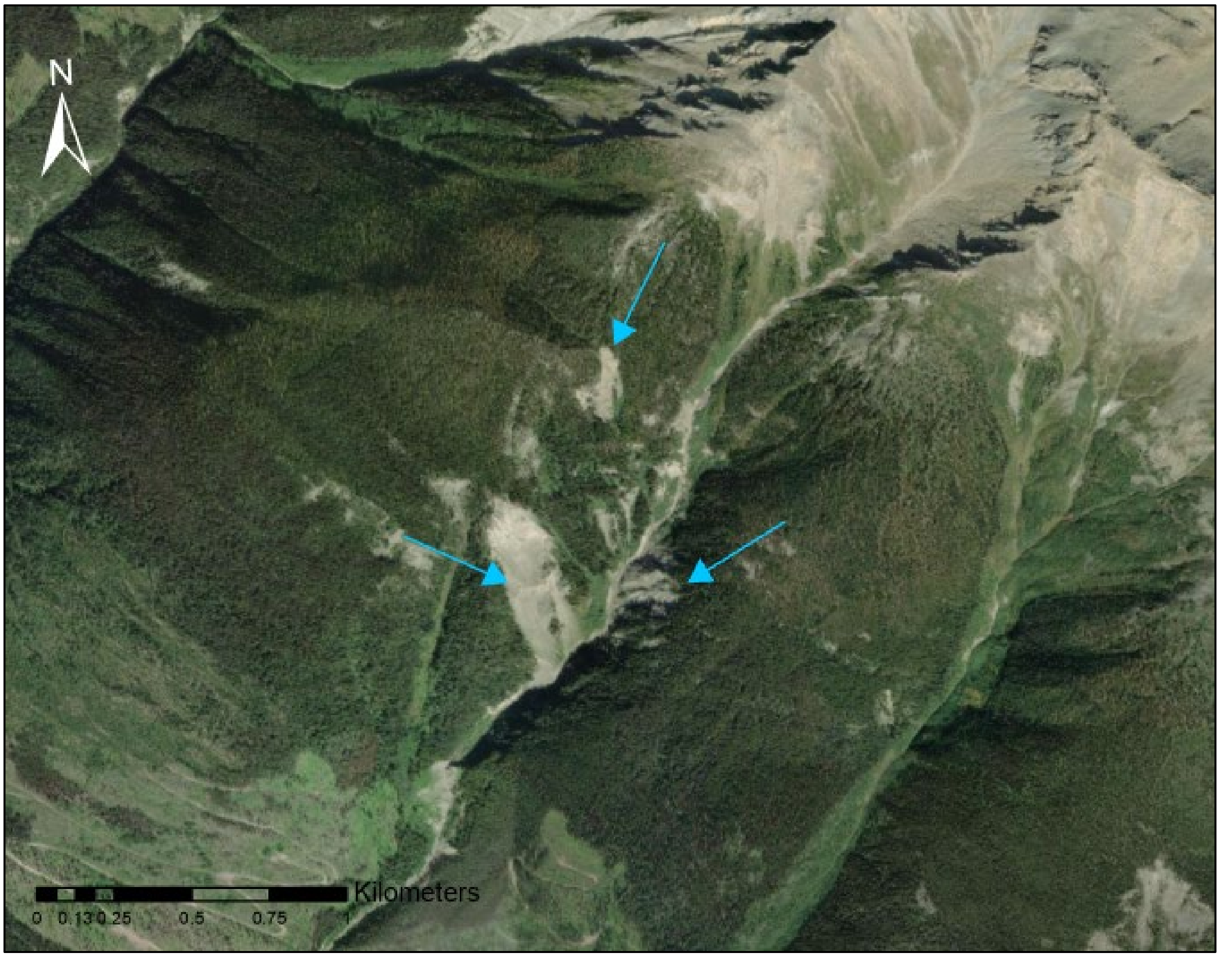

Figure F-10 Example of evidence for recent landslide or in-channel debris-flow initiation (blue arrows) within the basin of Goslin Creek, near Tete Jaun Cache (Imagery: Esri).

F-4.2 Fan Activity

The fan activity rating in Table F-2 is a measure of the frequency of steep creek events reaching the fan within the period of available records[3]. Features that suggest activity on the fan within the period of record include unvegetated channels, fresh debris deposits, and process-specific landforms such as debris-flow lobes and levees (Figure F-11). Outside of the available record period, the lidar hillshade can provide evidence of past events, which become muted over time and are not visible in satellite imagery or historical air photos.

BGC cautions the use of the fan activity rating as a quantitative measure of hazard activity levels on alluvial fans, due to its bias towards more recent events.

[3] For the purposes of this assessment, BGC defined the period of available records to be 1980 to present, for which there are readily and freely available air photo and recorded event records in the study area. The true number of recorded events at each geohazard area depends on the length and quality of air photo, imagery, and media records.

Table F-2 Relative fan activity for steep creeks organized by dominant process type. Fan activity refers to the frequency of recorded steep creek events reaching the fan.

Fan Activity[1,2]	Number of Recorded Events	Fan Observations	
		Debris-flood dominated creeks	Debris-flow dominated creeks
Very Low	None	• Vegetated mainstem. • No distinguishable debris-flood related landforms. • Uniform tree canopy of mature forest.	• No observable mainstem. • No distinguishable debris-flow related landforms. • Uniform tree canopy of mature forest.
Low	None	• Partially vegetated mainstem. • Muted channels or over bank deposits (most likely only visible in lidar). • Uniform tree canopy of mature forest.	• Vegetated mainstem. • Muted channels, lobes or levees (most likely only visible in lidar). • Uniform tree canopy of mature forest.
Moderate	0 to 1	• Unvegetated mainstem. • Channels and over bank deposits are visible in lidar, but potentially not in imagery. • Persistently includes swaths of mixed deciduous or conifer trees in riparian zone.	• Partially vegetated mainstem; • Channels, lobes or levees are visible in lidar, but potentially not in imagery. • Persistently includes swaths of mixed deciduous or coniferous trees associated with debris-flow landforms.
High	1 to 2	• Unvegetated mainstem; • Channels and over bank deposits are visible in imagery and lidar. • Persistently includes variable tree stand ages in riparian zone. • Regenerative vegetation and exposed sediment along channel. • Undersized channel in comparison with active floodplain width. • Partially vegetated bank erosion scars.	• Partially vegetated mainstem. • Channels, lobes or levees are visible in imagery and lidar. • Persistently includes swaths of regenerative (<10 year) or immature (<50 year) forest, potential areas of bare sediment.
Very High	8 (or at least two in the past 10 years where records are not available over a longer period)	• Unvegetated mainstem; • Channels and over bank deposits are visible in imagery and lidar. • Persistently includes areas of pioneer vegetation in riparian zone. • Fresh deposits are visible. • Undersized channel in comparison with active floodplain width. • Fresh bank erosion scars along mainstem.	• Fresh deposits are visible. • Channels, lobes or levees are visible in imagery and lidar. • Persistently includes swaths of bare sediment or low (<2 year) pioneer vegetation.
Cannot determine[3]	n/a	• Anthropogenic modifications across most of fan, and no evidence of past events in air photo record.	

Notes:

1. In cases where fan activity cannot be determined from available data, the basin activity rating was applied as the likelihood rating.
2. Very low vs. low classification cannot reliably be determined without lidar. A classification of low is conservatively applied in such cases.

Figure F-11 Example of a recent (2020) debris-flow deposit on Willox Creek, near McBride (Photo: Ministry of Transportation, 2020).

F-4.3 Avulsion Evidence

The fan activity rating in Table F-3 is a measure of the frequency of avulsions within the period of available records. Surface evidence for previous avulsions includes distinct changes in vegetation and the presence of relict channels, and lobes and deposits on the fan surface (e.g., Figure F-12). Outside of the available record, the lidar hillshade can provide evidence of past avulsions, which can become muted over time and are not visible in satellite imagery of historical airphotos. This rating is subject to greater uncertainty where development has obscured previous evidence for flow avulsions (e.g., channel modification or highly developed fans).

Fan-deltas (fans that form in standing water bodies, such as lakes, oceans and reservoirs) typically have a higher potential for avulsion than terrestrial (land-based) alluvial fans due to channel back-filling effects from the stream-water body interface (van Dijk et al., 2009; van Dijk et al., 2012). As such, these fans typically exhibit characteristics of a “Very Strong” or “Strong” avulsion evidence rating (Figure F-13). This characteristic behaviour can be disrupted if the channel is entrenched (highly incised) into the fan, and the base water level at any time of the year is well below the fan surface. Fan deltas with steeper gradients are less influenced by lake level and their avulsion rating does not need to be upgraded.

Figure F-12 Example of a previous avulsion on Swift Current Creek, located west of Mount Robson. Historical airphoto from 1973 (Government of BC).

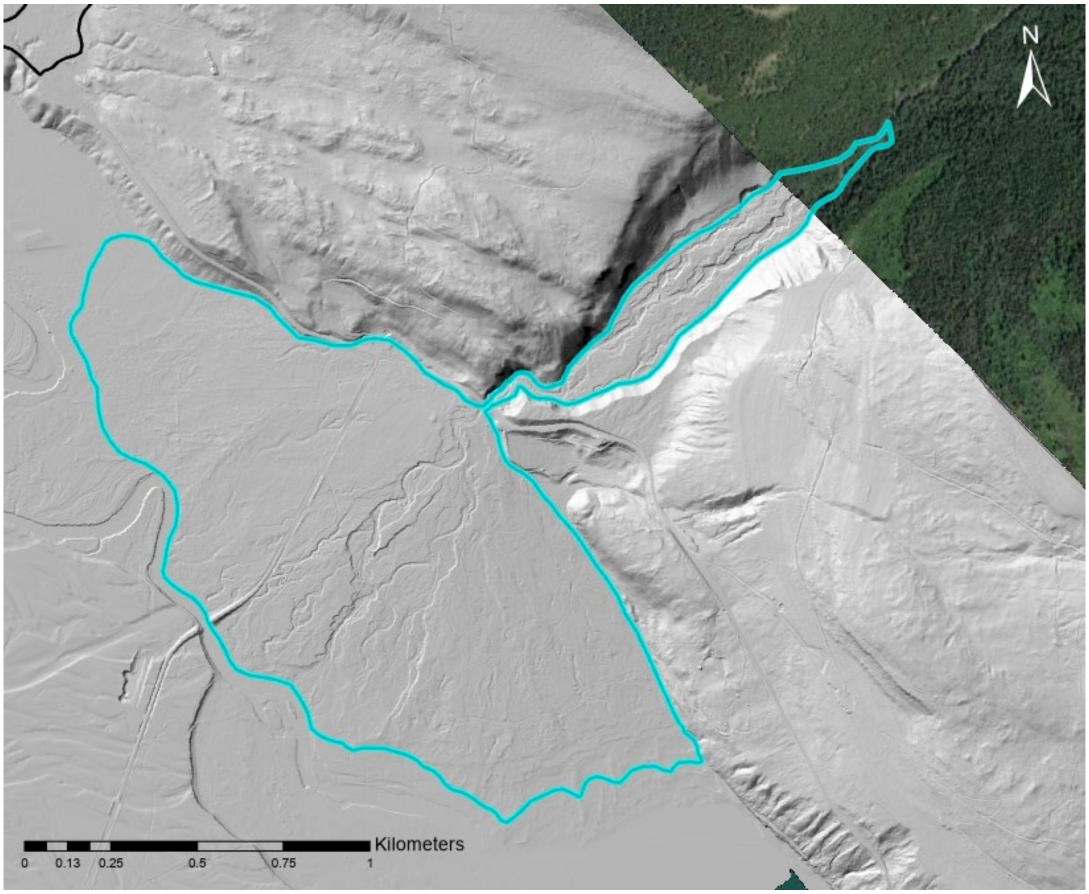

Figure F-13 Example of "Strong" avulsion evidence rating of a fan-delta at Packsaddle Creek near Valemount. Lidar data from Government of BC.

Table F-3 Evidence of previous avulsions criteria. These criteria refer to the frequency of observed events that avulsed on the fan.

Surface Evidence of Previous Avulsions[1]	Number of Recorded Events[2]	Description	Characteristic Observations[3]
Very Low	None	Active or historical channels cannot be identified in lidar or imagery.	Vegetated fan with consistent, mature tree stand age. No avulsion channels visible in lidar if available.
Low	None	Historical channels visible with lidar but they are muted and vegetated and not discernable on satellite imagery.	Vegetated fan with consistent, mature stand age. Muted historical channels visible in if available. lidar
Moderate	0 to 1	Historical channels on fan surface are visible in lidar and satellite imagery.	Swaths of young (<50 year) deciduous or coniferous vegetation exist in previous avulsion paths. Relict channels clear in lidar. Channels have similar characteristic geomorphic observations (e.g., debris-flow levees) as described in the fan activity rating.
Strong	1 to 2	An avulsion path is visible.	Swaths of bare sediment or low (<20 year) pioneer vegetation exist on previous avulsion path. Channels have similar characteristic geomorphic observations (e.g., debris-flow levees) as described in the fan activity rating.
Very Strong	8 (or at least two in the past 10 years where records are not available over a longer period)	At least one fresh avulsion path exist.	Swaths of bare sediment or low (<2 year) pioneer vegetation exist on previous avulsion paths. Channels have similar characteristic geomorphic observations (e.g., debris-flow levees) as described in the fan activity rating.

Notes:

1. Very low vs. low classification cannot reliably be determined without lidar. A classification of low is conservatively applied in such cases.
2. For the purposes of this assessment, BGC defined the record event span to be 1980 to present, for which there are readily and freely available air photo and recorded event records in the study area. The true number of recorded events at each geohazard area depends on the length and quality of air photo, imagery, and media records.
3. Fans classified as being a flood geohazard type are assessed according to these characteristics, but smaller flood events can be difficult to discern in air photos or satellite imagery. lidar, historical records and judgement is used where applicable. A low classification is conservatively applied as the lowest option for flood type fans.

F-4.4 Channel Confinement

BGC attributed a channel confinement rating to each alluvial fan using the terrain interpretation descriptions in Table F-4. Channel confinement is determined by the channel geometry on the fan, including relative bank height above the channel and identification of areas of potential loss of confinement, such as channel bends and changes in gradient (Figure F-14). Additionally, evidence of multiple channels in either the lidar hillshade or imagery suggests lack of channel confinement. As with avulsion evidence, the confinement of a channel can vary across a fan.

Note that where applicable, BGC used debris-flow and debris-floods susceptibility modelling (Flow-R) to further inform the attribution of the channel confinement ratings. Flow-R, developed by Horton et al. (2008, 2013) allows estimation of potential debris-flow and debris-flood hazard extent, based on a DEM and user-defined sources areas. BGC notes that Bornaetxea (2025) published recent debris flow susceptibility modelling for the Valemount Area. The results post-date BGC's assessment herein. They have been referenced in Appendix J as new information that may can inform future updates and steep creek hazard assessment within their study area.

Table F-4 Channel confinement rating criteria. Descriptions refer to on-fan observations.

Channel Confinement	Description
Very High	Deeply incised, straight channel; no obvious locations where confinement could be reduced during an event (e.g., channel bends, changes in channel gradient, channel constrictions).
High	Obvious (likely >15 m high) channel banks on lidar hillshade; no obvious locations where confinement could be reduced during an event (e.g., channel bends, changes in channel gradient, channel constrictions).
Moderate	Obvious (likely 5-15 m high) channel banks on lidar hillshade; some presence of locations where confinement could be reduced during an event (e.g., channel bends, changes in channel gradient, channel constrictions or areas of potential blockage).
Low	Minor or transient channel banks visible on lidar hillshade (likely < 5 m high), or obvious presence of locations where confinement could be reduced during an event (e.g., channel bends, changes in channel gradient, channel constrictions).
Very Low	Multiple channels visible on lidar hillshade. Minor or transient channel banks visible on lidar hillshade (likely < 5 m high), or obvious presence of locations where confinement could be reduced during an event (e.g., channel bends, changes in channel gradient, channel constrictions).

Figure F-14 Lidar hillshade over ESRI imagery of Parkridge Creek with a High channel confinement rating. Imagery from Google Earth.

F-4.5 Landslide Dam Outbreak Flood Potential

Some steep creek watersheds are prone to LDOFs, which could trigger flooding, debris floods, or debris flows with larger magnitudes than "typical" hazards. An example of this hazard in the RDFFG is large, slow moving landslide complex in the Dore River watershed, which has the potential to form a landslide dam (Figure F-15; BGC, March 10, 2021).

Table F-5 lists terrain criteria used to estimate LDOF potential. Ratings were assigned based on evidence of past landslide dams, presence of large landslides with the potential to travel to the valley floor, and presence of channel sections potentially susceptisble to blockage (e.g., channel constrictions).

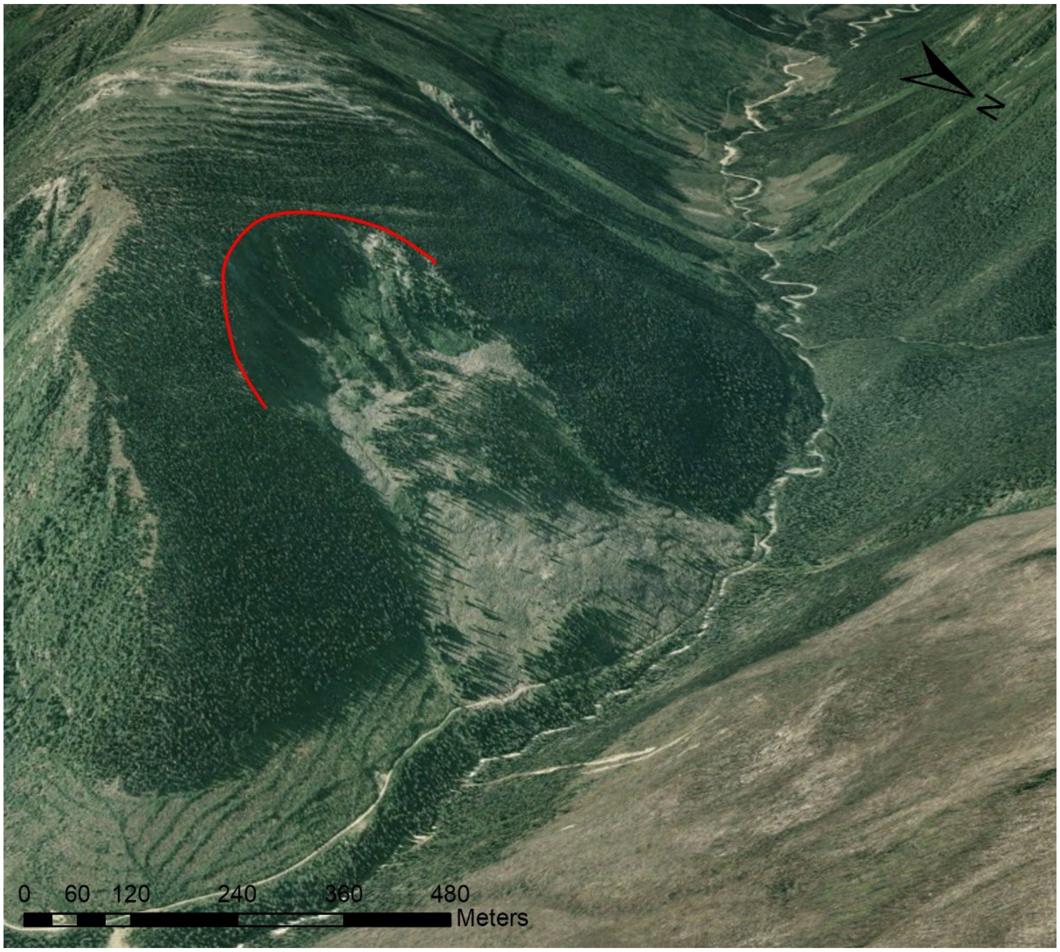

Figure F-15 Landslide on Boreal Creek, a tributary of Dore River. The red line indicates the crest of the slope movement that has pushed the creek towards the north. Imagery from Google Earth.

Table F-5 Landslide dam outbreak flood potential criteria.

Relative Frequency	LDOF Potential
Very Low	No evidence of historical landslides in the watershed. Main stream channel is broad and flat (e.g., floodplain).
Low	No evidence of historical landslides potentially large enough to reach the valley floor and block the river channel. No evidence of historical landslide dams in the main channel. Main stream channel is broad, with low angle to flat valley floor (e.g., floodplain).
Moderate	Evidence of historical landslides that are potentially large enough to reach the valley floor and block the river channel. No evidence of historical landslide dams in the main channel. Main stream channel has moderately steep valley walls and is partially confined (e.g., U-shaped valleys, glacial deposits, river terraces).
High	Evidence of historical landslides that are potentially large enough to reach the valley floor and block the river channel. Historical evidence of at least one landslide dam in the main channel. Main stream channel is entrenched and confined within a narrow valley and may have constrictions (e.g., bedrock canyon).
Very High	Presence of active landslides that are potentially large enough to reach the valley floor and block the river channel. Historical evidence of several landslide dams in the main channel. Main stream channel is entrenched and confined within a steep sided and narrow valley, resulting in multiple constriction points (e.g., bedrock canyon).

F-5 GAPS AND LIMITATIONS

Appendix J lists gaps and limitations for assets and hazards assessed in this study, including steep creeks.

REFERENCES

BGC Engineering Inc. (2021, March 10). Dore River Sustained Emergency Response – Geomorphic Assessment [Report]. Prepared for McElhanney Ltd.

Brideau, M.-A., Hancock, C.-A., Brayshaw, D., Lipovsky, P., Cronmiller, D., Friele, P., Geertsema, M., & Wells, G. (2025). Preliminary Canadian Landslide Database (10.0) [Data set]. Zenodo. https://doi.org/10.5281/zenodo.14585761

Bornaetxea, T, Blais-Stevens, A., Miller, B., Marchesini, I., 2025. Combination of statistical and conceptual approaches for debris-flow susceptibility modelling at a regional scale, British Columbia, Canada. CATENA,Volume 256, 2025, 109044, ISSN 0341-8162, https://doi.org/10.1016/j.catena.2025.109044.

Bruce Geotechnical Consultants Inc. (1999, January 28). *Robson Valley Hazard Land Study – Lamming Mills to Albreda, British Columbia* [Report]. Prepared for the Regional District of Fraser – Fort George.

Cannon, S.H. & Gartner, J.E. (2005). Wildfire-related debris flow from a hazards perspective. In: M. Jakob & O. Hungr (Eds), *Debris-flow hazards and related phenomena* (p. 363-386). Springer, Berlin, Heidelberg.

Church, M. (2013). Steep headwater channels. Chapter 9.28 in Shroder, J.F. (Eds.) Treatise on Geomorphology, vol. 9, Wohl, E. (ed.), Fluvial Geomorphology. San Diego, Academic Press: 528-549.

Church, M. & Jakob, M. (2020). What is a debris flood? *Water Resources Research, 56*(8), e2020WR027144. https://doi.org/10.1029/2020WR027144

Church, M. & Ryder, J.M. (1972). Paraglacial sedimentation: a consideration of fluvial processes conditioned by glaciation. *Geological Society of America Bulletin, 83*(10), 3059-3072. https://doi.org/10.1130/0016-7606(1972)83[3059:PSACOF]2.0.CO;2

Degraff, J.V., Cannon, S.H., & Gartner, J.E. (2015). Timing and susceptibility to post-fire debris flows in the western USA. *Environmental and Engineering Geoscience, 21*(4), 277-292. https://doi.org/10.2113/gseegeosci.21.4.277

de Haas, T., Densmore, A.L., Stoffel, M., Suwa, H., Imaizumi, F., Ballesteros-Cánovas, J.A., & Wasklewicz, T. (2017). Avulsions and the spatio-temporal evolution of debris-flow fans. *Earth-Science Reviews, 177*, 53-75. https://doi.org/10.1016/j.earscirev.2017.11.007

de Haas, T., Lau, C.-A. & Ventra, D. (2024). Debris-Flow Watersheds and Fans: Morphology, Sedimentology and Dynamics. In M. Jakob, S. McDougall, & P. Santi (Eds.), *Advances in Debris-flow Science and Practice*. Geoenvironmental Disaster Reduction. https://doi.org/10.1007/978-3-031-48691-3_1

Eaton, B.C., Moore, R.D., & Giles, T.R. (2010). Forest fire, bank strength, and channel instability: the “unusual” response of Fishtrap Creek, British Columbia. *Earth Surface Processes and Landforms, 35*, 1167-1183. https://doi.org/10.1002/esp.1946

Elliott, S.M., Hornberger, M.I., Rosenberry, D.O., Frus, R.J., & Webb, R.M. (2024). A conceptual framework to assess post-wildfire water quality: State of the science and knowledge gaps. *Water Resources Research*, 60, e2023WR036260. https://doi.org/10.1029/2023WR036260

Gartner, J.E., Kean, J.W., Rengers, F.K., McCoy, S.W., Oakley, N., Sheridan, G. (2024). Post-Wildfire Debris Flows. In M. Jakob, S. McDougall, & P. Santi (Eds.), *Advances in Debris-flow Science and Practice*. Geoenvironmental Disaster Reduction. Springer, Cham. https://doi.org/10.1007/978-3-031-48691-3_11

Government of Canada. (2016). Canadian Digital Elevation Model (CDEM) Product Specifications. Available online at http://ftp.geogratis.gc.ca, accessed December 2018.

Graber, A.P., Thomas, M.A., & Kean, J.W. (2023). How Long Do Runoff-Generated Debris-Flow Hazards Persist After Wildfire? *Geophysical Research Letters* 50 (19). https://doi.org/10.1029/2023GL105101

Hancock, C.-A. & Wlodarczyk, K. (2025). The role of wildfires and forest harvesting on geohazards and channel instability during the November 2021 atmospheric river in southwestern British Columbia, Canada. *Earth Surface Processes and Landforms* 50(1), e6065. https://doi.org/10.1002/esp.6065

HealthLink BC (2024, January). Wildfire: Its effects on drinking water quality [Online Resource]. Retrieved from https://www.healthlinkbc.ca/sites/default/files/documents/hfile49f.pdf

Horton, P., Jaboyedoff, M., & Bardou, E. (2008). Debris-flow susceptibility mapping at a regional scale. In Proceedings of the 4th Canadian Conference on Geohazards, edited by: Locat, J., Perret, D., Turmel, D., Demers, D., and Leroueil, S., Québec, Canada, 20-24 May 2008, 339–406.

Horton, P., Jaboyedoff, M., Rudaz, B., & Zimmermann, M. (2013). Flow-R, a model for susceptibility mapping of debris flows and other gravitational hazards at regional scale. *Natural Hazards and Earth System Sciences, 13*, 869-885. https://doi.org/10.5194/nhess-13-869-2013

Hungr, O., Leroueil, S., & Picarelli, L. (2014). Varnes classification of landslide types, an update. *Landslides*, *11*, 167-194. https://doi.org/10.1007/s10346-013-0436-y

Iverson, R.M. (2014). Debris flows: behaviour and hazard assessment. *Geology Today, 30(1)*, 15-20. https://doi.org/10.1111/gto.12037

Jakob, M. & Jordan, P. (2001). Design flood estimates in mountain streams – the need for a geomorphic approach. *Canadian Journal of Civil Engineering, 28*, 425-239. https://doi.org/10.1139/l01-010

Jakob, M., McDougall, S., Bale, S., & Friele, P. (2016). Regional Debris-flow Frequency-Magnitude Curves. GeoVancouver. Vancouver, BC.

Jakob, M., Stein, D., & Ulmi, M. (2012). Vulnerability of buildings to debris-flow impact. *Natural Hazards, 60(2)*, 241-261. https://doi.org/10.1007/s11069-011-0007-2

Jordan, P. (2012). Sediment yields and water quality effects of severe wildfires in southern British Columbia. *Wildfire and Water Quality: Processes, Impacts and Challenges.* Proceedings of a conference held in Banff, Canada, 11–14 June 2012. International Association of Hydrological Sciences Publ. 354.

Kellerhals, R. & Church, M. (1990). Hazard management on fans, with examples from British Columbia. In A.H. Rachocki & M. Church (Eds.), *Alluvial fans: a field approach* (pp. 335-354). John Wiley & Sons, Chichester, UK.

Lau, C.A. (2017). *Channel scour on temperate alluvial fans in British Columbia* (Master's thesis). Simon Fraser University, Burnaby, British Columbia. Retrieved from http://summit.sfu.ca/system/files/iritems1/17564/etd10198_CLau.pdf

MacKenzie, L., Eaton, B. C., & Church, M. (2018). Breaking from the average: Why large grains matter in gravel-bed streams. *Earth Surface Processes and Landforms*, *43*(15), 3190–3196. https://doi.org/10.1002/esp.4465

Major, J., Pierson, T., & Scott, K. (2005). Debris flows at Mount St. Helens, Washington, USA. *In:* M. Jakob & O. Hungr (Eds), *Debris-flow Hazards and Related Phenomena* (p. 685-731). Springer, Berlin Heidelberg.

Montgomery, D.R. & Buffington, J.M. (1997). Channel-reach morphology in mountain drainage basins. *Geological Society of America Bulletin, 109*, 596-611. https://doi.org/10.1130/0016-7606(1997)109<0596:CRMIMD>2.3.CO;2

Nardi, F., Annis, A., Di Baldassarre, G., Vivoni, E. R. & Grimaldi, S. (2019). GFPLAIN250m, a global high-resolution dataset of Earth's floodplains. *Scientific Data, 6*, 180309. https://doi.org/10.1038/sdata.2018.309

Pierson, T.C. (2005). Hyperconcentrated flow – transitional process between water flow and debris flow. In M. Jakob & O. Hungr (Eds.), *Debris-flow hazards and related phenomena* (p. 159-202). Springer-Praxis, Chichester, UK.

Raoelison, O.D., Valenca, R., Lee, A., Karim, S., Webster, J.P., Poulin, B.A., Mohanty, S.K. (2023). Wildfire impacts on surface water quality parameters: Cause of data variability and reporting needs. *Environmental Pollution, 317*, 120713. https://doi.org/10.1016/j.envpol.2022.120713

Ryder, J.M. (1971a). Some aspects of the morphometry of paraglacial alluvial fans in south-central British Columbia. *Canadian Journal of Earth Sciences, 8*, 1252-1264. https://doi.org/10.1139/e71-114

Ryder, J.M. (1971b). The stratigraphy and morphology of paraglacial alluvial fans in south-central British Columbia. *Canadian Journal of Earth Sciences, 8*, 279-298. https://doi.org/10.1139/e71-027

Schumm, S.A. (1977). *The fluvial system*. Wiley, New York, 338 p.

Stoffel, M., Allen, S.K., Ballestero-Canovas J.A., Jakob, M., & Oakley N. (2024). Climate Change Effects on Debris Flows. In M. Jakob, S. McDougall, & P. Santi (Eds.), *Advances in Debris-flow Science and Practice*. Geoenvironmental Disaster Reduction, https://doi.org/10.1007/978-3-031-48691-3_1

van Dijk, M., Kleihans, M.G., & Postma, G. (2009). Autocyclic behaviour of fan deltas: an analogue experimental study. *Sedimentology,* 56(5), 1569-1589. https://doi.org/10.1111/j.1365-3091.2008.01047.x

van Dijk, M., Kleihans, M.G., Postma, G., & Kraal, E. (2012). Contrasting morphodynamics in alluvial fans and fan deltas: effects of the downstream boundary. *Sedimentology, 59(7)*, 2125-2145. https://doi.org/10.1111/j.1365-3091.2012.01337.x

Wilford, D.J., Sakals, M.E., Innes, J.L, Sidle, R.C., & Bergerud, W.A. (2004). Recognition of debris-flow, debris-flood and flood hazard through watershed morphometrics: *Landslide*,*1*(1), 61–66. https://doi.org/10.1007/s10346-003-0002-0

Zubrycky, S., Mitchell, A., McDougall, S., Strouth, A., Clague, J.J., & Menounos, B. (2021). Exploring new methods to analyse spatial impact distributions on debris flow fans using data from south-western British Columbia. *Earth Surface Processes and Landforms*, *46*(12), 2395-2413. https://doi.org/10.1002/esp.5184

APPENDIX G
LANDSLIDE HAZARD ASSESSMENT

G-1 INTRODUCTION

This appendix describes methods used by BGC to assess landslide hazard at regional scale. The appendix is organized as follows:

- Section G-2 provides background information on the slope process types considered.
- Section G-3 describes methods to complete an inventory of landslide landforms.
- Section G-4 describes methods to define and review 'steep' slopes in relation to the landslide inventory.
- Section G-5 describes methods to develop a new hazard susceptibility model for deep-seated earth slides (DSEs) based on internal research and development by BGC.
- Section G-6 describes methods to develop a Landslide Hazard Areas of Interest layer based on a combination of the landslide inventory, steep slope map, and the landslide susceptibility map.
- The Landslide Hazard Areas of Interest layer is used to identify landslide hazard exposure for people and assets (Appendix H).

G-2 BACKGROUND

G-2.1 Landslide Terminology and Classification

Landslides are defined as "the movement of a mass of rock, debris or earth down a slope" (Cruden, 1991) and as "a physical system that develops in time through several stages" (Hungr et al., 2014). There are a number of other phrases/terms that are used interchangeably with the term "landslide" including mass movement, slope failure, and slope instability.

Landslide names are generated by determining an initiating material type for the landslide and a type of landslide movement. Common descriptors of landslide types are outlined below and summarized in Table G-1. Landslides are further described by their rate of movement summarized in Table G-2.

Table G-1 Landslide type classification (after Hungr et al. 2014).

Type of Movement	Rock	Soil
Fall	1. Rock fall*	2. *Boulder/debris/silt* fall*
Topple	3. Rock block topple*	5. *Gravel/sand/silt* topple*
	4. Rock flexural topple	
Slide	6. Rock rotational slide	11. *Clay/silt* rotational slide (surficial material slump)
	7. Rock planar slide*	12. *Clay/silt* planar slide
	8. Rock wedge slide*	13. *Gravel/sand/debris* slide*
	9. Rock compound slide	14. *Clay/silt* compound slide
	10. Rock irregular slide*	

Type of Movement	Rock	Soil
Spread	15. Rock slope spread	*16. Sand/silt* liquefaction spread*
		17. Sensitive clay spread*
Flow	18. Rock avalanche*	*19. Sand/silt/debris* dry flow
		20. Sand/silt/debris flowslide*
		21. Sensitive clay flow slide*
		22. Debris flow*
		23. Mud flow*
		24. Debris flood*
		25. Debris avalanche*
		26. Earthflow*
		27. Peat flow
Slope Deformation	28. Mountain slope deformation	30. Soil slope deformation
	29. Rock slope deformation	31. Soil creep
		32. Solifluction

Notes:

1. For material types in italics, use one only.
2. *Denotes movement types that usually reach extremely rapid velocities as defined by Hungr et al. (2014). The other landslide types are most often (but not always) extremely slow to very rapid (Table G-2).

Table G-2 Landslide velocity classification (after Hungr et al., 2014).

Description	Velocity (mm/s)	Typical Velocity
Extremely Rapid	> 5 x 10^{3}	5 m/s
Very Rapid	> 5 x 10^{1}	3 m/min
Rapid	> 5 x 10^{-1}	1.8 m/hr
Moderate	> 5 x 10^{-3}	13 m/month
Slow	> 5 x 10^{-5}	1.6 m/year
Very Slow	> 5 x 10^{-7}	16 mm/year
Extremely Slow	-	-

G-2.2 Factors Affecting Slope Stability

Slope failures are the result of gravitational forces acting on a mass, which results in slow creep, free fall, sliding along a failure surface, or flow as a slurry.

Two forces affecting the stability of slopes include: 1) Gravitational forces and water pressure in tension cracks which impose shear stress that causes the slope to move (force pulling it down); 2) Resisting forces (shear strength) that stabilize the slope and prevent movement (force holding it up). When gravitational forces exceed the resisting forces, a slope instability occurs. A simplified diagram of the forces affecting slope stability is shown in Figure G-1.

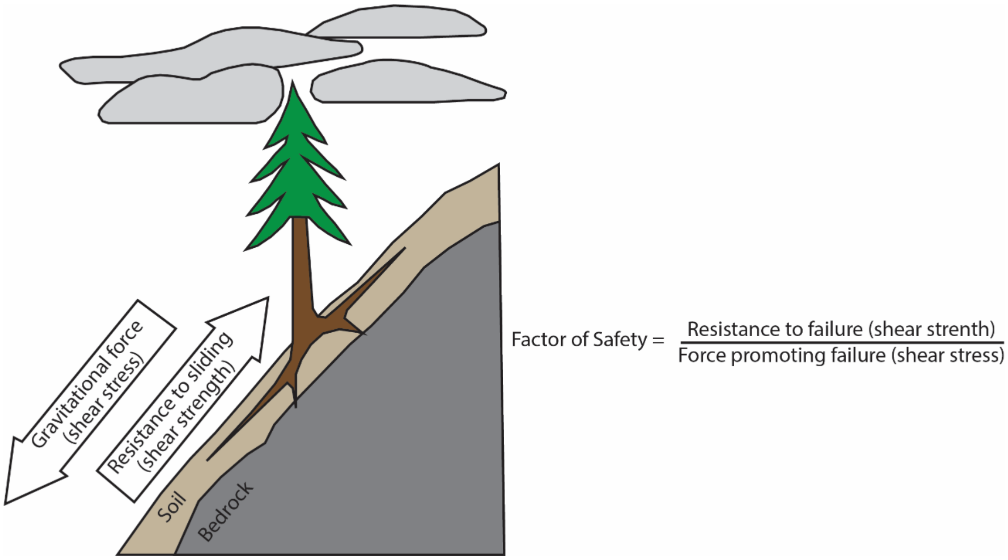

Figure G-1 Diagram of simplified forces acting on a slope (modified from BCMOF, 1994).

The stability and behavior of the slopes depend on different variables, including:

- Site topography and downslope materials
- Bedrock stratigraphy
- Material properties (including material structure and strength)
- Groundwater conditions
- Vegetation type and cover
- Anthropogenic modifications
- Seismic activity.

In addition, slopes can be sensitive to modifying factors, which change the shear stress and or shear strength over time and therefore affect the likelihood that slope instability can be triggered. Some changes in material and mass properties are gradual effects occurring over time, whereas some changes are almost immediate such as those from climatic events.

Landslides can have several causes (factors) that may reduce the stability of a slope and lead to failure in a progressive fashion. These include geological, morphological, physical, and human causes as outlined in Table G-3. The final impetus leading to slope failure may not be a gradual degradation of the landslide failure surface but instead some external stimuli ‘triggering’ slope failure. Examples of external stimuli, or triggering mechanisms, include intense rainfall, earthquake shaking, or human slope modification that result in failure by rapidly changing either shear stresses, or shear strength. Note that some triggering mechanisms can also be considered as causative factors in some cases. For example, an earthquake may not trigger a landslide, but weaken slope material, making the slope more susceptible to failure over time.

Table G-3 Factors that may reduce the stability of a slope (after Cruden and Varnes 1996).

1. Geological causes	a. Weak materials b. Weathered materials c. Jointed or fissured materials d. Adversely orientated discontinuity (bedding, rock joints, etc.) e. Contrast in permeability
2. Morphological causes	a. Glacial debuttressing b. Fluvial erosion of slope toe c. Subterranean erosion (solution, piping) d. Landslide deposition loading of slope or its crest e. Vegetation removal (forest fire, disease, wind storm, drought)
3. Physical causes	a. Intense rainfall* b. Rapid snowmelt* c. Prolonged exceptional precipitation* d. Earthquake* e. Freeze–and-thaw actions / weathering* f. Change in groundwater level*
4. Human causes	a. Excavation of slope or its toe* b. Loading of slope or its crest c. Deforestation d. Irrigation or water leakage from utilities* e. Surface water re-direction* f. Artificial vibration*

Note: * Can be either causative factors or triggering mechanisms.

G-2.3 Landslide Types

The following sections describe landslide types relevant to the Regional District of Fraser Fort George (Table G-1). Steep creek hazards (debris flows and debris floods) are described separately in Appendix F.

G-2.3.1 Rock Falls, Rock Slides and Rock Avalanches

Rock fall is a fragment of rock or boulder that detaches from a steep slope by sliding or toppling (Figure G-2). The rock or boulder may free-fall and break upon impact, or may begin rolling or bouncing down steeper slopes before arresting on flatter terrain. Rock falls are usually of limited volume (i.e., less than 10,000 m^3). When the volume is greater than 10,000 m^3, the process is called rock slide or rock collapse. Rock avalanche is an extremely rapid, flow-like motion of disintegrated rock mass that initiate as a large rock slide or rock fall.

Characteristics of rock falls, rock slides/collapse and rock avalanches include:

- Abrupt and extremely rapid landslide events (velocities of rock avalanches have been noted to be in excess of 200 km/hour).
- Their runout path is influenced by topography, which can deflect their trajectory.

- With increasing rock mass involved in a failure, movement changes from falling and bounding to a more flowing movement; this transition from rock fall to rockslide to rock avalanche is fluid and is sometime difficult to distinguish the actual process type
- Failures can run out past the toe of steep slopes. The runout distance depends on the fall height and the volume involved. Rock avalanches greater than about 1 Mm^3 in volume can have a high mobility and long run-out distances.

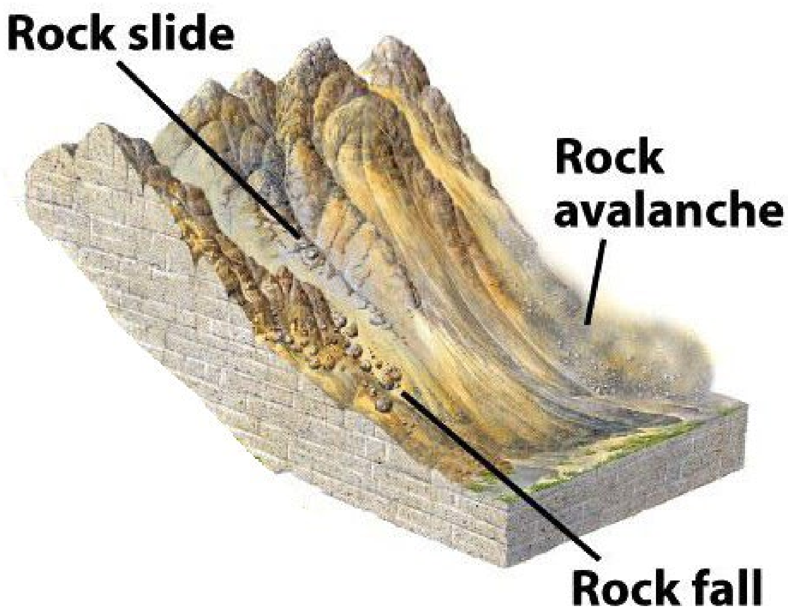

Figure G-2 Rock fall, rock slide, and rock avalanche schematic (from Louisiana State University website).

<u>Rock Fall, Rock Slide/Collapse and Rock Avalanche Event Causes</u>

Causal factors:

- Steep and sub-vertical rock slopes as source zones
- Bedrock discontinuities such as fractures, joints, fault and bedding planes that intersect with the slope configuration to form block geometries that can slide down and out of the slope or topple out of the slope
- Erosion at the base of slopes from rising rivers and streams or from human-related disturbances such as undercutting
- Mechanical weathering (tree roots or ice formation prying rock).

Trigger conditions:

- Rainfall or snowmelt events increasing water pressure in fissures
- Freeze-thaw cycles causing mechanical weathering of the rock mass
- Seismic events.

<u>Early Warning Signs</u>

Indicators of imminent rock fall can include terrain with overhanging rock or rock with open joints (fissures) or blocks that are separating from the surrounding rock. Fresh rock fall evidence includes recent rock fall impact marks, rock fragments in ditches, fresh rock faces at the source area, and torn soil layers at the slope crest.

Larger rock avalanches often show signs of instability before failure including:

- Slope deformation and slope cracks (See Section G-2.3.4)
- Vegetation disturbance
- Slow measurable movements
- Repeated small rockslides and rock falls.

G-2.3.2 Debris Avalanches and Debris Slides

Debris avalanche is an open-slope slide formed when an unstable slope collapses and the resulting fragmented debris rapidly moves down the slope (Figure G-3). Debris avalanches initiate as debris slides and occur on open slopes without confinement of an established channel.

Characteristics of debris avalanches include:

- Very rapid to extremely rapid shallow landslides with event velocities that range from 3 m/min to in excess of 80 km/hour
- Generally, originate from steep hillslopes or from within shallow hillslope depressions (hollow) where groundwater is concentrated
- Fragmented debris travels downslope, in some instances extending over 1 km downslope from the source zone
- Landslide dimensions range from head scarps spanning only a few meters in width to head scarps with widths of hundreds of meters.

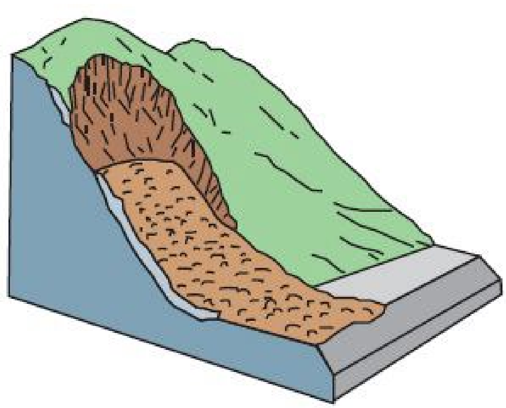

Figure G-3 Debris avalanche schematic (USGS, 2008).

Debris Avalanche Event Causes

Causal factors:

- Steep slopes
- Weak surficial material (overburden) over higher strength lower permeability material such as bedrock or glacial till
- Denuded vegetation due to forest fires or timber harvesting.

Trigger conditions:

- Intense rainfall, prolonged intense rainfall, rapid snowmelt, or rain on snow events
- Surface water concentration (e.g. associated with poorly constructed or maintained roads)
- Seismic events.

Early Warning Signs

If a debris avalanche event is triggered, the resulting slide could form rapidly with little warning. Early warning for the event can be any signs of land movement such as tension cracks, smaller landslides or progressively tilting trees. Small changes can indicate an increased immediate threat of a slide. Signs that might indicate moving debris include trees cracking or boulders knocking together; a trickle of flowing or falling mud or debris may precede a larger landslide.

G-2.3.3 Earth Slide

The main type of earth slides in the RDFFG project area are translational and rotational slides in glaciolacustrine deposits in the valley bottom (Figure G-4). These correspond to the *clay/silt rotational slide ("soil slump")* which Hungr et al. (20214) defined as: "Sliding of a mass of (homogeneous and usually cohesive) soil on a rotational rupture surface. Prominent main scarp and back-tilted landslide head. Normally extremely slow to rapid, but may be extremely rapid in sensitive or collapsive soils, and in over-consolidated (stiff) glaciolacustrine deposits." Translational earth slides are also possible in both glaciolacustrine, till, and colluvium material.

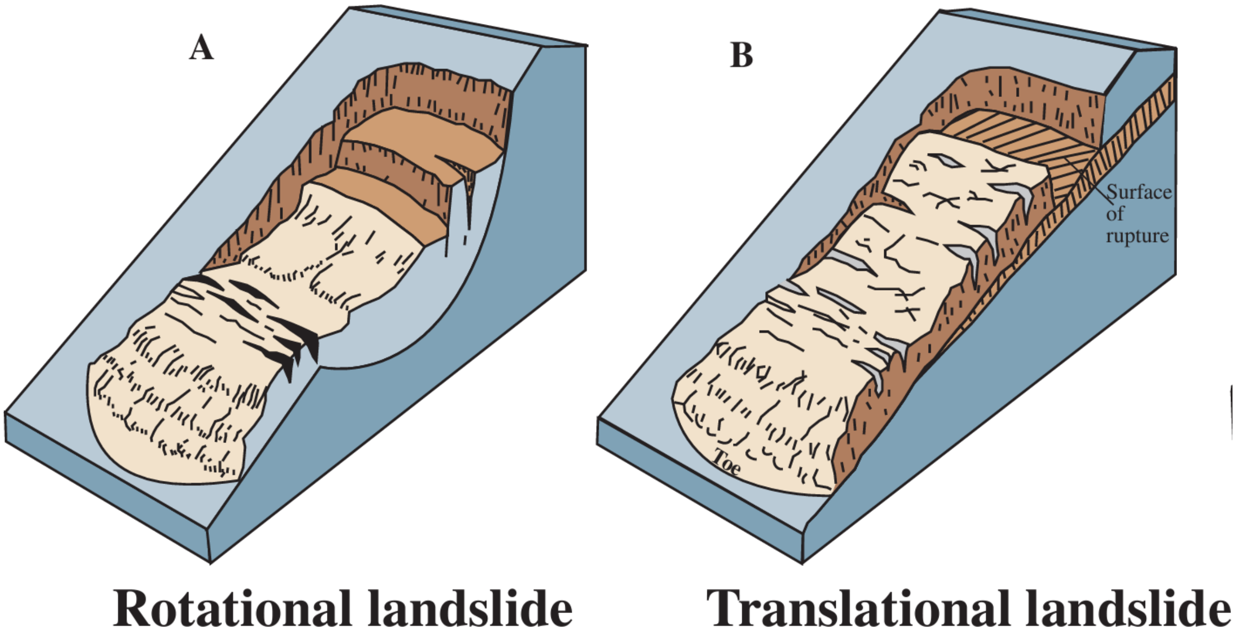

Figure G-4 Rotational and translational earth slide schematics (USGS, 2008).

Earth Slide Event Causes

Causal factors:

- Bank erosion
- Seasonal groundwater fluctuations
- Prolonged rainfall event
- Anthropogenic activity.

Trigger conditions:

- Rainfall event
- Anthropogenic activity
- Seismic activity
- Freeze-thaw.

Early Warning Signs

Presence of tension cracks, disturbed soil, damaged vegetation, tilted/damage infrastructure can be early warning signs of earth slides.

G-2.3.4 Mountain Slope Deformation

Mountain slope deformation also called deep-seated gravitation slope deformation, sackung, or rock mass creep, is defined by Hungr et al. (2014) as: *Large-scale gravitational deformation of steep, high mountain slopes, manifested by scarps, benches, cracks, trenches and bulges, but lacking a fully defined rupture surface. Extremely slow or unmeasurable movement rates*. Over time, slow mountain slope deformations can sometimes evolve into extremely rapid rock avalanches (Pedrazzini et al., 2013; see Section G-2.3.1), or they can deform at a slow to very slow rate for millennia (Hippolyte et al., 2012). Geomorphic features that can indicate past or present mountain slope deformation include grabens, trenches, uphill- and/or downhill-facing scarps, split ridges, and toe bulging (Figure G-5).

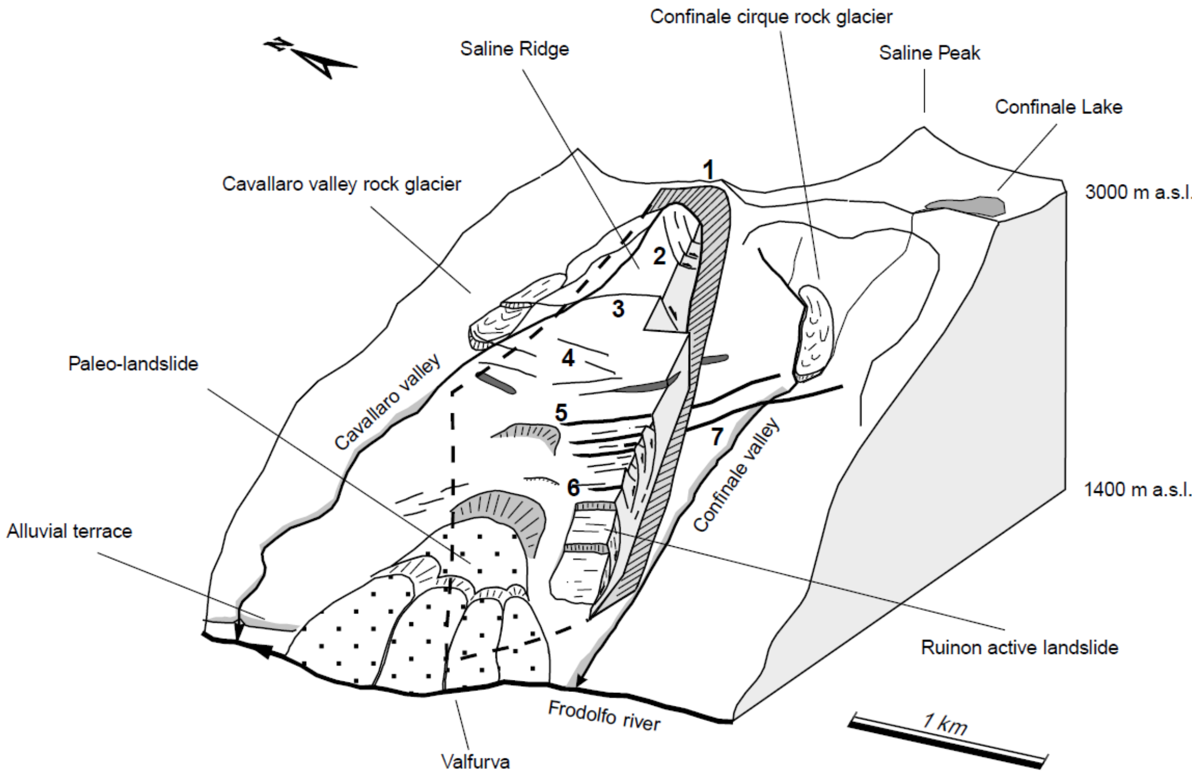

Figure G-5 Three-dimensional model of mountain slope deformation (Agliardi et al., 2001).

<u>Mountain Slope Deformation Causes</u>

Causal factors

- Stress distribution due to the interaction between rock mass strength and topography
- Glacial debuttressing
- Regional change in groundwater levels associated with climate change.

Trigger conditions

- Earthquake
- Progressive failure.

<u>Early Warning Signs</u>

Potential early warning indicators that a mountain slope deformation is transitioning for a large-scale rapid slope failure can include an increased rate of movement (from monitoring data or visual observations), increased rock fall activity or small rock slide on or around the mountain slope deformation feature.

G-3 LANDSLIDE INVENTORY

G-3.1 Summary

A landslide inventory identifies the locations where landslides have occurred in the past and where they are currently present. At the regional scale of study, BGC inventoried landslides as points at their initiation (start) zone. The landslide inventory contains both landslide events (discrete recorded events) and landslide features (landforms identified based their shape on lidar data, imagery, or based on InSAR analysis results).

In total, BGC compiled 1,232 landslide points based on previous work and interpretation of available lidar data, satellite imagery, and Interferometric synthetic aperture radar (InSAR)[1] analysis results. Project partners can access the full extent of available lidar data through their licensed access to Cambio web application. The compilation includes previous landslide inventories (Froese 1998; Bornaetxea et al., 2022; Brideau et al., 2024); landslides from surficial geology maps (Achard, 1973; Clague, 1998; Blais-Stevens & Clague, 2007a and 2007b), terrain mapping (Porter, 1999; Maynard et al., 2013a, b, c; Sacco et al., 2013a, b; Ward et al., 2013), and published geohazard literature (Choe et al., 2022). Comprehensive independent mapping of existing landslides was not undertaken by BGC as part of this project and the inventory is incomplete; several thousand additional landslides could likely be identified through review of the available lidar.

Table G-4 lists the characteristics assigned to each landslide point location.

Table G-4 Landslide point attributes.

Name	Description
Data Source	Source of the published landslide inventory containing a given point
Material Type	Classifies landslide as either being located within rock, or within soil
Movement Type	Classifies landslide as a fall, flow, slide, slope deformation, spread, or topple
Landslide Type	Combined values of Material Type and Movement Type
Comment	General notes on mapped landslide (e.g., data used as basis for interpretation, further classification of landslide beyond material and process)
Size	Qualitative assessment of landslide size, if known
Trigger	Interpreted trigger, if known

[1] TRE-Altamira prepared the InSAR analysis used in this project. The dataset used was ALOS-2 ScanSAR imagery from April 2015 and September 2021. It provided a 1-dimension (descending satellite line-of-sight) displacement information. Information was available for centre of the study area, approximately Bear Lake to the north and Tete Jaune Cache to the south. Results are displayed in the remote-sensing module of Cambio.

G-3.2 Limitations

Along with gaps and limitations related to other elements of the CDCRRA Project, Appendix J tabulates limitations associated with landslide inventory mapping, implications, and opportunities to resolve.

The primary limitation of a landslide inventory for determining hazard exposure is that it identifies only discrete locations where landslides have occurred. Hazard exposure assessment requires the spatial extents considered to have at least a minimum credible potential for landslides.

The following sections describe how BGC combined the landslide inventory with steep slope mapping (Section G-4) and hazard susceptibility mapping for deep-seated earth slides (Section G-5) to determine areas of interest for landslide hazard exposure.

G-4 STEEP SLOPE MAPPING

G-4.1 Summary

BGC defined “steep” slopes within the RDFFG as those with a slope angle greater than 30% and a relief greater than 10 m vertical over 90 m horizontal. Where regulations exist, a 30% slope gradient threshold has been previously used within the RDFFG to determine slope hazard development permit areas where a geotechnical assessment may be required as a condition of development approval.

BGC generated slope maps using a ‘medium resolution digital elevation model” (MRDEM) (NRCAN, 2025), which is a raster with 30 m pixel size available District-wide. The map covers 19,000 km^2 (36 %) of the RDFFG. All slopes exceeding 30% gradient and 10 m relief were conservatively assumed to have credible potential for landslide initiation and were included in the hazard exposure assessment.

G-4.2 Limitations

Appendix J describes limitations related to the preparation of slope maps based on a MRDEM. BGC highlights that, where existing, 1 m resolution lidar topography can resolve a higher proportion of steep slopes than the MRDEM (BGC, April 30, 2025). However, lidar is available for only part of the RDFFG. The MRDEM was generally considered reasonable at the scale of study, but may not identify potentially unstable but low-relief slopes such as river banks.

BGC compared the steep slope map with the landslide inventory to assess limitations of a slope map to capture the inventoried landslides. The results inform whether a steep slope map, on its own, is sufficient for the determination of hazard exposure to support decision making, or if further work is needed to define landslide hazard areas of interest for slopes gentler than 30%. BGC determined the following:

- Of the 1232 mapped landslide points, 825 (66%) occur on slopes gentler than 30%.
- The inventory includes 727 (roughly 60 %) landslide points classified as soil slides, of which 632 (87%) occur on slopes gentler than 30%.

These results indicate that while steep slope maps can reasonably capture some landslide types (e.g. rockfall and rock slides), additional work is needed to define credible potential for landslides on slopes gentler than 30%. Such gentle terrain is also the area typically favoured for development.

Section G-5 describes work funded under BGC's internal research and development program to analyse landslide hazard susceptibility for deep seated earth slides. The results help resolve limitations of slope threshold criteria to define areas of interest for hazard exposure and the regulation of land development.

G-5 DEEP-SEATED EARTH SLIDE SUSCEPTIBILITY MAPPING

To overcome the limitations of the steep slope map described in Section G-4, BGC developed a landslide susceptibility map specifically calibrated to identify deep-seated earth slides (DSEs)[2] on low-angle slopes in glacial soils. This susceptibility map spans a large portion of British Columbia and is designed to include regions where DSEs are possible, while excluding areas where such landslides are unlikely (e.g., the Rocky Mountains).

The development of the landslide susceptibility map followed a multi-step process, which included:

- Delineation of both the Area of Interest (AOI) and Analytical Study Area (ASA)
- Compilation of classifier data, which is comprised of raster-based thematic geospatial data
- Modeling and results generation
- Model validation and review
- Map visualization.

A high-level overview of each of these steps is provided in the following subsections.

G-5.1 Delineation of the area of interest (AOI) and analytical study area (ASA)

Figure G-6 shows the AOI (242,964 km²), the ASA (1,346 km²), and the extent of available lidar coverage.

The AOI defines the region where the landslide susceptibility model is expected to be applicable, as described above. After delineating the AOI boundary, BGC defined a 1 km × 1 km grid across the entire area and randomly selected grid cells overlapping with available lidar data for detailed mapping (ASAs). BGC then exhaustively mapped all landslides within each selected grid cell. In total, BGC mapped 653 DSEs within the ASAs covering approximately 90 km², or about 6% of the ASA

BGC then created a raster dataset that classifies each pixel within the ASA as either True (pixel is part of a mapped landslide) or False (pixel is not part of a mapped landslide). The extent of

[2] The landslide inventory outlined in Section G-3 does not include classification of soil slides into earth slides and other processes such as debris slides. In the evaluation of the steep slope map (Section G-4), susceptibility model (Section G-5), and landslide AOI map (Section G-6), the term deep-seated earthslide (DSE) refers to all landslide points classified as soil slides.

this raster dataset defines the ASA, which represents an area where BGC has a complete understanding of where landslide terrain does or does not exist, thus allowing assessment of the spatial probability of landslides within it. BGC used the ASA dataset for model training and validation.

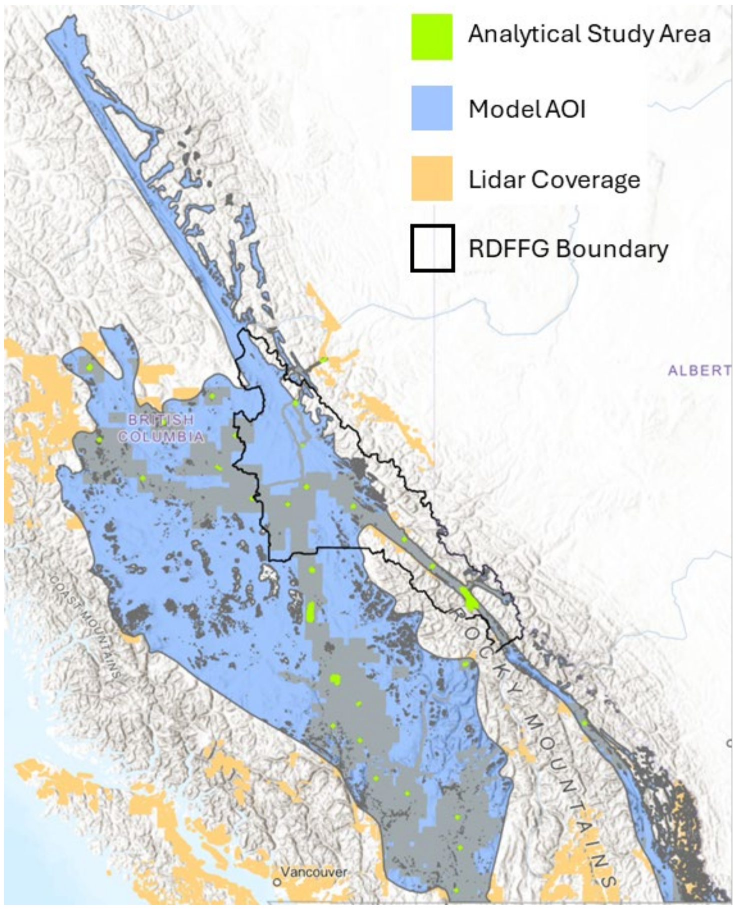

Figure G-6 Overview map showing the AOI, ASA, available lidar extents and the RDFFG boundary.

G-5.2 Classifier Data Compilation

Table G-5 summarizes the classifier data used in the susceptibility model described in Section G-5.3. BGC used the classifier data to train the model on terrain characteristics representative of DSEs within the ASA (i.e., where landslide presence and absence is known); the trained model then calculates a susceptibility value within the AOI (i.e., where landslide presence is unknown) based on the unique combination of values classifier data values for each pixel.

BGC selected classifier data based on assumed technical relevance and using datasets that are consistent throughout the AOI. Pixel size of the classifier datasets ranges from 20 m to 100 m. Where classifier data had continuous values, BGC used bins to produce a reasonably small number of statistically significant categories. These categories are assigned discrete values representing the range of the created bins.

Many of the geospatial themes considered for the model are not fully independent; for example, slope angle and relief are generally related and both likely correlated to soil type, surface expression and land cover. Independence of these variables was not considered in the creation of this model, but doing so could add value to the model and improve the results.

Table G-5 Summary of classifier data used in susceptibility model.

Classifier	Type	Description	Data Source and resolution
Aspect	Categorical	Raster representing the slope direction for a given pixel	MRDEM (NRCAN,2025) – 30 m pixel size
Flow Direction	Continuous	Raster representing the flow direction for a given raster cell	
Flow Accumulation	Categorical	Raster representing the area of upstream flow accumulation for a given raster cell	
Relief 3x3 Window	Continuous	Difference between maximum and minimum elevation within a 3x3 pixel (90 m) kernel surrounding a given raster cell	
Relief 15x15 Window	Continuous	Difference between maximum and minimum elevation within a 15x15 pixel (450 m) kernel surrounding a given raster cell	
Relief 30x30 Window	Continuous	Difference between maximum and minimum elevation within a 30x30 pixel (900 m) kernel surrounding a given raster cell	
Slope	Continuous	Slope angle for a given raster cell	
Slope 3x3 Window	Continuous	90th percentile slope value within a 3x3 pixel kernel surrounding a given pixel	
Slope 15x15 Window	Continuous	90th percentile slope value within a 15x15 pixel kernel surrounding a given pixel	
Slope 30x30 Window	Continuous	90th percentile slope value within a 30x30 pixel kernel surrounding a given pixel	
Topographic Wetness Index	Continuous	Raster representing topographic wetness index as described in Sørensen et al. (2006)	
Height Above Nearest Drainage	Continuous	Raster representing relative height above a watercourse for a given pixel. Created using the code base from Bartos (2020).	

Classifier	Type	Description	Data Source and resolution
Distance to Stream Order 1 and Above	Continuous	Raster representing distance to stream network, which was created according to the methodology outlined in Eilander (2025) with the MRDEM used as the primary input.	
Distance to Stream Order 3 and Above	Continuous		
Distance to Stream Order 6 and Above	Continuous		
Bedrock Geology	Categorical	Bedrock geology mapping for BC at 1:250,000 scale	BC Bedrock Geology Map - Cui et al,, 2021. – 100 m pixel size
Parent Material	Categorical	Provincial scale map of soil parent material	Heung et al., 2022 - 25 m cell size
Land Cover	Categorical	Raster-based landcover dataset	Government of Canada, 2020 - 30 m pixel size

G-5.3 Modelling and Results

In order to build the susceptibility model, BGC structured the geospatial data in a way that promotes efficiency in processing over such a large area (i.e., the AOI). This involved creating a vector grid where each grid cell contains a single attribute value for each classifier data and, within the ASA, a True or False classification denoting whether or not that grid cell falls within the extent of a mapped landslide.

BGC used an Extreme Gradient Boosting (XGBoost) machine learning model, which leverages gradient boosting to identify patterns in data, to develop the susceptibility model. The model was based on the XGBoost Python Package, an implementation of the model described in Chen and Guestrin (2016). All pixels within the ASA comprise the input for model training. The classifier data within this input dataset made up the “predictor” parameter for the model, and the binary landslide classification made up the “known value” parameter for the model. 80% of the input data was randomly selected for training and the remaining 20% of the input data was reserved for testing the model (to allow for unbiased testing of the model using data that has not been used in model training). XGBoost hyperparameters including learning rate, maximum tree depth, and regularization terms were tuned using cross-validation to prevent overfitting and enhance predictive accuracy. For a detailed account of the XG Boost Model, see Chen and Guestrin (2016).

BGC generated additional quantitative model metrics to evaluate model performance. The results are as follows:

- 87% true positive rate: proportion of landslide pixels within the ASA accurately classified by the model
- 93% true negative rate: proportion of non-landslide pixels within the ASA accurately classified by the model
- 7% False positive rate: proportion of non-landslide pixels within the ASA incorrectly classified as landslide pixels
- 13% false negative rate: proportion of landslide pixels within the ASA incorrectly classified as non-landslide pixels

A receiver operating curve (ROC), as shown in Figure G-7 plots the true positive rate against the false positive rate in order to understand the overall model accuracy. Stronger models typically show a curve that bows closer to the top-left corner of the plot, indicating a higher true positive rate and a lower false positive rate across various threshold settings. The area under the curve (AUC) quantifies the overall ability of the model to discriminate between classes, with a value of 1.0 indicating perfect classification and 0.5 suggesting no discriminative power, equivalent to random guessing. The model developed here achieved an AUC value of 0.96.

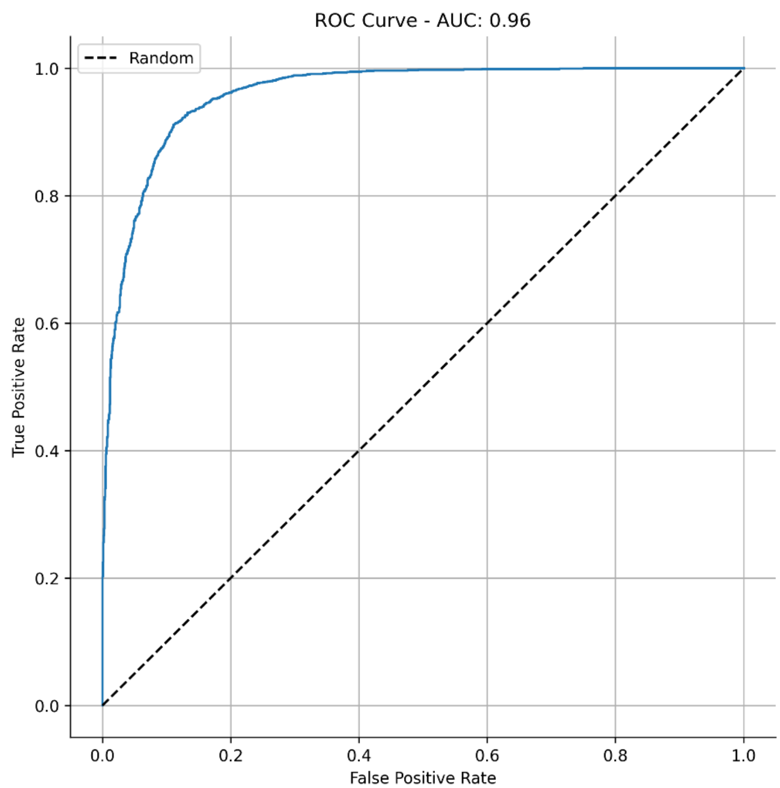

Figure G-7 Receiver operating curve (ROC) for the susceptibility model shown in blue. The ROC for a random model is shown for reference with as a black dashed line.

For all of these metrics, BGC distinguished between landslide and non-landslide based on a threshold susceptibility of 0.5 (i.e., a pixel is classified as landslide if the susceptibility value is equal or greater than 0.5). Exceeding this value for a given point means that the majority of the classification trees tested by the model classified the point as a landslide rather than as non-landslide.

After training and testing was completed, BGC applied the model to the entire AOI (i.e., where landslide presence and absence is unknown) to create the landslide susceptibility map.

G-5.4 Model Validation and Map Review

In addition to the evaluation of the quantitative model metrics discussed in Section G-5.3, BGC reviewed the practical utility and relevance of the resulting map (covering the AOI) through qualitative inspection of map outputs and statistical plots. Figure G-8 shows statistical plots representing the model evaluation criteria used to assess the utility and accuracy of the map. In all plots, the vertical axis represents the proportion of the map with a value that is greater than the corresponding value along the horizontal axis. The criteria illustrated in these plots are:

percentage area of the susceptibility map (vertical axis) versus susceptibility value (horizontal axis). This is a useful metric for evaluating the utility of the map, as the expectation is that the proportion of the map will decrease as susceptibility increases

True positive rate versus susceptibility value. This metric can be used to develop an understanding of how effective the model is at capturing known landslides within the ASA. Whereas the ROC shown in Figure G-7 plots true positive rate against true negative rate to evaluate overall model accuracy, the true positive rate versus susceptibility value plot (Figure G-8b) shows how true positive rate varies with changing susceptibility levels. This plot shows that the true positive rate diminishes as susceptibility rate increases. This is particularly useful in defining a binary susceptibility cutoff (discussed in Section G-5-6) as it provides context for what the true positive rate would be at a given susceptibility value, which, when combined with the ROC can also be used to understand the false positive rate at that threshold.

Susceptibility values for soil slide points in the landslide inventory from Brideau et al. (2024). This plot provides similar information to the plot in Figure G-8b but covers the entire AOI. The points in this inventory were not used in model training and provide an independent qualitative check on the ability of the model to capture landslide terrain (i.e., it would be expected that mapped landslide points would correspond with higher susceptibility values).

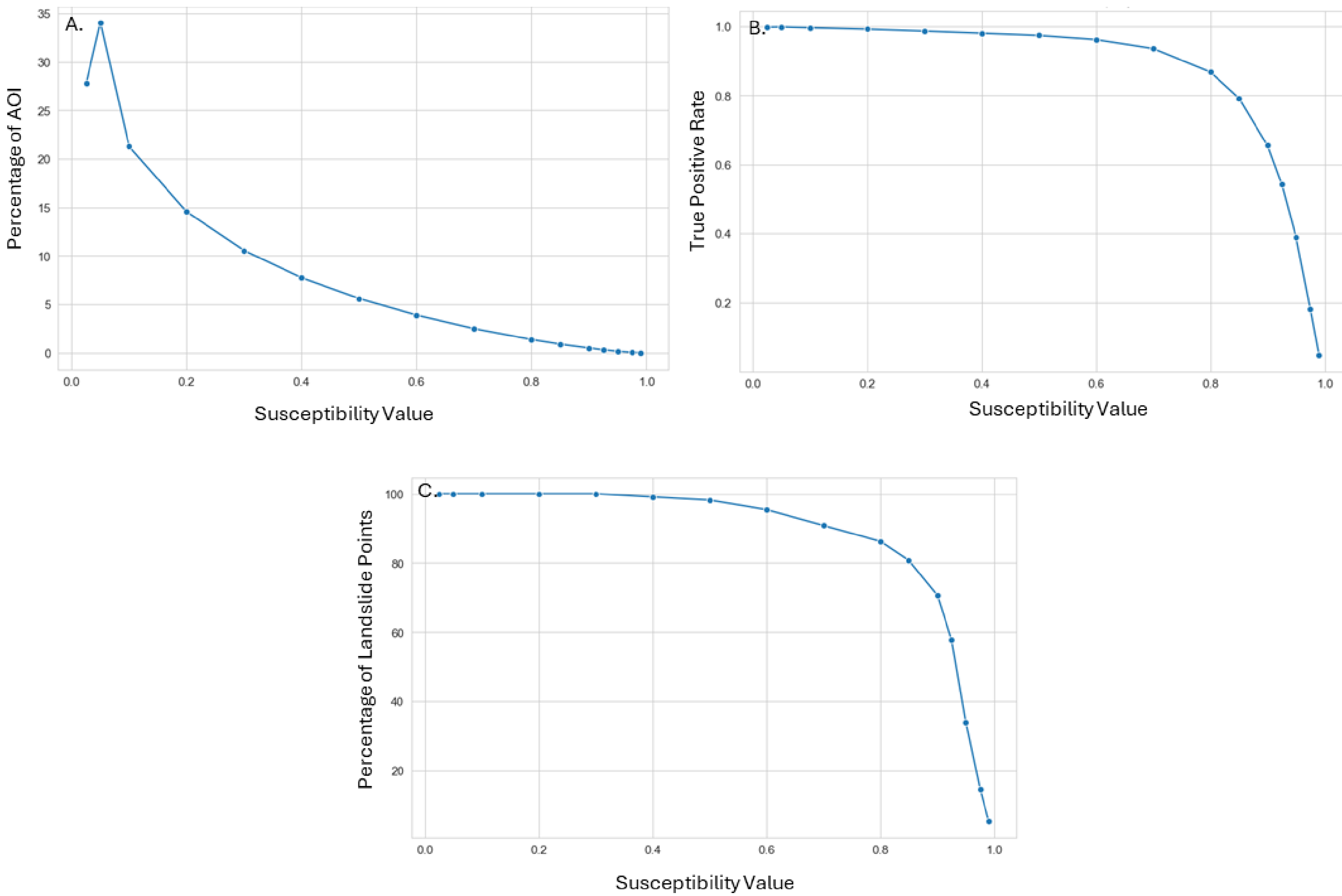

Figure G-8 a) Percentage of AOI covered assuming a given susceptibility threshold, b) true positive rate for a given susceptibility threshold, c) percentage of landslide points from Brideau et al. (2024) captured for a given susceptibility threshold.

While results reasonably capture landslide-susceptible terrain, Figure G-9 and Figure G-10 illustrate two examples of systematic sources of inaccuracy identified through qualitative review of the susceptibility map. Figure G-9 shows an area comprised of drumlin topography, which is being classified in a higher susceptibility range. This type of terrain is typically not associated with DSEs; however, the model likely made the classification based on the presence of relatively high relief within glacial lacustrine material, a configuration that is typically associated with DSEs. It is assumed here that the resolution/accuracy of the available surficial geology data is causing this systematic source of inaccuracy. Figure G-10 shows an area along the Fraser River with several mapped DSEs. The model has classified this area as having low susceptibility. It is assumed here that the 30 m pixel size of the raster data being used to calculate slope and relief is insufficient to capture the actual relief present. Further landslide mapping with a targeted effort to ensure that mapping is completed over a wide variety of terrain types, paired with parameter optimization and/or model tuning may improve the results and limit the impact of systematic misclassification similar to these examples.

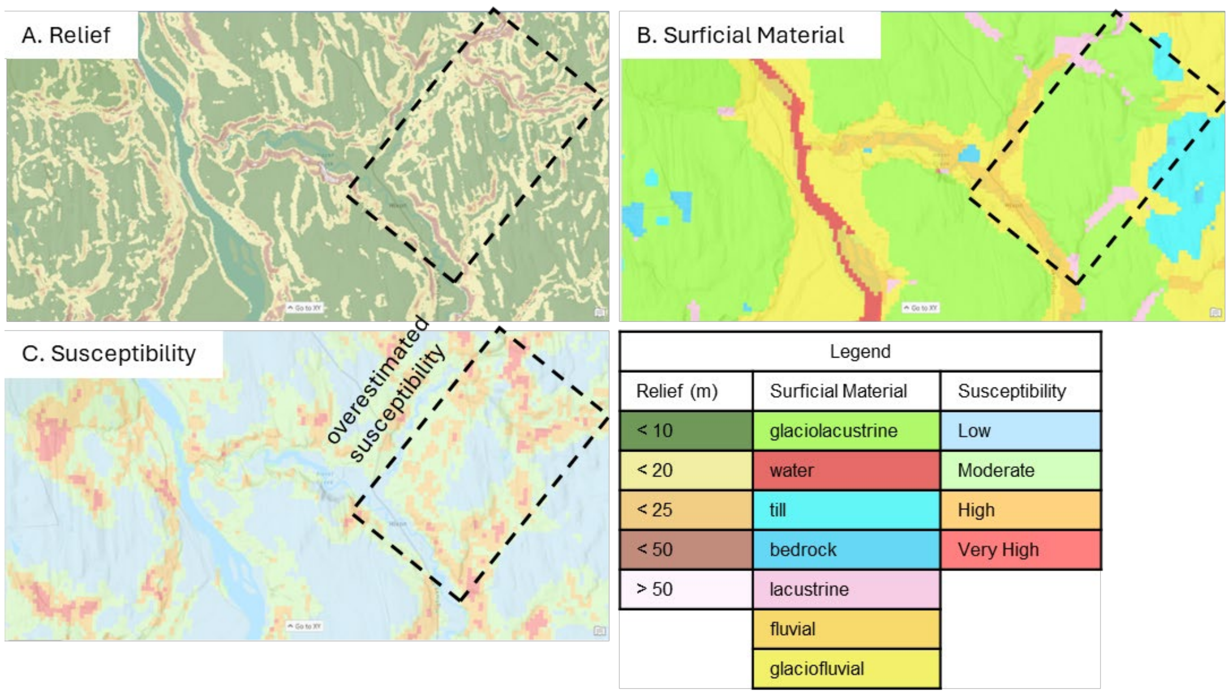

Figure G-9 Area where landslide susceptibility is being overstated due to the presence of drumlins.

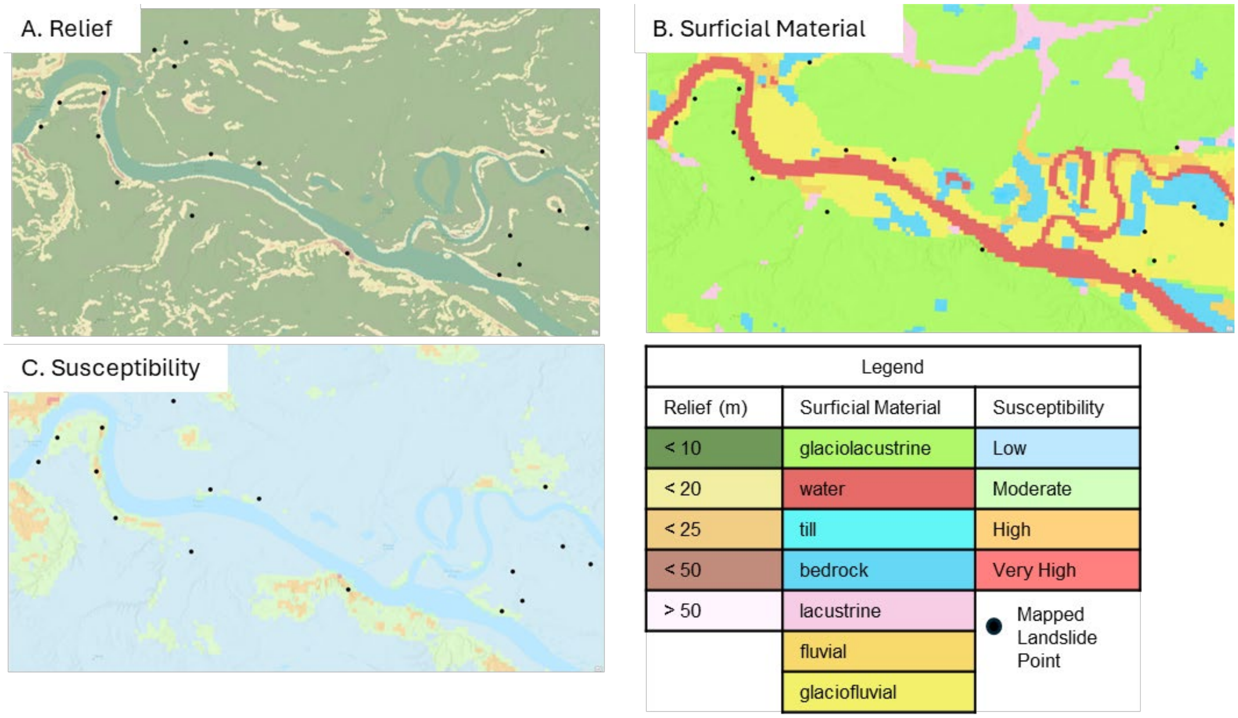

Figure G-10 Area where landslide susceptibility is being understated within a valley with several mapped DSEs.

G-5.5 Map Visualization

BGC (December 17, 2020) uses the term “spatial probability” to describe the proportion of landslide pixels within the ASA falling into a given susceptibility range. This framework provides a way to bin and visualize susceptibility results as the spatial probability of a landslide within a given pixel.

To generate the plot shown in Figure G-11, BGC binned the susceptibility model results into 100 equal-width intervals, each representing a 0.01 range in susceptibility values. The spatial probability is calculated for each bin. BGC then fitted a regression line to the binned data and identified intercepts along the regression line corresponding to specific spatial probability thresholds (Table G-5).

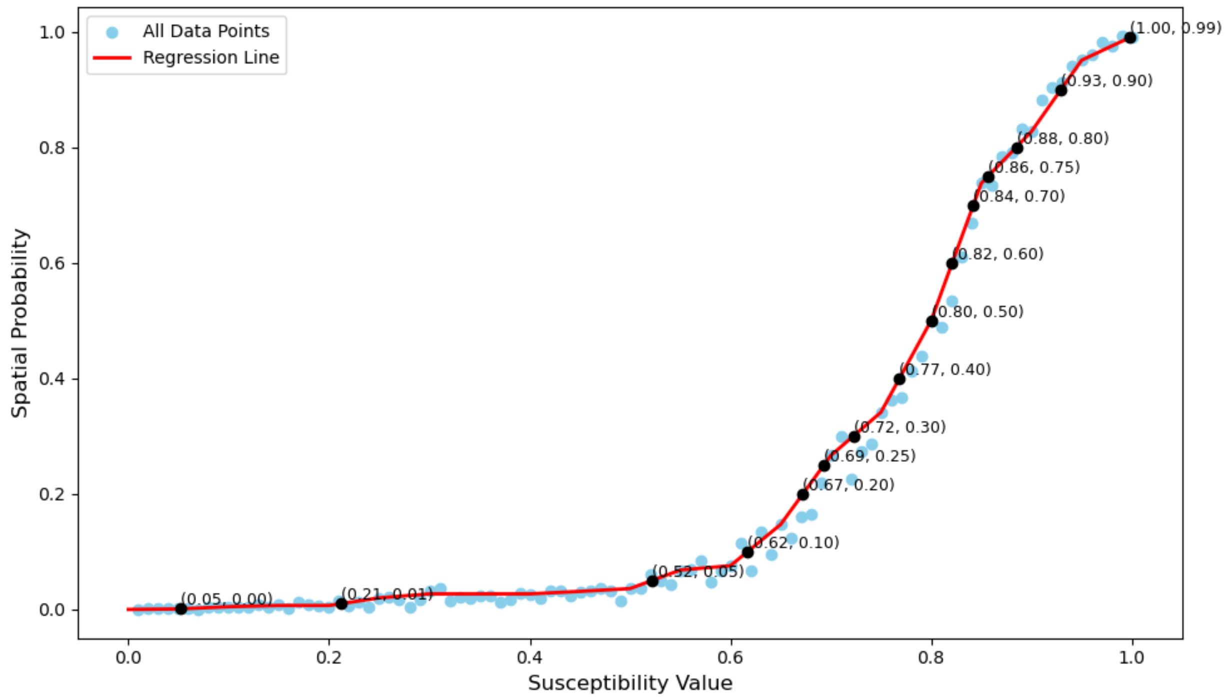

Figure G-11 Plot representing the data used to inform the translation of susceptibility values to spatial probability.

Table G-6 Overview of spatial data used to calculate spatial probability ranges within the ASA, and the total area corresponding to each range within both the ASA and AOI.

Spatial Probability Range		Susceptibility Value Range		ASA			AOI
From	To	From	To	Non -Landslide Pixels	Landslide Pixels	Proportion of Area in Range	Proportion of Area in Range
0%	0.1%	0	0.052	87014	28	66.26%	74.20%
0.1%	1%	0.05	0.212	15639	77	11.96%	12.10%
1%	5%	0.21	0.52	10310	234	8.03%	7.66%
5%	10%	0.52	0.62	2082	153	1.70%	1.50%
10%	20%	0.62	0.67	1033	159	0.91%	0.80%
20%	25%	0.67	0.69	332	75	0.31%	0.29%
25%	30%	0.69	0.72	482	180	0.50%	0.40%
30%	40%	0.72	0.77	713	345	0.81%	0.61%
40%	50%	0.77	0.8	407	332	0.56%	0.40%
50%	60%	0.8	0.82	290	310	0.46%	0.26%
60%	70%	0.82	0.84	215	407	0.47%	0.26%

Spatial Probability Range		Susceptibility Value Range		ASA			AOI
From	To	From	To	Non -Landslide Pixels	Landslide Pixels	Proportion of Area in Range	Proportion of Area in Range
70%	75%	0.84	0.86	131	347	0.36%	0.18%
75%	80%	0.86	0.89	232	851	0.82%	0.32%
80%	90%	0.89	0.93	305	2304	1.99%	0.49%
90%	100%	0.93	1	190	6197	4.86%	0.52%

G-5.6 Landslide Susceptibility Threshold

Table G-7 categorizes susceptibility from Low to High, using category breaks informed by Figure G-10 and Table G-7.

Table G-7 Landslide susceptibility classes.

Class	Approximate Spatial Probability	Susceptibility Range	Proportion of AOI
Low	< 1 %	< 0.212	86.3%
Moderate	1 - 10 %	0.212 - 0.617	9.2%
High	10 - 75%	0.617 - 0.857	3.2%
Very High	>75 %	> 0.857	1.3%

Regulatory decision making requires choosing a susceptibility level above which site-specific assessments may be warranted (e.g., required under bylaw where existing) to check for slope instability. Because the potential for landslides at any susceptibility cannot be entirely ruled out, the choice requires a tolerance for uncertainty. The objective is to capture as much unstable terrain as possible (avoid false negatives) without encompassing too much stable terrain (avoid false positives).

Within the RDFFG, the 1% (Low) threshold captures 364 of the 632 soil slides on slopes gentler than 30% (e.g., the slides missed by steep slope criteria), while adding 2450 km^2 (10 %) of area. A more conservative threshold substantially increases the coverage area, and a less conservative threshold captures less landslides without substantially reducing the coverage area. As such, BGC considered 1% as a reasonable threshold, given uncertainties and the information available. However, this threshold warrants further discussion (and potentially further landslide susceptibility model refinement) before adopting a threshold for regulatory decision-making purposes.

G-6 LANDSLIDE AREAS OF INTEREST MAP

Based on the results of the landslide inventory, steep slope mapping, and earth slide susceptibility mapping, BGC defined landslide "areas of interest" that meet one or more of the following criteria:

- Slope angle greater than 30% with a relief greater than 10 m vertical over 90 m horizontal
- Spatial probability of DSE presence greater than 1%
- Presence of an inventoried landslide.

The Landslide Hazard Area of Interest Map covers approximately 24,000 km^2 (46 %) of the RDFFG and includes:

- 1232 mapped landslide points (Section G-3)
- 19,000 km^2 of mapped steep slopes (Section G-4)
- 4000 km^2 where spatial probability of a DSE is greater than 1 % (Section G-5)
- 1500 km^2 where steep slope map and susceptibility criteria overlap.

Assets within the Landslide Area of Interest Map are assumed as exposed to landslide hazard.

REFERENCES

Achard, R.A., (1973). Five surficial geological maps of the Canoe river valley from the Columbia River to Valemount, British Columbia. GSC Open File, 163, scale 1:50,000.

Agliardi, F., Crosta, G., & Zanchi, A. (2001). Structural constraints on deep-seated slope deformation kinematics. *Engineering Geology, 59*(1-2), 83-102. https://doi.org/10.1016/S0013-7952(00)00066-1

Bartos, M. (2020). *pysheds: Simple and fast watershed delineation in Python* [Computer software]. Zenodo. https://doi.org/10.5281/zenodo.3822494

British Columbia Ministry of Forests (BCMOF). 1994. A Guide for Management of Landslide-Prone Terrain in the Pacific Northwest. Second Edition. Land Management Handbook Number 18. S.C. Chatwin, D.E. Howes, J.W. Schwab, and D.N. Swanston. Victoria, B.C.

BGC Engineering Inc. (2020, December 17). *North Eastern British Columbia landslide susceptibility map*. Prepared for BC Oil and Gas Research and Innovation Society (BC OGRIS).

BGC Engineering Inc. (2025, April 30). *Technical Memorandum – RDFFG Slope Maps: Topographic Analysis*. Prepared for RDFFG Electoral District A.

Blais-Stevens, A. & Clague, J.J. (2007a). *Surficial geology, Hixon, British Columbia*. Geological Survey of Canada, Open File 5272, scale 1:50,000.

Blais-Stevens, A., and Clague, J.J., (2007b). *Surficial geology, Ahbau Lake, British Columbia*. Geological Survey of Canada, Open File 5273, scale 1:50,000.

Bornaetxea, T., Blais-Stevens, A. & Miller, B. (2022). *Landslide inventory map of the Valemount area, British Columbia*. Geological Survey of Canada, Open File, 8926.

Brideau, M.-A., Hancock, C.-A., Brayshaw, D., Lipovsky, P., Cronmiller, D., Friele, P., Wells, G. 2024. Canadian Landslide Database, version 9.0. https://zenodo.org/records/13924556.

Chen, T. & Guestrin, C. (2016, June 10). XGBoost: A Scalable Tree Boosting System. https://doi.org/10.48550/arXiv.1603.02754

Clague, J.J. (1998). *Surficial Geology, Cluculz Lake, British Columbia*. Geological Survey of Canada, Open File 3638, Scale 1:100,000.

Choe, B-H., Blais-Stevens, A., Samsonov, S., & Dudley, J. (2022). *RADARSAT constellation mission (RCM) InSAR preliminary observations of slope movements in British Columbia, Alberta, and Nunavut*. Geological Survey of Canada Open File 8928.

Cruden, D.M. (199)1. A simple definition of a landslide. *Bulletin of the International Association of Engineering Geology, 43*, 27-29. https://doi.org/10.1007/BF02590167

Cruden, D.M. & Varnes, D.J. (1996). Landslide Types and Processes. Special Report, Transportation Research Board, National Academy of Sciences, 247, 36-75.

Cui, Y., Miller, D., Schiarizza, P., & Diakow, L.J. (2017). *British Columbia digital geology*. British Columbia Ministry of Energy, Mines and Petroleum Resources, British Columbia Geological Survey Open File 2017-8, 9p. Data version 2019-12-19.

Eilander, D. (2025). pyFlwDir (v0.5.10). Zenodo. https://doi.org/10.5281/zenodo.14889722

Froese, C.R. (1998). Landslides in the Morkill River Valley, British Columbia [M.Sc. thesis]. University of Alberta.

Government of Canada, Natural Resources Canada, Canada Centre for Remote Sensing. (2025, April 29). 2020 Land Cover of Canada. Natural Resources Canada, Federal Geospatial Platform. https://osdp-psdo.canada.ca/dp/en/search/metadata/NRCAN-FGP-1-ee1580ab-a23d-4f86-a09b-79763677eb47

Hippolyte, J.-C., Bourles, D., Leanni, L., & Braucher, R. (2012). 10Be ages reveal >12 ka of gravitational movement in a major sackung of the Western Alps (France). *Geomorphology, 171/172*, 139-153. https://doi.org/10.1016/j.geomorph.2012.05.013

Heung, B., Bulmer, C. E., Schmidt, M. G., & Zhang, J. (2022). Provincial-scale digital soil mapping using a random forest approach for British Columbia. *Canadian Journal of Soil Science, 102*(3), 597–620. https://doi.org/10.1139/cjss-2021-0090

Hungr, O., Leroueil, S. & Picarelli, L. (2014). Varnes classification of landslide types, an update. *Landslides, 11*, 167-194. https://doi.org/10.1007/s10346-013-0436-y

Maynard, D.E., Geertsema, M., Ward, B.C., & Sacco, D.A., (2013a). *Terrain map Weedon Lake (093J/11)*. Geoscience BC, Geoscience BC Map 2013-10-3, scale 1:50,000.

Maynard, D.E., Ward, B.C., Sacco, D.A., & Geertsema, M. (2013b). *Terrain map Great Beaver Lake (093J/05)*. Geoscience BC, Geoscience BC Map 2013-10-5, scale 1:50,000.

Maynard, D.E., Ward, B.C., Sacco, D.A., & Geertsema, M. (2013c). *Terrain map Bugle Lake (093J/06)*. Geoscience BC, Geoscience BC Map 2013-10-6, scale 1:50,000.

Natural Resources Canada (NRCAN). (2025). *Canadian Digital Elevation Model (CDEM) - Multiresolution DEM (MRDEM)* [Dataset]. Government of Canada. https://open.canada.ca/data/en/dataset/aa3d1f8b-36ae-517b-87fd-897e074ef160

Pedrazzini, A., Jaboyedoff, M., Loye, A., & Derron, M.-H. (2013). From deep seated slope deformation to rock avalanche: destabilization and transportation models of the Sierre landslide (Switzerland). *Tectonophysics, 605,* 149-198. https://doi.org/10.1016/j.tecto.2013.04.016

Porter, M., (1999). *Terrain assessment and preliminary stability analyses for a large history landslide in the Nechako River Valley* [M.Eng]. University of Alberta.

US Geological Survey (USGS). 2008. The Landslide Handbook — A Guide to Understanding Landslides. By L.M. Highland and M.D. Bobrowsky. USGS Circular 1325. Reston Virginia. pp. 129

Sacco, D.A., Ward, B.C., Geertsema, M., & Maynard, D.E., (2013a). *Terrain map Salmon Lake (093J/13)*. Geoscience BC, Geoscience BC Map 2013-10-1, scale 1:50,000.

Sacco, D.A., Ward, B.C., Geertsema, M., & Maynard, D.E., (2013b). *Terrain map Carp Lake (093J/14)*. Geoscience BC, Geoscience BC Map 2013-10-2, scale 1:50,000.

Sørensen, R., Zinko, U., & Seibert, J. (2006). On the calculation of the topographic wetness index: evaluation of different methods based on field observations. *Hydrology and Earth System Sciences, 10*, 101–112. https://doi.org/10.5194/hess-10-101-2006

Ward, B.C., Maynard, D.E., Sacco, D.A., & Geertsema, M., (2013). *Terrain map Carrier Lake (093J/12)*. Geoscience BC, Geoscience BC Map 2013-10-4, scale 1:50,000.

APPENDIX H
HAZARD EXPOSURE ANALYSIS

H-1 INTRODUCTION

For all mapped hazards, BGC identified where people and assets, collectively termed ‘valued assets’, are located and may be exposed to hazards. Table 5-1 in the main report shows the types of valued assets included. The same valued asset list is also provided in tabular results (Appendix I), and spatially in the layers published to Cambio.

This appendix describes the exposure analysis workflow and spatial logic. The descriptions and schematic figures in this appendix describe methods BGC implemented in Python Programming Language libraries. BGC optimized the process to minimize processing time for large datasets and generated summary reports (as shown in Appendix K). Appendix J describes gaps and limitations.

H-2 HAZARD EXPOSURE ASSESSMENT

H-2.1 Workflow

The hazard exposure analysis workflow follows a consistent order for each hazard type. This process is illustrated in Figure H-1. The workflow includes the following main steps:

1. Compile valued asset and hazard data inputs (Box 1 in Figure H-1)
2. Intersect hazard with valued assets (Box 2 in Figure H-1)
3. Summarize and generate hazard exposure results (Box 3 in Figure H-1).

BGC used a 100 m x 100 m (1 ha) grid as the spatial format to compute and summarize hazard exposure within each grid cell across the entire RDFFG (Step 3, above). BGC chose the 100 m x 100 m grid size to balance the level of detail required to meet the intended use case with the need to limit processing time required to generate the results. The size of the grid governs the size of areas summarized (Step 3), but not the resolution or results of the of exposure analysis (Steps 1 and 2). That is to say that changing the grid cell size does not change the results of the analysis.

BGC calculated hazard exposure summary statistics for each grid cell in the form of a summary of the asset values (e.g., population counts, monetary value of buildings and businesses, length of linear infrastructure) exposed and not exposed. Results in the various forms described in the main report are provided district-wide and for each project partner.

BGC assigned units of the value to exposed valued assets specific to each asset type (e.g., length, monetary value, or quantity). For those working with the geospatial data, BGC notes that a value of “NULL” was assigned to valued assets identified as ‘not-exposed’. For clarity, BGC notes that in rare cases the assessed value of a built form asset (i.e. a property with buildings on it) may be zero (0). This means that it is possible to have a value of zero for a built form exposed. Therefore, an grid cell has an exposure density of 0, this indicates that there is an exposed built form within this cell which has no value associated with it. If there are no exposed assets within a cell, this is indicated with a value of “NULL”.

Given the volume of data inputs and the regional-scale analysis, BGC optimized the hazard exposure analysis process to manage processing time.

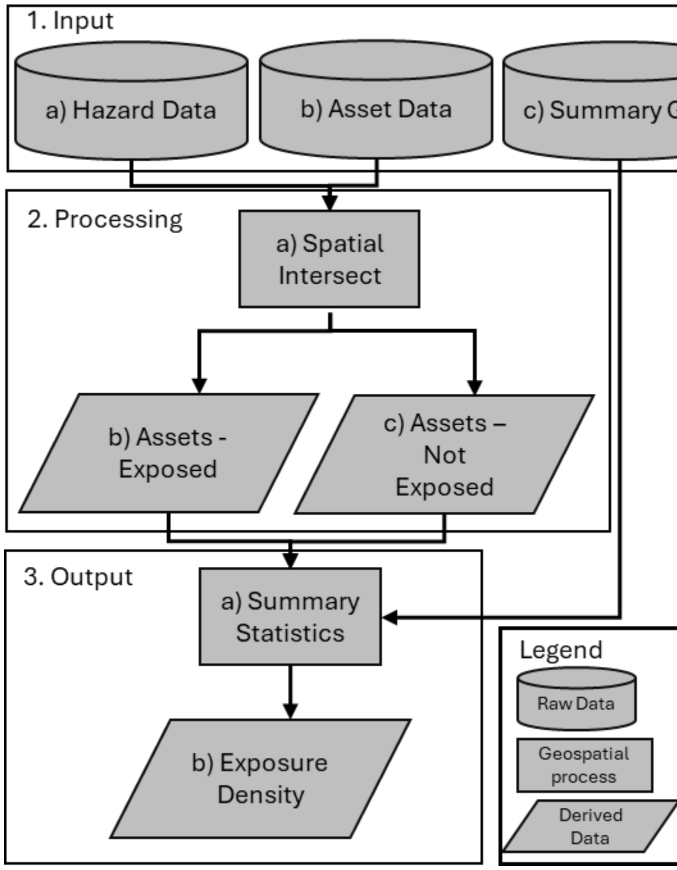

Figure H-1 Overview of the geospatial workflow implemented to assess hazard exposure across all valued assets and all hazards in this study.

H-2.2 Spatial Logic

H-2.2.1 General

Geometry of geospatial data representing valued assets can take the form of points (e.g., electrical power poles), polylines (e.g., roads), or polygons (e.g., cadastral land parcels). The workflow described in the previous section includes logic to identify exposure for each of these geometry types.

Table H-1 summarizes the logic for each geometry type illustrated in Figure H-2 (points), Figure H-3 (polylines), and Figure H-4 (polygons). If the valued asset intersects a mapped hazard area, BGC attributed the asset, accordingly. BGC designed the logic to calculate the total exposure of valued assets while maintaining the overall total for each valued asset. For example, the total assessed value of 'exposed' building improvements, plus the value of building improvements 'not exposed', must sum to the original total assessed value of all improvements.

Based on hazard-asset intersection, BGC calculated exposure "density", which is the sum of exposure within a given 100 m x 100 m grid cell (e.g., the total number of roads, or total value of exposed parcels). By normalizing values by area, exposure density provides an "apples to apples" way to view exposure across a jurisdiction. For example, consider multiple small parcels, each with the same value as a larger parcel. While they have the same value, the small parcels will have higher exposure density (higher exposure value per unit area), which may inform decisions to focus further work in more densely exposed areas.

Table H-1 description of geometry-based hazard exposure logic.

Geometry Type	Description of Hazard/Asset Intersect	Description of Exposure Density Calculation
Points	The spatial intersect between valued asset points and hazards, represented as a sub-set of exposed valued asset points.	Expressed as a count of exposed points per 100 m x 100 m grid cell
Polylines	The spatial intersect between linear valued assets and hazards, represented as a subset of polylines within the extent of the hazard.	Expressed as a length of exposed polyline segments per 100 m x 100 m grid cell
Polygons	The spatial intersect between valued asset areas and hazards, represented as a subset of polygons within the extent of the hazard.	Expressed as an area of exposed polygon areas or value (e.g. population) per 100 m x 100 m grid cell. Value (e.g., area) is proportioned where a polygon intersects more than one grid.

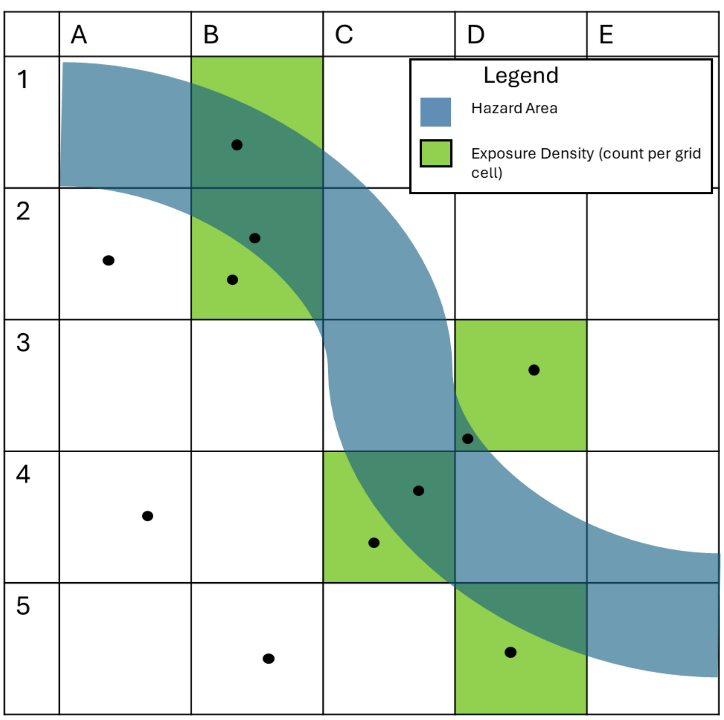

Figure H-2 Schematic of the hazard exposure calculation logic for point-based valued assets.

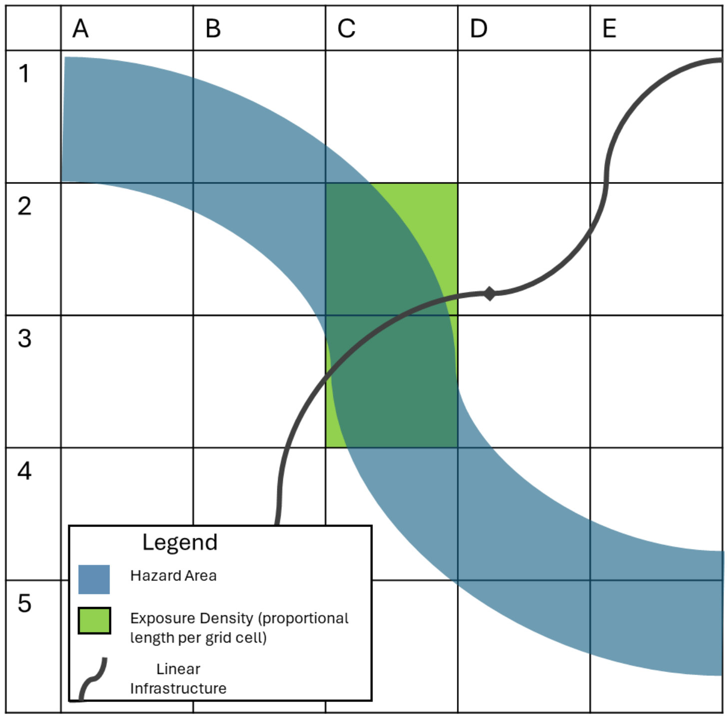

Figure H-3 **Schematic of the hazard exposure calculation logic for polyline-based valued assets.**

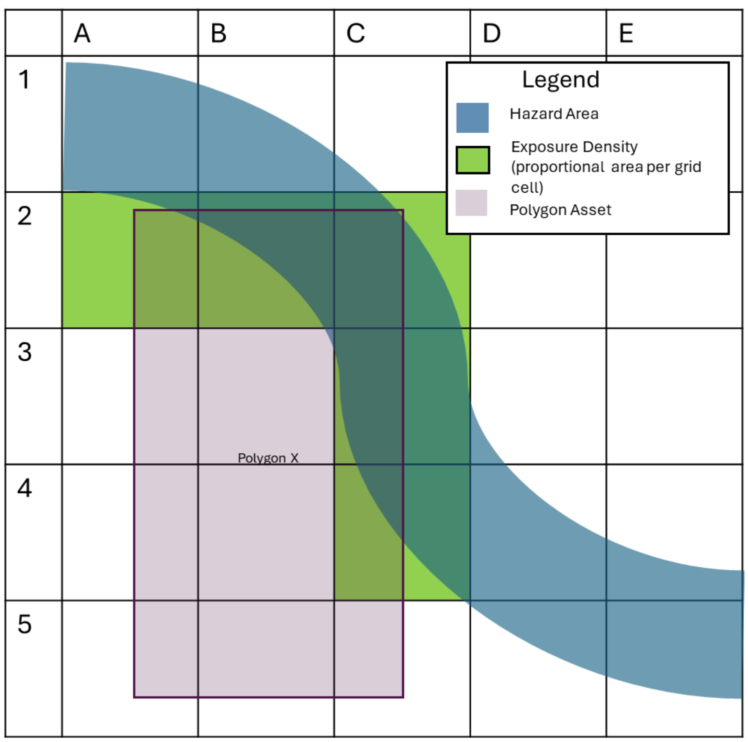

Figure H-4 **Schematic of the hazard exposure calculation logic for polygon-based valued assets.**

H-2.2.2 Spatial Logic - Populations

BGC analysed population exposure based on the Canadian Open Buildings Layer (Fortin, 2024) and the NRCAN human settlement layer (NRCAN 2022a, b). Both are based on Census data but have different spatial representation. Appendix J lists gaps and limitations associated with these data. BGC reported results from both sources in Appendix I. Where differences exist, population exposure shown on the Fact Sheets (Appendix M) conservatively shows the higher estimate.

Population exposure based on NRCAN (2022a) was assigned according to the general polygon logic described in Section H-3.

Figure H-5 illustrates the exposure logic for building footprint population data (Fortin, 2024). These data provide the most precise way to intersect population data with hazard areas. If a given building intersects with a hazard area, the total population of the building is considered exposed (even if only part of a building intersects). Where buildings extend across grid boundaries, the exposed population is distributed proportionally by area between the grid cells (i.e., cells B2, B3, and B4 in Figure H-5).

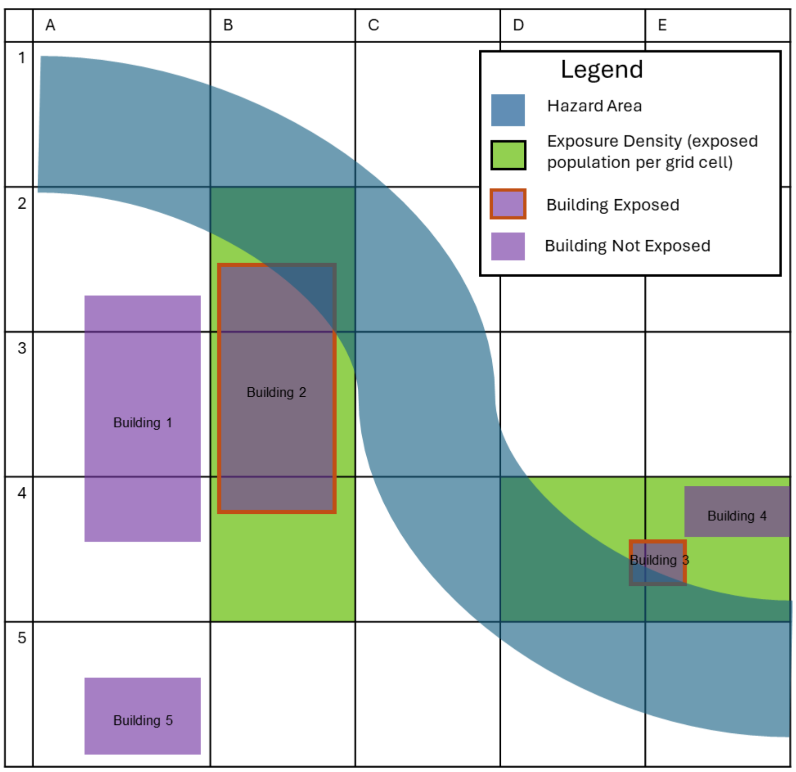

Figure H-5 Schematic of the hazard exposure calculation logic for population.

H-2.2.3 Spatial Logic – Improvement Values

Figure H-6 shows the exposure logic for cadastral parcels, where exposure level is measured by improvement value of the parcel. In this case, parcel exposure is calculated based on whether a parcel contains a building that intersects a hazard area. The exposure density calculation is the proportional distribution of improvement value amongst all cells that intersect the parcel. For example, Figure H-6 shows building #3 as exposed; therefore, the improvement value for Parcel 2 is distributed proportionally amongst cells C1, C2, C3, D1, D2, and D3. This logic preserves the requirement that the value of 'not exposed' plus 'exposed' must equal the original total value.

Parcel #3 in this figure represents a case where a parcel has improvement value associated with it (this implies that there is a building on the parcel), but no building present from the Open Buildings Layer (e.g., there is a data gap in the building footprints inventory). Where such data gaps exist, BGC based hazard exposure on the intersection of the parcel with the hazard (rather than being based on an exposed building). For example, building footprints are largely missing within the Village of McBride, and such logic is applied within McBride to analyse building improvement hazard exposure. In general, this logic results in a more conservative estimation of hazard exposure, as the parcel is counted as exposed if any part of the parcel intersects the hazard extent.

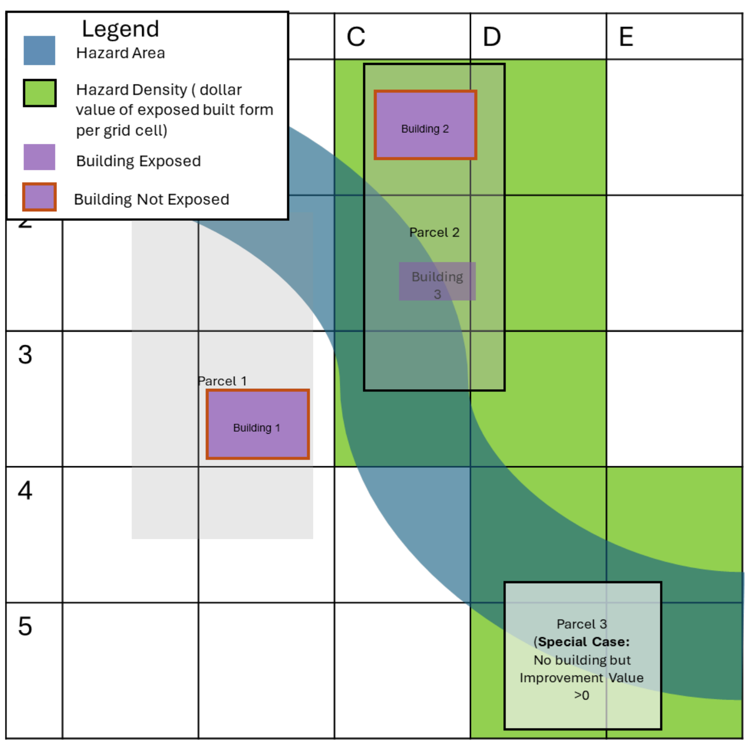

Figure H-6 Schematic of the hazard exposure calculation logic for cadastral parcels.

REFERENCES

Fortin, Maxim. (2024): Open Building Population Layer - Canada, derived from open-source computer-generated footprints and 2021 census data, URL: https://www.maximfortin.com/project/obpl-ca-2021/

Natural Resources Canada. (2022a). *Social Vulnerability to Natural Hazards in Canada.* Geological Survey of Canada Open File 8892

Natural Resources Canada. (2022b). *Physical Vulnerability to Natural Hazards in Canada*. Geological Survey of Canada Open File 8902

APPENDIX I
HAZARD EXPOSURE RESULTS (INCLUDED SEPARATELY)

APPENDIX J
GAPS AND LIMITATIONS

Input	Item	Description	Implications	Considerations to Resolve
Valued Assets	General	Gaps exist in the valued data model in terms of location, attributes, and data formats. Specifically, the layers are based on the best information available at the time of study but are not complete.	Potential gaps in information leading to underestimation of hazard threat (e.g. missing assets), or overestimation of hazard threat (e.g., where assets not located within hazard extents are still captured due to coarse resolution of datasets).	As a starting point for maintaining and updating asset data throughout the RDFFG, identify parties with roles and responsibilities related to compilation and management of valued asset data. In addition to those responsible for 'hard' assets, develop road map to geo-locate values defined through local and Indigenous knowledge.
	Summary - ICI Society Data	Much data about built environment valued assets in BC, including utility networks, is maintained by the Integrated Cadastral Information (ICI) Society. These data represent a valuable source of built environment data for disaster hazard threat and risk assessment. However, the data model requires substantial re-work (e.g. grouping, categorizing) to prepare for hazard threat analysis.	Increased effort and cost to prepare built environment data layers for hazard threat and risk analyses. This increase in effort increases multifold by each risk assessment completed that relies on these data.	In collaboration with ICI Society, review and consider updates to data organization and format to facilitate hazard threat, vulnerability and risk analysis.
	Population	Demographic breakdown of population totals in NRCAN (2022) is based on 2016 Census data (not 2021). Current Census data may under-represent populations with lower rates of response to census data requests, and for occupied areas not represented by Census data (e.g. non-residential. BGC also used two data sources to spatially represent and report population exposure: building footprints attributed with Census (2021) data, and the NRCAN settlement layers (also 2021 Census data). The building footprint layer is more precise for exposure analysis, but contains data gaps in some areas (e.g. Village of McBride).	Demographic breakdown of population exposure is limited to 2016 Census results. Population exposure based on building footprints will be underestimated where gaps in building footprint data exist.	Update hazard exposure analysis (re-run exposure analysis) when updated population data becomes available. Review exposure results based on both Population Total (2021 Census Building Footprint) and Population Total (2021 Census). McBride should ignore the building footprint - sourced population exposure results due to substantial data gaps.
	Built Forms (First Nations Reserves)	Built forms (parcel improvements) are not represented by BC Assessment (BCA) data on reserve lands. NRCAN physical exposure layer provides estimates of building replacement value aggregated at settlement area level of detail, but at lower resolution and without attribution amenable to vulnerability analysis. No data source for actively maintained built form data on FN reserves has been identified in a format amenable to regional scale, parcel or building resolution, hazard threat, vulnerability or risk analysis.	High uncertainty and likely underestimation of built form values on First Nations reserves, with subsequent implication for underestimation of loss due to hazards.	Review programs for the maintenance and distribution of built form geospatial data that can be efficiently accessed at province-wide scale (e.g. do not fragment data access between reserve areas).
	Built Forms (Data format)	BC Assessment data joined to cadastral fabric contains polygons at folio level of detail. For example, a condominium tower with many units (folios) will have many polygons stacked on top of each other. These were assigned a primary actual use and total value for spatial analysis.	More detailed analysis may require folio level of detail, such as to distinguish a retail ground floor from residential upper stories of a building for flood loss estimation.	Consider folio level of detail of spatial analysis for the completion of regional-local stages of assessment, where required to apply appropriate vulnerability criteria.
	Built Forms (Valuation)	Hazard threat analysis uses assessed built form values, which may differ from replacement costs.	Potential underestimation of disaster recovery costs where replacement costs exceed depreciated assessed built form values.	Maintain the use of a regularly updated dataset (BC Assessment); if replacement values are desired, consider BCA data fields as a data source for provincial scale estimation workflows.
	Built Forms (Building Footprints)	Available building footprints data does not characterize building type (built form actual use is derived from BC Assessment Actual Use codes). For example, if multiple footprints exist within a parcel, no attribute exists to distinguish between a main occupied structure and an out-building.	Exposure analysis conservatively considers hazard exposure to any building footprint within a parcel. This may over-estimate exposure if, for example, an unoccupied structure is exposed, but a main buildiing is outside the hazard extent.	For sites advanced to detailed assessment, complete site-specific checks of building footprint data to characterize at an individual building level of detail.
	Built Forms (Valuation)	There are two data sources for valuation -- parcel improvement value based on BC assessment data, which applies to all areas outside of first nations reserves, and Canada lands parcel building values, which is used within the boundaries of first nations reserves. In some cases the summary results may include exposed value from both sources as a result of the resolution of the grid summaries.	Conflicting built form exposure values	a consistent dataset applying to the entire province would eliminate this issue. The reducing the sizer of the 100 x 100 m grid cells may also help to limit the impact of this issue at the expense of more computational time required to generate results.
	Critical Facilities	Critical facilities were identified using a rules-based approach (BC Assessment Actual Use Descriptions), spatially represented by a point at the centroid of a given parcel. Given the source of data, facilities critical for reasons related to cultural importance are not included.	Local communities may have facilities critical for function in an emergency that are not identified at the scale of assessment, or that would not be identifiable without local knowledge (e.g. a parking lot containing emergency response resources).	Develop a plan to update and regularly maintain a critical facility inventory based on additional local knowledge of facilities critical for function during an emergency.
	Businesses	Total Annual Revenue data is based on uncertain categorical estimates within commercial data sources. Revenue cited for a given business location is not necessarily related to business activities at that location.	Uncertainly related to business disruption given hazard impact.	
	Environmental Values	Environmental values considered in the assessment (Old Growth Management Areas, Parks and Protected Areas, Fisheries Information Summary System (FISS) locations, and Species and Ecosystems at Risk) have very different vulnerabilities to hazard compared to the built environment.	Hazard thresholds selected for spatial hazard threat analysis are generalized for regional scale application. While spatial relations between hazards and ecosystems will inform subsequent steps of regional assessment, the term "threat" should be used with caution (is not comparable to built environment assets).	Consider additional hazard scenarios and threshold criteria in subsequent stages of assessment tailored more specifically to vulnerabilities within natural ecosystems.
	Linear facilities (road, rail, utilities)	Analysing hazard exposure for linear facilities is highly location-specific and may include mechanisms of damage not well represented by spatial intersection of hazard extent with an asset centerline.	Over-estimation of hazard threat for some hazard types that include a span (e.g. communication or electrical line) between tower locations located to either side of a hazard extent (e.g. flood area). Uncertain estimate of hazard threat for assets requiring distinct approaches for threat analysis (e.g. buried pipelines).	Many linear infrastructure operators in BC operate long-term asset and risk management programs maintained by consultants. Consider engagement with infrastructure operators and their consultants to identify opportunities to share resources, knowledge and tools, to advance shared risk management objectives.
	Municipal assets	Gaps exist for utilities and other asset data that is exclusively managed at a municipal level and not present within provincially compiled sources (ICI Society).	Underestimation of hazard threat for municipally managed assets not present within the database.	Consider municipally managed asset data sources for subsequent steps of local scale assessment

Input	Item	Description	Implications	Considerations to Resolve
	Riverine Flooding Tier 1 - Floodplain Identification	Tier 1 floodplain mapping is not of sufficient resolution to consider effects of structural flood mitigation (e.g., dikes). Mapping is limited to watersheds with at least 10 km^2 drainage area.	Under- or overestimation of credible riverine flood threat to valued assets. Watercourses less than 10 km^2 are not included, and may be subject to steep creek hazards (e.g. debris floods and debris flows) not included in hazard threat analysis.	With appropriate subject matter expertise, build on the hazard exposure analysis methods developed by this project with higher resolution flood hazard mapping where available, including additional scenarios and consideration of additional parameters of risk (vulnerability).
	Riverine Flooding Tier 2 - Flood Hazard Mapping	The models have not been calibrated due to limited local data. Modelling results are based on assumed parameters.	Lack of calibration may result in under- or over-estimation of flood hazard level.	After flood hazard events, allocate effort to collect time-sensitive information that is important for future model calibration, such as evidence for high-water marks.
		The models underestimate channel conveyance capacity.	Channel capacity that is larger than shown by the available digital elevation model may result in over-estimation of water levels and extents.	Collect river bathymetry and incorporate in the hydraulic models developed as part of this project.
		BGC developed the models based on current conditions; however, natural processes and human activities could alter the configuration of the study area in the future, potentially affecting the validity of the results.	Mapping results will become out of date as conditions change.	Develop a plan to refine existing mapping as conditions change. Reduce costs by treating hazard mapping as an asset that requires periodic maintenance to avoid becoming so out of date that it requires wholesale replacement.
		The numerical model assumes a fixed bed, excluding the effects of erosion and avulsion, which limits its ability to simulate geomorphological changes.	Lack of ability to consider hazard characteristics affected by a changing river bed, such as through bank erosion or channel avulsion.	Develop a plan to incorporate geomorphic mapping. As with bathymetry, reduce costs by treating additional assessment as part of a plan to refine hazard information (build on previous work).
		Climate change projections are subject to uncertainties due to variability among climate models, future emissions scenarios, and the representation of hydrological processes at regional scales.	Under- or overestimation of credible riverine flood threat to valued assets, as hazard changes in a changing climate.	Develop a plan to revisit climate change assumptions as part of a broader plan to maintain the currency of flood hazard information (along with bathymetry, geomorphology).
	Riverine Flooding	Tier 2 flood hazard maps were developed for select areas. The models were not calibrated due to limited local data and are representative of the terrain at the time of lidar acquistion.	Uncertainty of flood inundation extents. Modelling does not consider changes in the bed condition (degradation or aggradation of the channel bed).	Consider converting Tier 2 mapping areas to detailed floodplain mapping studies (Tier 3) to develop regulatory maps for high hazard areas.
	Landslide Inventory	BGC's hazard inventory is limited to identifying points placed at the initiation of landslide landforms. The accuracy of the landslide inventory depends, in part, on the resolution of the available terrain data. Lidar DEMs provide 1 m or better resolution. The landslide inventory is not exhaustive and has greater uncertainty in areas without lidar coverage.	More detailed assessment is anticipated to identify landslide locations not contained in the current inventory.	Update the landslide inventory as new events occur or when updated studies become available.
		Mapped landslide points do not provide information about their size, current level of activity (i.e., are they moving or have they not moved in decades/centuries/millennia), or the impact zone (runout extent) of past or future events. Landslide inventories also do not provide a comprehensive characterization of the location and probability of future landslide event.	The existence of a landslide indicates previous slope movement but does not necessarily imply current slope movement. Landslide point locations cannot indicate areas susceptible to first-time failure (e.g. where no landslide landform yet exists).	Use the landslide point inventory as a starting point for further hazard characterization as part of more detailed study.
	Landslide Susceptibility	Landslide susceptibility map is based on a model derived from approxiately 700 landslides. The model provides an estimate of landslide susceptibility based on various terrain perameters, which are static (e.g. slope angle, relief, surficial geology). The model is,therefore, also static and does not reflect changing conditions. Moreover, landslide susceptibility is measured as a spatial probability that a given location is within an existing earth landslide and does not provide any indication of activity level or temporal frequency. The model is also limited by the resolution of data inputs.	The landslide susceptibility map is a useful tool for understanding relative spatial distribution of landslide hazards and identifying areas of interest for further assessment. It does not replace more detailed landslide hazard characterization based on higher resolution information that may be available for certain sites.	Conduct further work to validate and improve the landslide susceptibility model--specifically include higher resolution surficial geology data as an input if such data becomes available. Combine landslide susceptibility with regional-scale InSAR analysis to identify areas of high susceptibility which have shown recent movement.
	Landslide Areas of Interest	Landslide areas of interest are intended to identify areas with credible potential for potential landslide initiation. Assessing landslide runout or landslide-affected areas within a setback behind the crest of escarpments was outside the scope of work.	Landslide hazard beyond the base or behind the crest of slopes may exist that was not mapped.	Conduct further work to characterize landslide hazard at the crest and base of escarpment slopes (e.g. in Prince George).
	Alluvial Fan Inventory	BGC's hazard inventory is limited to alluvial fans and is focused on settled areas. Alluvial fans exist in remote undeveloped areas that were not mapped. The presence of a fan indicates past geohazard occurrence, but the lack of a fan on a steep creek does not necessarily rule out the potential for future geohazard occurrence. The fan boundary approximates the extent of sediment deposition since the beginning of fan formation . Geohazards can potentially extend beyond the fan boundary due to localized flooding, where the fan is truncated by a lake or river, in young landscapes where fans are actively forming (e.g., recently deglaciated areas), or where large landslides (e.g., rock avalanches) trigger steep creek events larger than any previously occurring.	The fan inventory completed in this study should not be considered exhaustive. The potential for steep creek geohazards to extend beyond the limit of some mapped fan boundaries cannot be ruled out.	Update steep creek hazard information as new events occur or when updated studies become available.
		The accuracy of fan boundaries depend, in part, on the resolution of the available terrain data. Where available, lidar DEMs provide 1 m or better resolution, compared to 20+ m in areas without lidar. Mapped geohazard boundaries, even where lidar coverage is available, are approximate. The minimum geohazard area that was mapped with the available information is about 20 ha.	Local variations in terrain conditions over areas of 1 to 3 ha, or over distances of less than about 200 m, may not be visible. Future site investigations could alter the extents of the geohazards mapped by BGC. Because greater uncertainty exists when mapping alluvial fan boundareas in areas without lidar coverage, fan boundaries in these areas should be used with caution when making policy, regulatory, and risk management decisions.	In areas without lidar, update steep creek fan boundaries and characteristics once lidar data becomes available.
	Climate change (all hazards)	Quantitative consideration of climate change was limited to Tier 2 flood hazard mapping (via (via adjustments to projected 200-year flows)	Uncertainty of hazard exposure with ongoing climate change.	Consider climate change effects on remaining hazard types as part of more detailed assessment. Update results on a regular basis to maintain currency in a changing climate.

APPENDIX K
METADATA

Asset/Hazard Group	Cambio Layer Name	Dataset Name	Original Dataset Creator	Original Dataset Link	Citation	Metadata Creator	Date Published	Date Compiled	Date Modified	File Format	Methodology	Constraints	Coordinate System	Geometry Type
Population Within a Social Vulnerability Range	n/a	main.nhsl_social_fabric_indicators	NRCan	https://opendrr.github.io/national-human-settlement/en/	Natural Resources Canada. (2022a). Social Vulnerability to Natural Hazards in Canada. Geological Survey of Canada: Open File 8902. Natural Resources Canada. (2022b). Physical Vulnerability to Natural Hazards in Canada. Geological Survey of Canada. Open File 8892.	Matthew Buchanan, BGC	2021-11-23	2021-11-23	2021-11-23	Hixon_Q200_CC_depth_v0_reclass.tif	No changes from published dataset. All attributes dropped except Sauid, SVlt_Score	public	BC Albers	polygon
	n/a	main.physical	NRCan	https://opendrr.github.io/national-human-settlement/en/		Matthew Buchanan, BGC	2021-11-23	2021-11-23	2021-11-23	GeoPackage Data Table	No changes from published dataset. All attributes dropped except Sauid, Et_PopTransit	public	North America Albers Equal Area Conic	polygon
Built Form and Buildings	BC Assessment Data (Shown only outside of First Nations Reserves)	main.parcels_values	GeoBC, BC Assessment	https://www2.gov.bc.ca/gov/content/data/geographic-data-services/land-use/integrated-cadastral-fabric (retired)	Integrated Cadastral Information (ICI) Society. (2019, December 1). Utility Infrastructure [Database]. Retrieved from: https://www.icisociety.ca/services/our-data/.	Matthew Buchanan, BGC	2023-10-17	2023-10-17	2023-10-17	GeoPackage Data Table	Converted geopackage to Esri Geodatabase. Amalgamated parcel values from GEN_GROSS_IMPROVEMENT_VALUE SUBJECT TO CHANGE	?	North America Albers Equal Area Conic	polygon
		main.parcels_descriptions	GeoBC, BC Assessment	https://www2.gov.bc.ca/gov/content/data/geographic-data-services/land-use/integrated-cadastral-fabric		Matthew Buchanan, BGC	2023-10-17	2023-10-17	2023-10-17	GeoPackage Data Table	SUBJECT TO CHANGE	?	North America Albers Equal Area Conic	polygon
	Canada Lands (Shown only on First Nations Reserves)	main.fn_parcels	Canada Lands and FNESS	https://clss.nrcan-rncan.gc.ca/data-donnees/sgb_datasets/bc/		Matthew Buchanan, BGC				GeoPackage Data Table	No changes from published dataset	private	North America Albers Equal Area Conic	polygon
	Building Footprint	main.building_footprints	Maxim Fortin	https://maximfortin.com/project/obpl-ca-2021/	Fortin, Maxim (2024): Python code for the Open Building Population Layer - Canada, derived from open-source computer-generated footprints and 2021 census data.	Matthew Buchanan, BGC	2024-03-31			GeoPackage Data Table	No changes from published dataset	public	North America Albers Equal Area Conic	polygon
Critical Factilities	Critical Facility	main.critical_facilities	BGC and Regional Districts	n/a	BC Assessment Actual Use Descriptions grouped according to criteria listed in Section A-3 of Appendix A.	Matthew Buchanan, BGC	43252	43252	45236	GeoPackage Data Table	Point locations of critical facilities downloaded or received from cites and Regional Districts in BC. In areas where we didn't get data, points were determined from the centroid of parcels with these use_codes. usecodes = [515,446,447,625,620,287,270,640,505,424,600,650,286,285,630] Categorized into 9 categories. 1.Emergency Response Services 2.Emergency Response Resources 3.Utilities 4.Communication 5.Medical Facilities 6.Transportation 7.Environmental 8.Community 9.Food	private	North America Albers Equal Area Conic	polygon
Businesses	Business	main.business_points	Geografx	https://www.geografx.com/business-location-data-canada-us	Geographx. (2021). Business Location Database. Retrieved from: https://www.geografx.com/business-location-data-canada-us	Matthew Buchanan, BGC	2022-02-07	2022-02-07	2022-02-07	GeoPackage Data Table	No changes from published dataset. All attributes dropped except Name, Saldesc	public	North America Albers Equal Area Conic	point
Environmental Values	Fisheries	main.fisheries	GeoBC	http://www.env.gov.bc.ca/esd/distdata/ecosystems/bc50kfiss/hist_fish_dist/	BC Ministry of Environment (2006, July 25). BC Historical Fish Distribution 50k Spatial Dataset.	Matthew Buchanan, BGC	2018-03-27	2018-03-27	2018-03-27	GeoPackage Data Table	No changes from published dataset. All attributes dropped.	public	North America Albers Equal Area Conic	point
	Species and Ecosystems at risk	main.species_and_ecosystems_at_risk	BC Conservation Data Centre	https://catalogue.data.gov.bc.ca/dataset/species-and-ecosystems-at-risk-masked-secured-publicly-available-occurrences-cdc	BC Conservation Data Centre (2018). Endangered Species and Ecosystems – Masked Occurrences Data. Retrieved from: https://catalogue.data.gov.bc.ca/dataset?type=Application	Matthew Buchanan, BGC	2018-03-27	2018-03-27	2018-03-27	GeoPackage Data Table	No changes from published dataset. All attributes dropped.	public	North America Albers Equal Area Conic	polygon
	n/a	main.old_growth_management_areas	BC Data Catalogue	https://catalogue.data.gov.bc.ca/dataset/old-growth-management-areas-legal-current	BC Deparment of Provincial Stewardship Strategies and Planning. (2009). Old Growth Management Areas - Legal Current. Retrieved from: https://catalogue.data.gov.bc.ca/dataset/old-growth-management-areas-legal-current	Matthew Buchanan, BGC	2008-02-13	2008-02-13	2009-07-16	GeoPackage Data Table	No changes from published dataset. All attributes dropped.	public	North America Albers Equal Area Conic	polygon
	Provincial Park	main.provincial_parks	BC Data Catalogue	https://catalogue.data.gov.bc.ca/dataset/bc-parks-ecological-reserves-and-protected-areas	BC Data Catalog (2018). BC Parks, Ecological Reserves and Protected Areas. Retrieved from: https://catalogue.data.gov.bc.ca/dataset/bc-parks-ecological-reserves-and-protected-areas	Matthew Buchanan, BGC	2011-03-08	2011-03-08	2024-05-14	GeoPackage Data Table	No changes from published dataset. All attributes dropped except PROT_NAME	public	North America Albers Equal Area Conic	polygon
Roads	Road	main.road	BC Road Atlas GeoBC	https://www2.gov.bc.ca/gov/content/data/geographic-data-services/topographic-data/roads	GeoBC. (2024). Digital Road Atlas. Retrieved from: https://www2.gov.bc.ca/gov/content/data/geographic-data-services/topographic-data/roads	Matthew Buchanan, BGC	2018-05-03	2018-05-03	2018-05-03	GeoPackage Data Table	Road data from BC Road Atlas joined to MoTI traffic data. All attributes dropped except TRANSPORT_LINE_ID,TRANSPORT_LINE_TYPE_CODE,TRANSPORT_LINE_SURFACE_CODE,SUMMER_CLA	public	North America Albers Equal Area Conic	line
	Bridge	main.mott_bridges	BC Data Catalogue	https://catalogue.data.gov.bc.ca/dataset/ministry-of-transportation-mot-road-structures		Matthew Buchanan, BGC	2018-05-03	2018-05-03	2018-05-03	GeoPackage Data Table		public	North America Albers Equal Area Conic	line
	Culvert	main.mott_culverts	BC Data Catalogue	https://catalogue.data.gov.bc.ca/dataset/ministry-of-transportation-mot-road-structures		Matthew Buchanan, BGC	2018-05-03	2018-05-03	2018-05-03	GeoPackage Data Table		public	North America Albers Equal Area Conic	point
Railway	Railway	main.railway	NRCan	https://open.canada.ca/data/en/dataset/ac26807e-a1e8-49fa-87bf-451175a859b8	Natural Resources Canada. (2019). National Railway Network - GeoBase Series. Retrieved from: https://open.canada.ca/data/en/dataset/ac26807e-a1e8-49fa-87bf-451175a859b8	Matthew Buchanan, BGC	2013-12-06	2013-12-06	2013-12-06	GeoPackage Data Table	No changes from published dataset. All attributes dropped.	public	North America Albers Equal Area Conic	line
Utilities (Linear Infrastruc	Petroleum Pipeline	main.petroleum_line	ICI Society	https://www.icisociety.ca/	Integrated Cadastral Information (ICI) Society. (2019, December 1). Utility Infrastructure [Database]. Retrieved from: https://www.icisociety.ca/services/our-data/.	Matthew Buchanan, BGC	2018-08-07	2018-08-07	2018-08-07	GeoPackage Data Table	No changes from published dataset. All attributes dropped.	not public	North America Albers Equal Area Conic	line
	Communication Line	main.communication_line	ICI Society	https://www.icisociety.ca/	Integrated Cadastral Information (ICI) Society. (2019, December 1). Utility Infrastructure [Database]. Retrieved from: https://www.icisociety.ca/services/our-data/.	Matthew Buchanan, BGC	2018-08-07	2018-08-07	2018-08-07	GeoPackage Data Table	No changes from published dataset. All attributes dropped.	not public	North America Albers Equal Area Conic	line
	Electrical Line	main.electrical_line	ICI Society	https://www.icisociety.ca/	Integrated Cadastral Information (ICI) Society. (2019, December 1). Utility Infrastructure [Database]. Retrieved from: https://www.icisociety.ca/services/our-data/.	Matthew Buchanan, BGC	2018-08-07	2018-08-07	2018-08-07	GeoPackage Data Table	No changes from published dataset. All attributes dropped.	not public	North America Albers Equal Area Conic	line
	Water Line	main.water_line	ICI Society and others	https://www.icisociety.ca/	Integrated Cadastral Information (ICI) Society. (2019, December 1). Utility Infrastructure [Database]. Retrieved from: https://www.icisociety.ca/services/our-data/.	Matthew Buchanan, BGC	2018-08-07	2018-08-07	2018-08-07	GeoPackage Data Table	No changes from published dataset. All attributes dropped.	not public	North America Albers Equal Area Conic	line
Utilities (Point Infrastructure)	Electrical Point	main.electrical_points	ICI Society	https://www.icisociety.ca/	Integrated Cadastral Information (ICI) Society. (2019, December 1). Utility Infrastructure [Database]. Retrieved from: https://www.icisociety.ca/services/our-data/.	Matthew Buchanan, BGC	2018-08-07	2018-08-07	2018-08-07	GeoPackage Data Table	No changes from published dataset. All attributes dropped.	not public	North America Albers Equal Area Conic	point
	Communication Point	main.communication_points	ICI Society	https://www.icisociety.ca/	Integrated Cadastral Information (ICI) Society. (2019, December 1). Utility Infrastructure [Database]. Retrieved from: https://www.icisociety.ca/services/our-data/.	Matthew Buchanan, BGC	2018-08-07	2018-08-07	2018-08-07	GeoPackage Data Table	No changes from published dataset. All attributes dropped.	not public	North America Albers Equal Area Conic	point
	Petroleum Point	main.petroleum_point	ICI Society	https://www.icisociety.ca/	Integrated Cadastral Information (ICI) Society. (2019, December 1). Utility Infrastructure [Database]. Retrieved from: https://www.icisociety.ca/services/our-data/.	Matthew Buchanan, BGC	2018-08-07	2018-08-07	2018-08-07	GeoPackage Data Table	No changes from published dataset. All attributes dropped.	not public	North America Albers Equal Area Conic	point
	Water Point	main.water_point	various	n/a		Matthew Buchanan, BGC	2018-08-07	2018-08-07	2024-03-31	GeoPackage Data Table	No changes from published dataset. All attributes dropped.	not public	North America Albers Equal Area Conic	point
Riverine Flooding	Tier 1 (Floodplain Identification), > 10km2	main.clearwater_floodplain	BGC	Geodatabase included with project.	This project. Adapted from BGC Engineering Inc. (April 19, 2024). Mapping for Floodplain Identification (Stage 1). Final report prepared for BC Hydro.	Matthew Buchanan, BGC	2024-01-12	2024-01-12	2024-01-12	GeoPackage Data Table		public	North America Albers Equal Area Conic	polygon
Alluvial Fans	Steep Creek Fan Boundary	main.alluvial_fans	BGC	Geodatabase included with project.	This project.	Matthew Buchanan, BGC			2025-05-06	GeoPackage Data Table		public	North America Albers Equal Area Conic	polygon
Landslides	Landslide Hazard Areas of Interest	main.landslide_1pct_sus_w_inv	BGC	Geodatabase included with project.	This project.	Matthew Buchanan, BGC			2025-05-06	GeoPackage Data Table		public	North America Albers Equal Area Conic	polygon
Asset/Hazard Grid	Density_****	main.grid_summary	BGC	Geodatabase included with project.	This project.	Matthew Buchanan, BGC			2025-05-06	GeoPackage Data Table		public	North America Albers Equal Area Conic	polygon
Riverine Flooding	Tier 2 (Base Level Hazard Maps)	Velocity (flow m3/s)	BGC	Geodatabase included with project.	This project.	Matthew Buchanan, BGC	2024-01-12	2024-01-12	2024-01-12	GeoTIFF		private	UTM Zone 11	raster
		Depth (flow m3/s)	BGC	Geodatabase included with project.	This project.	Matthew Buchanan, BGC	2024-01-12	2024-01-12	2024-01-12	GeoTIFF		private	UTM Zone 11	raster

APPENDIX L
GEOSPATIAL DATA (INCLUDED SEPARATELY)

APPENDIX M
RESULTS FACT SHEETS (INCLUDED SEPARATELY)